PowerTech Belgrade 2023

LEADING INNOVATIONS FOR RESILIENT & CARBON-NEUTRAL POWER SYSTEMS

25-29 JUNE, 2023, BELGRADE, SERBIA

TT08 | Modelling, operation, control, and stability analysis of low-inertia power systems

Federico Milano, UCD, Ireland

Petros Aristidou, Cyprus University of Technology, Cyprus
Junru Chen, Xinjiang University, China
Ahsan Murad, DIgSILENT GmbH, Germany
Taulant Kërçi, EirGird, TDO, Ireland

Abstract

- The tutorial discusses the dynamic analysis and operation of low-inertia grids, that grid with high penetration of converter-interfaced generation. The module is organized into two parts. The first part focuses on operation and control, whereas the second part deals with modelling and stability analysis. The module blends industry experience and recent trends in academic research. The industry point of view is represented by EirGrid that operates the Irish grid up to 75% non-synchronous instantaneous power generation and DIgSILENT that will share their experience with the implementation of converter and their controllers in a power system software tool. The academic presentations discuss state-of-the-art concepts on the modelling of security constrained optimal power flow problems for low-inertia systems; as well as recent advances in the synchronization stability and modelling of grid-connected converters and their controllers. All presentations include several illustrative examples based on both benchmark and real-world systems.

Course Outline

- **8:30 – 10:30 Part I**

  Introduction

  Petros Aristidou: Blending optimization methods with dynamic analysis for low-inertia power systems

  Taulant Kërçi: Dynamic Response of Inverter-based Resources in Ireland and Northern Ireland Power Systems

  Ahsan Murad: Distributed generation modeling, simulation and system studies using DIgSILENT PowerFactory

- **10:30 – 10:45 Break**
- **10:45 – 12:45 Part II**

  Junru Chen: Synchronization stability of grid-connected converters

  Federico Milano: Complex modelling of converter-interfaced generation

  Closure

Petros Aristidou

Petros Aristidou got his Diploma from the Department of Electrical & Computer Engineering at the National Technical University of Athens (Greece) in 2010 and his PhD at the University of Liege (Belgium) in 2015. During his PhD, he worked on domain decomposition methods for real-time dynamic security assessment of transmission systems. He took a position as a Postdoctoral Researcher at the Power Systems Laboratory at ETH Zurich (Switzerland) for one year, working on developing new control algorithms for future low-inertia power systems. Between 2016-2019 he was a Lecturer at the University of Leeds (UK), where he led the Smart Grids Lab. Since January 2020, he has been a Lecturer in Sustainable Power Systems at the Cyprus University of Technology. His expertise is in power system dynamics, planning, and control, and he has participated in several working groups looking into the challenges of low-inertia systems. Recent projects and publications can be found at https://sps.cut.ac.cy

Blending optimization methods with dynamic analysis in low-inertia power systems

Dr. Petros Aristidou

Sustainable Power Systems Lab
Department of Electrical Engineering, Computer Engineering & Informatics,
Cyprus University of Technology

TT08 | Modelling, operation, control, and stability analysis of low-inertia power systems

25 June 2023

Outline

1. Low-inertia Power Systems and their Challenges
2. Economic and Secure Operation of Low-inertia Grids
3. Using Dynamic Optimization
4. Using Dynamic Simulation Software
5. Using Simplified Models or Approximations
6. Concluding Remarks and Open Work

Low-inertia Power Systems and their Challenges

Transformation of power systems and new challenges

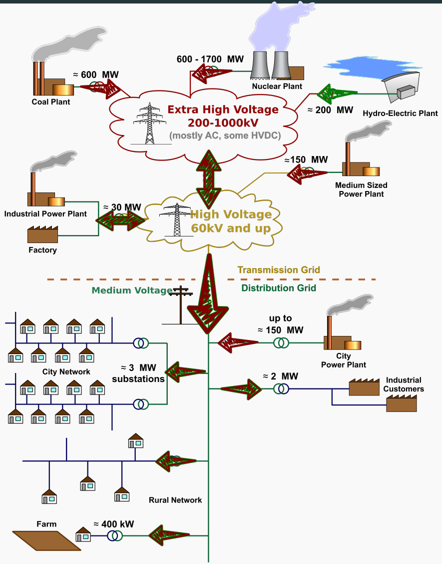

Transformation of power systems and new challenges

- **Operation of the grid close or above the physical limits.** *Pushing them closer to the stability boundaries.*
- **Bi-directional flows.** *Most of the system protections and operation practices were not designed for this.*
- **Increased uncertainty.** *Intermittent generation, new consumption profiles and patterns, unknown consumer response.*
- **Decommission of conventional generation units.** *Loss of synchronous generators and their controls.*

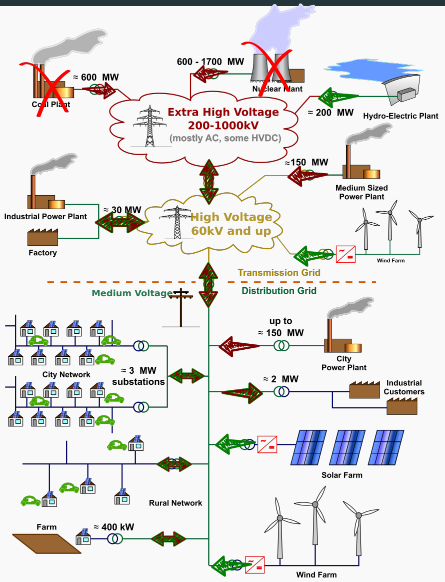

Transformation of power systems and new challenges

- **Operation of the grid close or above the physical limits.** *Pushing them closer to the stability boundaries.*
- **Bi-directional flows.** *Most of the system protections and operation practices were not designed for this.*
- **Increased uncertainty.** *Intermittent generation, new consumption profiles and patterns, unknown consumer response.*
- **Decommission of conventional generation units.** *Loss of synchronous generators and their controls.*

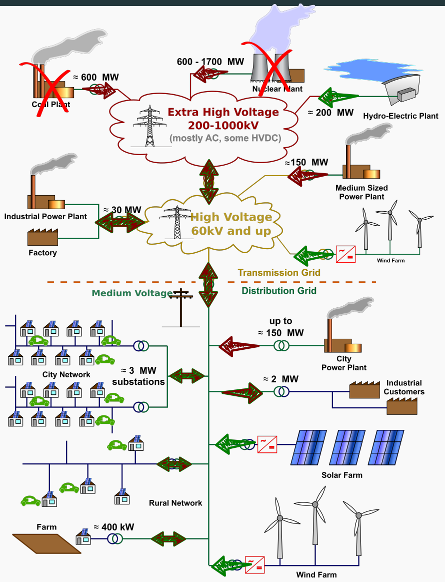

Low-inertia power systems

Definition: Power systems with increased percentage of **power-electronics**-interfaced resources and reduced percentage of **synchronous-generator**-based power plants.

Alternative title: Power-electronics-dominated power systems

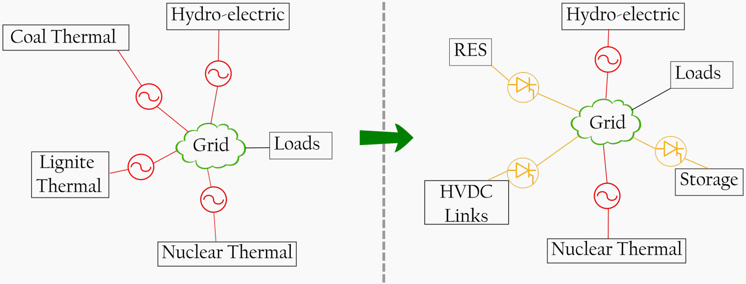

Low-inertia transition

Synchronous generators:

- **Inherently** provide an energy buffer to the system in the form of **kinetic energy** that supports the system in case of power imbalances
- **Inherently** provide short-circuit current in case of fault to help detect and clear the faults.
- Support the system voltages (as a voltage source and through AVR)
- Support the system with primary frequency control to arrest frequency

Converter-based generators:

- Do not provide kinetic inertia. Can provide synthetic inertia – but not **inherently**
- Do not provide short-circuit current **inherently**
- Do not support the system voltages **inherently**
- Cannot participate in frequency control unless renewable curtailments are made, or storage is installed

Some of the arising dynamic problems

- **Frequency security problems**: Lower inertia and frequency controlability. After a contingency, lower nadir and higher ROCOF.

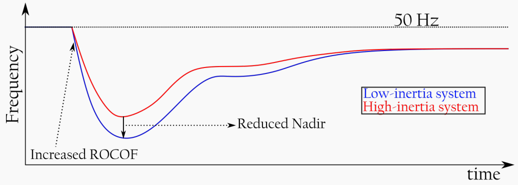

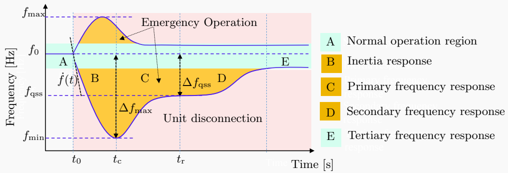

Some of the arising dynamic problems

- **Frequency security problems**: Lower inertia and frequency controlability. After a contingency, lower nadir and higher ROCOF.
- **Voltage security problems**: Decreased system stiffness (Short-Circuit-Ratio). After a short-circuit, lower dips, larger dip durations, and slower recovery.

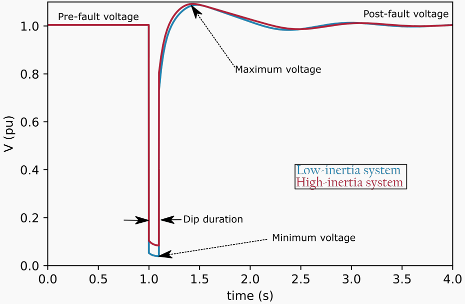

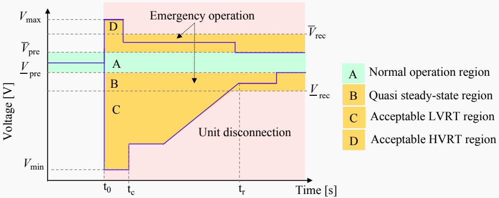

Some of the arising dynamic problems

- **Frequency security problems**: Lower inertia and frequency controlability. After a contingency, lower nadir and higher ROCOF.
- **Voltage security problems**: Decreased system stiffness (Short-Circuit-Ratio). After a short-circuit, lower dips, larger dip durations, and slower recovery.
- **Protection problems**: Lower short-circuits currents that impact the system fault levels. This affects all of the protection schemes and the critical clearing time of the system.

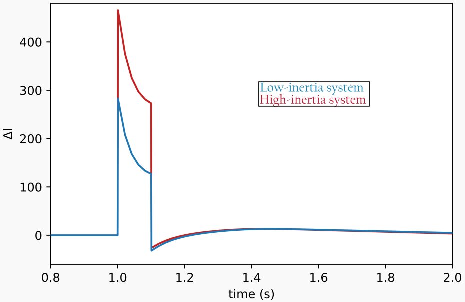

Many open questions and problems for industry and academia

TT08: Modelling, operation, control, and stability analysis of low-inertia power systems

- How do we operate low-inertia grids to ensure dynamic security?
- What are some of the most urgent challenges faced by the industry?
- How do we simulate and analyze the dynamic performance of low-inertia grids?
- How do we ensure the stability of low-inertia grids?
- How do we model the new components and controls involved in low-inertia grids?

Economic and Secure Operation of Low-inertia Grids

Economic Operation of power systems

Objective: Find the most economical solution to a problem related to the operation or planning of power systems, subject to technical and operational constraints $\rightarrow$ {**economical**, **feasible**, **secure**}

Examples: Economic Dispatch, Unit Commitment, Expansion planning, Optimal resource placement, AC Optimal Power Flow (OPF), etc.

Recent developments:

- Better modelling to increase the fidelity of optimization models.
- Techniques to improve the treatment of non-convex constraints while ensuring accuracy to increase performance.
- Methods targeted specifically to distribution networks.
- Machine Learning models and data-driven techniques to increase performance.
- Dynamic constraints to ensure dynamic security of solutions.

Economic Operation of power systems

Objective: Find the most economical solution to a problem related to the operation or planning of power systems, subject to technical and operational constraints $\rightarrow$ {**economical**, **feasible**, **secure**}

Examples: Economic Dispatch, Unit Commitment, Expansion planning, Optimal resource placement, AC Optimal Power Flow (OPF), etc.

Recent developments:

- Better modelling to increase the fidelity of optimization models.
- Techniques to improve the treatment of non-convex constraints while ensuring accuracy to increase performance.
- Methods targeted specifically to distribution networks.
- Machine Learning models and data-driven techniques to increase performance.
- Dynamic constraints to ensure dynamic security of solutions.

Unit Commitment with AC OPF Constraints

Objective:

Minimize: Dispatch + Operation costs

Subject to:

- Forecasted or real-time input data (load demand, system topology, generation profiles, costs)
- Technical and operational constraints
- Security constraints
- Environmental constraints (e.g., CO_2 limits, limit in using fossil fuel, etc.)

Unit Commitment with AC OPF Constraints

Objective:

Minimize: Dispatch + Operation costs

Subject to:

- Forecasted or real-time input data (load demand, system topology, generation profiles, costs)
- Technical and operational constraints
- Security constraints
- Environmental constraints (e.g., CO_2 limits, limit in using fossil fuel, etc.)

$$\min_{\chi \in \Omega, z \in \{0,1\}} \quad \Theta(\chi, z) \tag{1a}$$

$$\text{s.t.} \quad \Phi(\chi, z) = 0, \tag{1b}$$

$$\Lambda(\chi, z) \leq 0 \tag{1c}$$

- Operation decision (χ) variables (unit dispatching, load shifting/disconnection, battery charging, etc.)
- Unit commitment (z) variable (units to be committed)
- Equality constraints (1b)
- Inequality constraints (1c)

Technical constraints (for a multi-period problem)

Dispatchable Generation Constraints → Describe the behaviour of the generating units

$$0 \leq p_{st} \leq \overline{p}_s \cdot z_s, \quad -\overline{q}_s \cdot z_s \leq q_{st} \leq \overline{q}_s \cdot z_s, \quad -\mathrm{rp}_s^{\mathrm{dn}} \leq p_{st} - p_{s(t-1)} \leq \mathrm{rp}_s^{\mathrm{up}}, \qquad \forall s, t$$

$$0 \leq p_{rt} \leq \tilde{p}_{rt} \cdot z_r, \quad -\tan \overline{\phi}_r \cdot \tilde{p}_{rt} \cdot z_r \leq q_{rt} \leq \tan \overline{\phi}_r \cdot \tilde{p}_{rt} \cdot z_r, \qquad \forall r, t$$

Battery Behaviour and Constraints → Describe the behaviour of the batteries

$$0 \leq p_{bt}^{\mathrm{dch}} \leq \overline{p}_b^{\mathrm{dch}} \cdot z_{bt}^{\mathrm{dch}}, \quad 0 \leq p_{bt}^{\mathrm{ch}} \leq \overline{p}_b^{\mathrm{ch}} \cdot z_{bt}^{\mathrm{ch}}, \quad z_{bt}^{\mathrm{dch}} + z_{bt}^{\mathrm{ch}} = z_b, \qquad \forall b, t$$

$$\underline{e}_b \cdot z_b \leq e_b^{\mathrm{ini}} + \sum_{\tau=1}^{t} \left(\xi_b^{\mathrm{ch}} \cdot p_{b\tau o}^{\mathrm{ch}} - \frac{1}{\xi_b^{\mathrm{dch}}} \cdot p_{b\tau}^{\mathrm{dch}} \right) \leq \overline{e}_b \cdot z_b, \qquad \forall b, t$$

$$\sum_{t \in \mathscr{T}} \left(\xi_b^{\mathrm{ch}} \cdot p_{bt}^{\mathrm{ch}} - \frac{1}{\xi_b^{\mathrm{dch}}} \cdot p_{bt}^{\mathrm{dch}} \right) = 0, \qquad \forall b$$

Technical constraints (for a multi-period problem)

AC Power Flow Equations $\rightarrow$ Dictate the loading of the lines, the currents, and voltages

$$s^{\mathrm{d}}_{it} - \sum_{g \in \mathscr{G}^i} s_{gt} = \sum_{\eta(l^+)=i} S_{(l^+)t} + \sum_{\eta(l^-)=i} S_{(l^-)t} \qquad \forall i, t$$

$$S_{(l^+)t} = V_{\eta(l^+)t} \left(I_{(l^+)t}\right)^*, \qquad S_{(l^-)t} = V_{\eta(l^-)t} \left(I_{(l^-)t}\right)^*, \qquad \forall l, t$$

$$I_{(l^+)t} = y^s_l \left(V_{\eta(l^+)t} - V_{\eta(l^-)t}\right) + y^{sh}_l V_{\eta(l^+)t}, \qquad \forall l, t$$

$$I_{(l^-)t} = y^s_l \left(V_{\eta(l^-)t} - V_{\eta(l^+)t}\right) + y^{sh}_l V_{\eta(l^-)t}, \qquad \forall l, t$$

Line Thermal Loading and Bus Voltage Constraints

$$P^2_{lt} + Q^2_{lt} \le \left(\overline{S}_l\right)^2 \quad \text{or} \quad |I_{lt}| \le \overline{I}_l \qquad \forall l, t$$

$$\underline{V} \le V_{it} \le \overline{V} \qquad \forall i, t$$

Incorporating static and dynamic security constraints

Challenge: How do we ensure that our optimal solution is also **secure against contingencies** (e.g., N-1 secure)?

- **Static security:** After the fault, the **post-fault steady-state** system should be able to supply the loads while complying with the security constraints (voltage, current, generator limits, etc.).
- **Dynamic security:** The system should be able to **survive the transient** response immediately after the fault.

Examples of faults considered:

- Loss of a generator (conventional or renewable).
- Network faults (loss of line, transformer, etc.)

Example: Frequency response of a system after tripping a generator

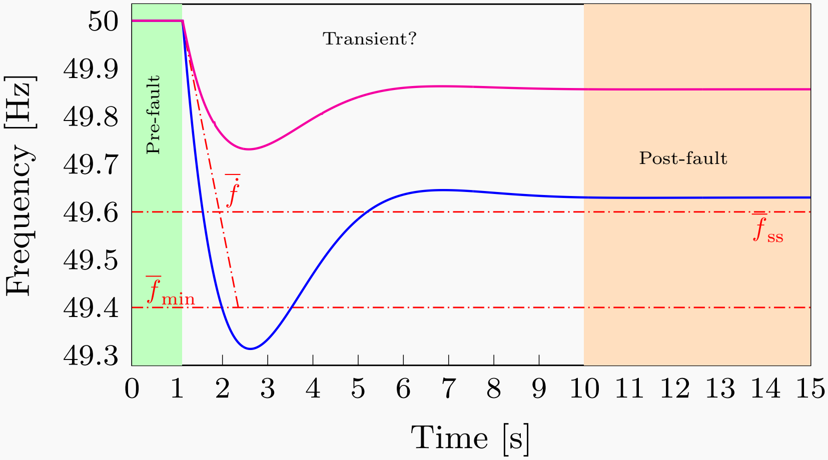

3-bus example

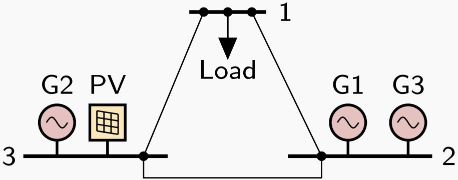

UC-ACOPF Solution (€):

- $P_{PV} = 30$ MW
- $z_1 = 1,\ P_1 = 40.2$ MW
- $z_2 = z_3 = 0$ (Generators 2+3 disconnected)

Data:

- $P_i^{max} = 100$ MW, $P_i^{min} = 10$ MW
- $Cost_{G1} \leq Cost_{G2} \leq Cost_{G3}$
- $H_1 \leq H_2 \leq H_3$
- $Load = 70$ MW
- $P_{PV} = 30$ MW, $Cost_{PV} = 0$

3-bus example

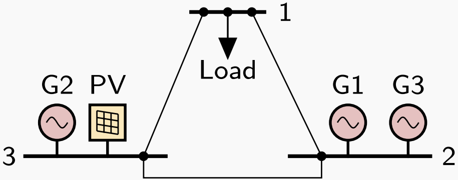

UC-ACOPF Solution (€):

- $P_{PV} = 30$ MW
- $z_1 = 1,\ P_1 = 40.2$ MW
- $z_2 = z_3 = 0$ (Generators 2+3 disconnected)
- **Not N-1 secure**

Data:

- $P_i^{max} = 100$ MW, $P_i^{min} = 10$ MW
- $Cost_{G1} \leq Cost_{G2} \leq Cost_{G3}$
- $H_1 \leq H_2 \leq H_3$
- $Load = 70$ MW
- $P_{PV} = 30$ MW, $Cost_{PV} = 0$

3-bus example

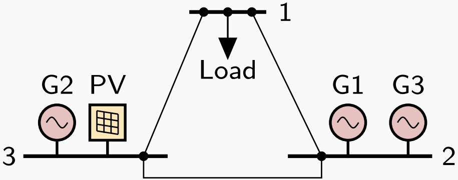

Data:

- $P_i^{max} = 100$ MW, $P_i^{min} = 10$ MW
- $Cost_{G1} \leq Cost_{G2} \leq Cost_{G3}$
- $H_1 \leq H_2 \leq H_3$
- $Load = 70$ MW
- $P_{PV} = 30$ MW, $Cost_{PV} = 0$

UC-ACOPF Solution (€):

- $P_{PV} = 30$ MW
- $z_1 = 1,\ P_1 = 40.2$ MW
- $z_2 = z_3 = 0$ (Generators 2+3 disconnected)
- **Not N-1 secure**

UC-ACOPF Solution with static security constraints (€€):

- $P_{PV} = 30$ MW
- $z_1 = 1,\ P_1 = 30.2$ MW
- $z_2 = 1,\ P_2 = 10$ MW
- $z_3 = 0$ (Generator 3 disconnected)

3-bus example

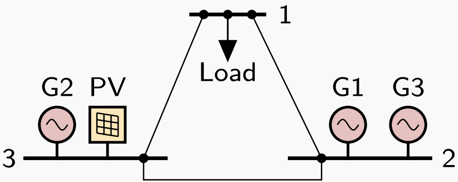

Data:

- $P_i^{max} = 100$ MW, $P_i^{min} = 10$ MW
- $Cost_{G1} \leq Cost_{G2} \leq Cost_{G3}$
- $H_1 \leq H_2 \leq H_3$
- $Load = 70$ MW
- $P_{PV} = 30$ MW, $Cost_{PV} = 0$

Dynamic Security Assessment of solution:

Trip G1:

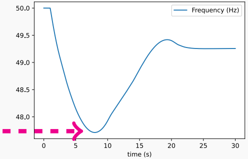

Nadir

ROCOF

Trip G2:

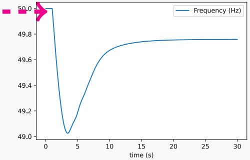

Trip PV:

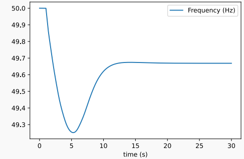

3-bus example

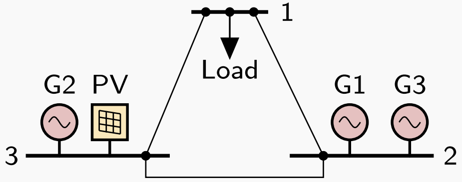

Data:

- $P_i^{max} = 100$ MW, $P_i^{min} = 10$ MW
- $Cost_{G1} \leq Cost_{G2} \leq Cost_{G3}$
- $H_1 \leq H_2 \leq H_3$
- $Load = 70$ MW
- $P_{PV} = 30$ MW, $Cost_{PV} = 0$

Dynamic Security Assessment of solution:

- Change the power dispatch?
- Replace a generator with another generator with better characteristics (H, R, T, etc.)?
- Add one more generator?
- Add some other device to provide support (battery, flywheel, etc.)?

How do we decide the most economical and dynamically secure solution?

3-bus example

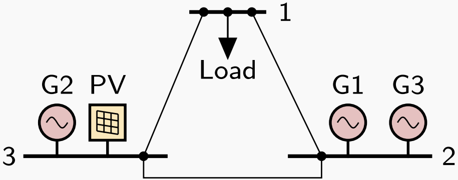

UC-ACOPF Solution with static and dynamic security constraints (€€€):

- $P_{PV} = 30$ MW, $P_1 = 20.2$ MW, $P_2 = 10$ MW, $P_3 = 10$ MW

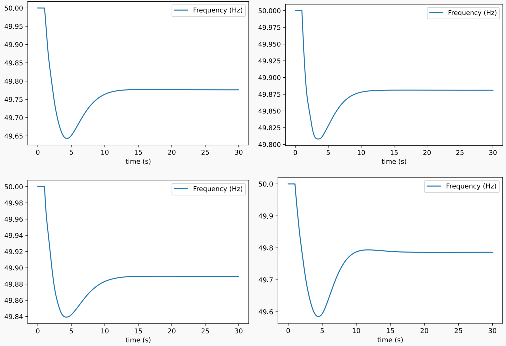

Data:

- $P_i^{max} = 100$ MW, $P_i^{min} = 10$ MW
- $Cost_{G1} \leq Cost_{G2} \leq Cost_{G3}$
- $H_1 \leq H_2 \leq H_3$
- $Load = 70$ MW
- $P_{PV} = 30$ MW, $Cost_{PV} = 0$

Incorporating static and dynamic security constraints

How to model the post-fault static security?

- We require that the system must survive after the considered faults.
- For each fault we want to consider, we add a new set of power-flow constraints for the **post-fault** (*pof*) operation.
- The **pre-fault** (*prf*) unit commitment decision variables z are changed to z' where the faulted component operation is set to zero.

$$\min_{\chi\in\Omega, z\in\{0,1\}} \quad \Theta^{\mathrm{prf}}(\chi^{\mathrm{prf}}, z) \tag{2a}$$

$$\text{s.t.} \quad \Phi^{\mathrm{prf}}(z, \chi^{\mathrm{prf}}) = 0 \tag{2b}$$

$$\Lambda^{\mathrm{prf}}(z, \chi^{\mathrm{prf}}) \leq 0 \tag{2c}$$

$$\Phi^{\mathrm{pof}}(z', \chi^{\mathrm{pof}}) = 0 \tag{2d}$$

$$\Lambda^{\mathrm{pof}}(z', \chi^{\mathrm{pof}}) \leq 0 \tag{2e}$$

Incorporating static and dynamic security constraints

How to model the post-fault dynamic security?

- The transient period is described by the **solution** of an **Initial-Value Problem of Differential-Algebraic Equations** (IVP DAE):
  - Model:

$$F(\chi^{\mathrm{prf}}, z', \boldsymbol{x}, \dot{\boldsymbol{x}}, \tau) = 0, \qquad \tau \in [0, T]$$

    where $\boldsymbol{x}$ are the **differential-algebraic states** of the IVP DAE problem.
  - The system is non-linear and hybrid (continuous and discrete variables).
  - The **structure** of the DAE depends on the unit commitment decision variables after a contingency is applied (z').
  - The **initial values** of the DAE model $\boldsymbol{x}_0$ depend on the pre-fault operational decision variables (χ^{prf}).
- The solution requires performing a **numerical integration** of the DAEs for every planning period and every contingency.

Optimization with Differential and Algebraic Equations

$$
\begin{aligned}
\min_{\chi \in \Omega, z \in \{0,1\}} \quad & \Theta^{\mathrm{prf}}(\chi^{\mathrm{prf}}, z) \\
\text{s.t.} \quad & \Phi^{\mathrm{prf}}(z, \chi^{\mathrm{prf}}) = 0 \\
& \Lambda^{\mathrm{prf}}(z, \chi^{\mathrm{prf}}) \leq 0 \\
& F(\chi^{\mathrm{prf}}, z', \boldsymbol{x}, \dot{\boldsymbol{x}}, \tau) = 0,\ \tau \in [0, T] \\
& \rho(\chi^{\mathrm{prf}}, z', \boldsymbol{x}, \dot{\boldsymbol{x}}, \tau) \leq 0,\ \tau \in [0, T]
\end{aligned}
$$

Bethany Nicholson, John D. Siirola, Jean-Paul Watson, Victor M. Zavala, and Lorenz T. Biegler. "pyomo.dae: a modeling and automatic discretization framework for optimization with differential and algebraic equations." Mathematical Programming Computation 10(2) (2018): 187-223.

Optimization with Differential and Algebraic Equations

$$\begin{aligned}
\min_{\chi\in\Omega, z\in\{0,1\}} \quad & \boxed{\begin{aligned} &\Theta^{\mathrm{prf}}(\chi^{\mathrm{prf}}, z) \\ \text{s.t.} \quad & \Phi^{\mathrm{prf}}(z, \chi^{\mathrm{prf}}) = 0 \\ & \Lambda^{\mathrm{prf}}(z, \chi^{\mathrm{prf}}) \leq 0 \end{aligned}} \\
& F(\chi^{\mathrm{prf}}, z', \boldsymbol{x}, \dot{\boldsymbol{x}}, \tau) = 0, \; \tau \in [0, T] \\
& \rho(\chi^{\mathrm{prf}}, z', \boldsymbol{x}, \dot{\boldsymbol{x}}, \tau) \leq 0, \; \tau \in [0, T]
\end{aligned}$$

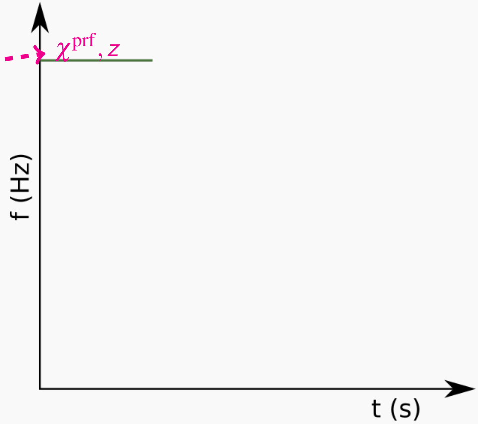

Optimization with Differential and Algebraic Equations

$$
\begin{aligned}
\min_{\chi\in\Omega, z\in\{0,1\}} \quad & \boxed{\Theta^{\text{prf}}(\chi^{\text{prf}}, z)} \\
\text{s.t.} \quad & \Phi^{\text{prf}}(z, \chi^{\text{prf}}) = 0 \\
& \Lambda^{\text{prf}}(z, \chi^{\text{prf}}) \leq 0 \\
& F(\chi^{\text{prf}}, z', \boldsymbol{x}, \dot{\boldsymbol{x}}, \tau) = 0,\ \tau \in [0, T] \\
& \rho(\chi^{\text{prf}}, z', \boldsymbol{x}, \dot{\boldsymbol{x}}, \tau) \leq 0,\ \tau \in [0, T]
\end{aligned}
$$

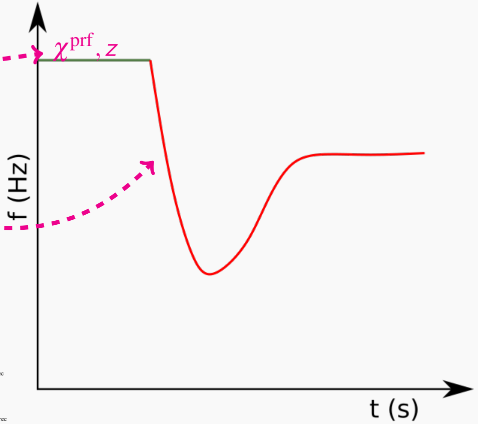

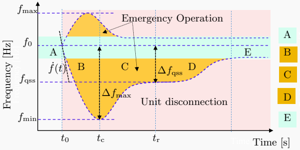

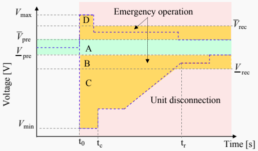

Bethany Nicholson, John D. Siirola, Jean-Paul Watson, Victor M. Zavala, and Lorenz T. Biegler. "pyomo.dae: a modeling and automatic discretization framework for optimization with differential and algebraic equations." Mathematical Programming Computation 10(2) (2018): 187-223.

Using Dynamic Optimization

Optimization with Differential and Algebraic Equations

$$
\begin{aligned}
\min_{\chi\in\Omega, z\in\{0,1\}} \quad & \boxed{\Theta^{\text{prf}}(\chi^{\text{prf}}, z)} \\
\text{s.t.} \quad & \Phi^{\text{prf}}(z, \chi^{\text{prf}}) = 0 \\
& \Lambda^{\text{prf}}(z, \chi^{\text{prf}}) \le 0 \\
& \boxed{F(\chi^{\text{prf}}, z', \boldsymbol{x}, \dot{\boldsymbol{x}}, \tau) = 0,\ \tau \in [0, T]} \\
& \boxed{\rho(\chi^{\text{prf}}, z', \boldsymbol{x}, \dot{\boldsymbol{x}}, \tau) \le 0,\ \tau \in [0, T]}
\end{aligned}
$$

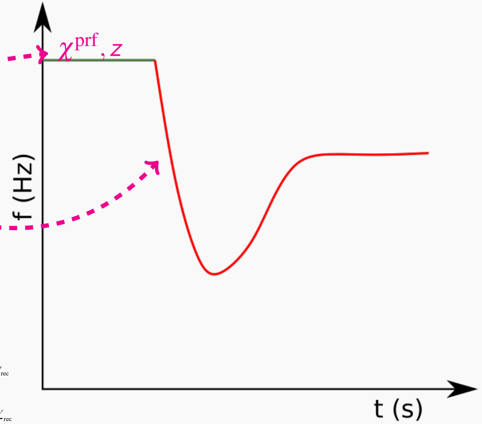

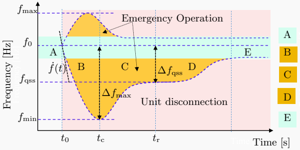

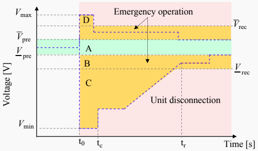

Bethany Nicholson, John D. Siirola, Jean-Paul Watson, Victor M. Zavala, and Lorenz T. Biegler. "pyomo.dae: a modeling and automatic discretization framework for optimization with differential and algebraic equations." Mathematical Programming Computation 10(2) (2018): 187-223.

Optimization with Differential and Algebraic Equations

$$
\begin{aligned}
\min_{\chi \in \Omega, z \in \{0,1\}} \quad & \Theta^{\mathrm{prf}}(\chi^{\mathrm{prf}}, z) \\
\text{s.t.} \quad & \Phi^{\mathrm{prf}}(z, \chi^{\mathrm{prf}}) = 0 \\
& \Lambda^{\mathrm{prf}}(z, \chi^{\mathrm{prf}}) \leq 0 \\
& F_d(\chi^{\mathrm{prf}}, z', \boldsymbol{x}[kh]) = 0,\ k = 0 \dots N \\
& \rho_d(\chi^{\mathrm{prf}}, z', \boldsymbol{x}[kh]) \leq 0,\ k = 0 \dots N
\end{aligned}
$$

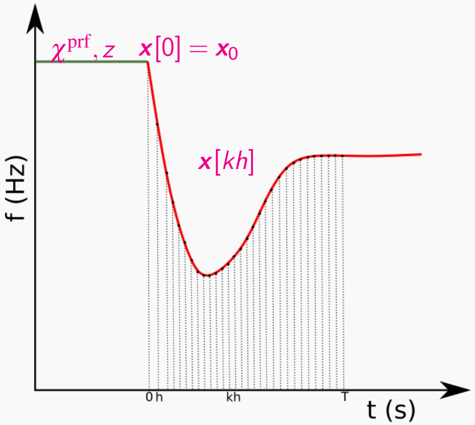

DAE discretization:

- Trapezoidal, BDF, etc.
- Non-linear algebraic equations

Optimization with Differential and Algebraic Equations

Comments:

- **Available tools**: Pyomo.DAE, ACADO, APMonitor, etc.
- Require **continuous** DAE systems. Power system dynamics are characterized by hybrid DAEs (limits, discrete controllers, etc.).
- Each simulation time-step introduces a new set of **coupling** variables $\boldsymbol{x}[kh]$!
- How does it scale? Is it feasible for normal power system applications?

Optimization with Differential and Algebraic Equations

Comments:

- **Available tools**: Pyomo.DAE, ACADO, APMonitor, etc.
- Require **continuous** DAE systems. Power system dynamics are characterized by hybrid DAEs (limits, discrete controllers, etc.).
- Each simulation time-step introduces a new set of **coupling** variables $\boldsymbol{x}[kh]$!
- How does it scale? Is it feasible for normal power system applications?

3-bus example:

- **Initial UC-ACOPF problem**: **15 variables** (12 continuous and 3 binary)
- **DAEs**: 134 states
- **Discretized equation variables** ($T = 15$ s with $h = 10$ ms):

$$134 \cdot \frac{15}{0.01} = 201000$$

- **Considering 4 contingencies for N-1**:

$$\sim 600\,000$$

- **Overall problem size**: $\sim 600\,015$

Bethany Nicholson, John D. Siirola, Jean-Paul Watson, Victor M. Zavala, and Lorenz T. Biegler. "pyomo.dae: a modeling and automatic discretization framework for optimization with differential and algebraic equations." Mathematical Programming Computation 10(2) (2018): 187-223.

Using Dynamic Simulation Software

AC-OPF with dynamic security constraints through dynamic simulations

$$
\begin{aligned}
\min_{\chi^{\mathrm{prf}} \in \Omega} \quad & \Theta^{\mathrm{prf}}(\chi^{\mathrm{prf}}, z) \\
\text{s.t.} \quad & \Phi^{\mathrm{prf}}(z, \chi^{\mathrm{prf}}) = 0 \\
& \Lambda^{\mathrm{prf}}(z, \chi^{\mathrm{prf}}) \leq 0 \\
& F(\chi^{\mathrm{prf}}, z', \boldsymbol{x}, \dot{\boldsymbol{x}}, \tau) = 0, \; \tau \in [0, T] \\
& \rho(\chi^{\mathrm{prf}}, z', \boldsymbol{x}, \dot{\boldsymbol{x}}, \tau) \leq 0, \; \tau \in [0, T]
\end{aligned}
$$

A. Nakiganda, P. Aristidou, "Resilient Microgrid Scheduling with Secure Frequency and Voltage Transient Response", IEEE Transactions on Power Systems, 2022.

AC-OPF with dynamic security constraints through dynamic simulations

$$\min_{\chi^{\text{prf}} \in \Omega} \Theta^{\text{prf}}(\chi^{\text{prf}}, z)$$

$$\text{s.t.} \quad \Phi^{\text{prf}}(z, \chi^{\text{prf}}) = 0$$

$$\Lambda^{\text{prf}}(z, \chi^{\text{prf}}) \leq 0$$

$$\boxed{\begin{aligned} &F(\chi^{\text{prf}}, z', \boldsymbol{x}, \dot{\boldsymbol{x}}, \tau) = 0, \ \tau \in [0, T] \\ &\rho(\chi^{\text{prf}}, z', \boldsymbol{x}, \dot{\boldsymbol{x}}, \tau) \leq 0, \ \tau \in [0, T] \end{aligned}}$$

Move to external simulator

Methodology:

- Move sub-problem into a dynamic simulator
- Extract sensitivities to critical voltage and frequency values using multiple simulations
- Formulate linear feasibility cuts for the optimization problem
- Iterate between optimization and dynamic simulation until the solution is feasible and dynamically secure

A. Nakiganda, P. Aristidou, "Resilient Microgrid Scheduling with Secure Frequency and Voltage Transient Response", IEEE Transactions on Power Systems, 2022.

AC-OPF with dynamic security constraints through dynamic simulations

Step 1: Solve AC-OPF (no dynamic constraints)

$$\min_{\chi^{\mathrm{prf}}\in\Omega} \Theta^{\mathrm{prf}}(\chi^{\mathrm{prf}}, z)$$

$$\text{s.t.} \quad \Phi^{\mathrm{prf}}(z, \chi^{\mathrm{prf}}) = 0$$

$$\Lambda^{\mathrm{prf}}(z, \chi^{\mathrm{prf}}) \leq 0$$

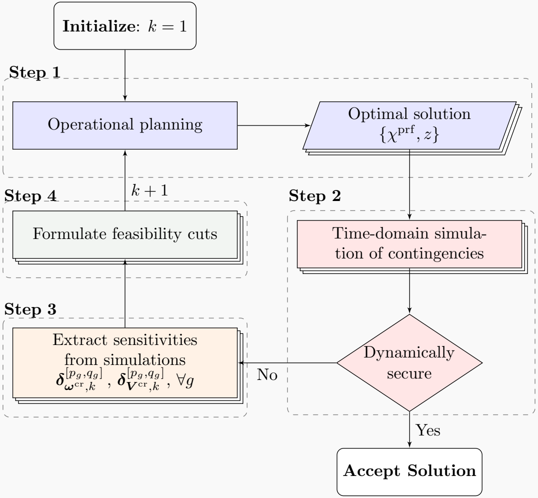

AC-OPF with dynamic security constraints through dynamic simulations

Step 2+3: Call dynamic simulator for each contingency and extract sensitivities

$$F(\chi^{\mathrm{prf}}, z', \boldsymbol{x}, \dot{\boldsymbol{x}}, \tau) = 0,\ \tau \in [0, T]$$
$$\rho(\chi^{\mathrm{prf}}, z', \boldsymbol{x}, \dot{\boldsymbol{x}}, \tau) \leq 0,\ \tau \in [0, T]$$

Step 4: Formulate feasibility cuts (see next slide)

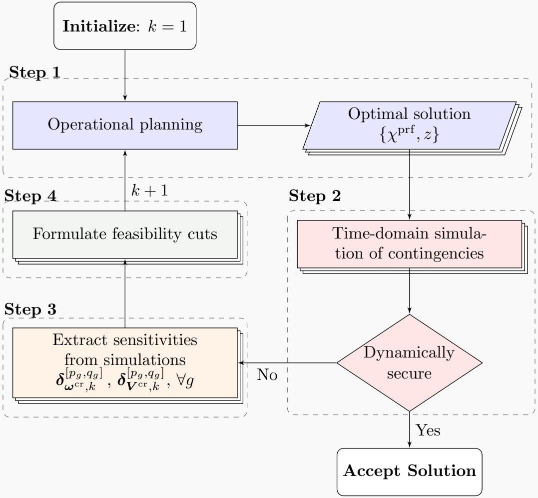

AC-OPF with dynamic security constraints through dynamic simulations

Step 1: Solve AC-OPF with feasibility cuts

$$
\begin{aligned}
\min_{\chi^{\mathrm{prf}} \in \Omega} \quad & \Theta^{\mathrm{prf}}(\chi^{\mathrm{prf}}, z) \\
\text{s.t.} \quad & \Phi^{\mathrm{prf}}(z, \chi^{\mathrm{prf}}) = 0 \\
& \Lambda^{\mathrm{prf}}(z, \chi^{\mathrm{prf}}) \leq 0 \\
& + \text{ Feasibility cuts}_k
\end{aligned}
$$

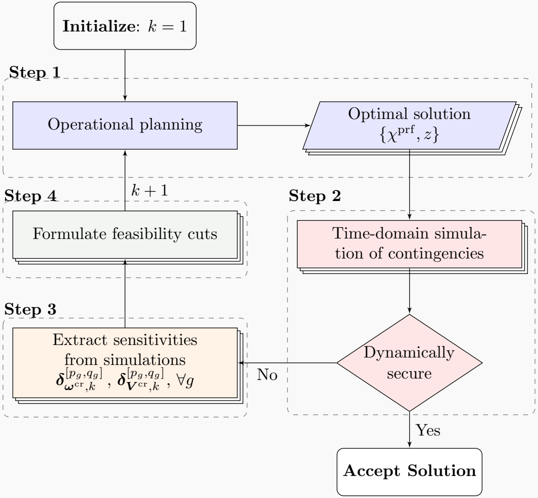

AC-OPF with dynamic security constraints through dynamic simulations

Frequency feasibility cuts for $cr = \{$**min, max, ROCOF, qss**$\}$:

$$\boldsymbol{\omega}^{\mathrm{cr}}_{(k+1)} \leq \boldsymbol{\omega}^{\mathrm{cr}}_{\gamma} + \boldsymbol{\delta}^{p_{\mathrm{g}}}_{\boldsymbol{\omega}^{\mathrm{cr}},\gamma} \cdot (\boldsymbol{p}_{\mathrm{g},(k+1)} - \boldsymbol{p}_{\mathrm{g},\gamma}) \quad + \boldsymbol{\delta}^{q_{\mathrm{g}}}_{\omega^{\mathrm{cr}},\gamma} \cdot (\boldsymbol{q}_{\mathrm{g},(k+1)} - \boldsymbol{q}_{\mathrm{g},\gamma}),\ \forall \gamma = 1, \ldots, k \tag{3a}$$

$$\boldsymbol{\omega}^{\mathrm{min}}_{k+1} \geq \underline{\boldsymbol{\omega}}^{\mathrm{min}}, \qquad \boldsymbol{\omega}^{\mathrm{max}}_{k+1} \leq \overline{\boldsymbol{\omega}}^{\mathrm{max}}, \qquad \underline{\dot{\boldsymbol{\omega}}} \leq \dot{\boldsymbol{\omega}}_{k+1} \leq \overline{\dot{\boldsymbol{\omega}}}, \qquad \underline{\boldsymbol{\omega}}^{\mathrm{qss}} \leq \boldsymbol{\omega}^{\mathrm{qss}}_{k+1} \leq \overline{\boldsymbol{\omega}}^{\mathrm{qss}} \tag{3b}$$

Voltage feasibility cuts for $cr = \{$**min, max,qss**$\}$:

$$\begin{aligned} \boldsymbol{V}^{\mathrm{cr}}_{(k+1)} \leq \boldsymbol{V}^{\mathrm{cr}}_{\gamma} + \sum_{g \in \{\mathscr{S},\mathscr{C}\}} \Big(& \boldsymbol{\delta}^{p_g}_{V^{\mathrm{cr}}_g,\gamma} \cdot (\boldsymbol{p}_{g,(k+1)} - \boldsymbol{p}_{g,\gamma}) \\ & + \boldsymbol{\delta}^{q_g}_{V^{\mathrm{cr}}_g,\gamma} \cdot \left(\boldsymbol{q}_{g,(k+1)} - \boldsymbol{q}_{g,\gamma}\right)\Big),\ \forall \gamma = 1, \ldots, k \end{aligned} \tag{4a}$$

$$\boldsymbol{V}^{\mathrm{min}}_{k+1} \geq \underline{\boldsymbol{V}}^{\mathrm{min}}, \qquad \boldsymbol{V}^{\mathrm{max}}_{k+1} \leq \overline{\boldsymbol{V}}^{\mathrm{max}}, \qquad \underline{\boldsymbol{V}}^{\mathrm{rec}} \leq \boldsymbol{V}^{\mathrm{rec}}_{k+1} \leq \overline{\boldsymbol{V}}^{\mathrm{rec}} \tag{4b}$$

A. Nakiganda, P. Aristidou, "Resilient Microgrid Scheduling with Secure Frequency and Voltage Transient Response", IEEE Transactions on Power Systems, 2022.

Transient frequency and voltage security

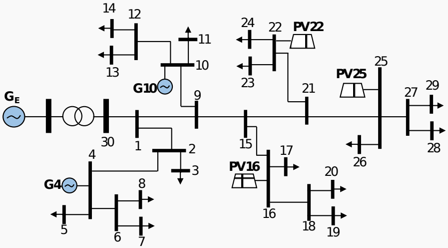

- Pyomo + Gurobi for the optimization
- PyRAMSES for the dynamic simulation
- Daily operation costs (24-hours):

No transient	Only frequency	Frequency and Voltage
€19203	€22070	€38000

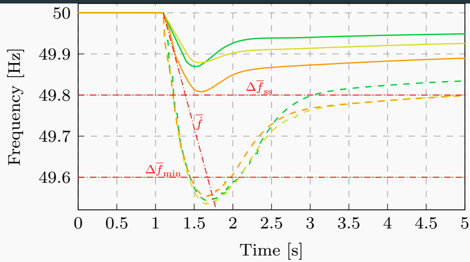

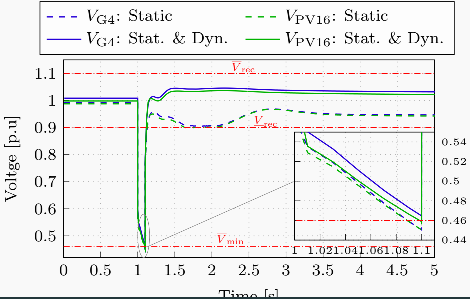

AC-OPF with dynamic security constraints through dynamic simulations

Benefits:

- Many free and commercial dynamic simulators available (PyRAMSES, Dome, DigSilent Powerfactory, PSS/e, etc.)
- Pre-existing models in most dynamic simulators $\rightarrow$ reduces the modelling effort
- Much better computational performance than the dynamic optimization solution $\rightarrow$ $\{$in parallel, very fast, specialized software$\}$.
- Able to incorporate protections, discrete events, wide-area controls, etc.

A. Nakiganda, P. Aristidou, "Resilient Microgrid Scheduling with Secure Frequency and Voltage Transient Response", IEEE Transactions on Power Systems, 2022.

AC-OPF with dynamic security constraints through dynamic simulations

Benefits:

- Many free and commercial dynamic simulators available (PyRAMSES, Dome, DigSilent Powerfactory, PSS/e, etc.)
- Pre-existing models in most dynamic simulators $\rightarrow$ reduces the modelling effort
- Much better computational performance than the dynamic optimization solution $\rightarrow$ {in parallel, very fast, specialized software}.
- Able to incorporate protections, discrete events, wide-area controls, etc.

Issues:

- Hard to provide proof for the convergence of the iterative algorithm (especially when discrete events/protections are considered)
- Hard to extract sensitivities for dispatch variables (z)
- Might have conflicting feasibility cuts for different dynamics (e.g., active power impacts both frequency and voltage)

A. Nakiganda, P. Aristidou, "Resilient Microgrid Scheduling with Secure Frequency and Voltage Transient Response", IEEE Transactions on Power Systems, 2022.

Using Simplified Models or Approximations

Expansion planning with dynamic constraints through simplified models

$$
\begin{aligned}
\min_{\chi^{\text{prf}} \in \Omega, z \in \{0,1\}} \quad & \Theta^{\text{prf}}(\chi^{\text{prf}}, z) \\
\text{s.t.} \quad & \Phi^{\text{prf}}(z, \chi^{\text{prf}}) = 0 \\
& \Lambda^{\text{prf}}(z, \chi^{\text{prf}}) \leq 0 \\
& F(\chi^{\text{prf}}, z', \boldsymbol{x}, \dot{\boldsymbol{x}}, \tau) = 0,\ \tau \in [0, T] \\
& \rho(\chi^{\text{prf}}, z', \boldsymbol{x}, \dot{\boldsymbol{x}}, \tau) \leq 0,\ \tau \in [0, T]
\end{aligned}
$$

A. Nakiganda, P. Aristidou, "Resilient Microgrid Scheduling with Secure Frequency and Voltage Transient Response", IEEE Transactions on Power Systems, 2022.

Expansion planning with dynamic constraints through simplified models

$$
\begin{aligned}
\min_{\chi^{\mathrm{prf}}\in\Omega, z\in\{0,1\}} \quad & \Theta^{\mathrm{prf}}(\chi^{\mathrm{prf}}, z) \\
\text{s.t.} \quad & \Phi^{\mathrm{prf}}(z, \chi^{\mathrm{prf}}) = 0 \\
& \Lambda^{\mathrm{prf}}(z, \chi^{\mathrm{prf}}) \leq 0 \\
& \boxed{\begin{aligned} & F(\chi^{\mathrm{prf}}, z', \boldsymbol{x}, \dot{\boldsymbol{x}}, \tau) = 0,\ \tau \in [0, T] \\ & \rho(\chi^{\mathrm{prf}}, z', \boldsymbol{x}, \dot{\boldsymbol{x}}, \tau) \leq 0,\ \tau \in [0, T] \end{aligned}}
\end{aligned}
$$

Replace with simplified model

Solve with decomposition-based algorithm

Methodology:

- We simplify the DAE IVP and replace it with a simplified or approximate model that can be handled in optimization problems
- We decompose the resulting optimization problem and use an iterative method to solve (e.g., Bender's decomposition)
- Iterate between the sub-problems until the solution is secure

A. Nakiganda, P. Aristidou, "Resilient Microgrid Scheduling with Secure Frequency and Voltage Transient Response", IEEE Transactions on Power Systems, 2022.

Expansion planning with frequency dynamic constraints

Frequency response aggregate model:

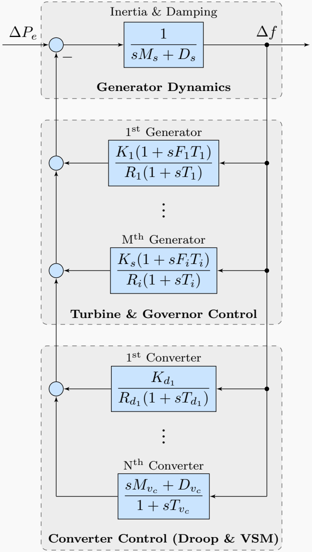

Expansion planning with frequency dynamic constraints

Frequency response aggregate model:

$$G(s) = \frac{\Delta f(s)}{\Delta P(s)}$$

$$= \Bigg(\underbrace{(sM_s + D_s)}_{\text{SGs swing dynamics}} + \underbrace{\sum_{i \in \mathscr{S}} \frac{K_i(1+sF_iT_i)}{R_i(1+sT_i)}}_{\text{SGs turbine \& governor response}}$$

$$+ \underbrace{\sum_{d \in \mathscr{C}^d} \frac{K_d}{R_d(1+sT_d)}}_{\text{droop-based CIGs}} + \underbrace{\sum_{v \in \mathscr{C}^v} \frac{sM_v + D_v}{1+sT_v}}_{\text{VSM-based CIGs}} \Bigg)^{-1}$$

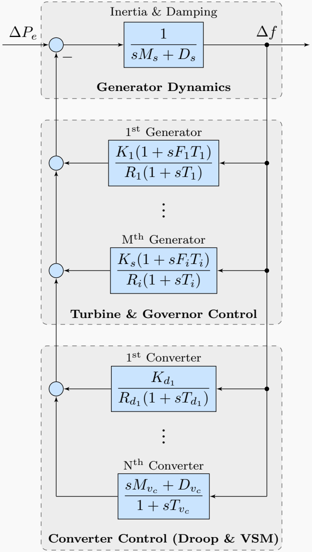

Critical parameters of frequency response aggregate model for a step-wise disturbance:

$$\dot{f}_{\max} = \dot{f}(t_0^+) = -\frac{\Delta P}{M}, \tag{5a}$$

$$\Delta f_{\mathrm{ss}} = -\frac{\Delta P}{D + R_s}, \tag{5b}$$

$$\Delta f_{\kappa}^{\max} = -\Delta P \cdot \underbrace{\frac{1}{D + R_s}\left(1 + \sqrt{\frac{T(R_s - F_s)}{M}}e^{-\zeta \omega_n t_m}\right)}_{h(D,R_s,F_s,M)} \tag{5c}$$

$$\approx -\Delta P \cdot \left(h_\kappa + \frac{\partial h_\kappa}{\partial D}\left(D - D_\kappa\right) + \frac{\partial h_\kappa}{\partial R_s}\left(R_s - R_{s,\kappa}\right) + \frac{\partial h_\kappa}{\partial F_s}\left(F_s - F_{s,\kappa}\right) + \frac{\partial h_\kappa}{\partial M}\left(M - M_\kappa\right)\right)$$

Expansion planning with frequency dynamic constraints

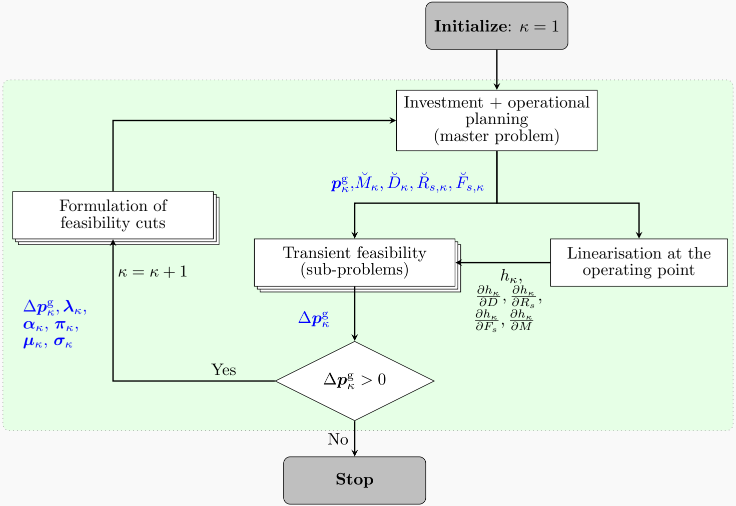

A. Nakiganda, S. Dehghan, U. Markovic, G. Hug, P. Aristidou, "A Stochastic-Robust Approach for Resilient Microgrid Investment Planning Under Static and Transient Islanding Security Constraints", IEEE Transactions on Smart Grid, 2022.

Expansion planning with frequency dynamic constraints

Sub-problem at iteration k:

$$\min_{\Delta \boldsymbol{p}_\kappa^{\mathrm{g}}} |\Delta \boldsymbol{p}_\kappa^{\mathrm{g}}| \tag{6a}$$

$$\text{s.t. } \underline{\dot{f}}^{\max} \le \frac{\left(\boldsymbol{p}_\kappa^{\mathrm{g}} + \Delta \boldsymbol{p}_\kappa^{\mathrm{g}}\right)}{\frac{\check{M}}{P_\kappa^{\mathrm{base}}}} \le \overline{\dot{f}}^{\max}, \tag{6b}$$

$$\underline{\Delta f}^{\mathrm{ss}} \le \frac{\left(\boldsymbol{p}_\kappa^{\mathrm{g}} + \Delta \boldsymbol{p}_\kappa^{\mathrm{g}}\right)}{\frac{\check{D}}{P_\kappa^{\mathrm{base}}} + \frac{\check{R}_s}{P_{\kappa,s}^{\mathrm{base}}}} \le \overline{\Delta f}^{\mathrm{ss}} \tag{6c}$$

$$\underline{\Delta f}^{\max} \le \left(\boldsymbol{p}_\kappa^{\mathrm{g}} + \Delta \boldsymbol{p}_\kappa^{\mathrm{g}}\right) \cdot \left(h_\kappa + \frac{\partial h_\kappa}{\partial D} \frac{\left(D - \check{D}_\kappa\right)}{P_\kappa^{\mathrm{base}}} + \frac{\partial h_\kappa}{\partial R_s} \frac{\left(R_s - \check{R}_{s,\kappa}\right)}{P_{\kappa,s}^{\mathrm{base}}} \right. \tag{6d}$$

$$\left. + \frac{\partial h^\kappa}{\partial F_s} \frac{\left(F_s - \check{F}_{s,\kappa}\right)}{P_{\kappa,s}^{\mathrm{base}}} + \frac{\partial h^\kappa}{\partial M} \frac{\left(M - \check{M}_\kappa\right)}{P_\kappa^{\mathrm{base}}} \right) \le \overline{\Delta f}^{\max} \tag{6e}$$

Expansion planning with frequency dynamic constraints

Feasibility cuts:

$$
\begin{aligned}
\Delta \boldsymbol{p}^{\mathrm{g}}_{\nu} + \boldsymbol{\lambda}_{\nu}(\boldsymbol{p}^{\mathrm{g}}_{\kappa+1} - \boldsymbol{p}^{\mathrm{g}}_{\nu}) + \boldsymbol{\alpha}_{\nu}(M_{\kappa+1} - M_{\nu}) + \boldsymbol{\pi}_{\nu}(D_{\kappa+1} - D_{\nu}) \\
+ \boldsymbol{\mu}_{\nu}(R_{s,\kappa+1} - R_{s,\nu}) + \boldsymbol{\sigma}^{\nu}(F_{s,\kappa+1} - F_{s,\nu}) \leq 0, \qquad \forall \nu = 1, \ldots, \kappa
\end{aligned}
\tag{7}
$$

where dual variables

- $\boldsymbol{\lambda}_{\kappa} \rightarrow$ generator power
- $\boldsymbol{\alpha}_{\kappa} \rightarrow$ aggregated inertia
- $\boldsymbol{\pi}_{\kappa} \rightarrow$ damping
- $\boldsymbol{\mu}_{\kappa} \rightarrow$ droop
- $\boldsymbol{\sigma}_{\kappa} \rightarrow$ turbine power fraction

Expansion planning with frequency dynamic constraints

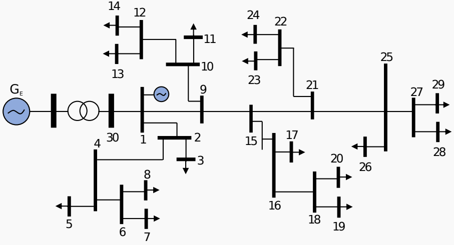

- Pyomo + Gurobi for the optimization
- Investment candidates:

	SG_1	SG_2	PV_1	PV_2	PV_3
Annualized investment cost ($)	-	40000	70000	65000	60000
Capacity (kW)	280	350	350	350	350
$M\,(s)$	14	14	14	-	-
D (p.u.)	0.9	0.9	0.9	-	-
K (p.u.)	1	1	1	1	-
R (p.u.)	0.03	0.03	-	0.05	-
F (p.u.)	0.35	0.35	-	-	-

	Only Static	**Static & Dynamic**
Costs and decisions		
Total cost ($)	223390	242740
Investment cost ($)	61000	131000
Investment decisions	PV_3	PV_1, PV_3
Operational cost ($)	162390	111740
Demand disconnection penalty	14536	5337
Computational performance		
Number of iterations	-	4
Computation time (s)	612	3386
Inertia support		
M (s)	7.84	17.64
D (p.u)	0.50	1.13

A. Nakiganda, S. Dehghan, P. Aristidou, "Inertia-Aware Microgrid Investment Planning Using Tractable Decomposition Algorithms", under review.

Expansion planning with dynamic constraints through simplified models

Benefits:

- Easier to provide proof for the convergence of the iterative algorithm (decomposition-based algorithms are well-studied)
- Able to handle discrete decision variables (z) through the dual variables of inertia, damping, etc.
- Faster convergence (compared to dynamic simulation-based).
- Better computational performance than the dynamic optimization solution.

Expansion planning with dynamic constraints through simplified models

Benefits:

- Easier to provide proof for the convergence of the iterative algorithm (decomposition-based algorithms are well-studied)
- Able to handle discrete decision variables (z) through the dual variables of inertia, damping, etc.
- Faster convergence (compared to dynamic simulation-based).
- Better computational performance than the dynamic optimization solution.

Issues:

- Only focuses on one type of dynamics (unlike the dynamic simulation-based). Difficult to build simplified models focusing on multiple dynamics.
- Not able to incorporate protections, discrete events, wide-area controls, etc.
- Still complicated to implement and computationally intensive.

UC-ACOPF with dynamic constraints through piece-wise linear constraints

$$
\begin{aligned}
\min_{\chi^{\mathrm{prf}} \in \Omega, z \in \{0,1\}} \quad & \Theta^{\mathrm{prf}}(\chi^{\mathrm{prf}}, z) \\
\text{s.t.} \quad & \Phi^{\mathrm{prf}}(z, \chi^{\mathrm{prf}}) = 0 \\
& \Lambda^{\mathrm{prf}}(z, \chi^{\mathrm{prf}}) \leq 0 \\
& F(\chi^{\mathrm{prf}}, z', \boldsymbol{x}, \dot{\boldsymbol{x}}, \tau) = 0, \, \tau \in [0, T] \\
& \rho(\chi^{\mathrm{prf}}, z', \boldsymbol{x}, \dot{\boldsymbol{x}}, \tau) \leq 0, \, \tau \in [0, T]
\end{aligned}
$$

UC-ACOPF with dynamic constraints through piece-wise linear constraints

$$
\begin{aligned}
\min_{\chi^{\text{prf}} \in \Omega, z \in \{0,1\}} \quad & \Theta^{\text{prf}}(\chi^{\text{prf}}, z) \\
\text{s.t.} \quad & \Phi^{\text{prf}}(z, \chi^{\text{prf}}) = 0 \\
& \Lambda^{\text{prf}}(z, \chi^{\text{prf}}) \leq 0 \\
& \boxed{\begin{aligned} & F(\chi^{\text{prf}}, z', \boldsymbol{x}, \dot{\boldsymbol{x}}, \tau) = 0, \; \tau \in [0, T] \\ & \rho(\chi^{\text{prf}}, z', \boldsymbol{x}, \dot{\boldsymbol{x}}, \tau) \leq 0, \; \tau \in [0, T] \end{aligned}}
\end{aligned}
$$

Replace with piece-wise linear constraints computed offline

Methodology:

- We use the full or simplified model to extract piece-wise linear constraints to be embedded in the optimization problem
- Incorporate in the optimization problem
- Solve once the optimization problem

M. Paturet, U. Markovic, S. Delikaraoglou, E. Vrettos, Petros Aristidou, G. Hug, "Stochastic Unit Commitment in Low-Inertia Grids", IEEE Transactions on Power Systems, 2020.

UC-ACOPF with dynamic constraints through piece-wise linear constraints

Compute PWL constraints for Nadir:

$$\min_{\Psi} \sum_{\eta} \left(\max_{1\le\nu\le\overline{\nu}} \left\{ a_\nu R_g^{(\eta)} + b_\nu F_g^{(\eta)} + c_\nu M^{(\eta)} + d_\nu \right\} - \Delta f_{\max}\left(R_g^{(\eta)}, F_g^{(\eta)}, M^{(\eta)}\right) \right)^2,$$

- $\Psi = \{a_\nu, b_\nu, c_\nu, d_\nu, \forall \nu\}$
- η denoting the evaluation point
- ν referring to the number of PWL segments

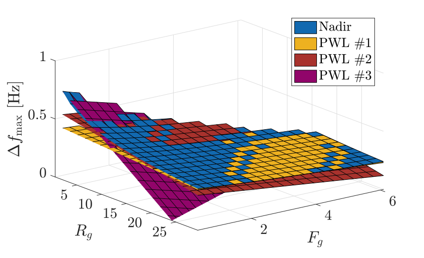

PWL of the nadir constraint for $M = 9$.

Linearization	Computational time [s]
PWL ($\eta = 3, \nu = 4$)	70
PWL ($\eta = 4, \nu = 4$)	7200

UC-ACOPF with dynamic constraints through piece-wise linear constraints

- IEEE RTS-96 power system consisting of areas 1+2
- 20 generators and 16 wind farms

Type	H_i [s]	K_i [p.u.]	F_i [p.u.]	R_i [p.u.]	D_i [p.u.]
Nuclear	4.5	0.98	0.25	0.04	0.6
CCGT	7.0	1.1	0.15	0.01	0.6
OCGT	5.5	0.95	0.35	0.03	0.6
VSM	6.0	1.0	-	-	0.6
Droop	-	1.0	-	0.05	-

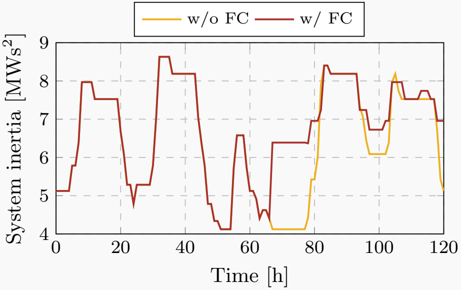

Hour	**65**	**66**	**67**	**68**	**69**	**70**	**71**	**72**	**73**
w/o FC	6	5	4	4	4	4	4	4	4
w/ FC	6	5	10	10	10	10	10	10	10

Concluding Remarks and Open Work

Concluding remarks

- The transition towards low-inertia grids pushes grids to operate closer to their dynamic stability boundaries – with more erratic, faster, and uncertain dynamic performance.
- Optimizing their operation **without** considering the dynamic stability will inadvertently lead to unstable and dangerous situations

- Some first steps have been made, but many issues need to be addressed:
  - Incorporating multiple stability and protection constraints in the same optimization problem (frequency, voltage, oscillations, fault levels, SCR, etc.)
  - Bringing the solution algorithms and implementations closer to industrial grade
  - Convergence and optimality proofs for solutions (improve the maths behind the techniques)
  - Bring ML methods in the picture?

Presentation based on...

- A. M. Nakiganda, S. Dehghan, P. Aristidou, "Inertia-Aware Microgrid Investment Planning Using Tractable Decomposition Algorithms", under review.
- A. M. Nakiganda, P. Aristidou, "Resilient Microgrid Scheduling with Secure Frequency and Voltage Transient Response", IEEE Transactions on Power Systems, 2022.
- A. Venkatraman, U. Markovic, D. Shchetinin, E. Vrettos, P. Aristidou, G. Hug, "Improving Dynamic Performance of Low-Inertia Systems through Eigensensitivity Optimization", IEEE Transactions on Power Systems, 2021.
- M. Paturet, U. Markovic, S. Delikaraoglou, E. Vrettos, P. Aristidou, G. Hug, "Stochastic Unit Commitment in Low-Inertia Grids", IEEE Transactions on Power Systems, 2020.

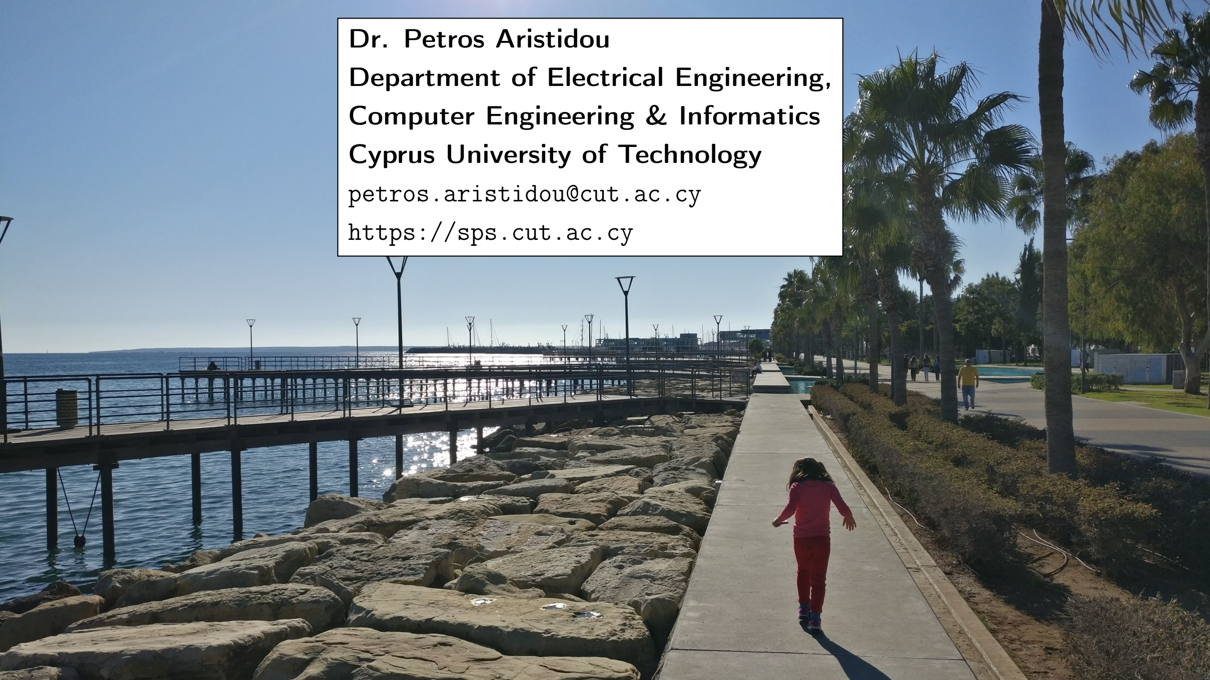

Dr. Petros Aristidou

Department of Electrical Engineering,

Computer Engineering & Informatics

Cyprus University of Technology

petros.aristidou@cut.ac.cy

https://sps.cut.ac.cy

Example: DAE models and controls

Inverter-based generator

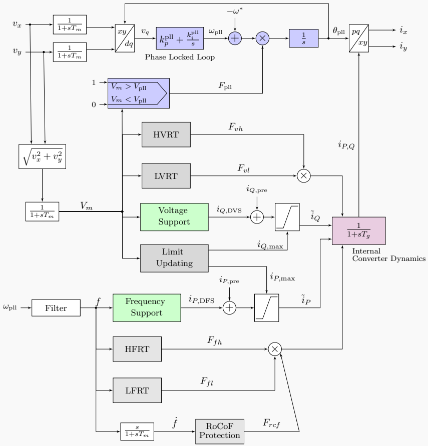

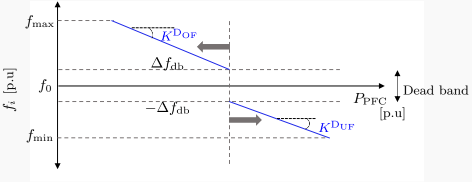

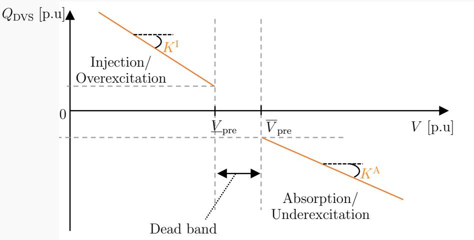

Example: DAE models and controls

Synchronous generator

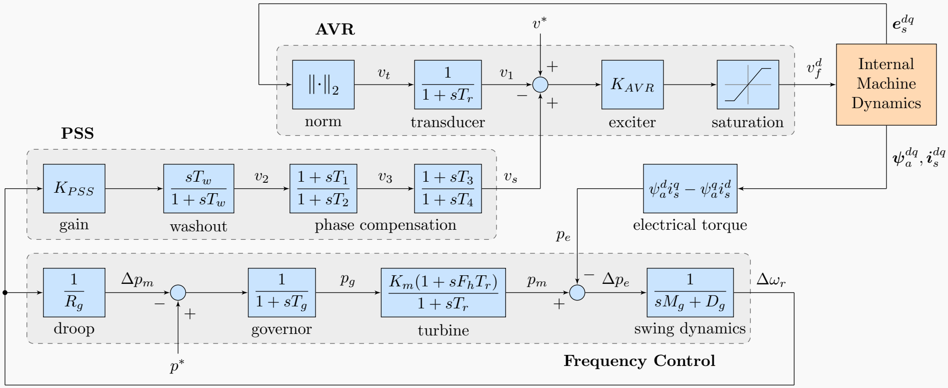

Frequency aggregate model parameters

$$M_s = \sum_{i \in \Omega^{\mathrm{S}}} M_i \frac{P_i}{P_{b_s}}, \qquad D_s = \sum_{i \in \Omega^{\mathrm{S}}} D_i \frac{P_i}{P_{b_s}}, \quad R_s = \sum_{i \in \Omega^{\mathrm{S}}} \frac{K_i}{R_i} \frac{P_i}{P_{b_s}}, \tag{8a}$$

$$F_s = \sum_{i \in \Omega^{\mathrm{S}}} \frac{K_i F_i}{R_i} \frac{P_i}{P_{b_s}}, \qquad M_c = \sum_{v \in \Omega_v^{\mathrm{C}}} M_v \frac{P_{c_v}}{P_{b_c}}, \quad D_c = \sum_{v \in \Omega_v^{\mathrm{C}}} D_v \frac{P_{c_v}}{P_{b_c}}, \tag{8b}$$

$$R_c = \sum_{d \in \Omega_d^{\mathrm{C}}} R_d \frac{P_{c_d}}{P_{b_c}}, \qquad M = \frac{M_s P_{b_s} + M_c P_{b_c}}{P_{b_g} + P_{b_c}}, \quad D = \frac{D_s P_{b_s} + D_c P_{b_c} + R_c P_{b_c}}{P_{b_s} + P_{b_c}}. \tag{8c}$$

P_i and P_c denote the active power capacity of the SG and CIG, respectively, scaled over their respective sums of active power capacity of all connected SGs and CIGs, P_{b_s} and P_{b_c}. The energy reserve capability for inertia and primary frequency response of CIG units is defined as a function of the DC-side capacitor storage unit connected to the generator. The contribution of each CIG to the M and D for frequency control was based on the capacity of the DC-side capacitor of the associated unit.

Frequency aggregate model analysis

By assuming a stepwise disturbance in the active power $\Delta P_e(s) = -\Delta P/s$, where ΔP is the net power change, the time-domain expression for frequency deviation ($\omega(t) \equiv \Delta f(t)$) can be derived as follows:

$$\omega(t) = -\frac{\Delta P}{M}\left(\frac{1}{T\omega_n^2} + \frac{1}{\omega_d}e^{-\zeta\omega_n t}\left(\sin\omega_d t - \frac{1}{\omega_n t}\sin\omega_d t + \phi\right)\right) \tag{9}$$

where $\omega_d = \omega_n\sqrt{1-\zeta^2}$ and $\phi = \sin^{-1}\left(\sqrt{1-\zeta^2}\right)$.

The RoCoF can be obtained by solving $\dot{\omega}(t)$, where the maximum RoCoF occurs at $t_r = 0^+$, i.e., $\dot{\omega}_{max} = \dot{\omega}(t_r)$, derived as indicated in (5a). The frequency nadir described in (5c) occurs at the time instance t_m when $\dot{\omega}(t_m) = 0$, whereas the quasi-steady-state frequency given in (5b) is derived from (9) for $t \to \infty$.

Taulant Kërçi

Taulant Kërçi received the B.Sc. and M.Sc. degrees in electrical engineering from the Polytechnic University of Tirana, Albania, in 2011 and 2013, respectively, and the Ph.D. degree in electrical engineering from University College Dublin, Ireland, in November 2021. From June 2013 to October 2013, he was with the Albanian DSO with the metering and new connection department. From November 2013 to January 2018, he was with the Albanian TSO at the SCADA/EMS office. In September 2021, he joined the Irish TSO, EirGrid plc, where he is currently a senior lead engineer. He is (co-)author of 1 book chapter and more than 20 journals/conferences papers. His research interests include power system operations and dynamics, as well as co-simulation of power systems and electricity markets.

25/06/2023

Dynamic Response of Inverter-based Resources in the Ireland and Northern Ireland Power Systems

Taulant Kërçi
Senior Lead Engineer
Future Operations

EirGrid SONI

Contents

- Background
- Dynamic Model Validation
  - Overview
  - Examples of System Wide Model Validation
- Dynamic Response of Large Energy Users (LEUs)
- Q & A

EirGrid SONI

Background

Background: All-Island Power System Overview

Peak Demand: 7.0 GW
Installed Wind: 5.88 GW
Peak Wind: 4.58 GW

Wind/Solar Connections

■ Transmission ■ Distribution

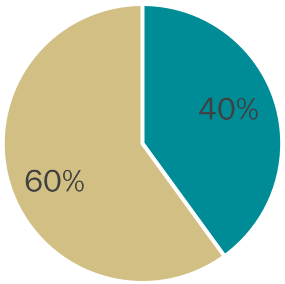

Two Control Centres

- Jurisdictional Transmission Control
- All-Island Scheduling and Dispatch

Source: *https://www.eirgridgroup.com/how-the-grid-works/renewables/*

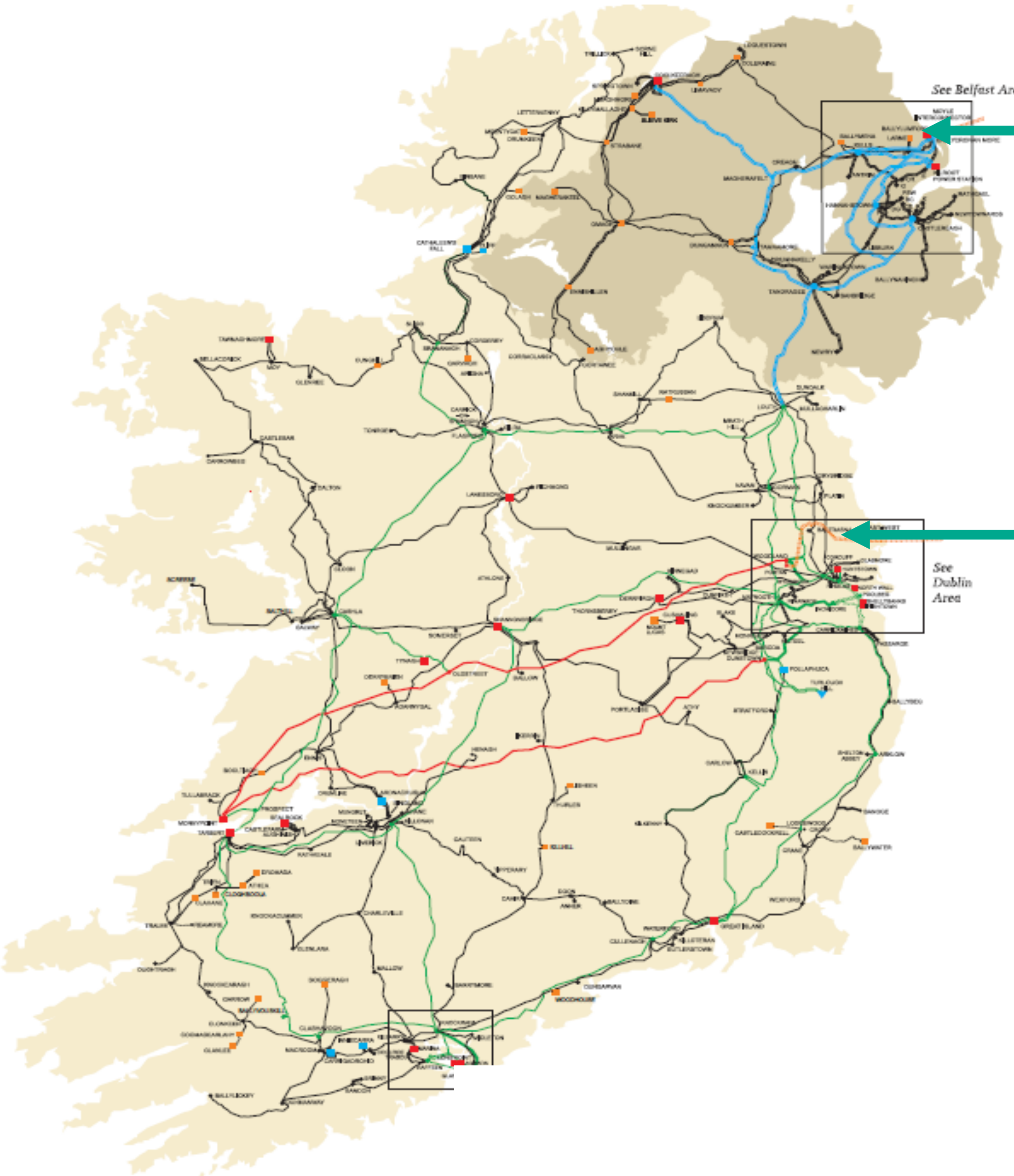

Moyle
+/- 500 MW
HVDC (LCC)
to Great Brittan

EWIC
+/- 500 MW
HVDC (VSC)
to Great Brittan

EirGrid SONI

Background: Installed Wind Capacity and Renewable Electricity as % of Demand

Evolution of Wind Capacity in the All-Island Power System

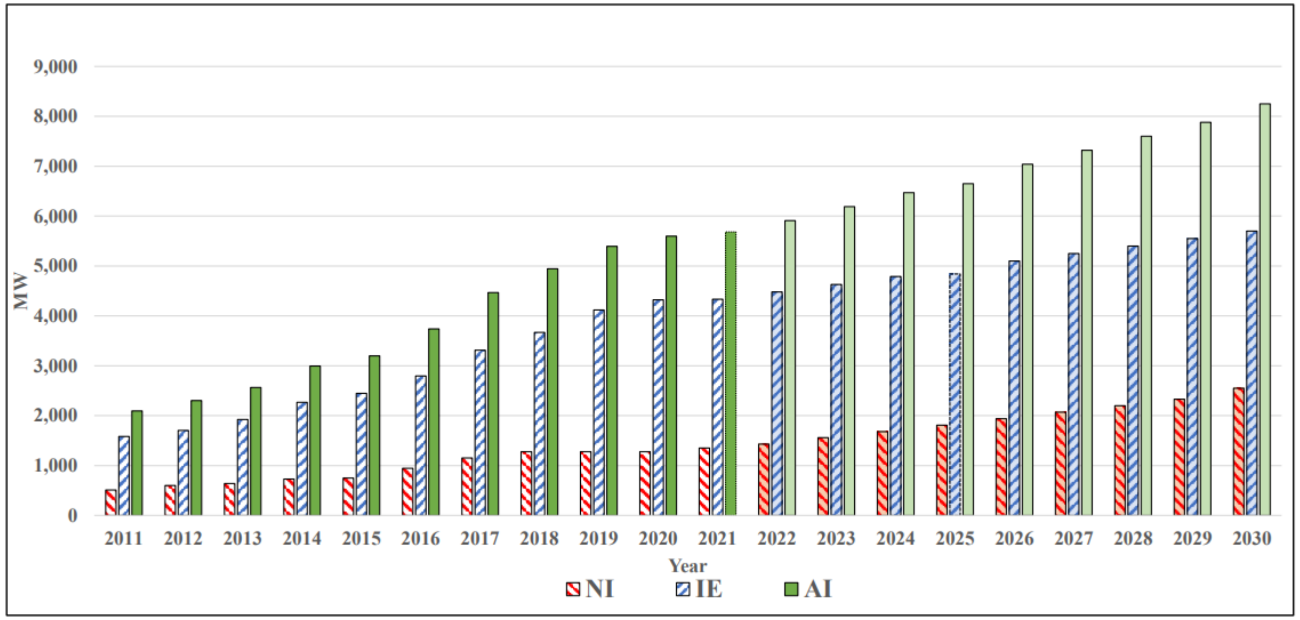

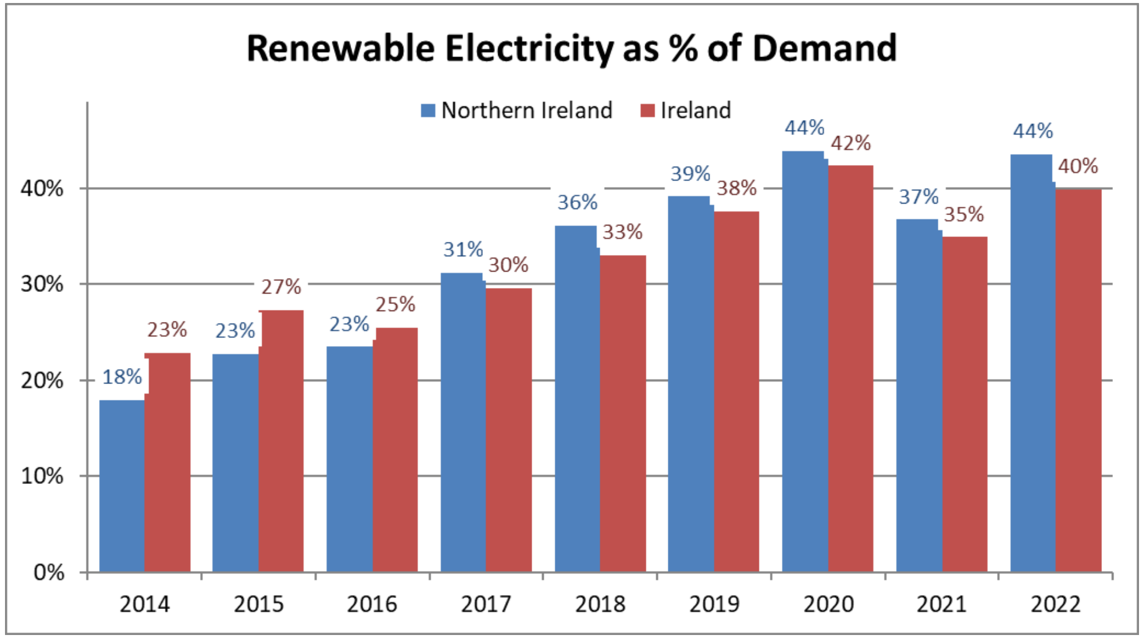

Source: *Hurtado, M., Kërçi, T., Tweed, S., Kennedy, E., Kamaluddin, N., & Milano, F. (2023).* *[Analysis of Wind Energy Curtailment in the Ireland and Northern Ireland Power Systems](). arXiv preprint arXiv:2302.07143.*

Source: *[https://www.eirgridgroup.com/how-the-grid-works/renewables/]()*

EirGrid SONI

Background: Maintaining Dynamic Stability in the All-Island Power System

Milestones to 2030 – Dynamic Stability

Key Changes: Greenlink HVDC · LCIS · North South Interconnector, Celtic HVDC · Offshore Wind · Potential Further Interconnection

Policy	22H2	23H1	23H2	24H1	24H2	25H1	25H2	26H1	26H2	27H1	27H2	28H1	28H2	29H1	29H2	2030
Inertia	23 GWs	20 GWs (All Island)		20 GWs (All Island)			Regional Inertia		~ 20 GWs (Regional or All Island)	~ 20 GWs (Regional or All Island)						~ 20 GWs (Regional or All Island)
RoCoF	1 Hz/s	1 Hz/s														1 Hz/s
System Strength						New EirGrid & SONI Policy									Updated EirGrid & SONI Policy	Enduring System Strength Policy
SNSP	75%			~ 80%	~ 80 %			Constraint Relaxed ~ 85%	Constraint Removed			~ 90%				~ 95%
MUON	8 (5 in IE, 3 in NI)	7 (All Island)		7 (All Island)					Constraint Relaxed ~ 6	Constraint Removed ~6	~ 5 (All Island)		~ 4 (All Island)			~ 3 (All Island)

Key: Information gathering · Analysis System Studies · Operational trial · Trial Review Policy Update · Ongoing monitoring

Source: [EirGrid & SONI Operational Policy Roadmap 2023-2030]

Dynamic Model Validation: Overview

- 24/7 Online analysis in Belfast and Dublin Control Rooms:
  - Real-Time cases every **5 minutes.**
  - Look-ahead cases run every hour for 8 future timepoints
- Fully integrated in EMS
- Online VSAT & TSAT
- Real-Time and Look-Ahead system security assessments:
  - Steady state voltage security
  - Steady state transfer limits
  - Dynamic stability
- Offline study mode functionality

Look-ahead Security Assessment Tool (LSAT)

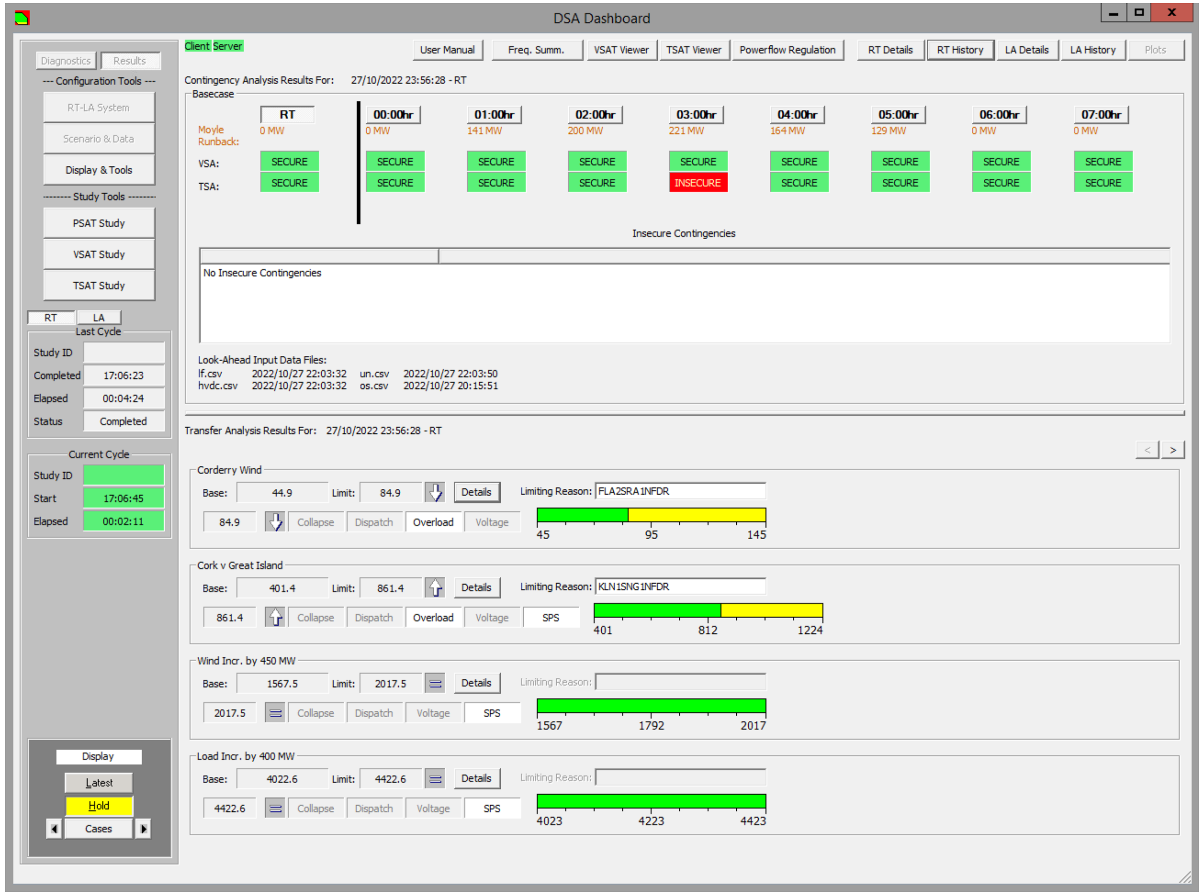

EirGrid SONI

Dynamic Model Validation: Overview

- **Why?**
  - Dynamic models used in critical decision support tools such as Look-ahead Security Assessment Tool (LSAT)
  - Regular validation need to be performed to assess the “health” of the models and the adequacy of tool outcomes
  - EirGrid & SONI perform regular dynamic model validation to identify and track model behavior

Offline testing → Pre-production (test) server → Production (live) server → Model Validation

Dynamic Model Validation: Overview

Data Gathering
- Event selection: Generator trips and system fault
- PMU data gathering and screening
- LSAT cases gathering

Case Set-up
- Data preparation scripts + manual adjustments
- Matching Power Flow data, Monitor and contingency data
- Dynamic models

Simulation
- Dynamic Simulation
- Playback Simulation

Analysis
- Quantitative
- Qualitative

Dynamic Model Validation: Overview

Customer requirements to submit WECC models:

- Submission of WECC model with <u>site specific parameters</u> at least 3 months before energisation
- Grid Code compliance tests
- Submission of validation report for WECC model parameters no later than 6 weeks after grid code testing

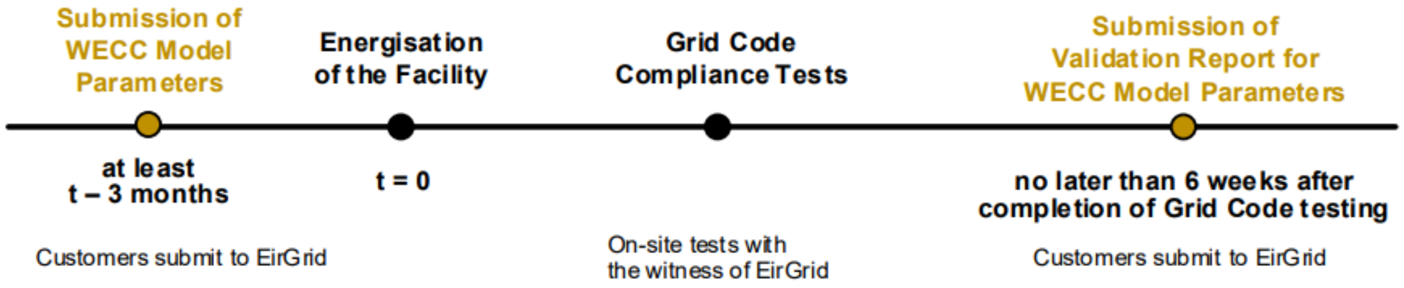

Source: https://www.eirgridgroup.com/site-files/library/EirGrid/Requirements-for-WECC-Model-Submission-v1.0.pdf

Dynamic Model Validation: Timescales of Interest

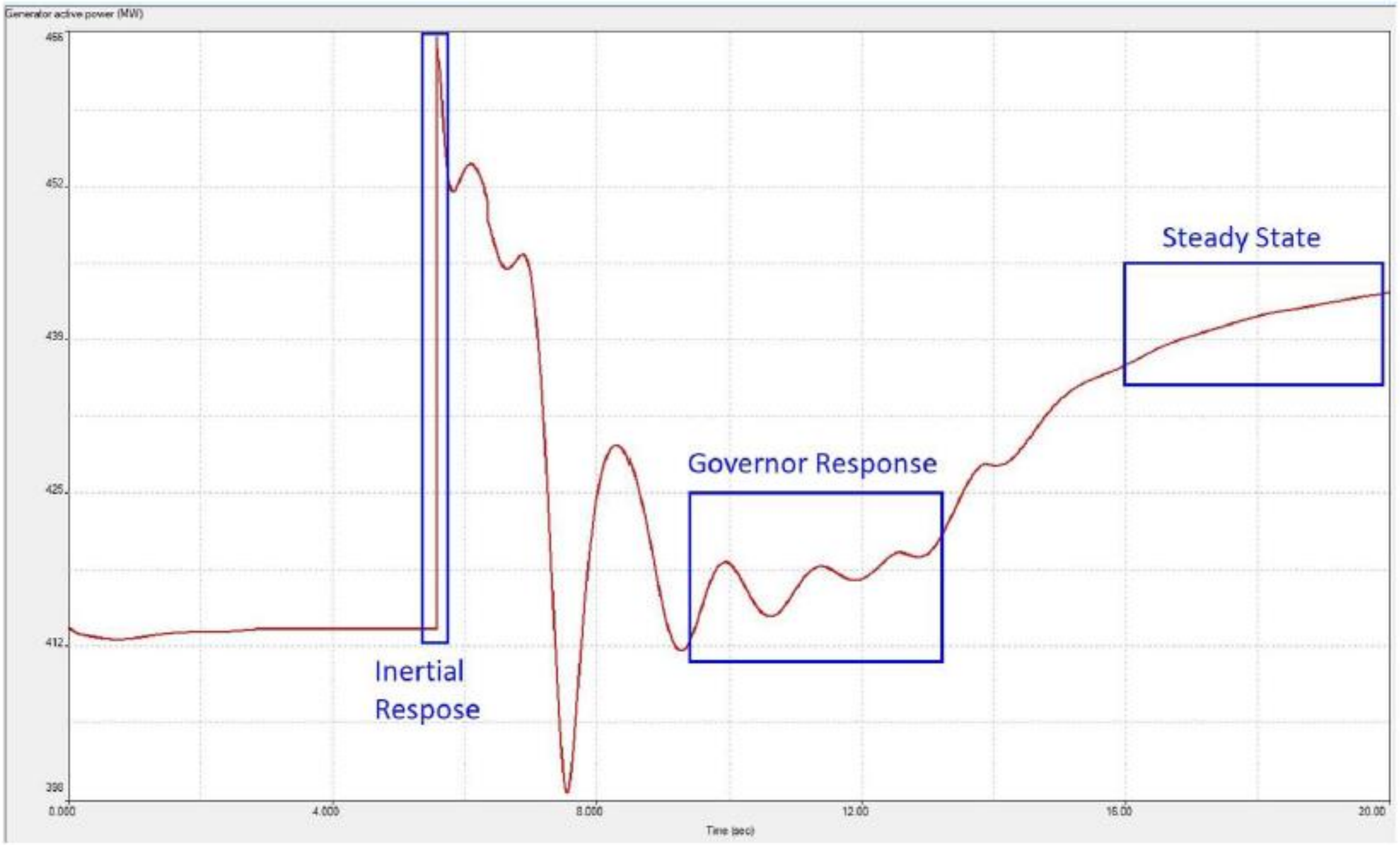

Dynamic Model Validation: Importance of Accurate Models

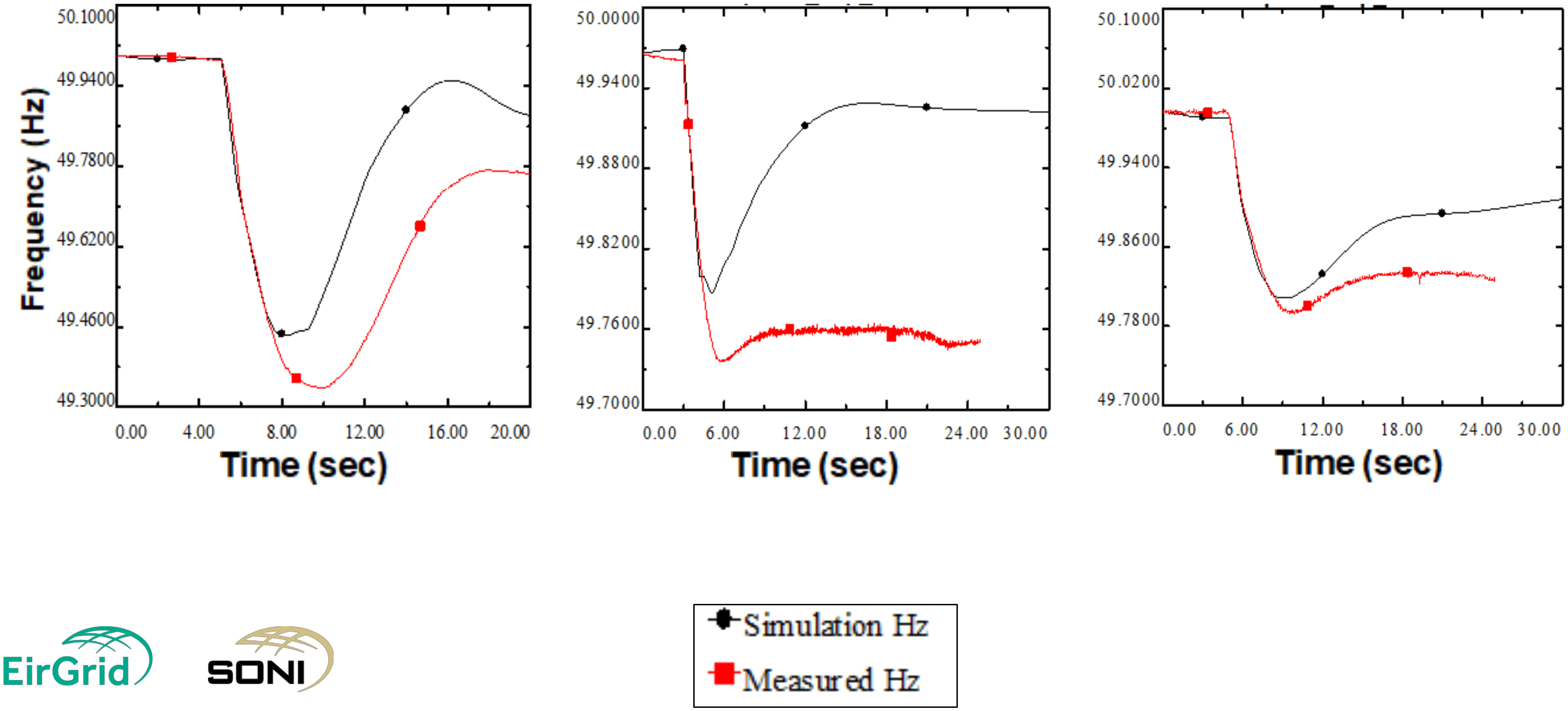

Dynamic Model Validation: Examples of System Wide Model Validation

Wind Farms

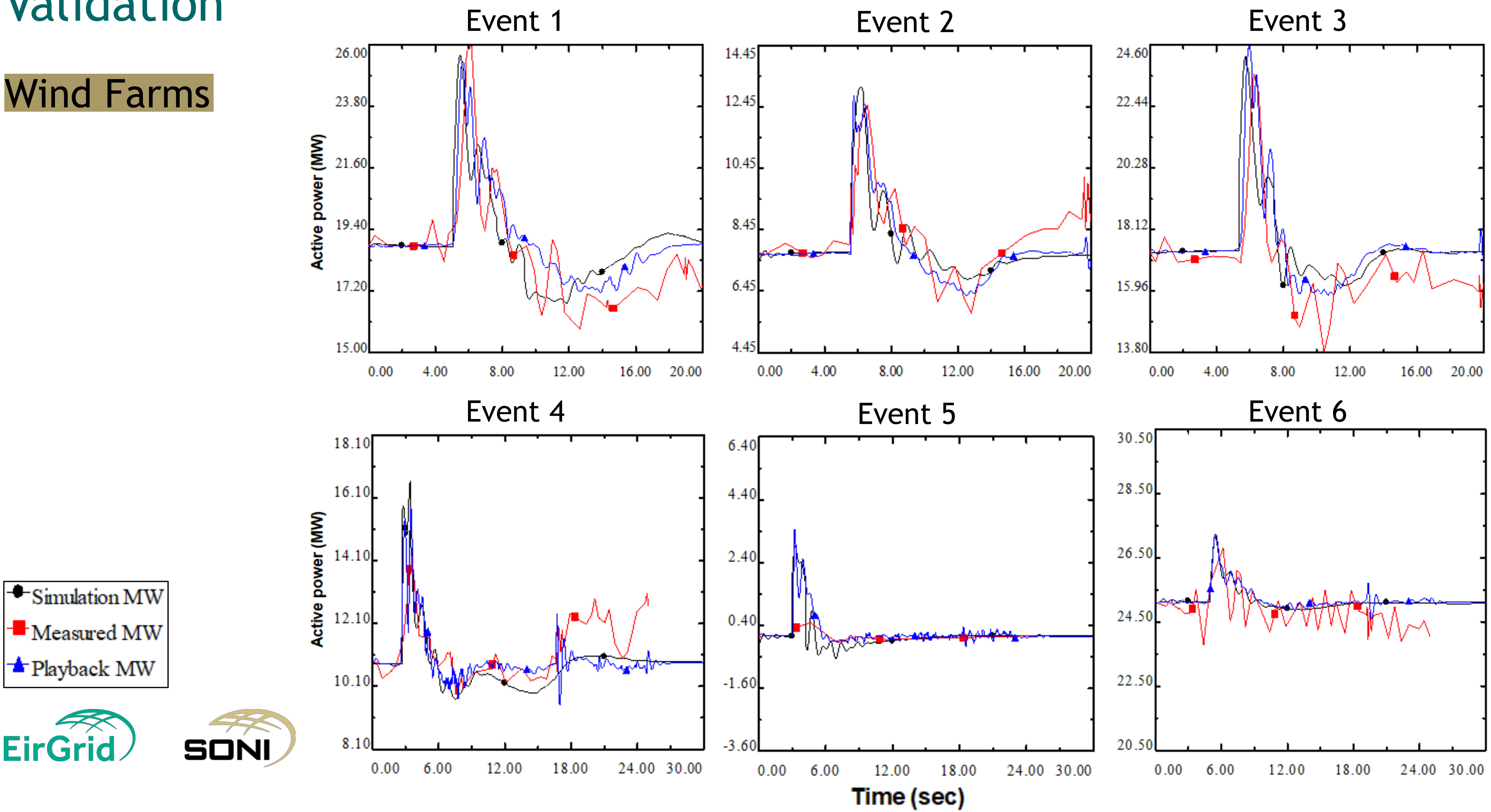

Dynamic Model Validation: Examples of System Wide Model Validation

HVDC Interconnector

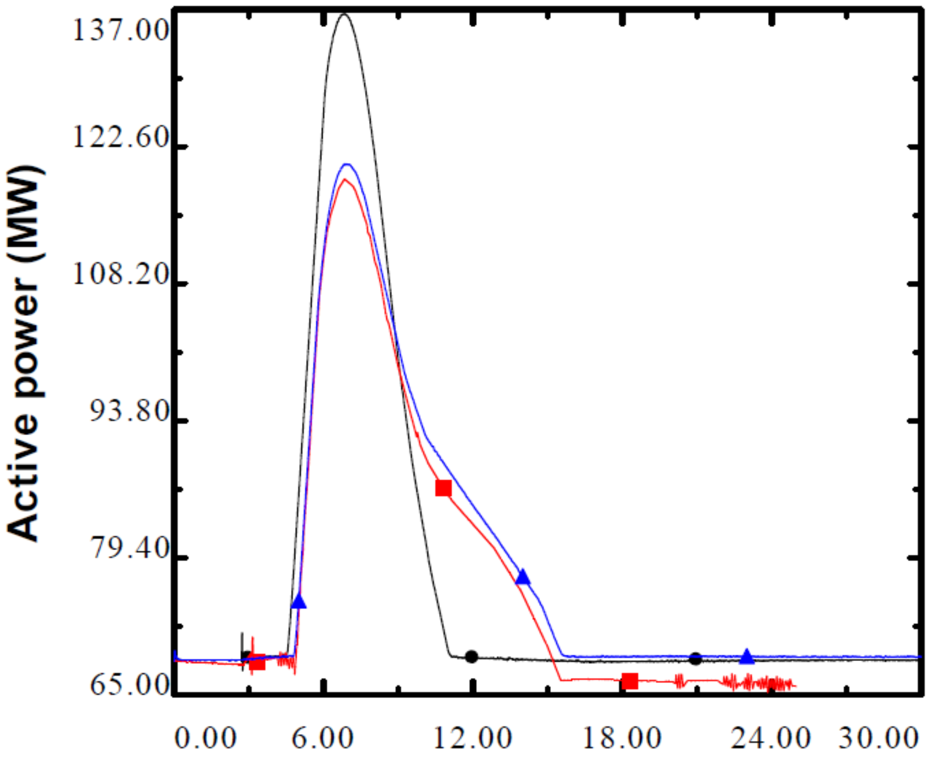

BESS

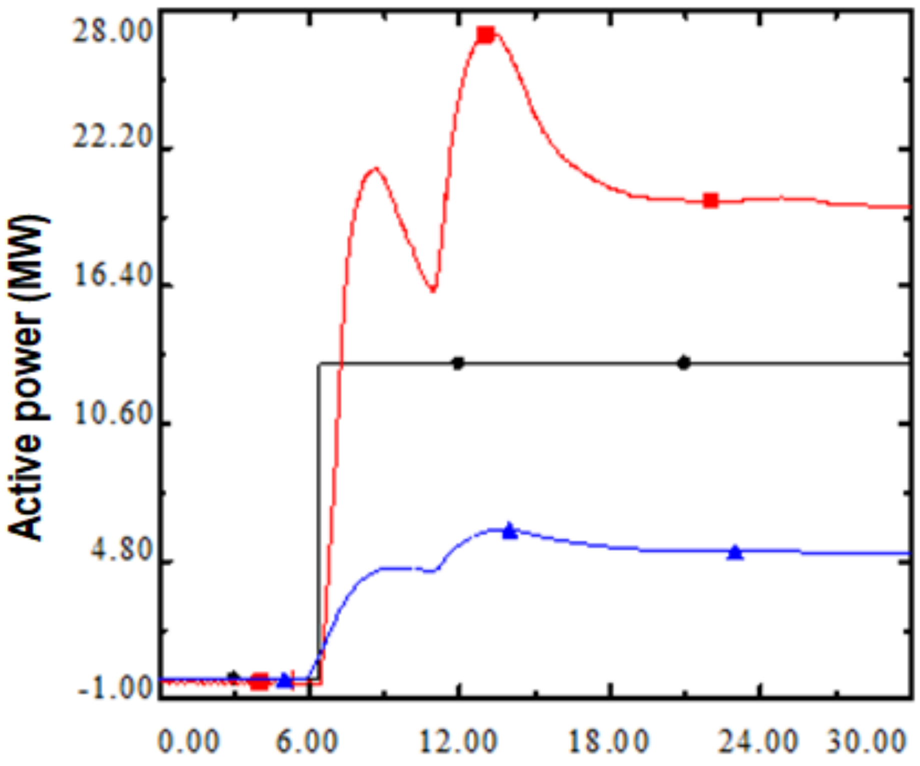

Simulation MW
Measured MW
Playback MW

Dynamic Model Validation: Examples of System Wide Model Validation

Example of impact of tuning (frequency droop) on BESS unit response

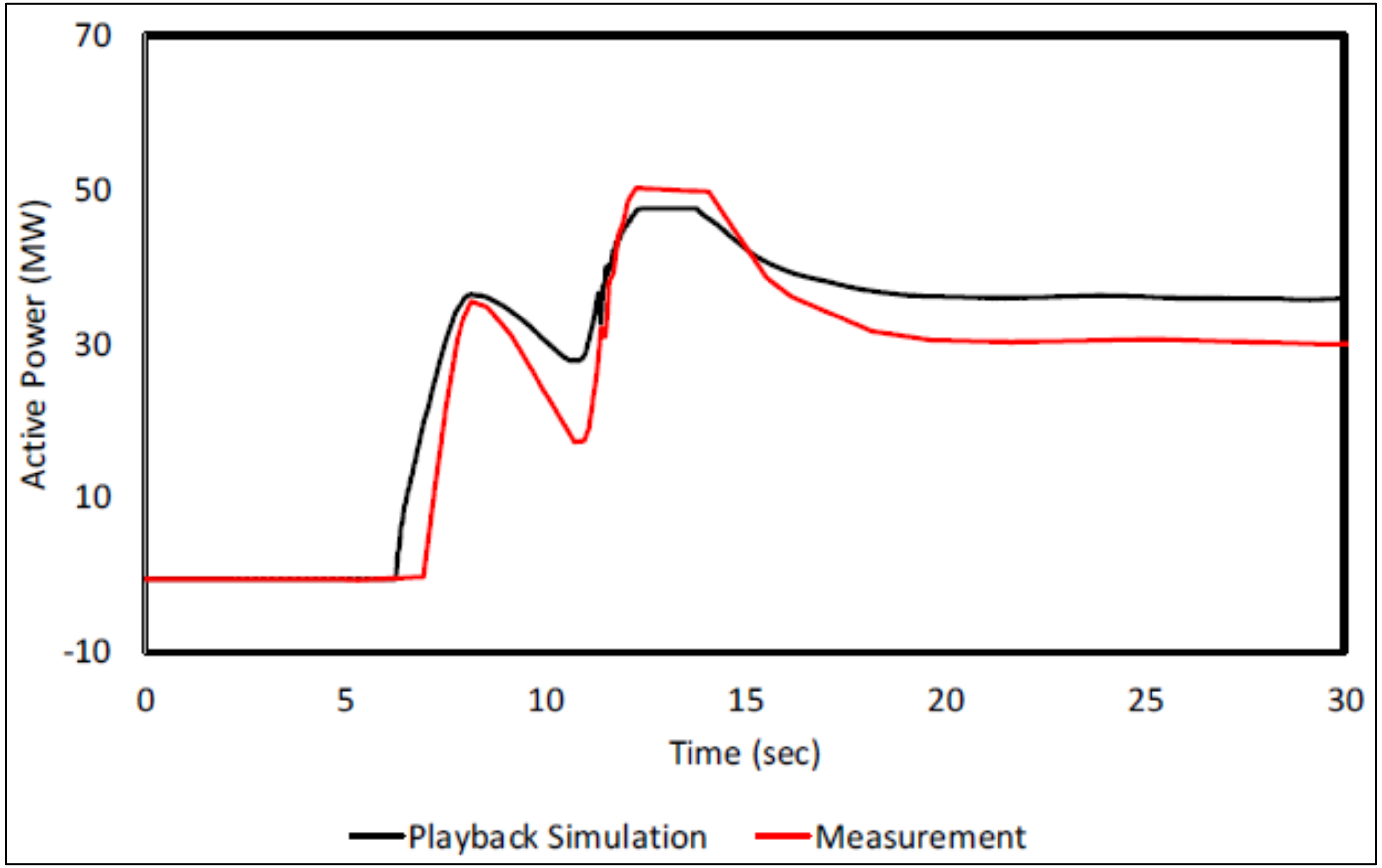

Dynamic Model Validation: Examples of System Wide Model Validation

Example of impact of tuning on BESS unit response

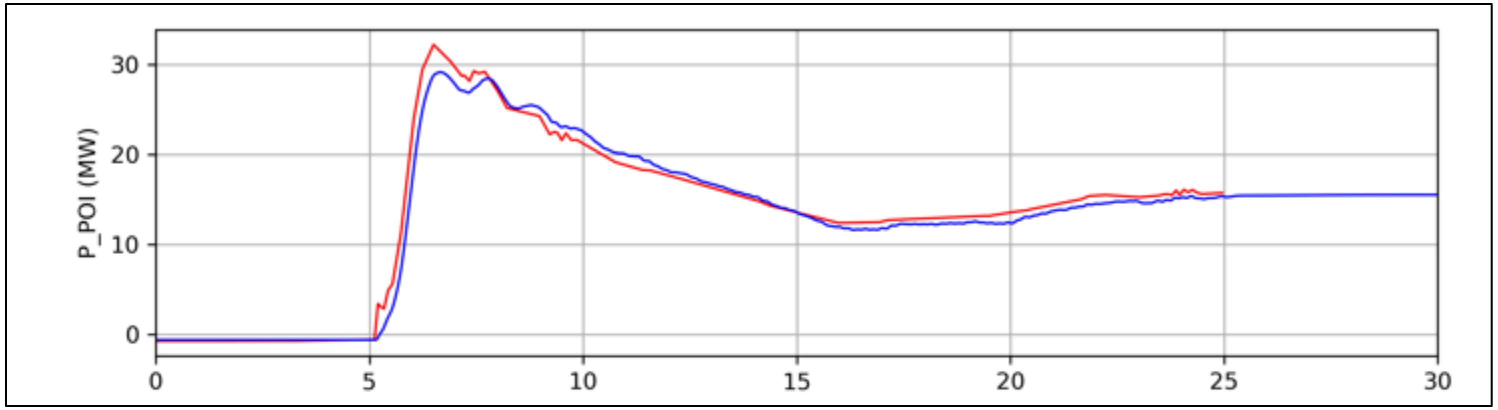

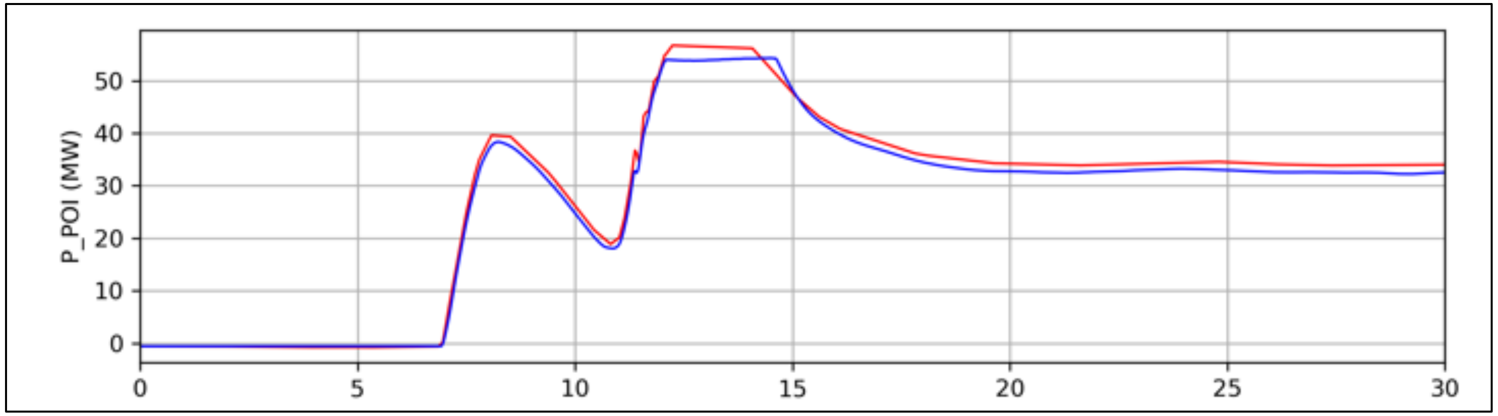

Dynamic Response of Large Energy Users (Data Centres)

EirGrid SONI

Dynamic Response of Large Energy Users (LEUs)

- Large Energy Users (LEU):
  - 1.6 GW connected or contracted Data Centres (DC) (currently 520 MW connected)
  - A significant proportion of this extra load is contracted to materialize in the Dublin region
  - Favorable climate and renewable electricity in Ireland
  - Can account for 30% of peak demand by 2030
- DC Load Characteristics:
  - Critical IT load
  - Electrical design based on redundancy, including UPS and on-site generation
  - Protection schemes can switch the source of power from the electricity grid to the backup generators without interruption
  - Sensitive protection settings: Under/Over Voltage, Under/Over Frequency, RoCoF

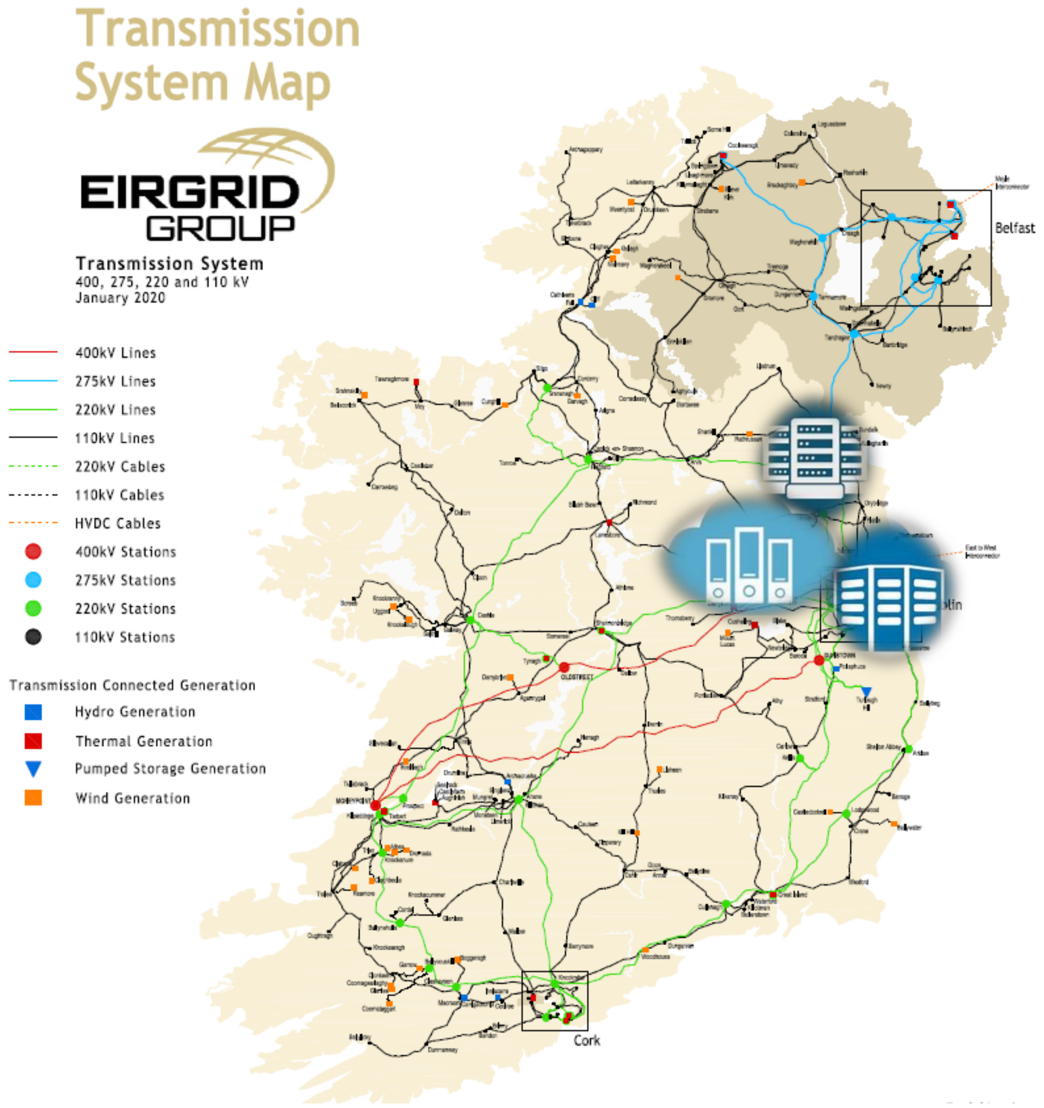

Dynamic Response of Large Energy Users (LEUs)

How to explore the potential of converter based demand?

Demand Unit Case: Data Centers

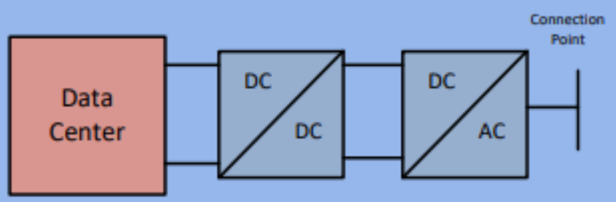

- Large increase in demand capacity is expected in the next years
- Voltage Source Converter interfaced to the grid
- Big potential to provide LFSM, FSM, reactive power capability and voltage control

Future research topic:

- Demonstrate highest TRL level of Data Center Demand Facility that comply with CNC requirements (Q and U control, FSM, LFSM-U/O, FRT and grid forming)
- Develop effective simulation models for Transmission connected Data center facilities (RMT, EMT and frequency domain)

entsoe

EirGrid SONI

Source: ENTSO-E, Stability Management in Power Electronics Dominated Systems

Dynamic Response of Large Energy Users (LEUs)

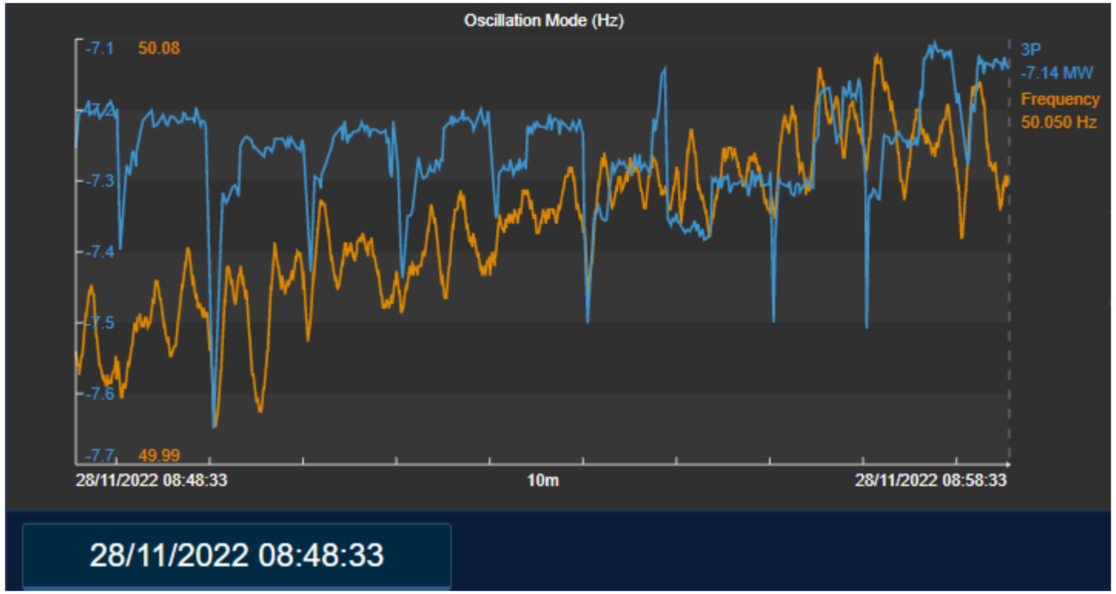

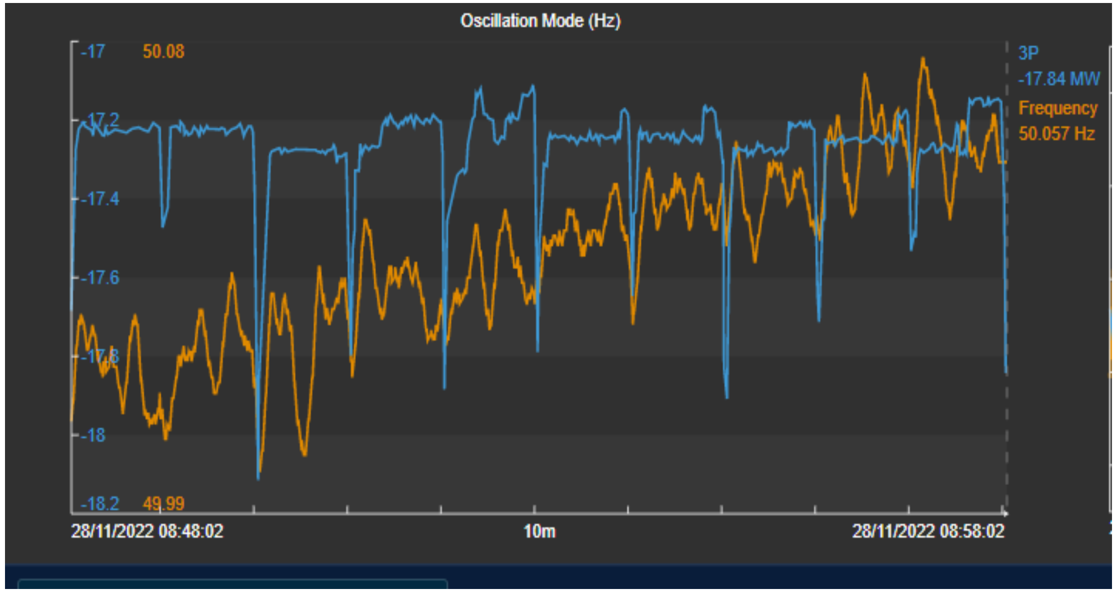

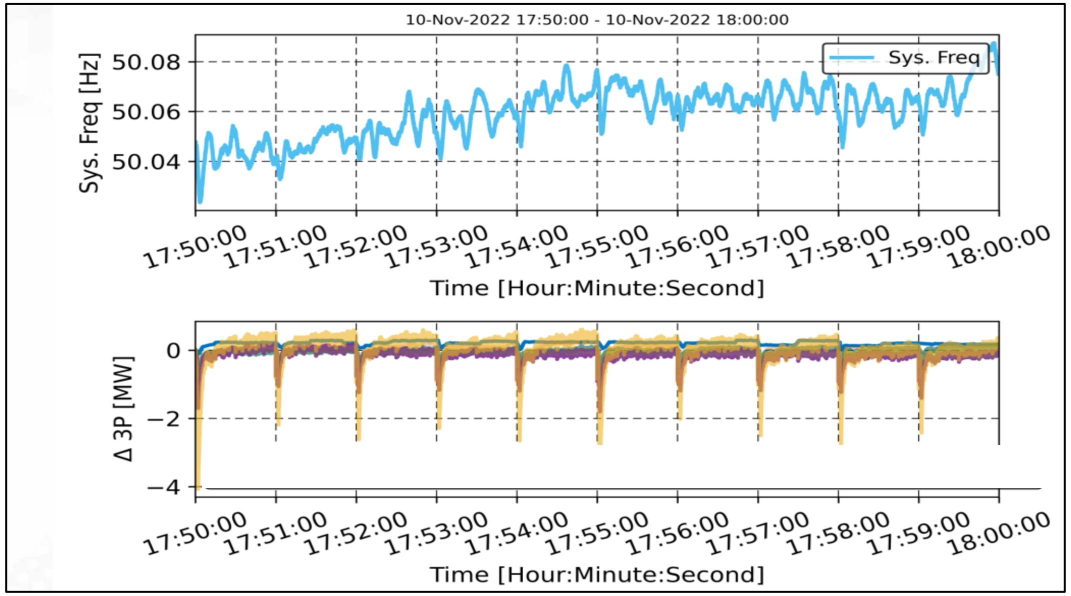

Dynamic Response of Large Energy Users (LEUs): Case Studies on Behaviour

1. 07/01/2022 System Fault

- Lightening strike on a 220kV Circuit Killonan - Kilpaddoge in Co. Limerick
- Phase-Phase (ST) fault caused the voltage drop to 0.41 p.u. at Kilpaddodge 110kV in North Kerry

2. 13/12/2022 System Fault

- At 16:57 hours on Tuesday 13 December 2022, the Kellystown - Woodland 220 kV line tripped, reclosed and tripped for a single phase to ground fault (RE)
- The fault clearance times were approximately 80 ms and 98 ms
- Failure of polymeric insulator was the cause

Voltage Induced Frequency Rise - Step Through

Severe System Fault

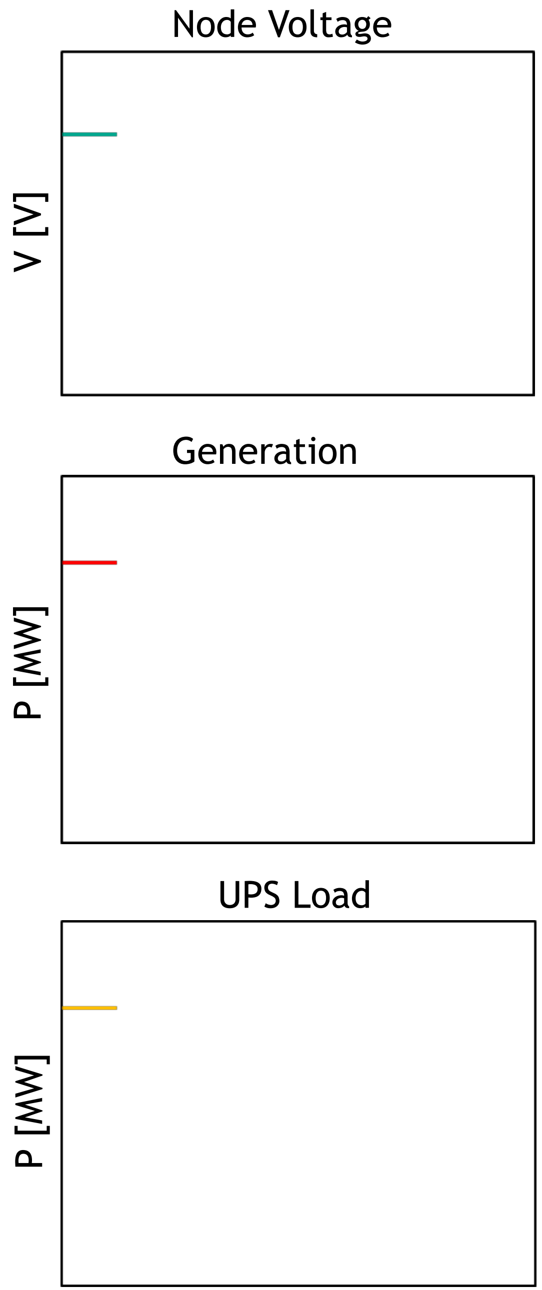

Voltage Induced Frequency Rise - Step Through

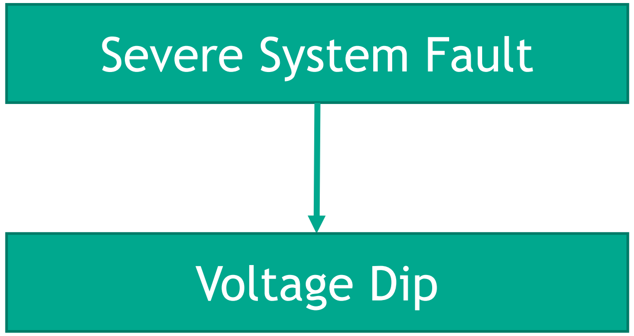

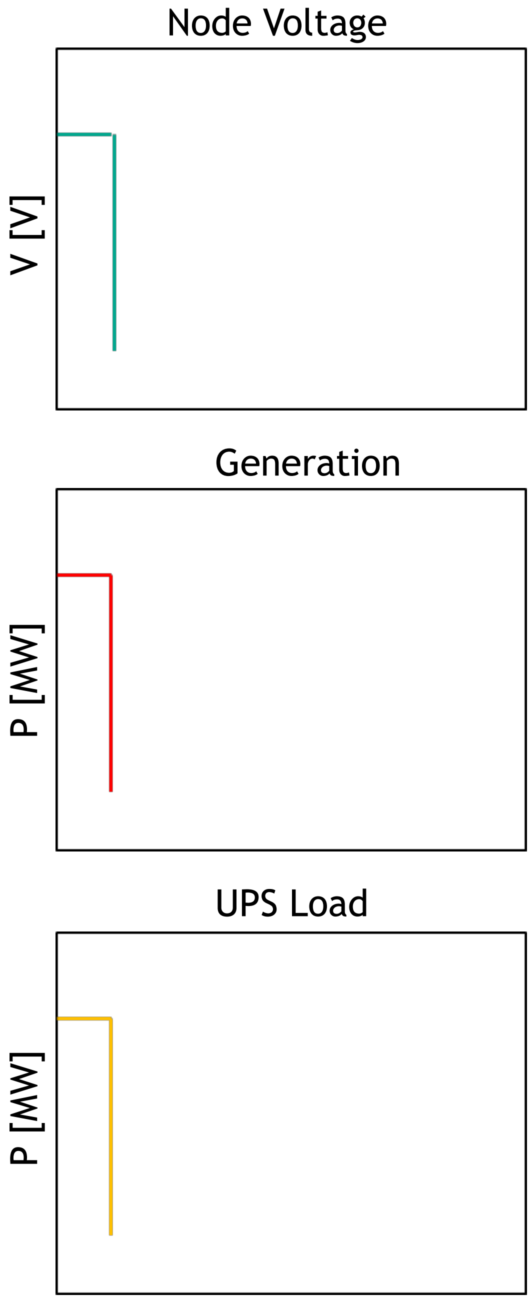

Voltage Induced Frequency Rise - Step Through

Severe System Fault

↓

Voltage Dip

↓

G - Reduction temporarily
UPS Load - Reduction permeant

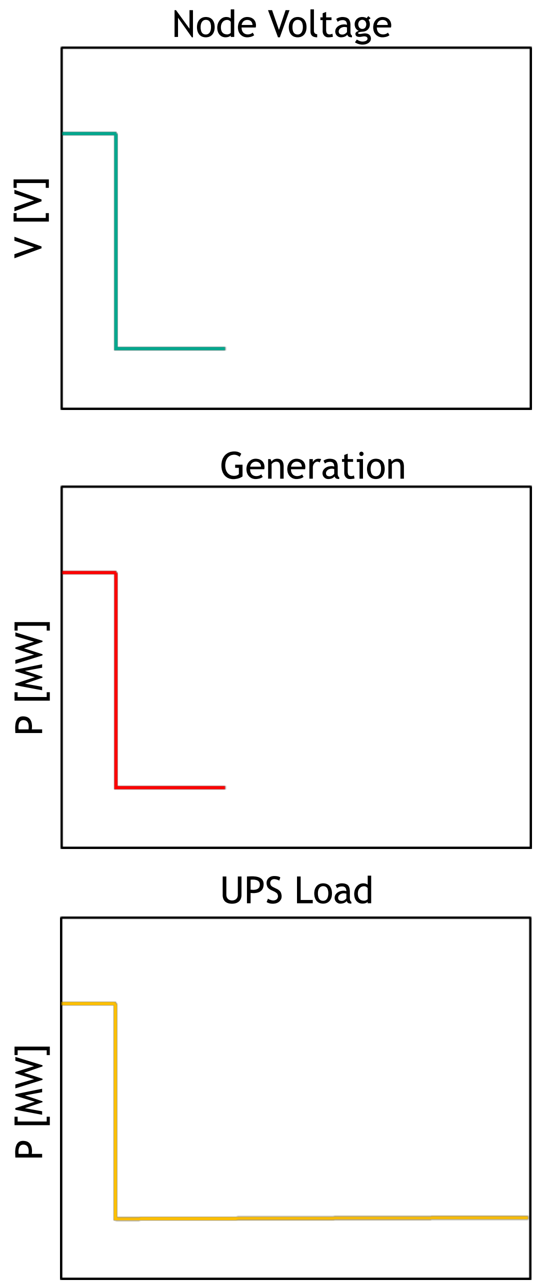

Voltage Induced Frequency Rise - Step Through

Severe System Fault

↓

Voltage Dip

↓

G - Reduction temporarily
UPS Load - Reduction permeant

↓

Fault Cleared

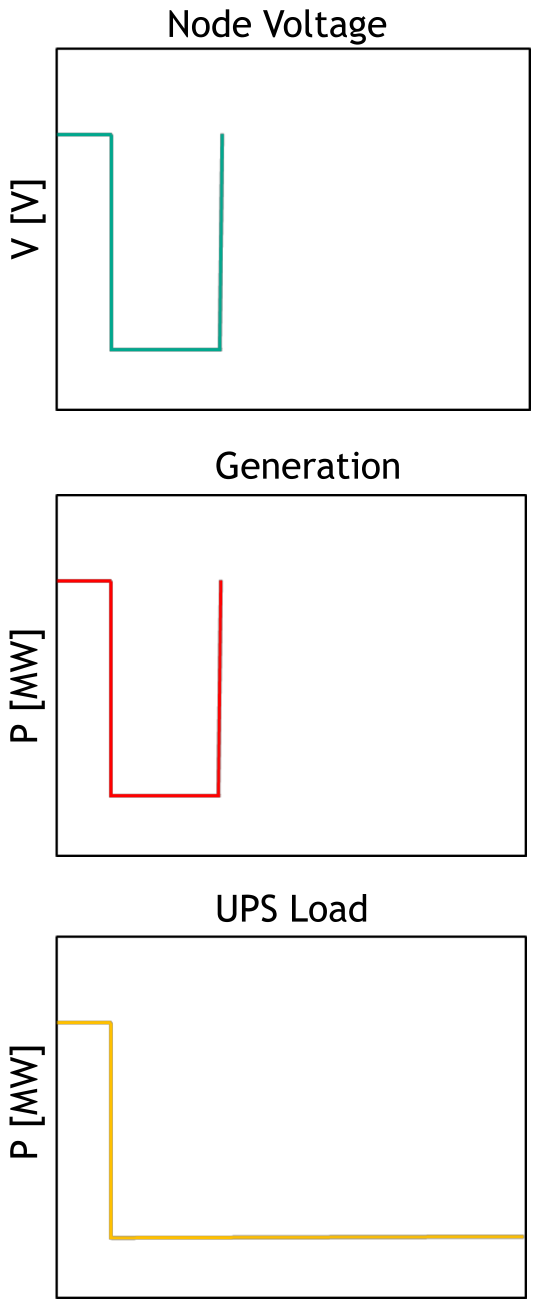

Voltage Induced Frequency Rise - Step Through

Severe System Fault

Voltage Dip

G - Reduction temporarily
UPS Load - Reduction permeant

Fault Cleared

Temporary Energy Imbalance

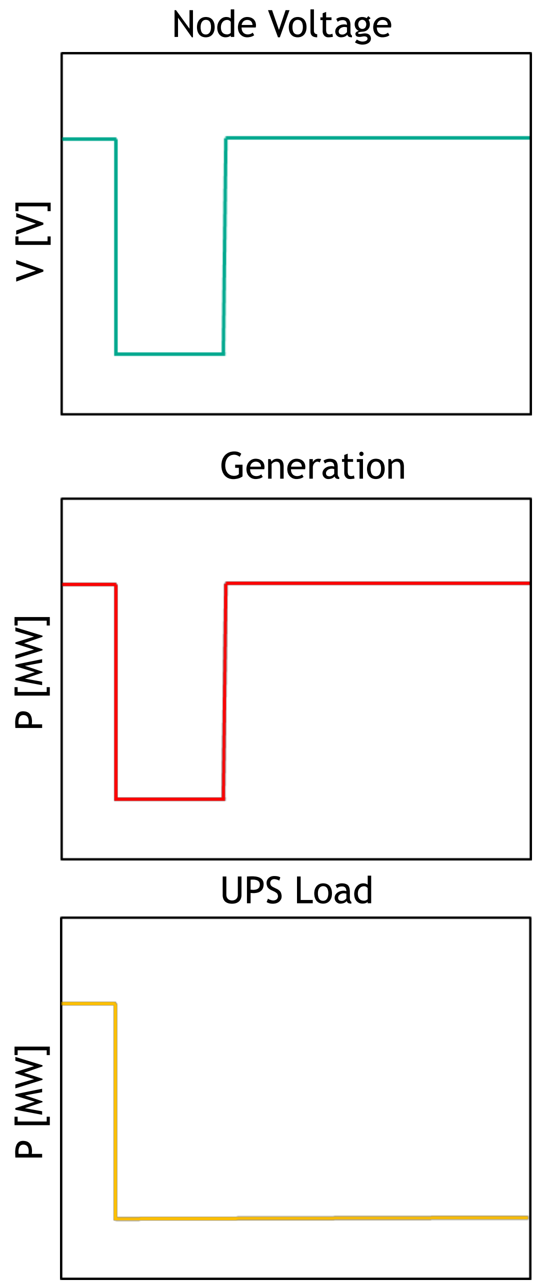

07/01/2022 System Fault

Lightening strike on a 220kV Circuit
Killonan - Kilpaddoge in Co. Limerick

Phase to Phase Fault at Killonan - Kilpaddoge 220kV

- 07/01/2022: Lighting strike on a 220kV circuit in County Limerick

- Phase to Phase Fault (ST)
- Fault cleared after 61ms
- Cause of fault was lightening
- V [p.u.] reached minimum voltage at Kilpaddoge 110kV T131

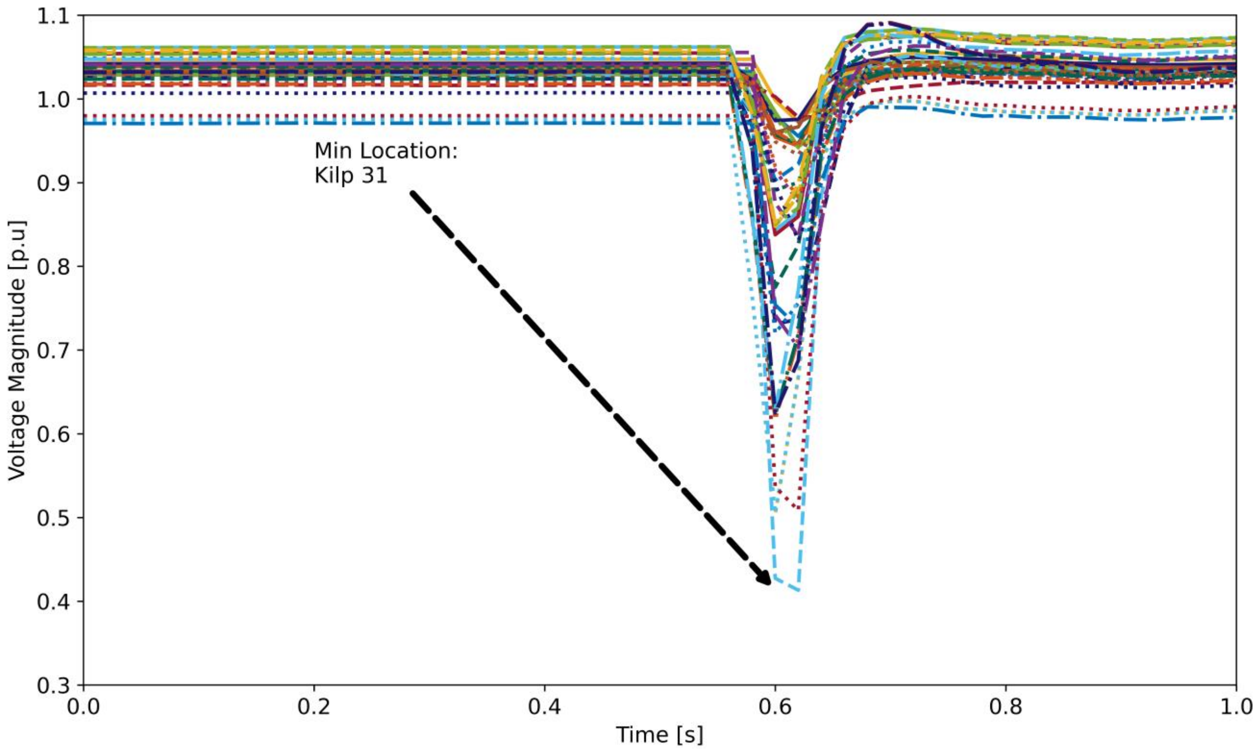

Load dropped from Data Centres for Killonan- Kilpaddoge 220 kV Fault

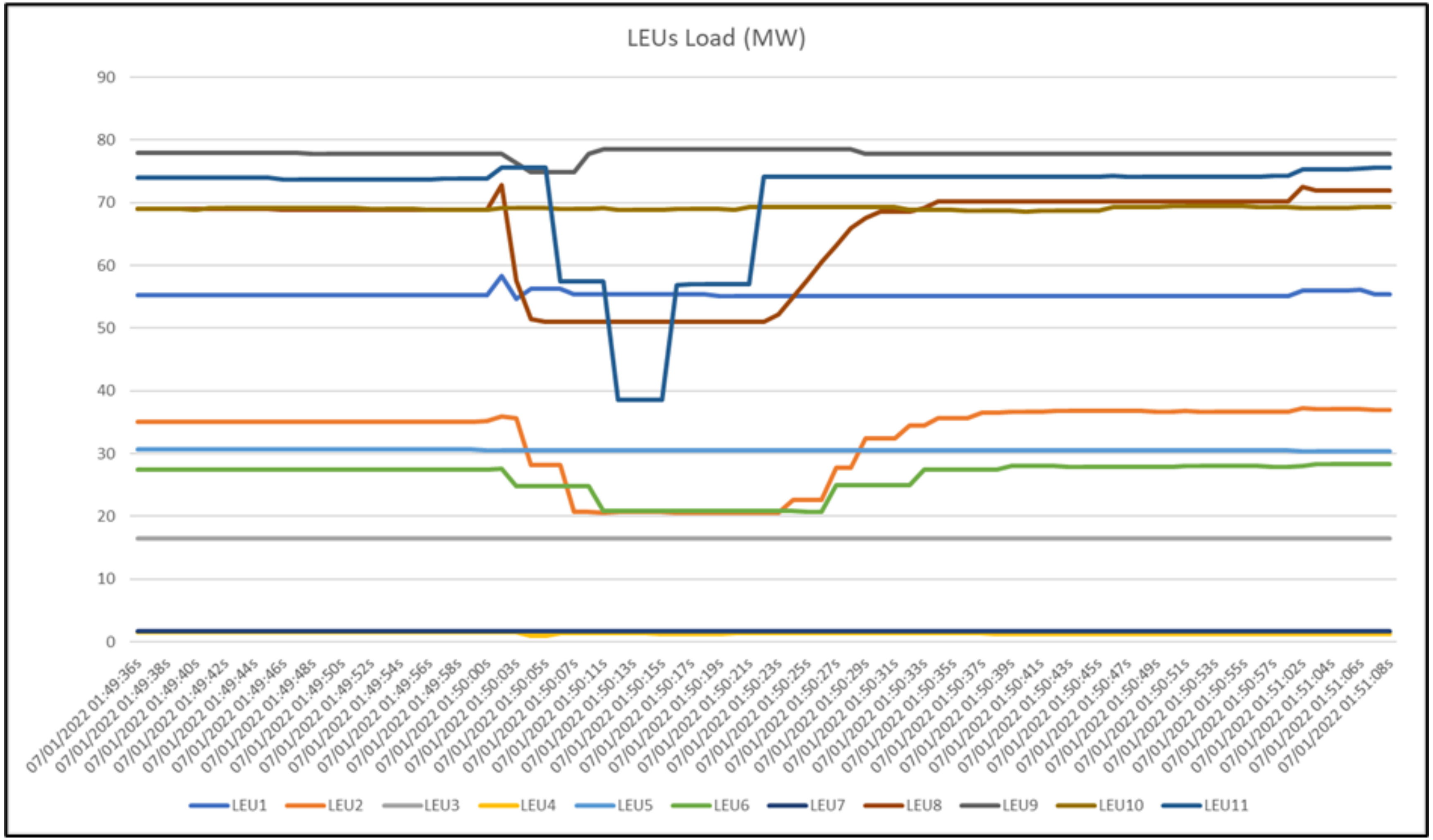

Load dropped from Data Centres for Killonan- Kilpaddoge 220 kV Fault

Wind/Demand

LSAT predictions vs recorded events for the Killonan-Kilpadogge trip:

	Simulated	Recorded data	Difference
LEUs load tripped	363.79 MW	74 MW	289.79 MW
Wind tripped	365.56 MW	200 MW	165.56 MW

System Frequency

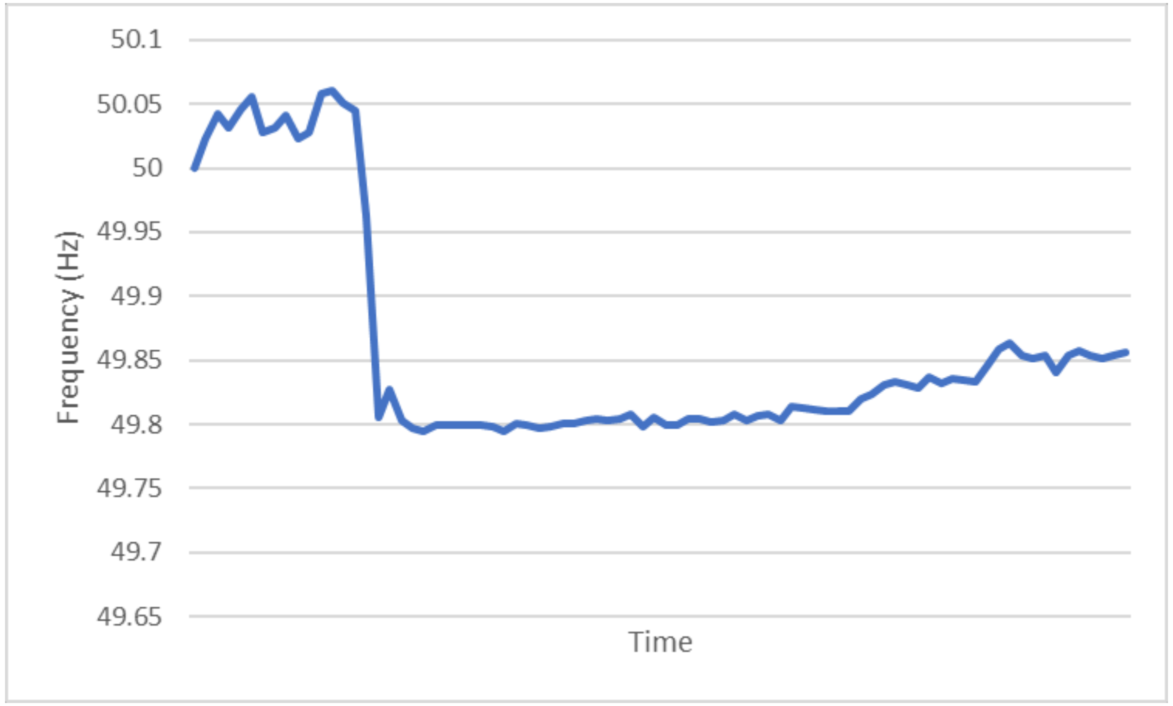

13/12/2022 System Fault

- At 16:57 hours on Tuesday 13 December 2022, the **Kellystown - Woodland 220 kV line** tripped, reclosed and tripped for a single phase to ground fault (RE)
- The fault clearance times were approximately 80 ms and 98 ms
- Failure of Polymeric insulator

Voltage Magnitude Response – [p.u.] (ALL PMU's)

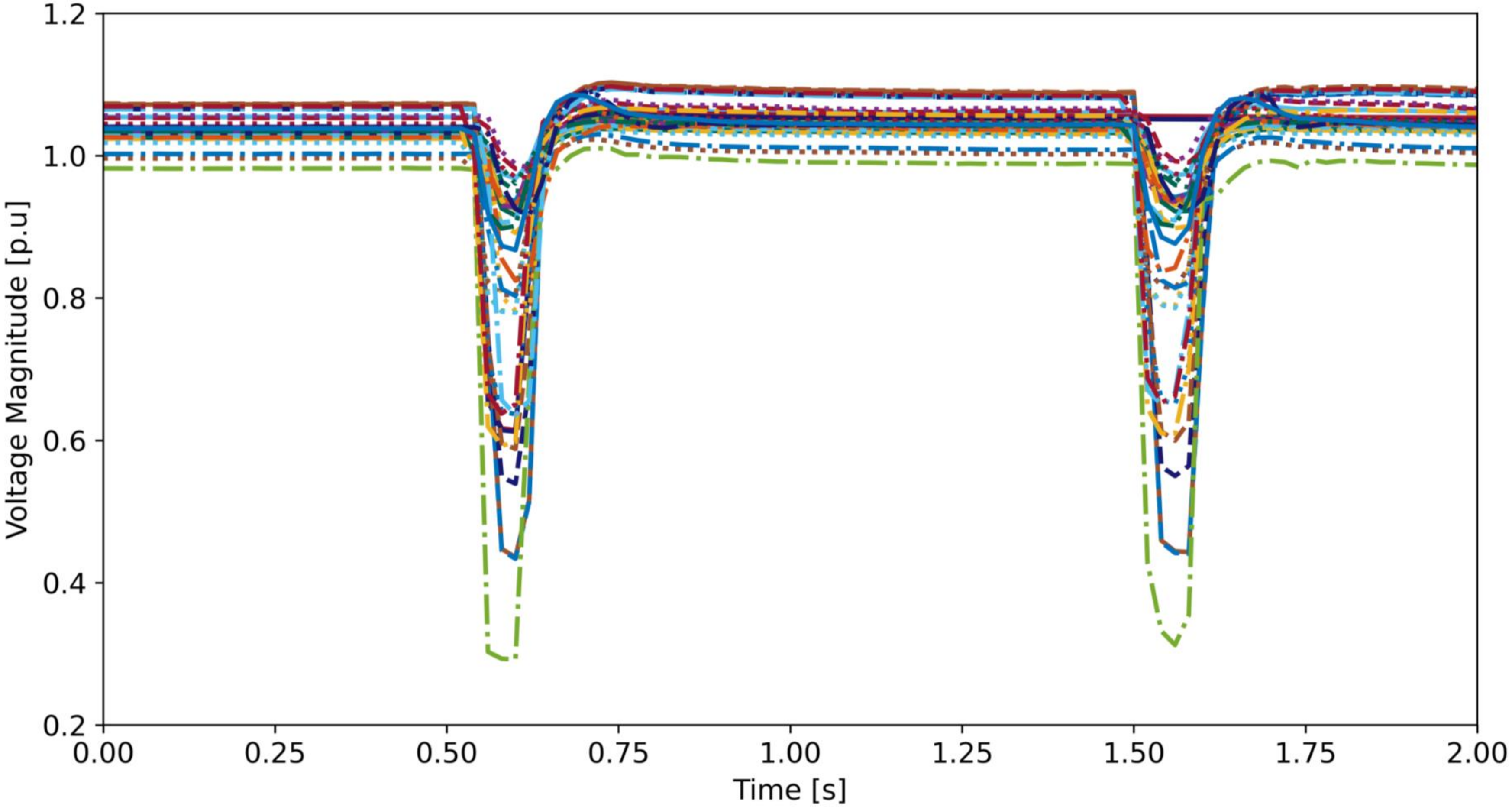

EirGrid SONI

Voltage Magnitude Response – [p.u.] (Dublin PMU’s)

EMS - Dublin

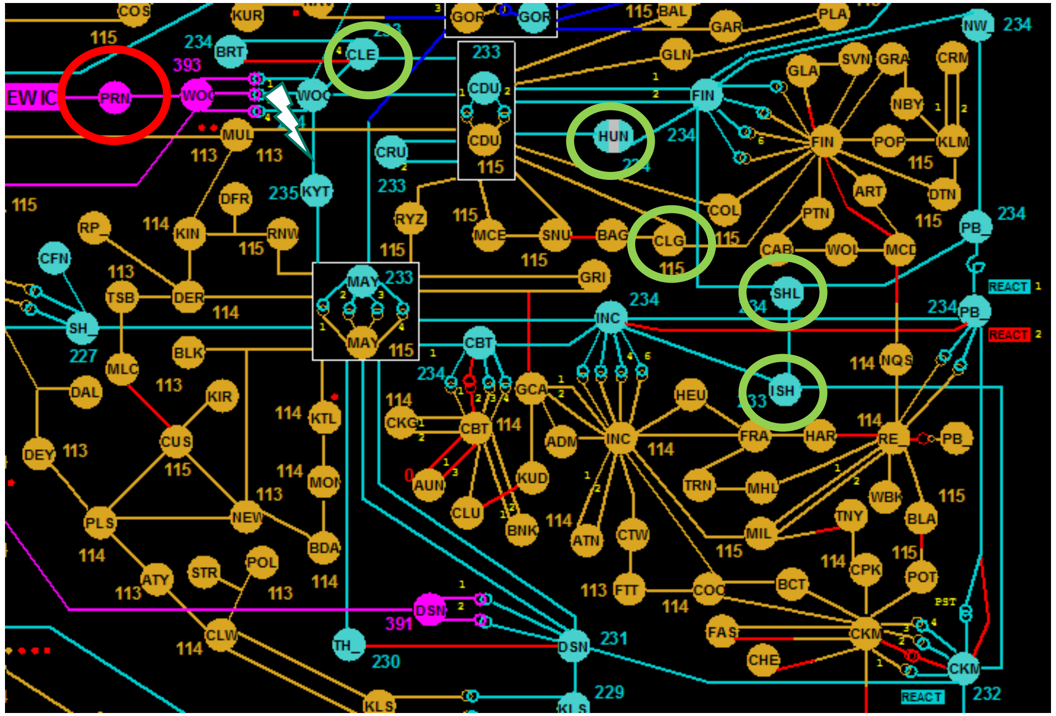

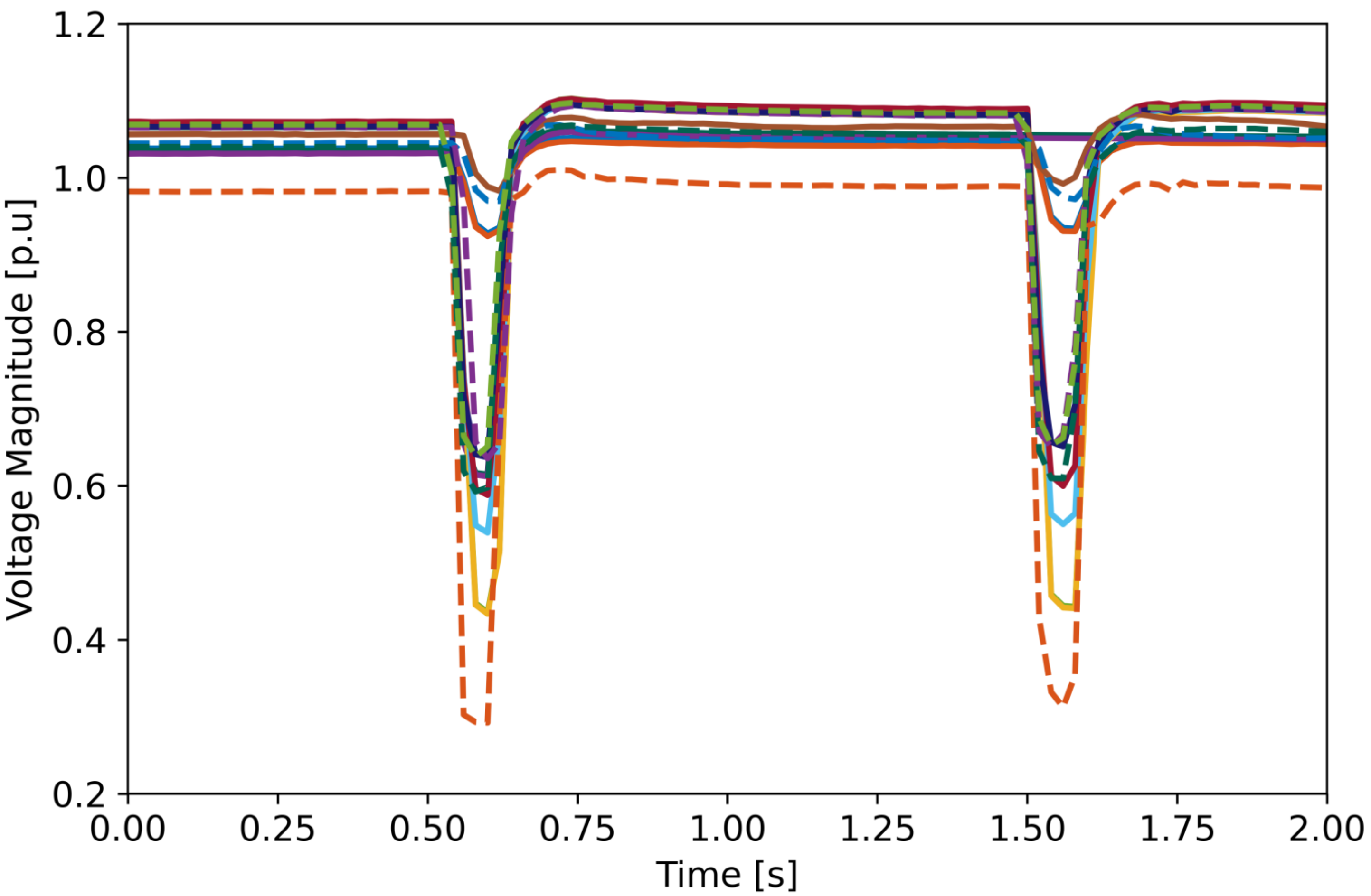

EirGrid SONI

Load dropped from Data Centres for Kellystown-Woodland Fault 13/12/2022

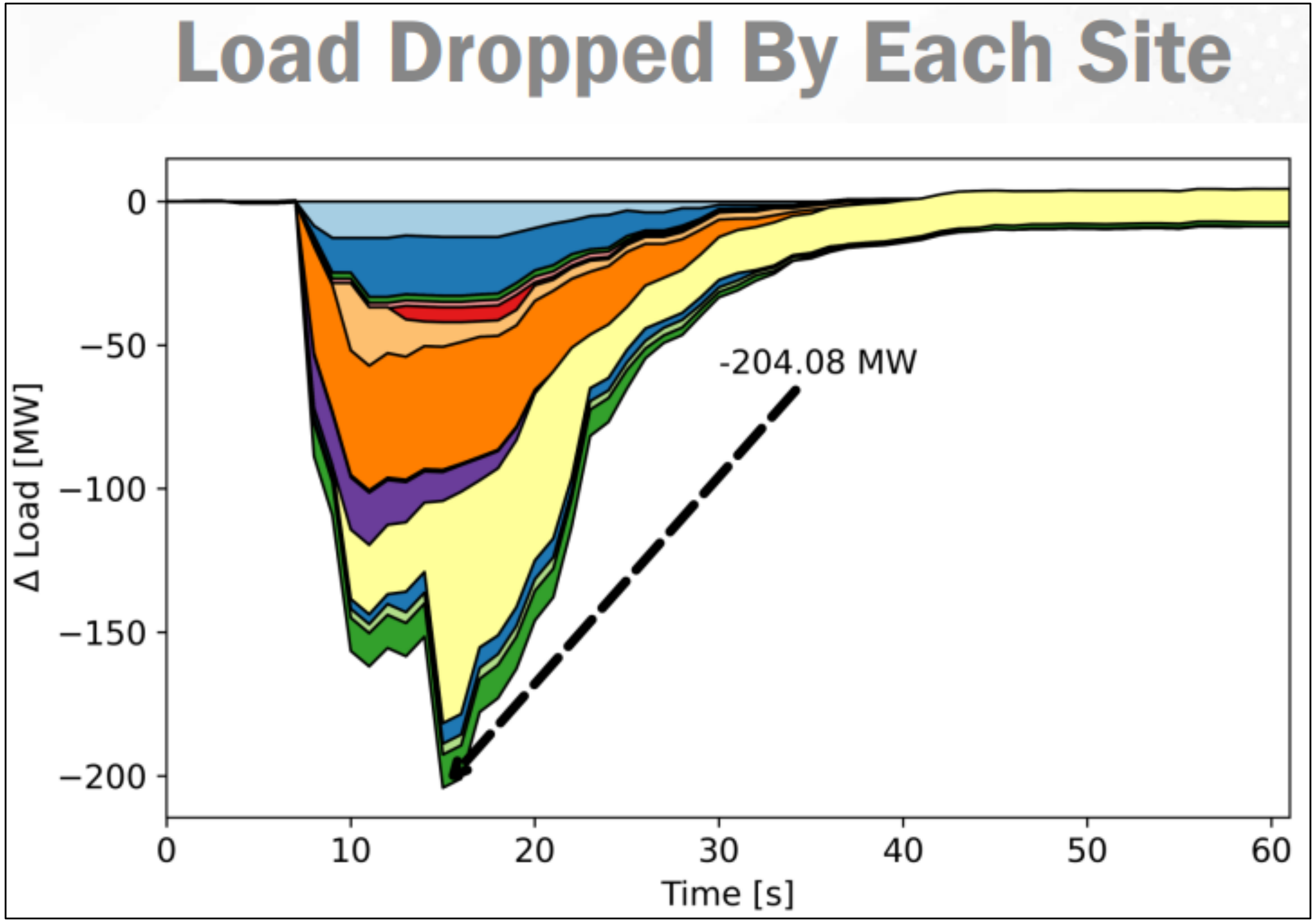

Impact on System Frequency

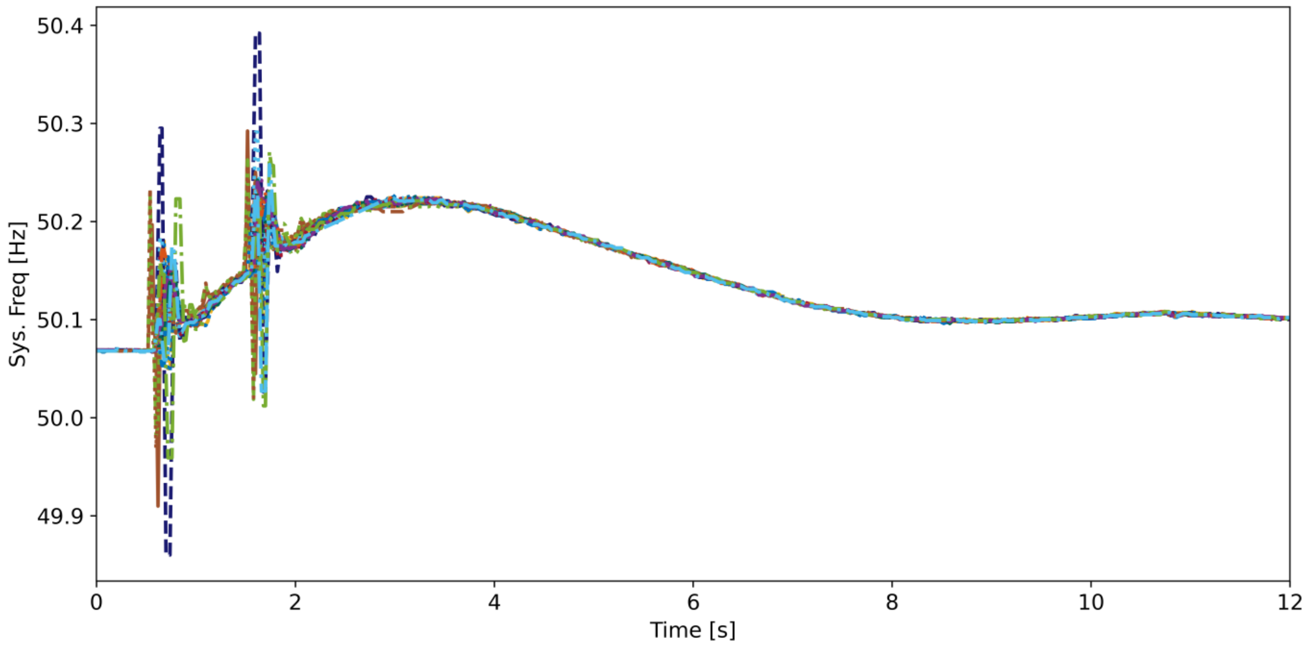

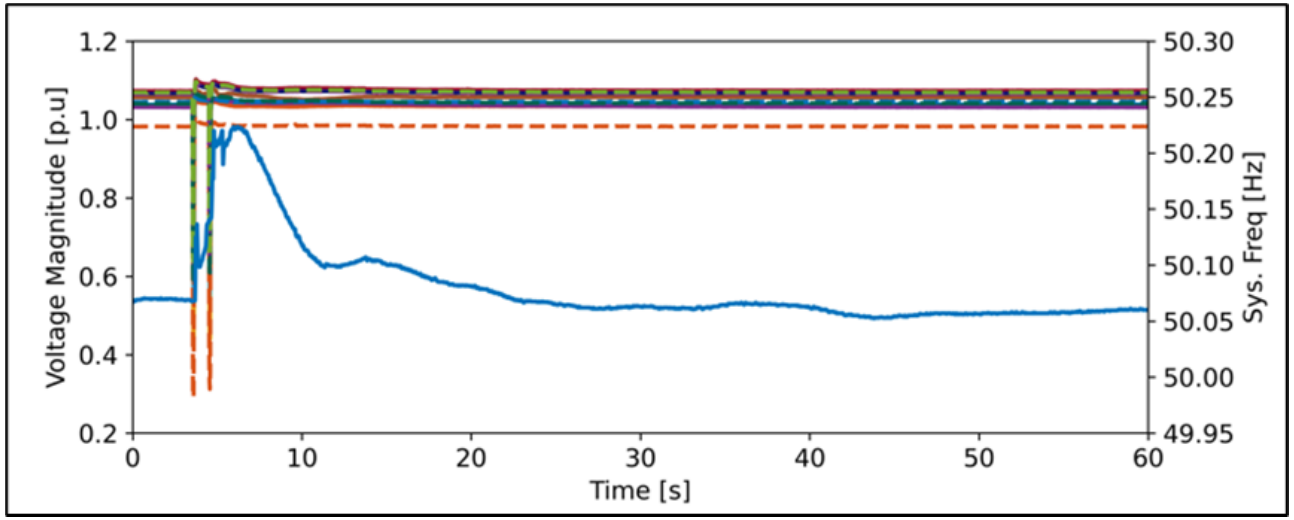

Grid Code and Network Code on Demand Connection requirements

Grid Code

CC.7.4.2 **Demand Facilities, Closed Distribution Systems** and **Distribution Systems** shall:

CC.7.4.2.1 Remain synchronised to the **Transmission System** and operate within the frequency ranges and time periods specified in *Table CC.7.4.2.1*.

Table CC.7.4.2.1: Minimum Time Periods for ***Demand Facilities*****, Closed Distribution Systems** and **Distribution Systems** *to Remain Operational without Disconnecting*

Frequency Range	Time Period
47 – 47.5 Hz	20 seconds
47.5 – 48.5 Hz	90 minutes
48.5 – 49 Hz	90 minutes
49 – 51 Hz	Unlimited
51 – 51.5 Hz	90 minutes
51.5 – 52 Hz	60 minutes

CC.7.4.2.2 Remain synchronised to the **Transmission System** and operate within the ranges of the **Transmission System Voltage** at the connection point, for an unlimited time period, as specified below:

(i) 400 kV system: 360 kV to 420 kV (0.9 p.u. – 1.05 p.u.)

(ii) 220 kV system: 198 kV to 245 kV (0.9 p.u. – 1.114 p.u.)

(iii) 110 kV system: 99 kV to 123 kV (0.9 p.u. – 1.118 p.u.)

European Network Code on Demand Connection

Ireland and Northern Ireland	47,5 Hz-48,5 Hz	90 minutes
	48,5 Hz-49,0 Hz	To be specified
	49,0 Hz-51,0 Hz	Unlimited
	51,0 Hz-51,5 Hz	90 minutes

Article 18

Information exchange

Article 21

Simulation models

Article 12

General frequency requirements

1. Transmission-connected demand facilities, transmission-connected distribution facilities and distribution systems shall be capable of remaining connected to the network and operating at the frequency ranges and time periods specified in Annex I.

EirGrid and SONI’s Proposed Phased Approach

Proposed Approach:

Phase 1 (Short-Term)	Phase 2 (Long-Term)
• Collect LEUs updated protection settings • Request changes to the highlighted protection settings to align with Code requirements and avoid system issues	• Update the Transmission/Network Codes (and potentially the Distribution Codes) to more comprehensively define standards including, among others, performance requirements (i.e., fault ride through), models and testing like generators

Fault Ride Through

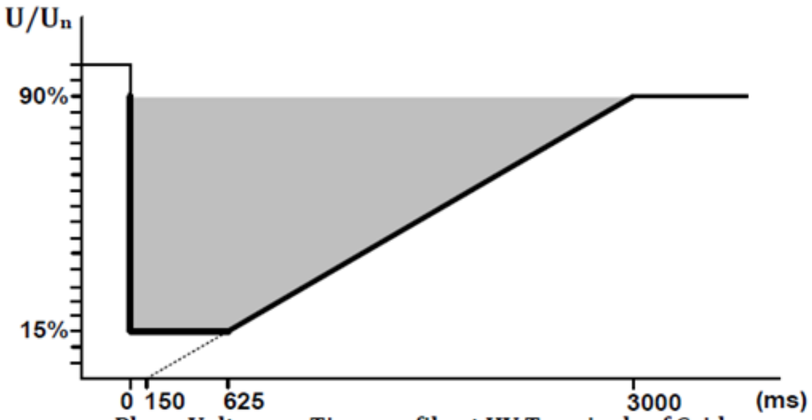

Phase Voltage vs Time profile at HV Terminals of Grid-Connected Transformer

Q & A

Email: Taulant.Kerci@Eirgrid.com

Ahsan Murad

Ahsan Murad received a B.Sc. degree in electrical engineering from IUT, Bangladesh, in 2009 and a double M.Sc. degree in Smart Electrical Networks and Systems from KU Leuven, Belgium, and KTH, Sweden, in 2015. He completed his Ph.D. with the Department of Electrical and Electronic Engineering, University College Dublin, Ireland, in 2019. He is currently working with DIgSILENT GmbH, Germany as an application engineer.

POWERFACTORY

Distributed generation modeling, simulation and system studies using DIgSILENT *PowerFactory*

POWER SYSTEM SOLUTIONS
MADE IN GERMANY

Agenda

- Introduction
- Modeling and Simulation
  - Dynamic simulation concepts in *PowerFactory*
  - Hybrid and clocked dynamic models using DSL and Modelica
  - Interoperability of Modelica models using FMI standard
  - Implementation and validation
- System Study
  - Unintentional electrical islands
- Outlook and conclusions

Introduction

- An increased penetration of converter-interfaced distributed technologies
- Significant impact on the overall dynamic response of the system
- Interaction between the controllers of these converters and the rest of the system
- Challenges on different levels, e.g., modeling, validation, simulation, model exchange etc
- This presentation
  - **shows how *PowerFactory* can be used to address the challenges above**
  - **discusses one system study conducted using *PowerFactory* to show the impact of distributed technologies on island detection**

Distributed generation modeling, simulation and system studies using DIgSILENT *PowerFactory*

POWERFACTORY

POWER SYSTEM SOLUTIONS
MADE IN GERMANY

Simulation and Time-Scales

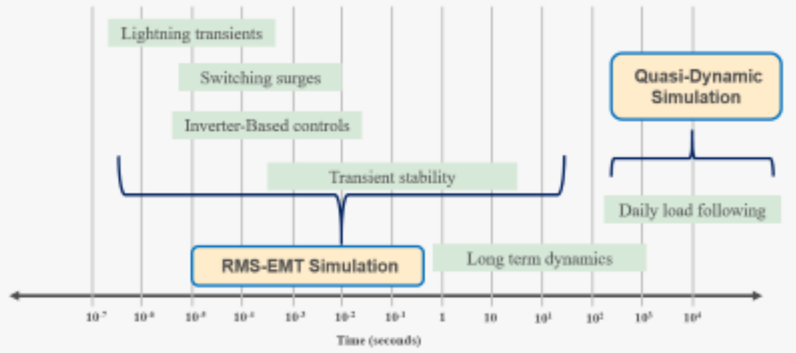

System Studies: Unintentional Electrical Islands

- *IEEE 1547*
  - *Island network, intended: A planned island network.*
  - *Island network, unintentional: An Unplanned Island Network.*
- DIN VDE V 0126-1-1
  - *In the case of unintentional islanding, this process [islanding] takes place outside the control of the grid operator. Voltage and frequency of the disconnected sub-network are not to be influenced by the grid operator*
- DIN VDE V 0126-2
  - *"[...] an island that is intentionally generated, usually to restore power to the utility system affected by a disturbance or to maintain supply. The generation and loads may be with any combination of customer-owned and utility-owned facilities, but there is an unspoken or explicit agreement between the controlling utility and the operators at the customer-owned generating station for this situation."*
- **Unintentional islanding:** *serious challenge due to the increasing number of converter interfaced distributed generation (DGs)*

Conclusions

- DIgSILENT *PowerFactory* capabilities on modeling and simulation to study dynamic performance at different time scales with converter-interfaced technologies
- Modeling: DSL and Modelica
- Modelica models are interoperable as model exchange and co-simulation using FMI standard
- Manufacturer-sourced control model import using FMI standard
- Model validation challenges
- System study: unintentional islands will become more frequent with the increasing number of distributed generation

Thank you for your attention

Ahsan Murad
a.murad@digsilent.de

Simulation and Time-Scales

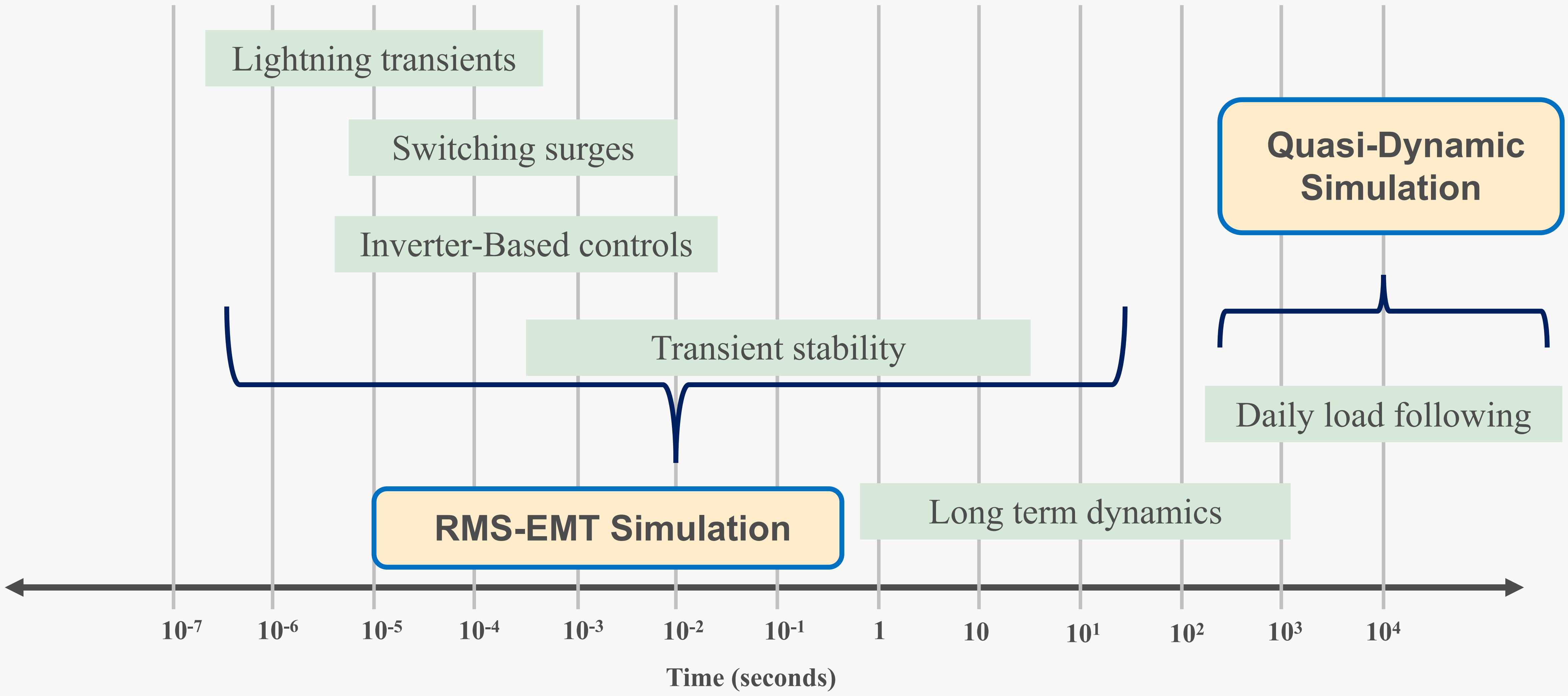

RMS-EMT Dynamic Modeling

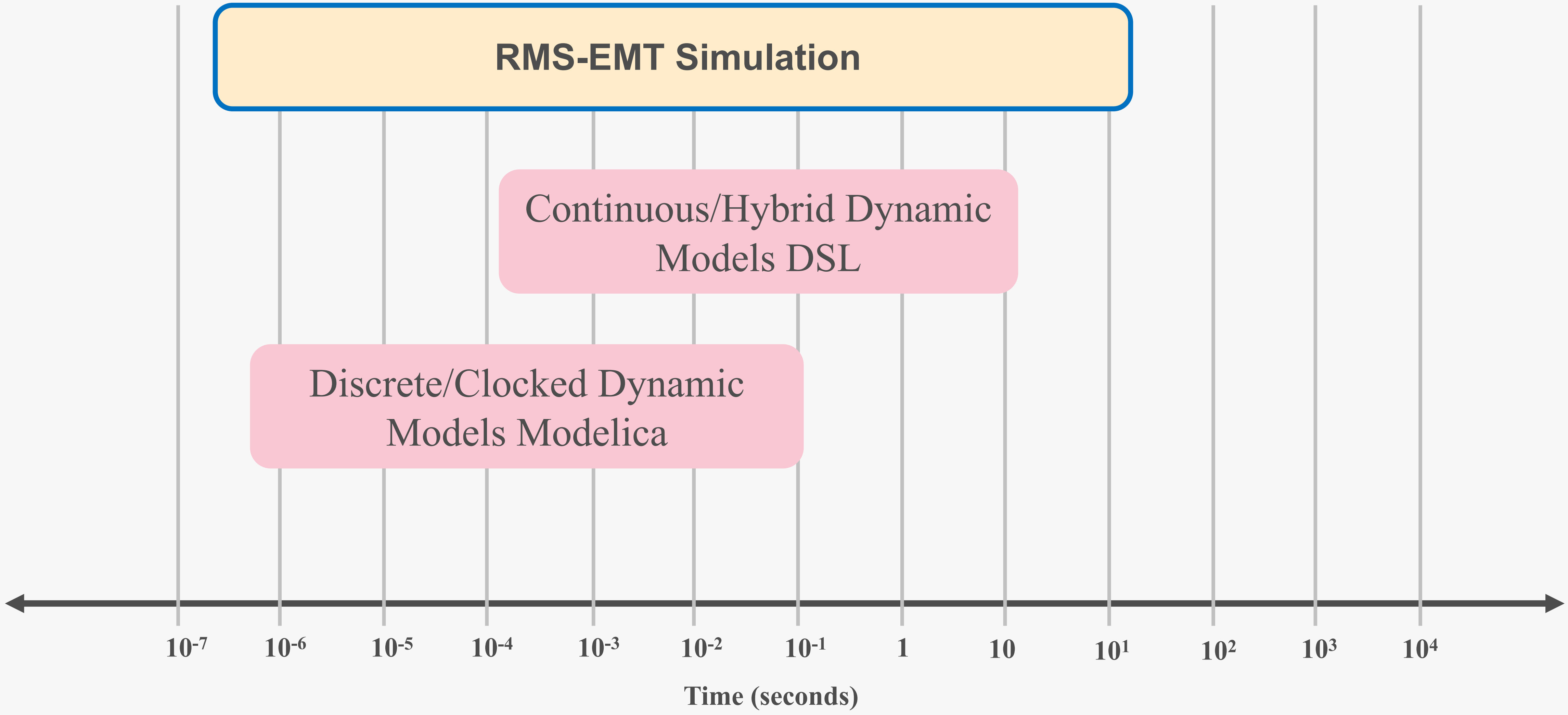

DSL and MODELICA

DSL: DIgSILENT Simulation Language

DSL:

- Developed and owned by DIgSILENT
- Continuous System Simulation Language
- Mathematical description of (time-) continuous linear and non-linear systems
- Causal modeling
- Hybrid modeling

29.4. DSL: THE DIGSILENT SIMULATION LANGUAGE

29.4 DSL: The *DIgSILENT* Simulation Language

The *DIgSILENT* Simulation Language (DSL) is used to design and simulate dynamic models for representing various dynamic systems, including controllers of electrical equipment as well as other components used in electric power systems.

Modelica: An open modeling language

Modelica language:

- Object-oriented modeling language
- Acausal and equation based
- Supports multi-domain modeling
- Synchronous/clocked language elements
- Hybrid modeling

Modelica Language

Modelica® – A Unified Object-Oriented Language for Systems Modeling

Language Specification

Version 3.6

DIgSILENT Library Dynamic Models

- **Application**
  - Production Specification (https://www.digsilent.de/en/)
- **Models**
  - Network models
  - Dynamic controller models
  - Application examples

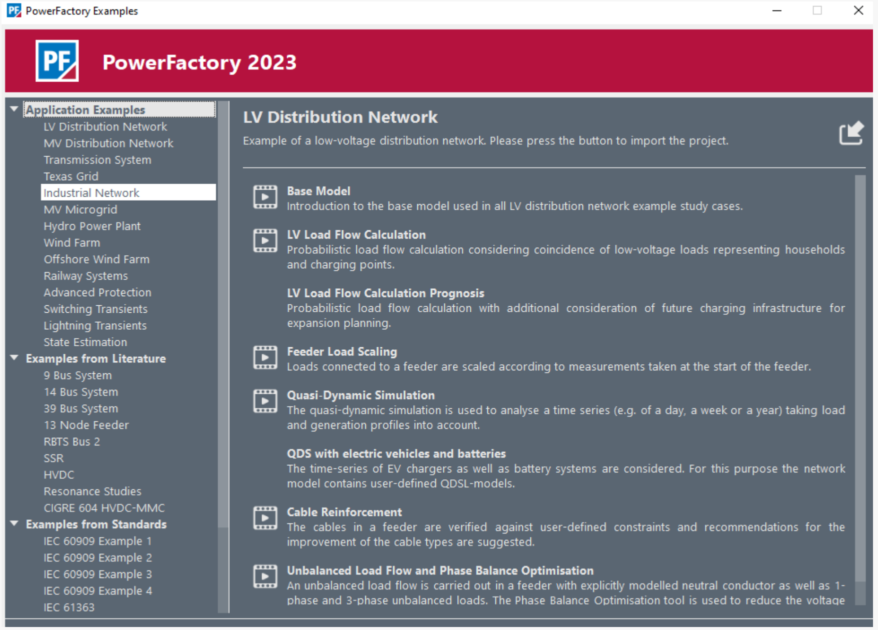

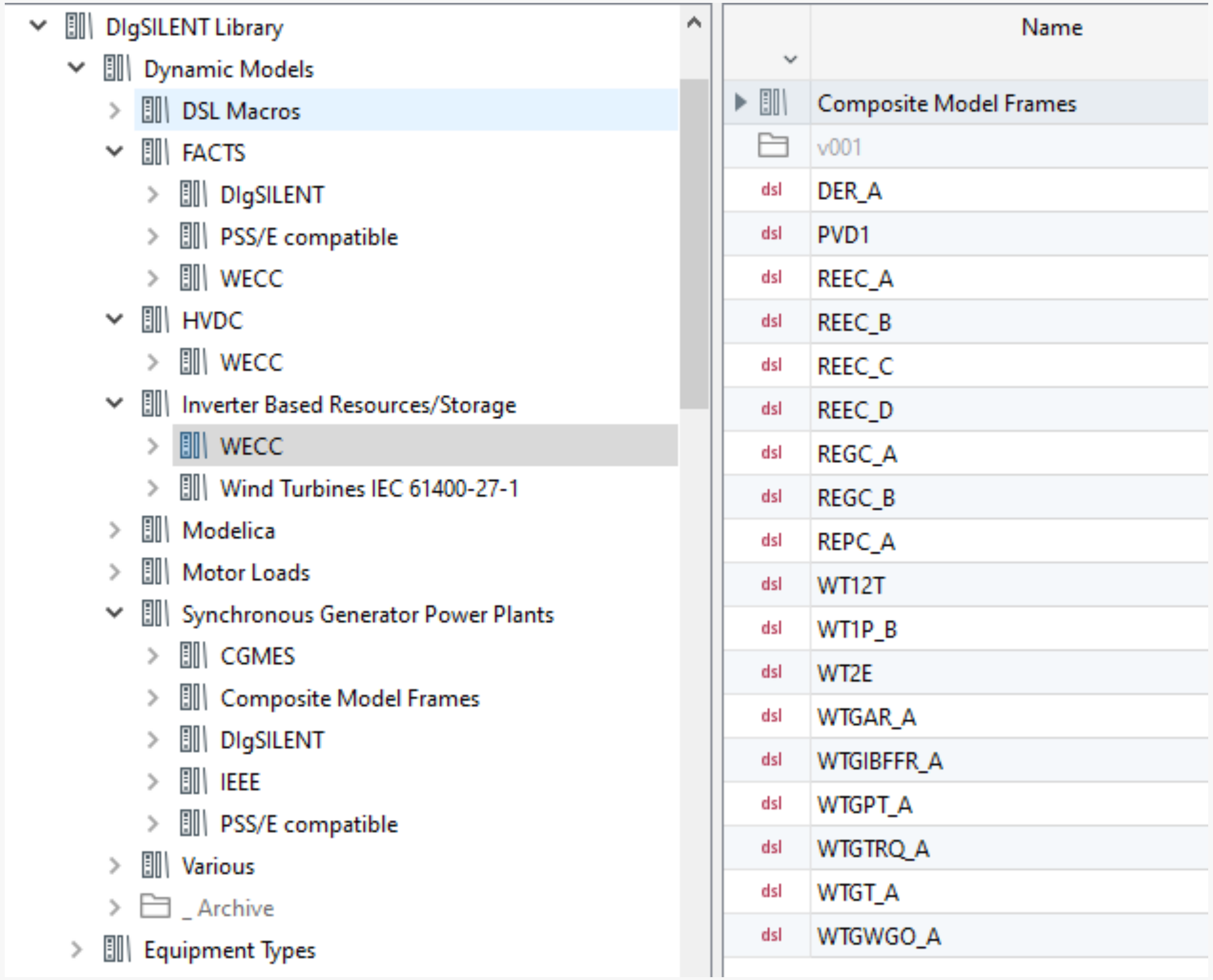

Example I

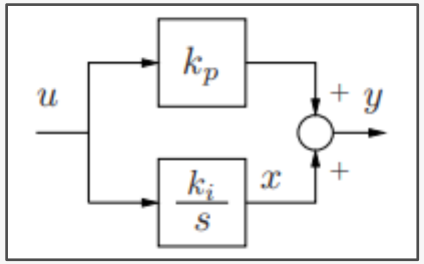

Hybrid Model (DSL)

Additional equations

```
inc(y)=0
inc(x)=0
u = select(time() < 0.1,1 - uref,1.01 - uref)
y = kp*u + x
x.= ki*u
```

Clocked Model (Modelica)

Algorithm after first tick

```
u := if time < 0.1 then 1 - uref else 1.01 - uref;
x := previous(x)+ki*interval()*previous(u);
y := kp*u+x;
```

- Global Macros
  - Characteristics
  - Comparators
  - Constants
  - DSL Special Functions
  - Deadbands
  - Delays
  - Derivatives
  - Electric Power
  - Filters
  - Gains
  - Higher Order Transfer Functions
  - Integrators
  - Lead-lag Blocks
  - Limiters
  - Logic Functions
  - Math Functions
  - Mechanical
  - PI(D) Controllers
  - Signals
  - Switches / Selectors
  - Timers
  - Transformations
  - Unit Conversion

- **Library**
  - Connectors
    - RealInput
    - RealOutput
    - IntegerInput
    - IntegerOutput
    - BooleanInput
    - BooleanOutput
  - Global Models
    - Digital
      - Filters
      - Integrators
      - Math
      - Nonlinear
      - Operators
      - Sources
      - Switches
      - Transformations
      - TypeCasting

Example II: PWM Converter

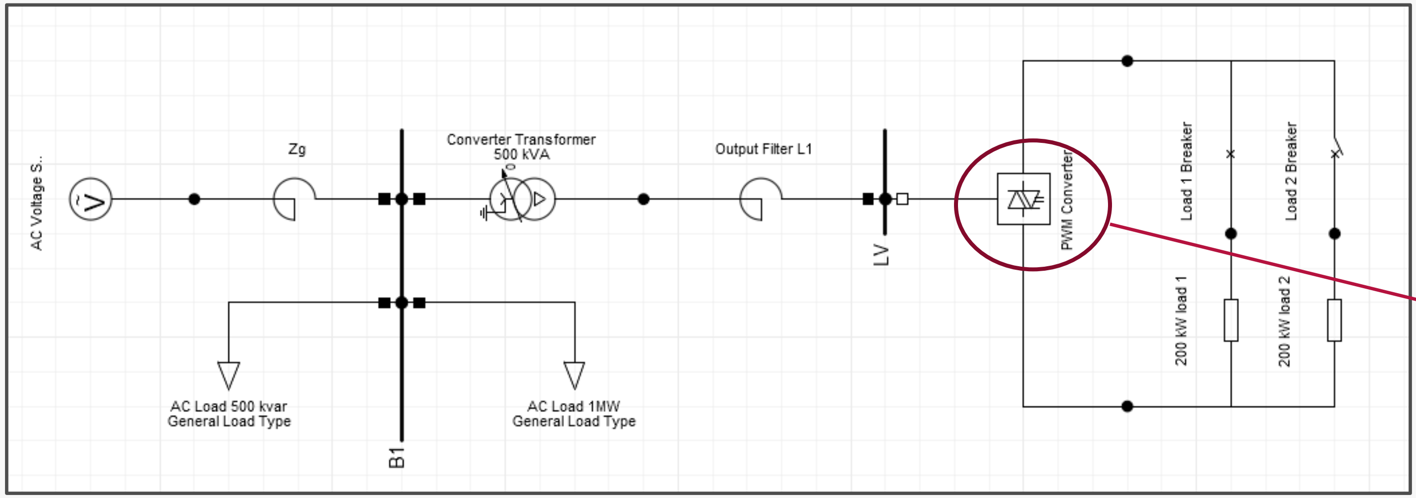

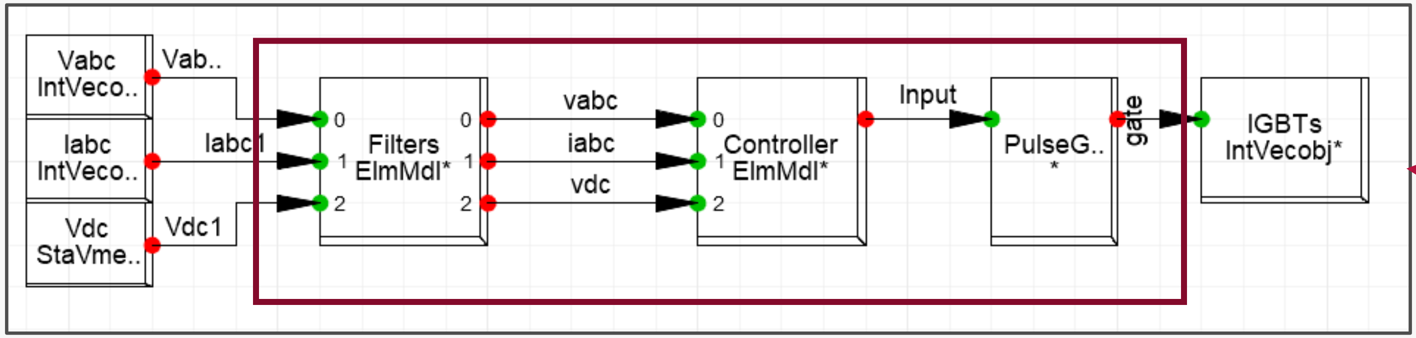

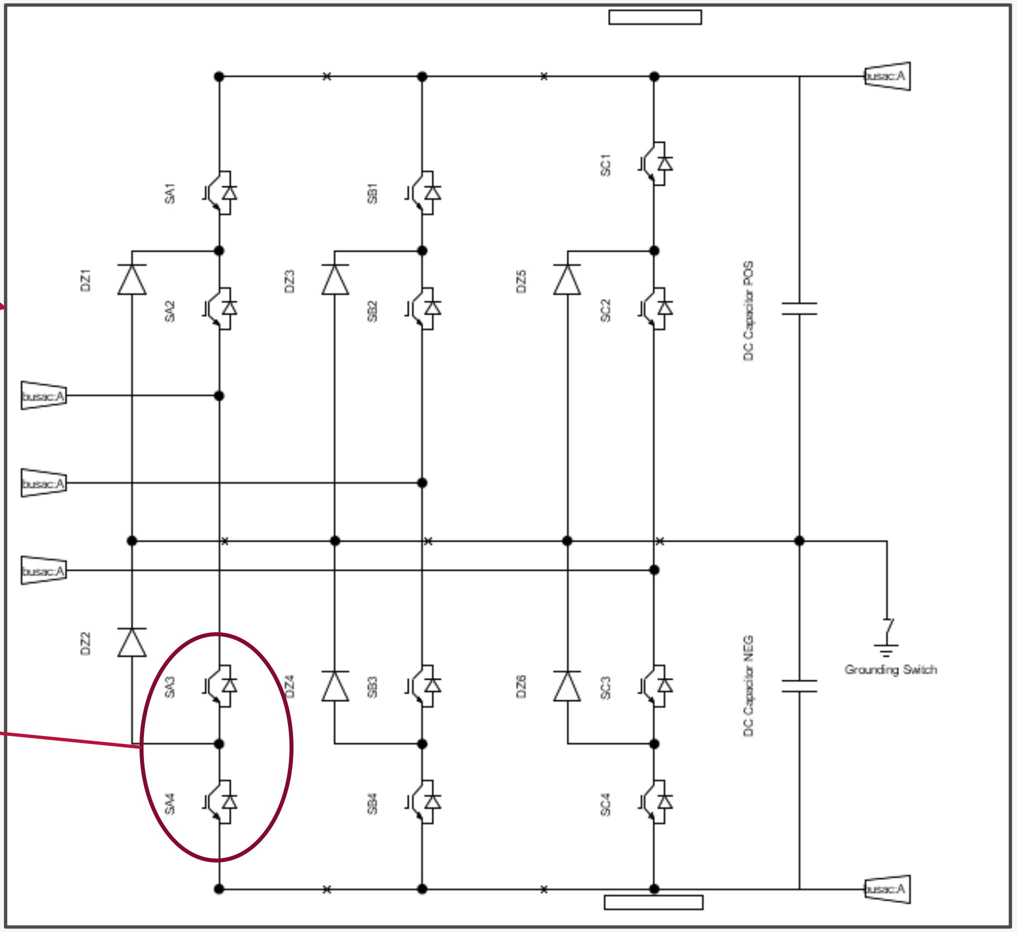

- Controllers
  - DSL
  - Modelica

Controller: DSL

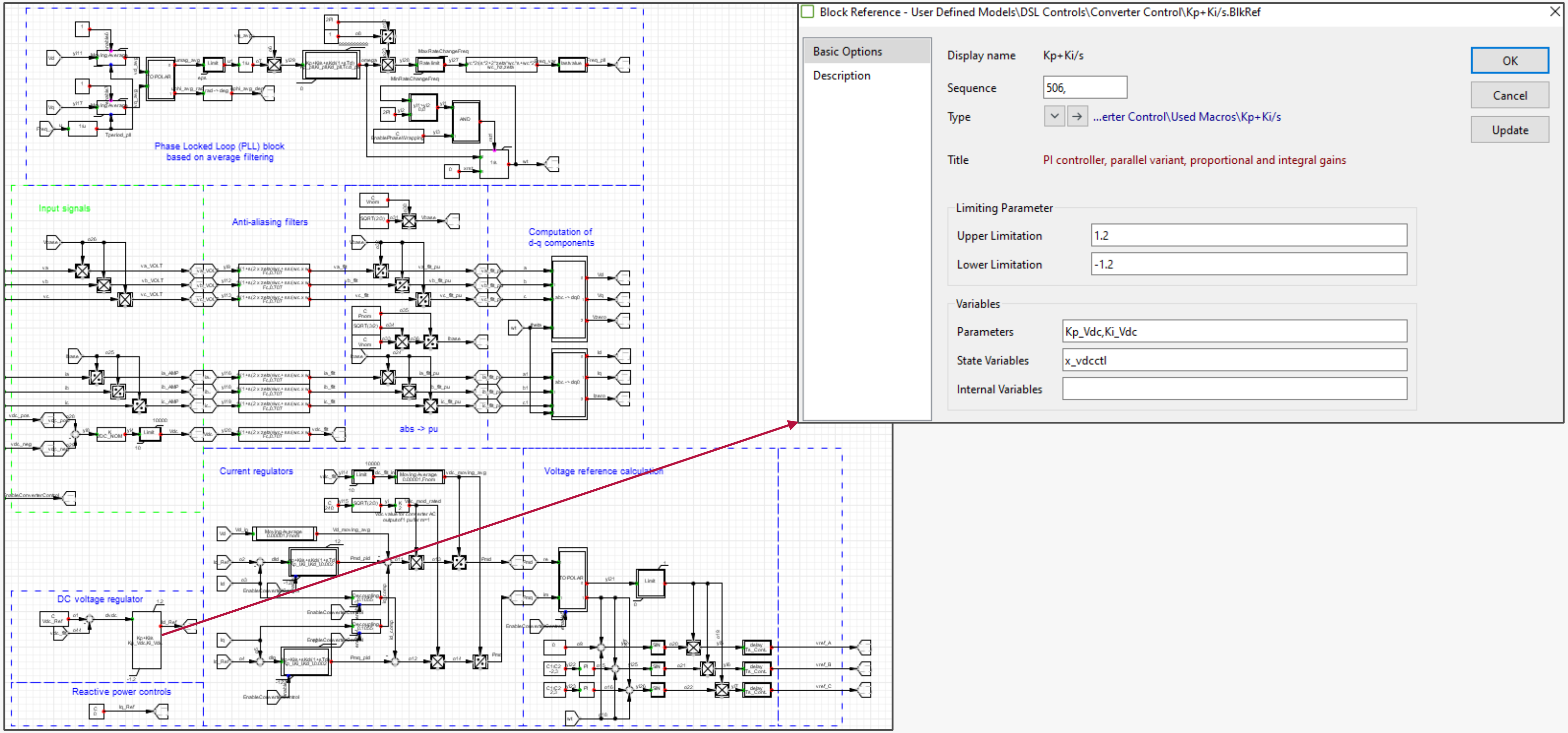

Controller: Modelica

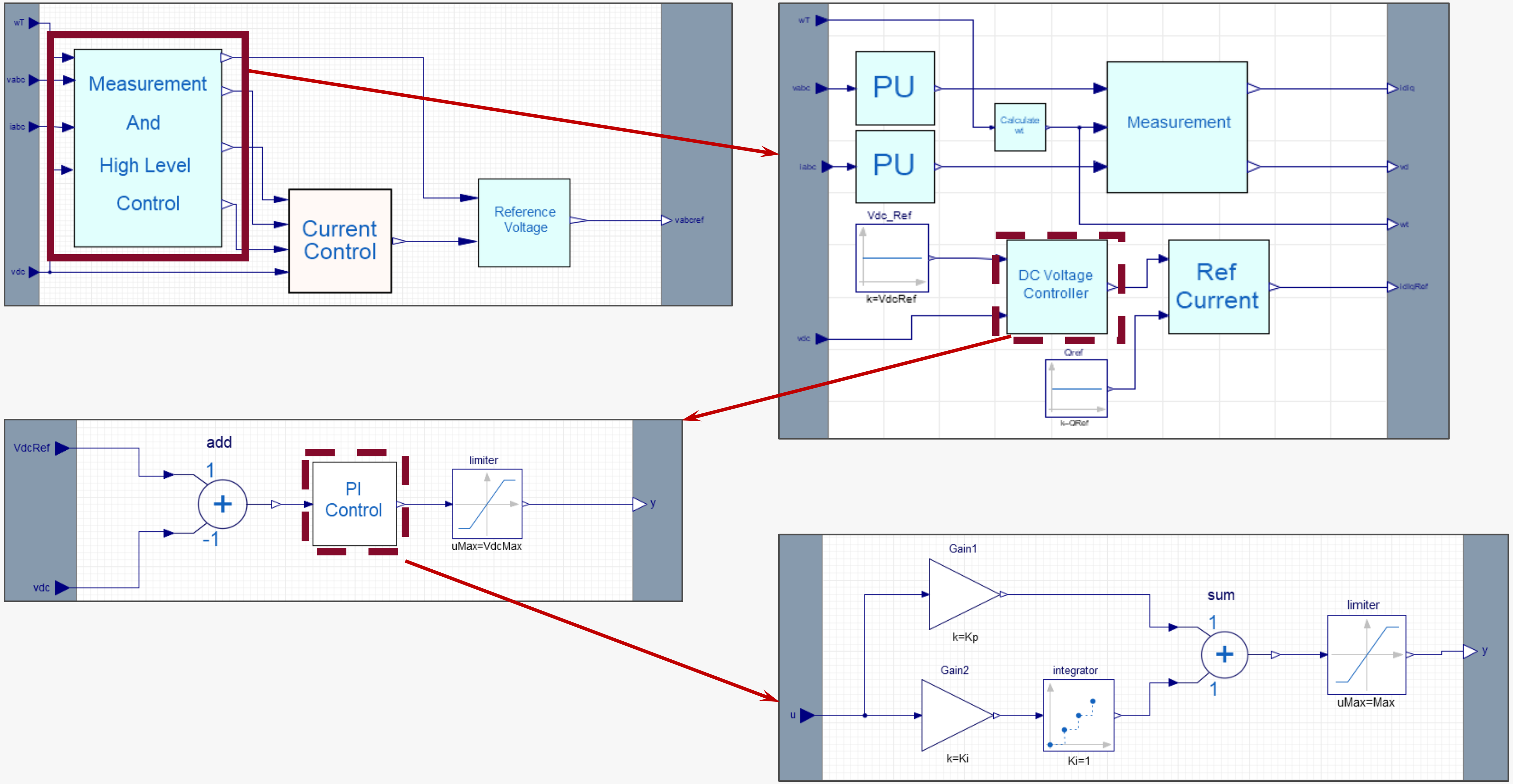

Comparison

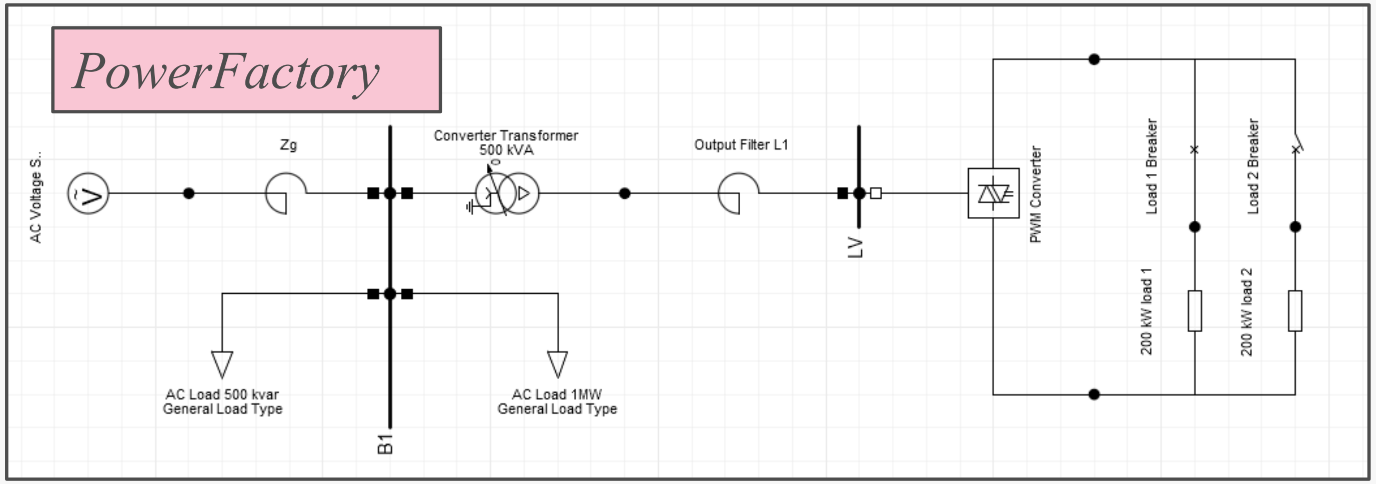

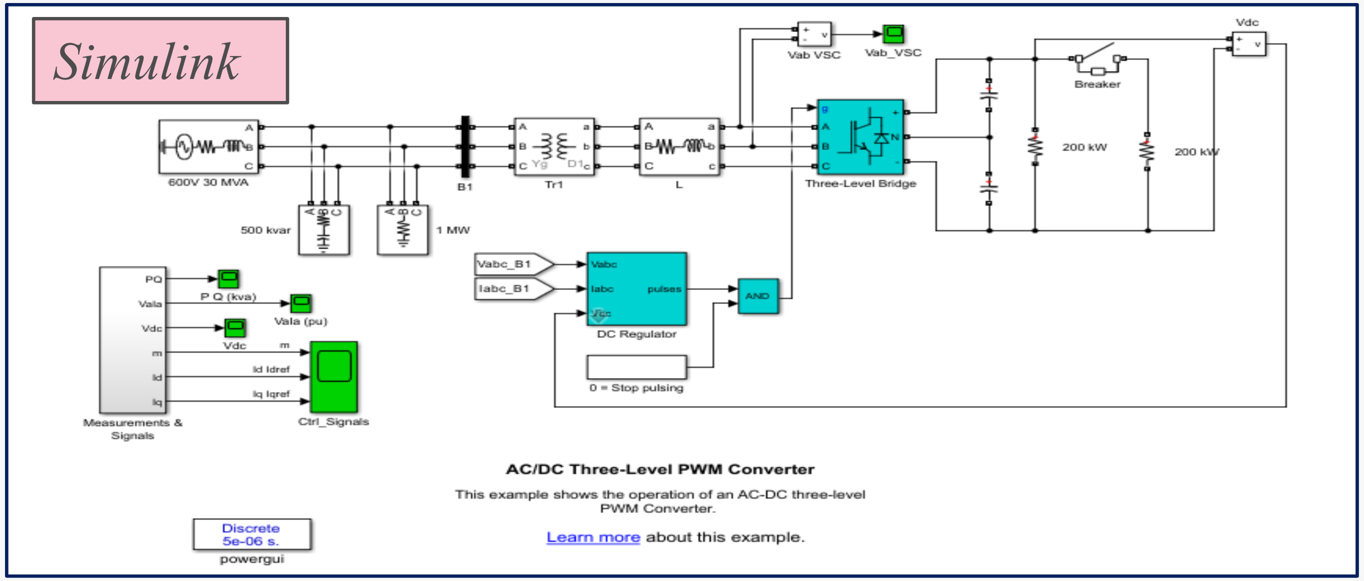

- Comparison of results between *PowerFactory* (EMT) and *Matlab-Simulink*
- AC/DC Three-Level PWM converter controllers are implemented using Modelica and DSL graphical modeling
- DC voltage response: satisfactory match

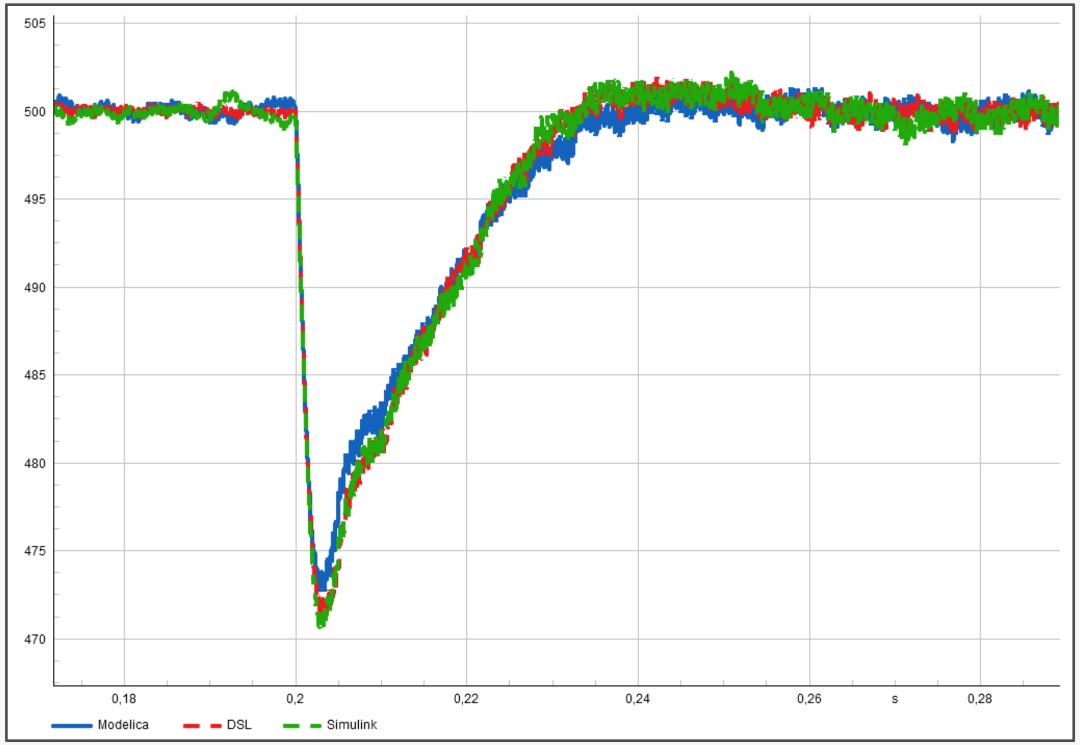

Interoperability of Modelica Models

- Why interoperability?
- **Challenges**
  - manufacturer models
  - several interfaces (IEC 61400-27, FMI)

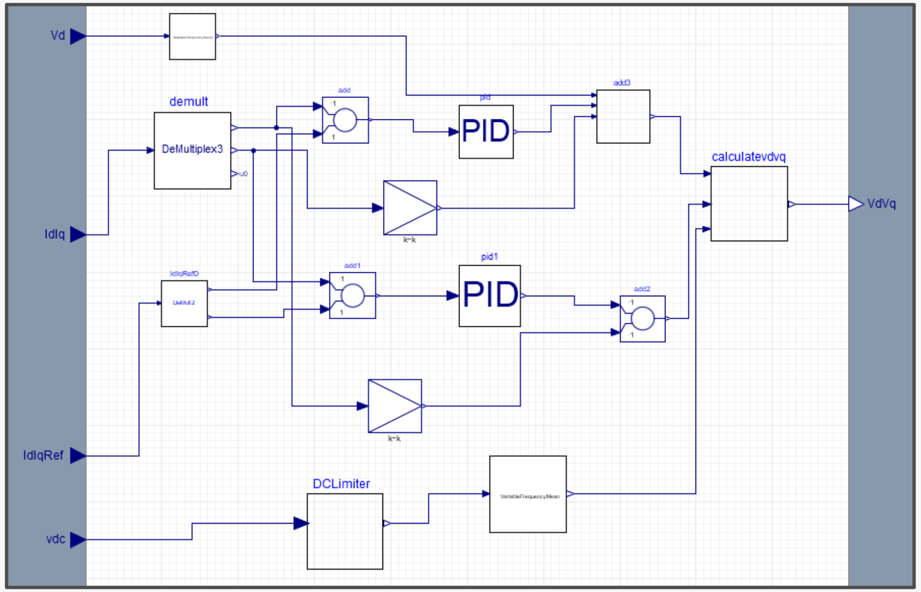


```
if IntMethod == 1 then
x := previous(y)+k*Ts*0.5*previous(u);
y := if y > uMax then uMax else if y < uMin then uMin else x+k*Ts*0.5*u;
elseif IntMethod == 2 then
y := if y > uMax then uMax else if y < uMin then uMin else previous(y)+k*Ts*previous(u);
end if;
```

Sequential Code Generation

Simulate in PF

Functional Mock-up Interface

Portable model to external tools, e.g. *Matlab*

FMI - Overview

- The **[Functional Mock-up Interface (FMI)]** is a free standard that defines a container and an interface to exchange dynamic models using a combination of XML files, binaries and C code, distributed as a ZIP file

- **Advantages:**
  - Convenient way of producing, sharing and using simulation components
  - Efficiently couples multi-disciplinary simulations
  - One FMU: exchange between different tools
  - Supports many features: event iteration, data types etc and well tested

- **Functional Mock-up Interface (FMI) – version 2 supported since *PowerFactory* 2022**
  https://fmi-standard.org/

- **FMI Supported Tools:**
  https://fmi-standard.org/tools/

- **Repository:**
  https://github.com/modelica/fmi-standard

- **FMI interface Types:**
  - Co-simulation
  - Model Exchange

fmi Functional Mock-up Interface

The leading standard to exchange dynamic simulation models

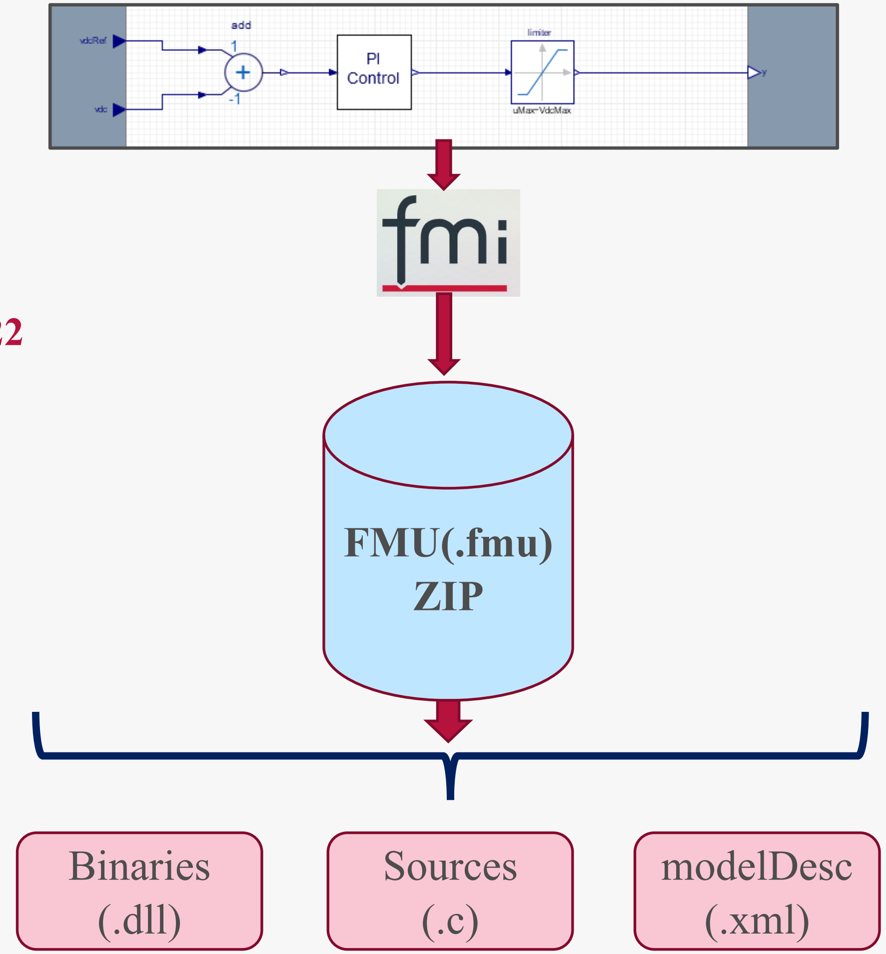

Interoperability of Modelica Models

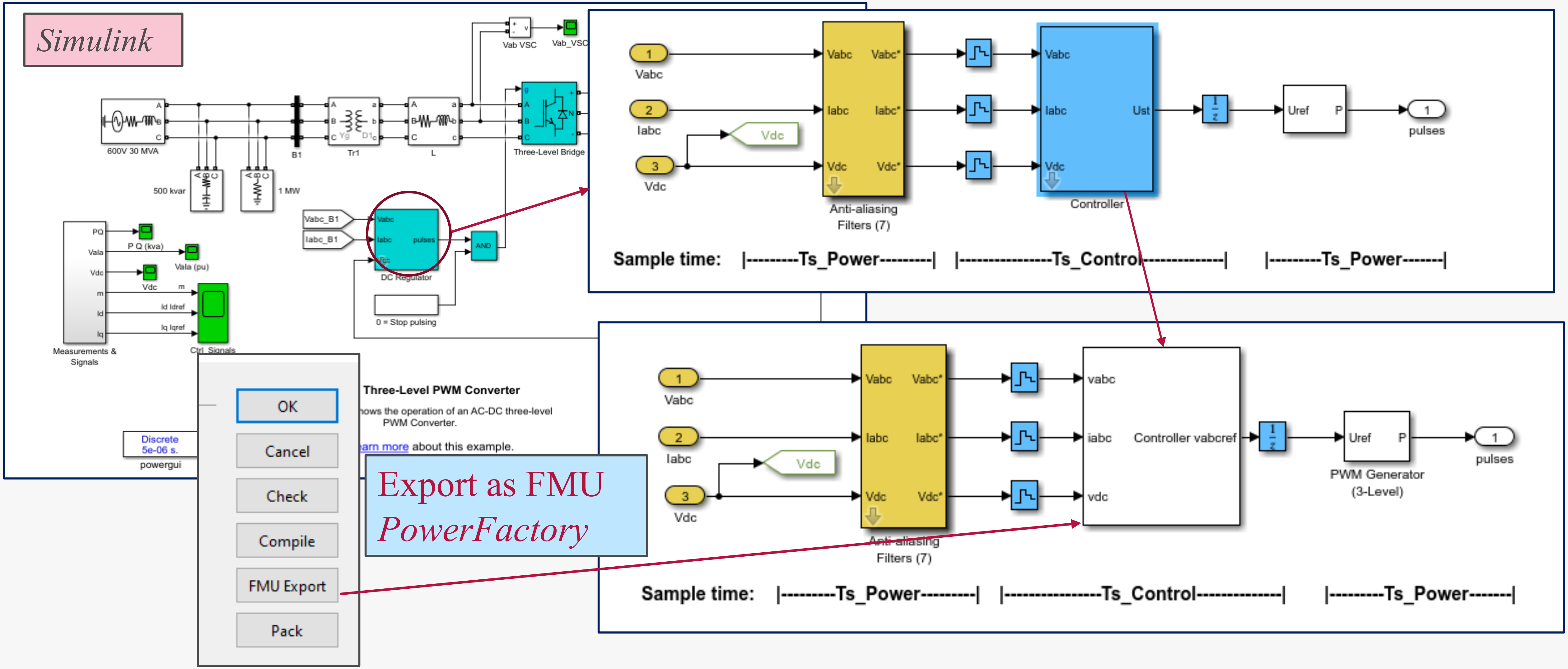

Interoperability of Modelica Models

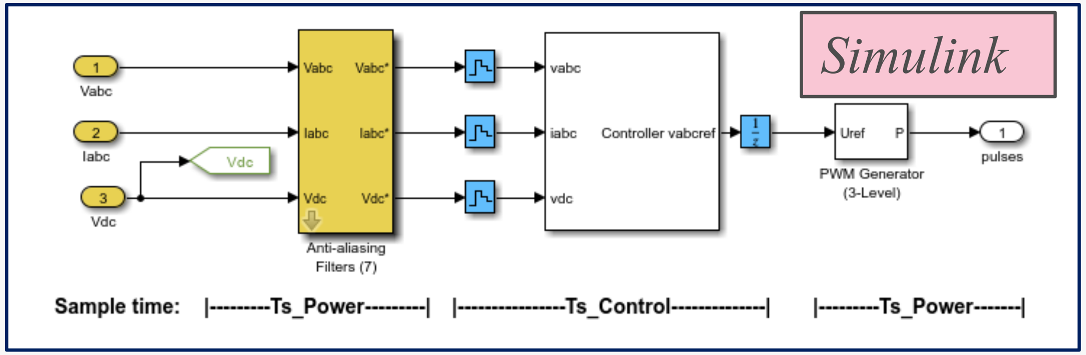

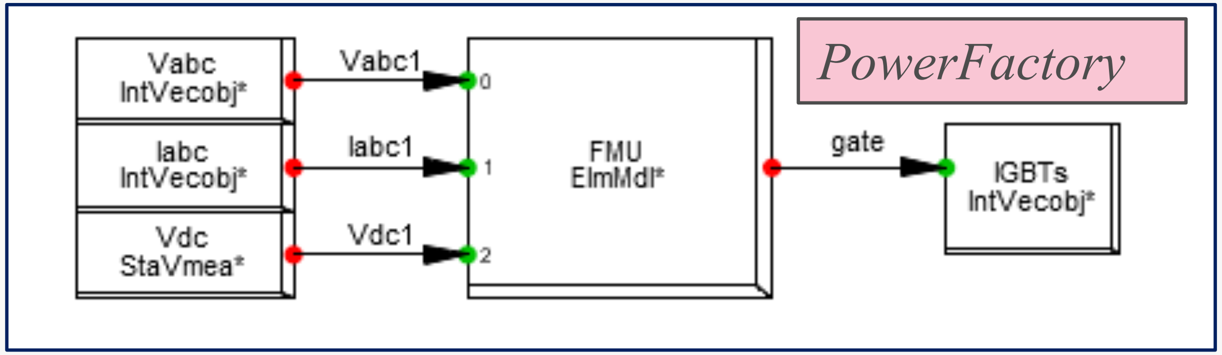

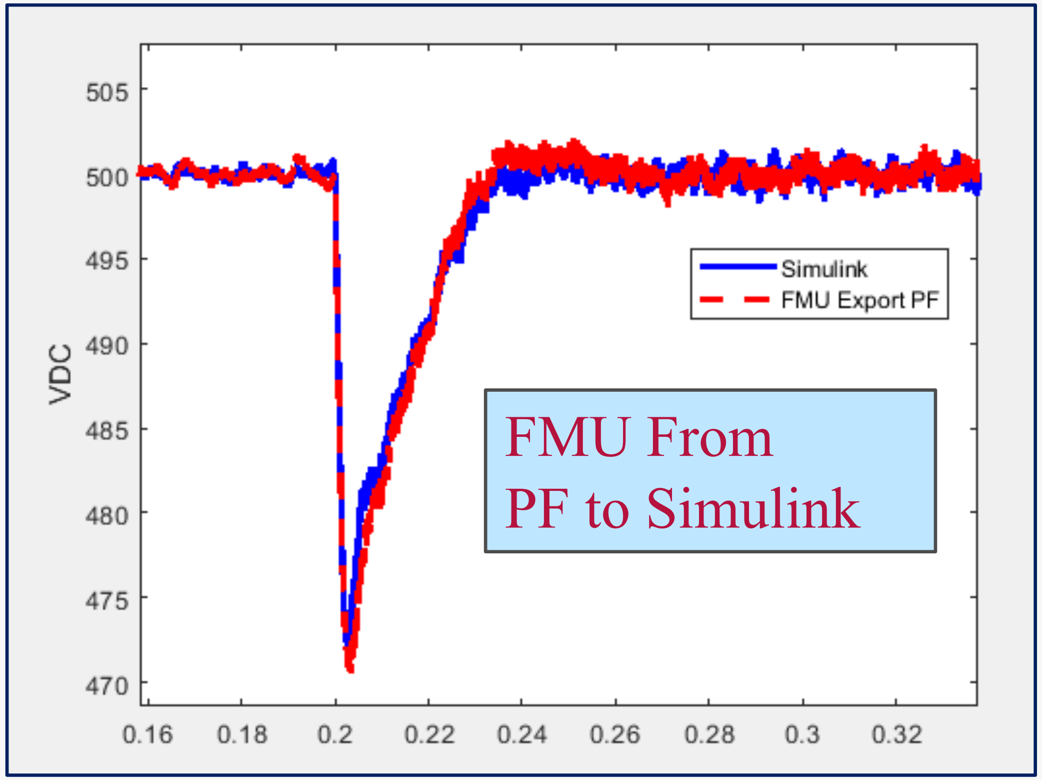

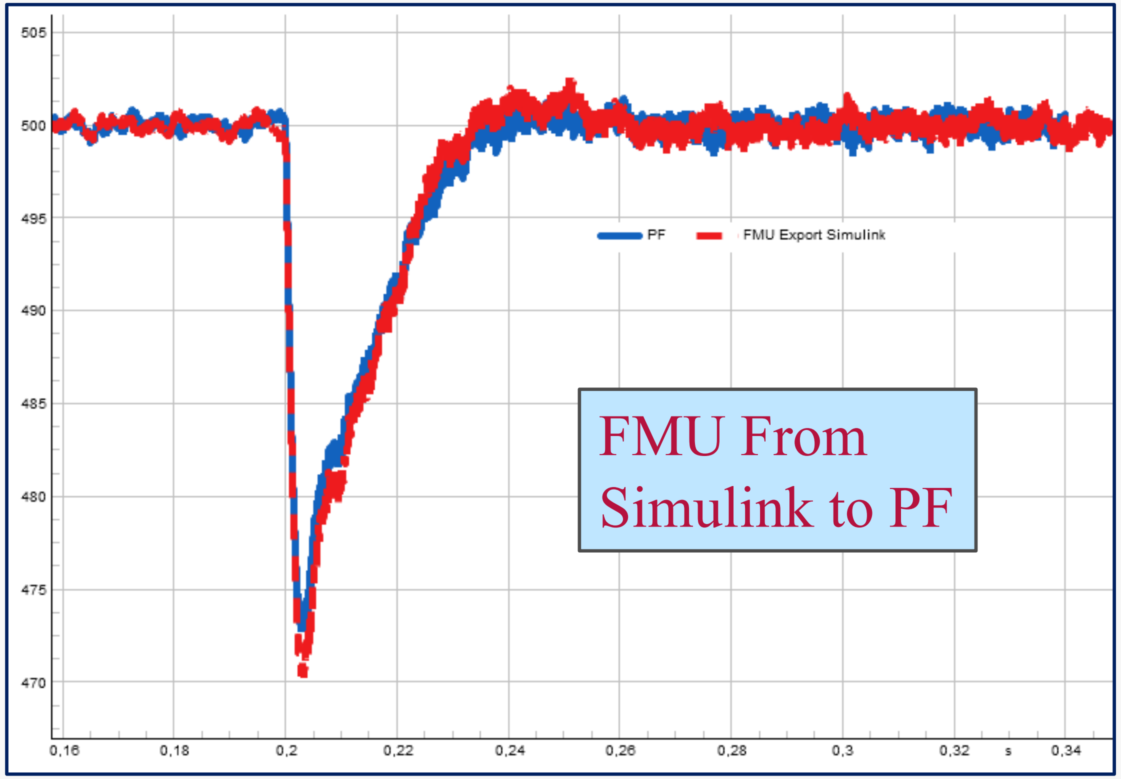

Model Validation

- **Interaction between continuous dynamic and events**
  - current and other limiters
  - switching between different controls
  - anti-windup on integrators
  - deadband
  - deadtime
  - protection
  - reset
  - blocking
  - fault ride through
- **Issues**
  - non-convergence
  - trajectory deadlock
  - toggling/chattering
  - spurious oscillations
- **Implementation and validation need to be carefully done**

- **Example: anti-windup on the PI controller**
  - compare hybrid and clocked implementation

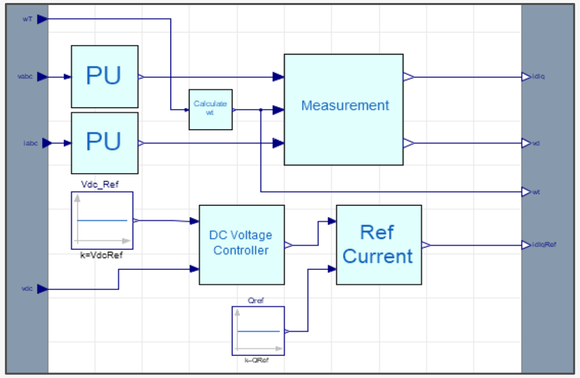

$$\text{If } y \geqslant w_{\max} : w = w_{\max} \text{ and } \dot{x} = 0 \,,$$
$$\text{If } y \leqslant w_{\min} : w = w_{\min} \text{ and } \dot{x} = 0 \,,$$
$$\text{Otherwise} : w = y = k_p u + x \text{ and } \dot{x} = k_i u \,.$$

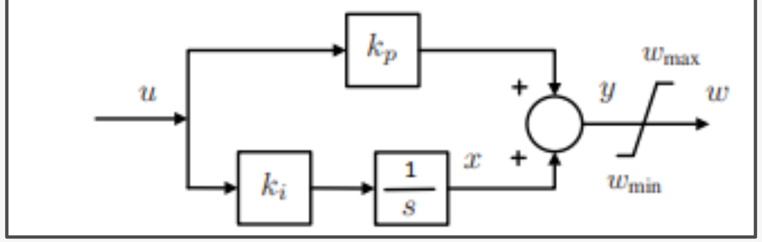

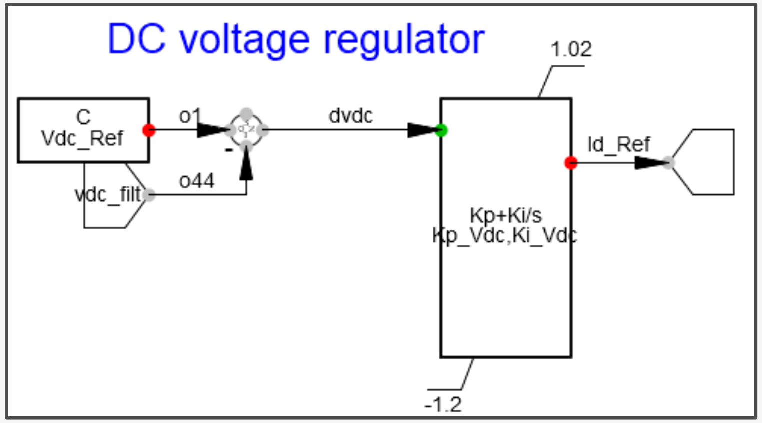

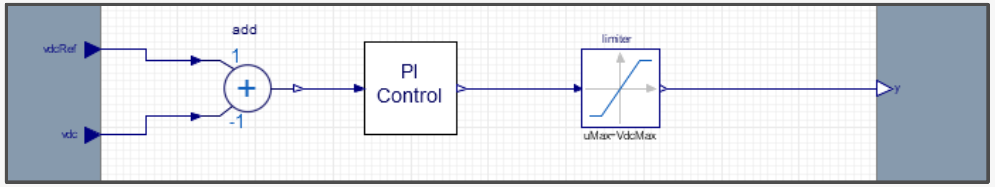

Trajectory Deadlock and Chattering

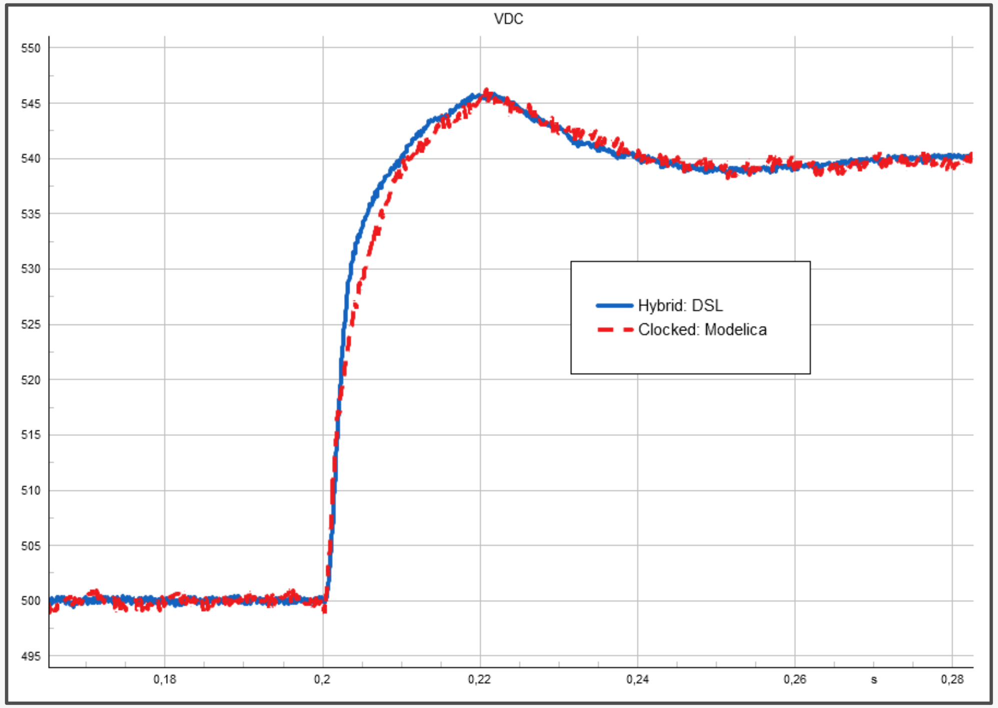

Errors (0) | Warnings (260) | Information (21) | Events (4) | Others (0) | Filter as you type | Clear all filters

```
(t=200:755 ms) No convergence. Maximum number of outer-loop iterations for dynamic model equations of element 'dsl Converter Control' has been reached.
(t=200:755 ms) No convergence. Maximum number of outer-loop iterations for dynamic model equations of element 'dsl Converter Control' has been reached.
(t=200:755 ms) No convergence. Maximum number of outer-loop iterations for dynamic model equations of element 'dsl Converter Control' has been reached.
(t=200:755 ms) No convergence. Maximum number of outer-loop iterations for dynamic model equations of element 'dsl Converter Control' has been reached.
(t=200:757 ms) No convergence. Maximum number of outer-loop iterations for dynamic model equations of element 'dsl Converter Control' has been reached.
(t=200:757 ms) No convergence. Maximum number of outer-loop iterations for dynamic model equations of element 'dsl Converter Control' has been reached.
(t=200:757 ms) No convergence. Maximum number of outer-loop iterations for dynamic model equations of element 'dsl Converter Control' has been reached.
(t=200:757 ms) No convergence. Maximum number of outer-loop iterations for dynamic model equations of element 'dsl Converter Control' has been reached.
(t=200:757 ms) No convergence. Maximum number of outer-loop iterations for dynamic model equations of element 'dsl Converter Control' has been reached.
(t=200:765 ms) No convergence. Maximum number of outer-loop iterations for dynamic model equations of element 'dsl Converter Control' has been reached.
(t=200:765 ms) No convergence. Maximum number of outer-loop iterations for dynamic model equations of element 'dsl Converter Control' has been reached.
(t=200:765 ms) No convergence. Maximum number of outer-loop iterations for dynamic model equations of element 'dsl Converter Control' has been reached.
(t=200:765 ms) No convergence. Maximum number of outer-loop iterations for dynamic model equations of element 'dsl Converter Control' has been reached.
(t=200:785 ms) No convergence. Maximum number of outer-loop iterations for dynamic model equations of element 'dsl Converter Control' has been reached.
(t=200:785 ms) No convergence. Maximum number of outer-loop iterations for dynamic model equations of element 'dsl Converter Control' has been reached.
(t=200:785 ms) No convergence. Maximum number of outer-loop iterations for dynamic model equations of element 'dsl Converter Control' has been reached.
(t=200:785 ms) No convergence. Maximum number of outer-loop iterations for dynamic model equations of element 'dsl Converter Control' has been reached.
(t=200:811 ms) No convergence. Maximum number of outer-loop iterations for dynamic model equations of element 'dsl Converter Control' has been reached.
(t=200:811 ms) No convergence. Maximum number of outer-loop iterations for dynamic model equations of element 'dsl Converter Control' has been reached.
(t=200:811 ms) No convergence. Maximum number of outer-loop iterations for dynamic model equations of element 'dsl Converter Control' has been reached.
(t=200:811 ms) No convergence. Maximum number of outer-loop iterations for dynamic model equations of element 'dsl Converter Control' has been reached.
(t=200:811 ms) No convergence. Maximum number of outer-loop iterations for dynamic model equations of element 'dsl Converter Control' has been reached.
(t=200:811 ms) No convergence. Maximum number of outer-loop iterations for dynamic model equations of element 'dsl Converter Control' has been reached.
(t=400:000 ms) Simulation successfully executed.
```

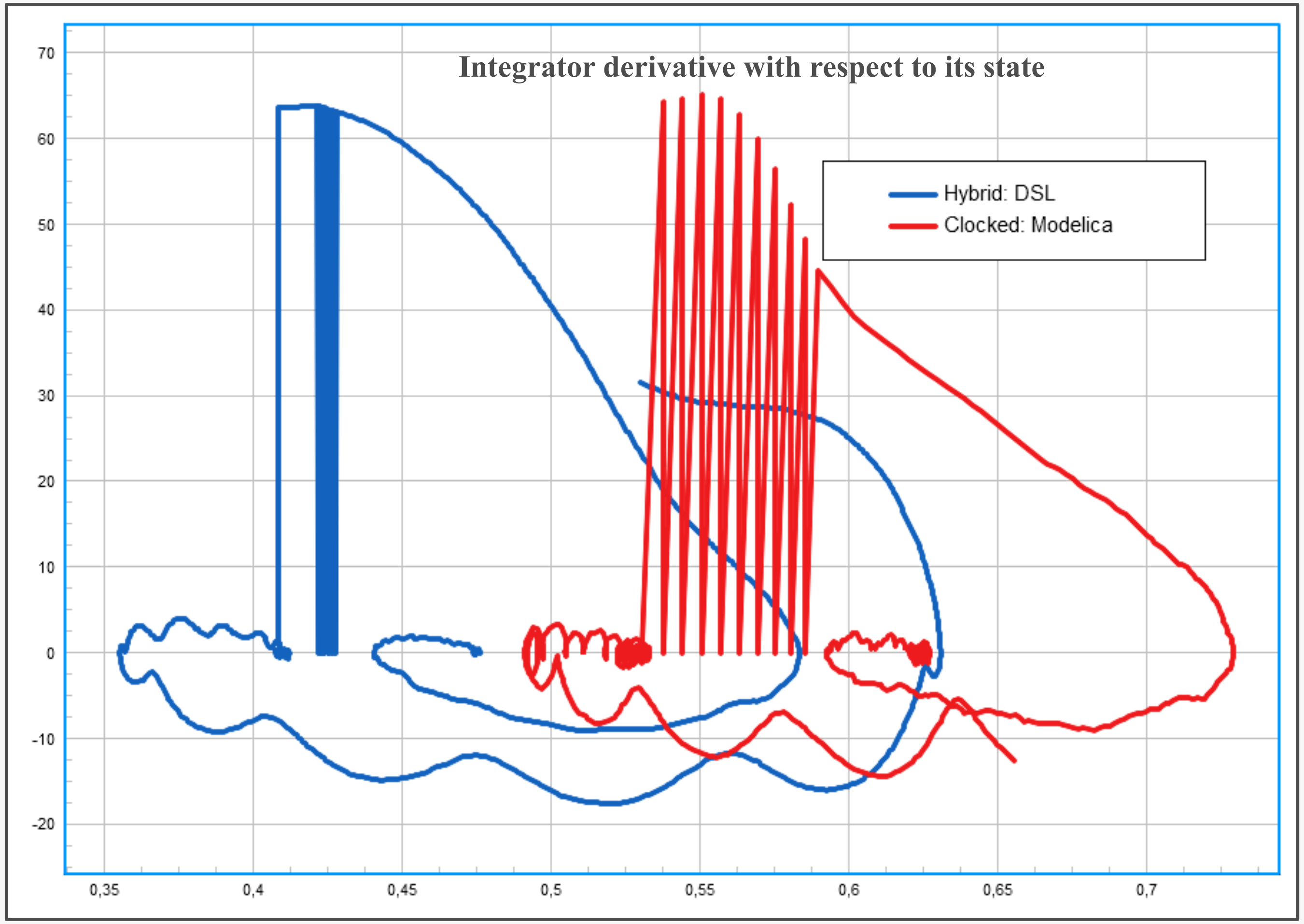

- *PowerFactory* accurately captures the trajectory deadlock and chattering
- Hybrid model: non-convergences and chattering
- Clocked model: only shows chattering

Trajectory Deadlock and Chattering

- Hybrid model implementation considering the sliding mode
- No deadlock (no non-convergence issues) and chattering
- Clocked model: possible to remove chattering

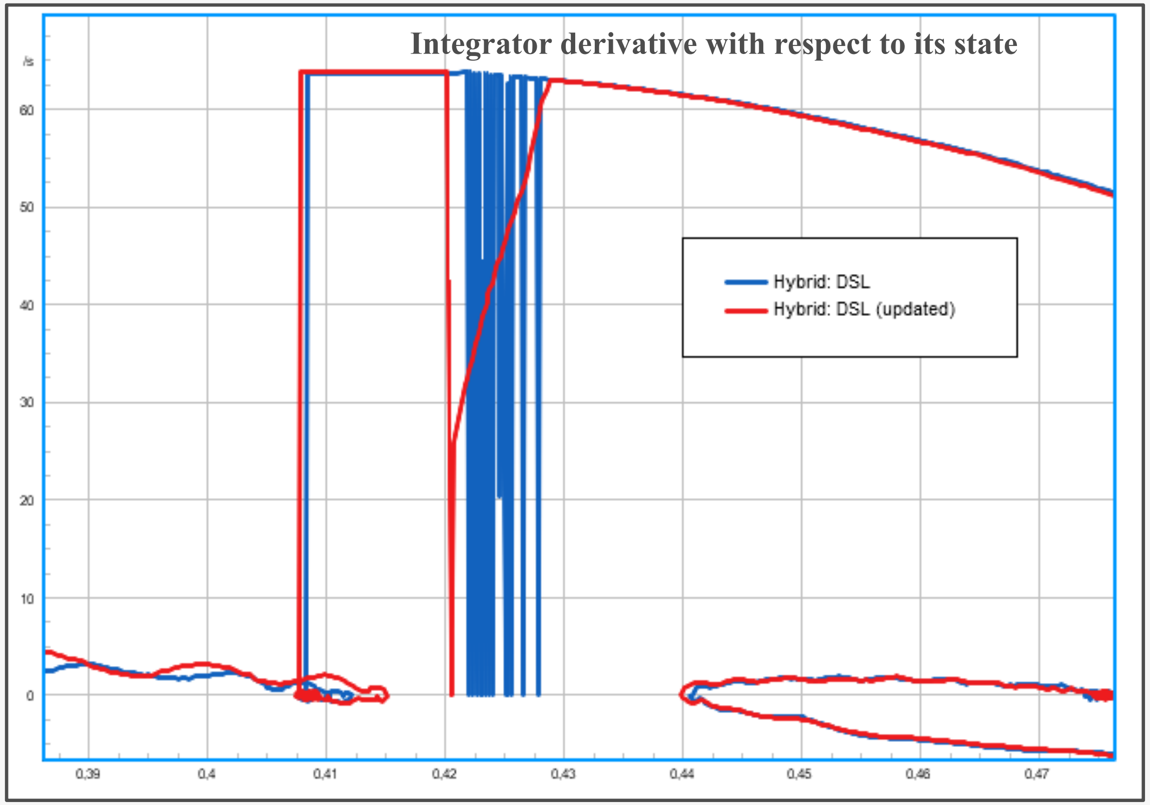

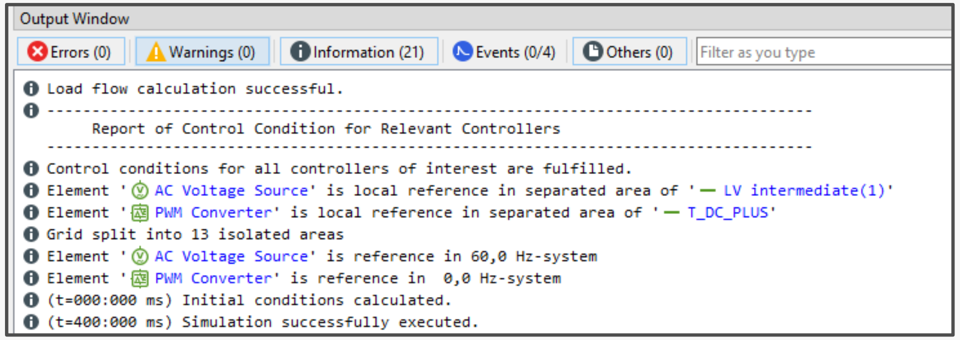

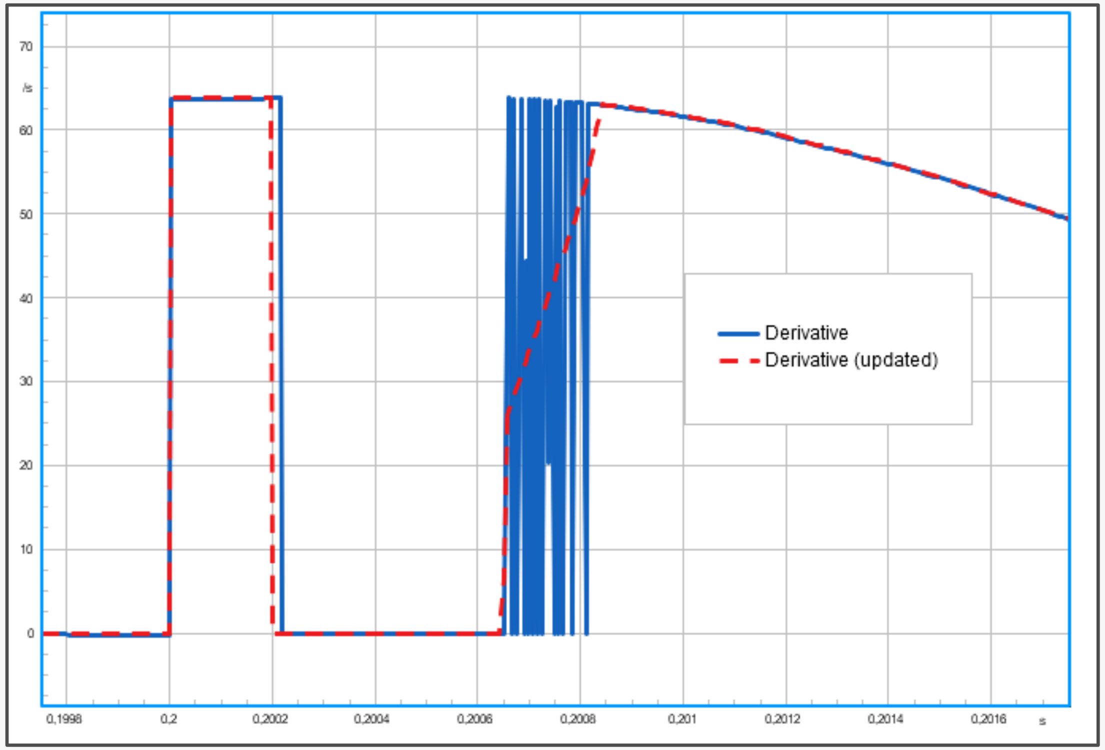

Response of the integrator derivative

Murad, Mohammed Ahsan Adib, and Federico Milano. "Chattering-free modelling and simulation of power systems with inclusion of filippov theory." *Electric Power Systems Research* 189 (2020): 106727.
Fabozzi, Davide, et al. "Semi-implicit formulation of proportional-integral controller block with non-windup limiter according to IEEE Standard 421.5-2016." *Bulk Power Systems Dynamics and Control Symposium (IREP)*. 2017.

System Studies: Unintentional Electrical Islands

- ***IEEE 1547***
  - *Island network, intended: A planned island network.*
  - *Island network, unintentional: An Unplanned Island Network.*

- **DIN VDE V 0126-1-1**
  - *In the case of unintentional islanding, this process* [islanding] *takes place outside the control of the grid operator. Voltage and frequency of the disconnected sub-network are not to be influenced by the grid operator*

- **DIN VDE V 0126-2**
  - "[...] *an island that is intentionally generated, usually to restore power to the utility system affected by a disturbance or to maintain supply. The generation and loads may be with any combination of customer-owned and utility-owned facilities, but there is an unspoken or explicit agreement between the controlling utility and the operators at the customer-owned generating station for this situation.*"

- **Unintentional islanding:** *serious challenge due to the increasing number of converter interfaced distributed generation (DGs)*

IEEE: 1547 IEEE Standard for Interconnecting Distributed Resources with Electric Power Systems (2003)
VDE: DIN VDE 0126-1-1 Automatic switching point between a grid-parallel self-generation system and the public low-voltage grid. Vol. 1, 2013

Detection Methods

- Voltage and frequency can not be controlled or influenced by the network operator
- A successful automatic reclosing is reduced
- Liability for damages

- **Why island detection?**
  - A disconnection unit is implemented in each DG
  - Disconnects the DG from the electrical grid, if voltage and frequency exceed bounds

- **References**

  - S. Palm and P. Schegner, "Fundamentals of detectability and detection methods of unintentional electrical islands," *2015 IEEE Eindhoven PowerTech*, Eindhoven, Netherlands, 2015, pp. 1-6.
  - Palm, Sebastian. *Untersuchung und Bewertung von Verfahren zur Inselnetzerkennung,-prognose und-stabilisierung in Verteilnetzen*. BoD–Books on Demand, 2019.

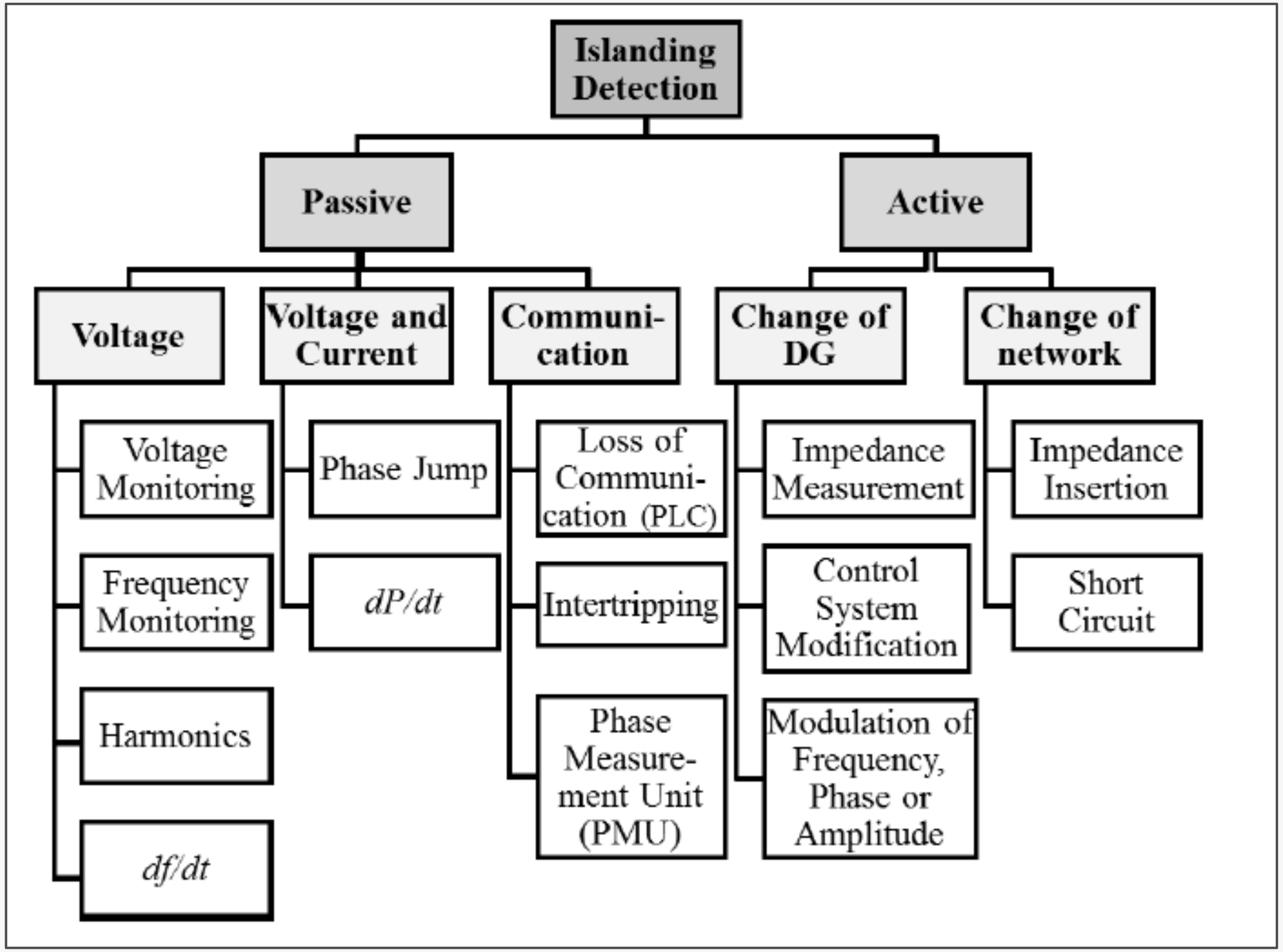

Network Model

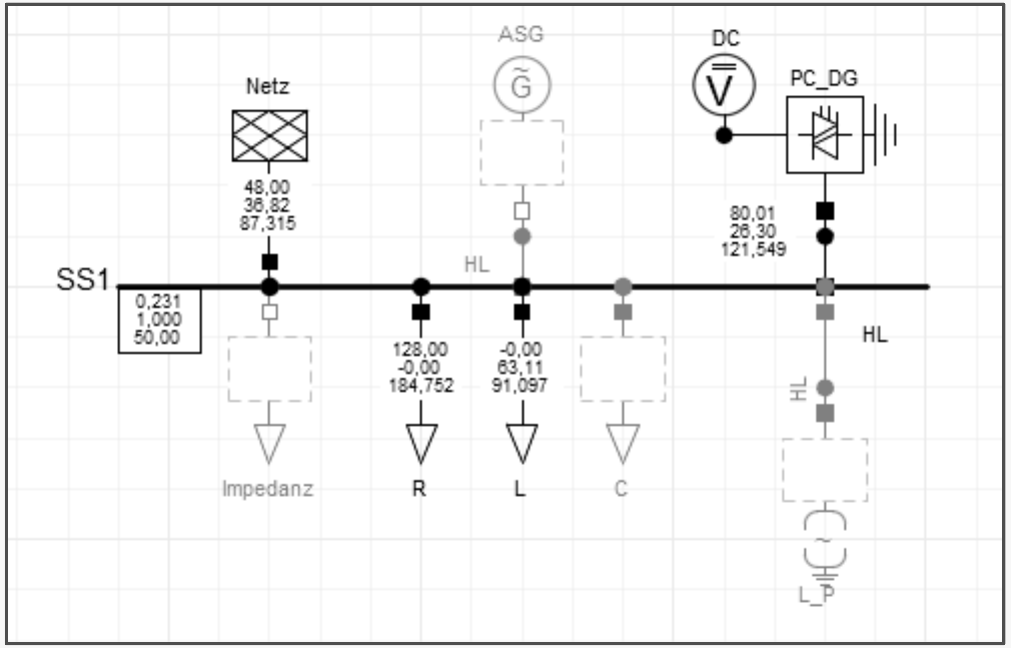

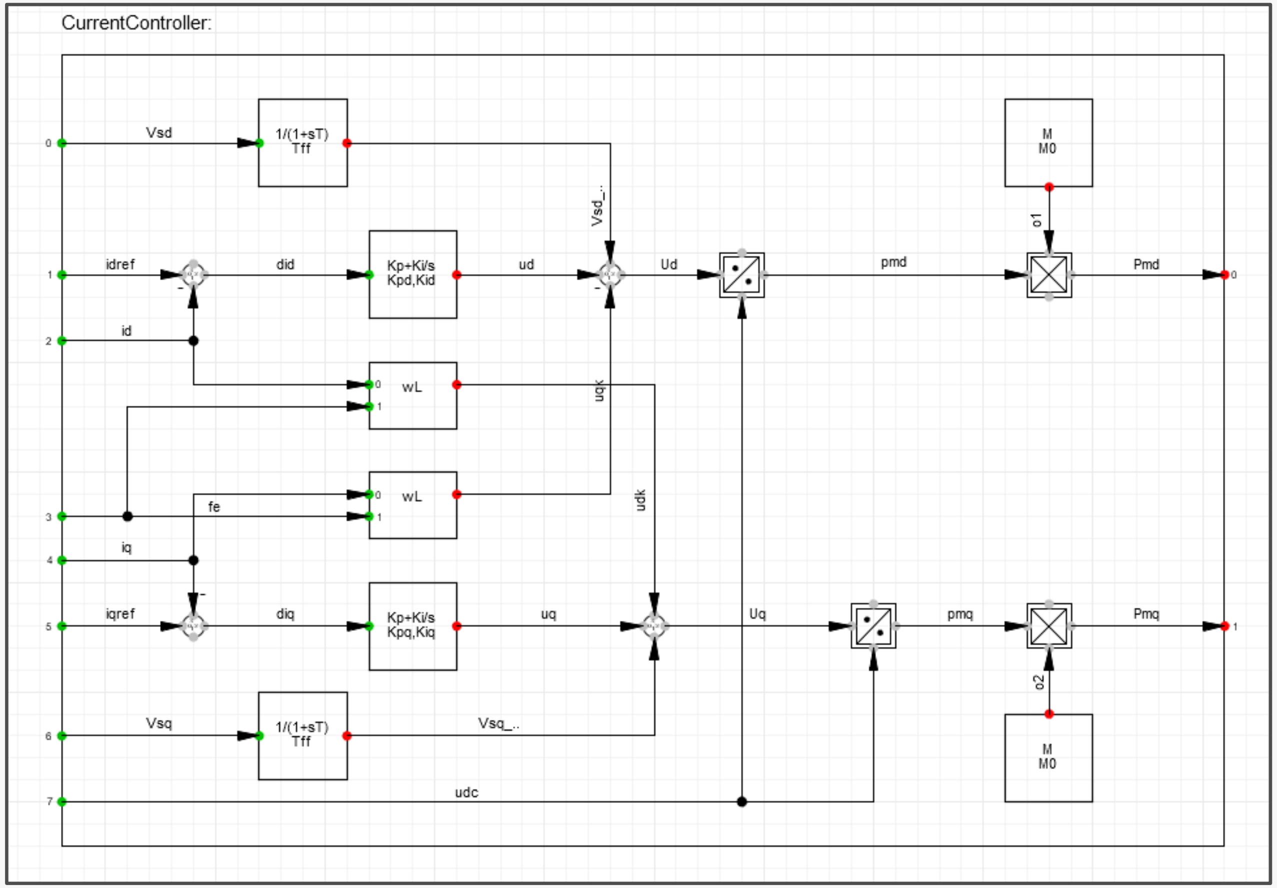

$$\Delta P_{\mathrm{DG}} = 20 \cdot P_{\mathrm{M}} \cdot \frac{50.2 - f\,/\mathrm{Hz}}{50}$$

Results

- Type of distributed generation: inverter
- Load type: R-L
- Detection method: voltage and frequency based
- Simulation:
  - each square with a side length 5%
  - 1025 simulations in each scenario
  - automate using DPL scripting

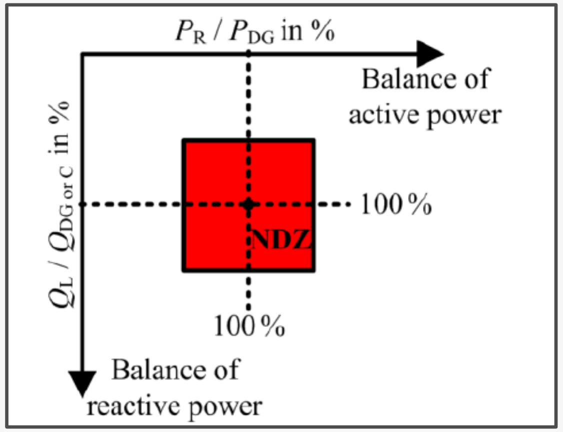

- A_{NDZ} in sq%
  - Without P(f): 650, With: 3475
- Reacting to frequency-dependent power reduction makes around 5 times bigger

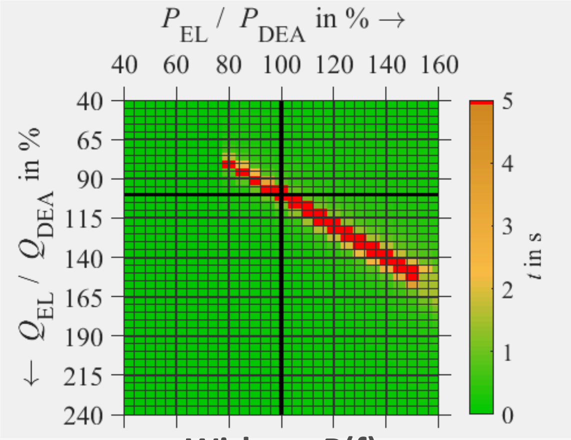

Without P(f)

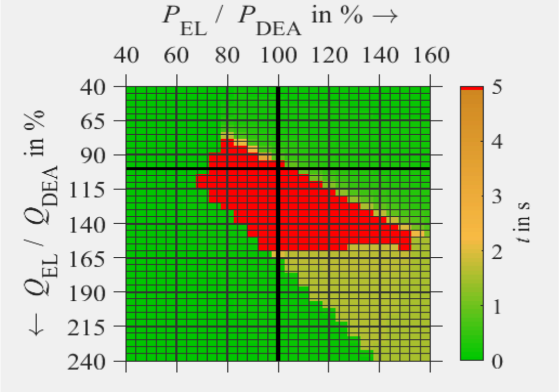

With P(f)

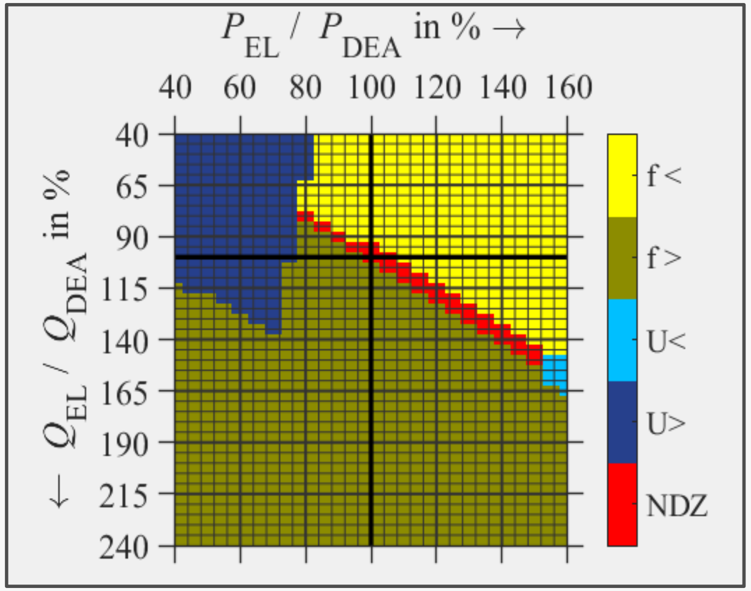

Without P(f)

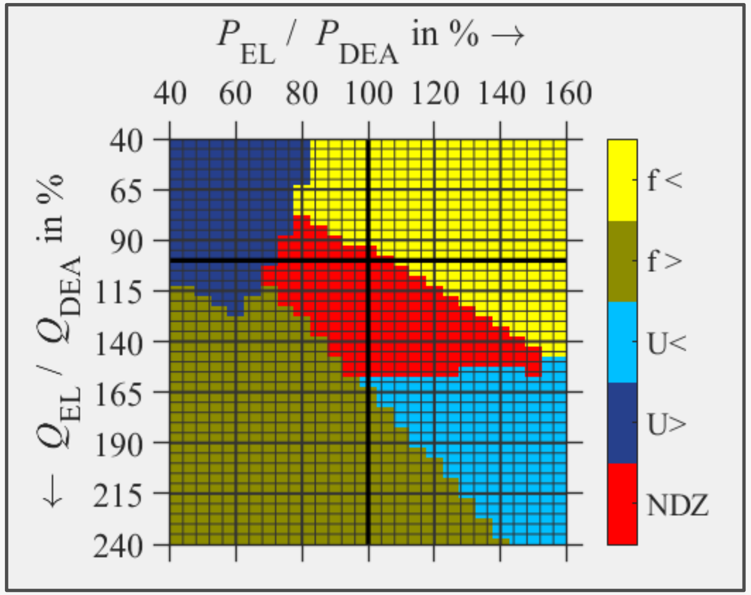

With P(f)

Conclusions

- DIgSILENT *PowerFactory* capabilities on modeling and simulation to study dynamic performance at different time scales with converter-interfaced technologies
- Modeling: DSL and Modelica
- Modelica models are interoperable as model exchange and co-simulation using FMI standard
- Manufacturer-sourced control model import using FMI standard
- Model validation challenges
- System study: unintentional islands will become more frequent with the increasing number of distributed generation

Thank you for your attention

Ahsan Murad
a.murad@digsilent.de

Break: see you in 15 minutes!

PowerTech Belgrade 2023

LEADING INNOVATIONS FOR RESILIENT & CARBON-NEUTRAL POWER SYSTEMS

25-29 JUNE, 2023, BELGRADE, SERBIA

Junru Chen

Junru Chen (S'17, M'19) received the Ph.D. in 2019 and the ME Electrical Energy Engineering in 2016 from University College Dublin, Dublin, Ireland. He was a Senior Researcher in University College Dublin and visiting scholar in Aalborg University, Denmark in 2020. He was a visiting doctoral student in Kiel University, Germany in 2018 and Tallinn University of Technology, Estonia, in 2019. Since 2020 he is an Associate Professor at Xinjiang University, China. He has been honored with the 2019 Chinese Government Award for Outstanding Self-financed Students Abroad. His current research interests include power electronics control, modeling, stability, and application.

新疆大學 Xinjiang University

Synchronization Stability of Grid-Connected Converters

Junru Chen

junru.chen@xju.edu.cn

Outline

1 Concept

1.1 Concept: *Synchronization Stability*

- **Synchronization Stability Definition**

➢ The ability of the **Synchronous machines** to remain synchronized to the grid after being subjected to a large disturbances (Original: conventional power system)

➢ The ability of the **electrical device or the system** to remain synchronized to the grid or other systems after being subjected to various disturbances (Extended: modern power system)

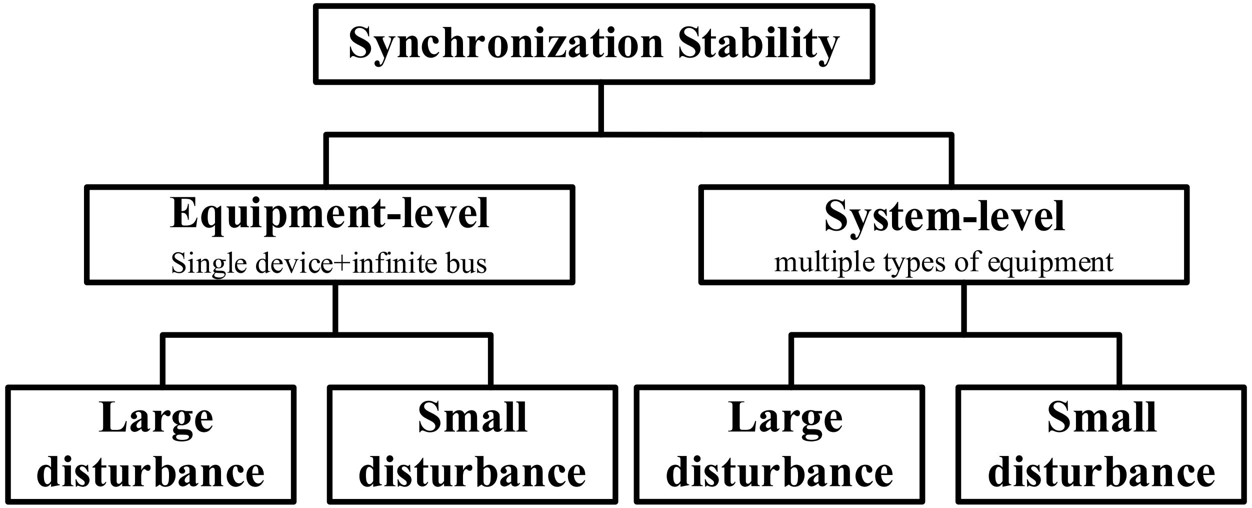

- Large disturbance: Nonlinear, electromechanical transient (100ms), Low-order model.
- Small disturbance: Linearization, electromagnetic transient (1ms), high-dimension model.

1.2 Concept: *Grid-Connected Convert*

- **Grid-Forming Convert (GFM)**

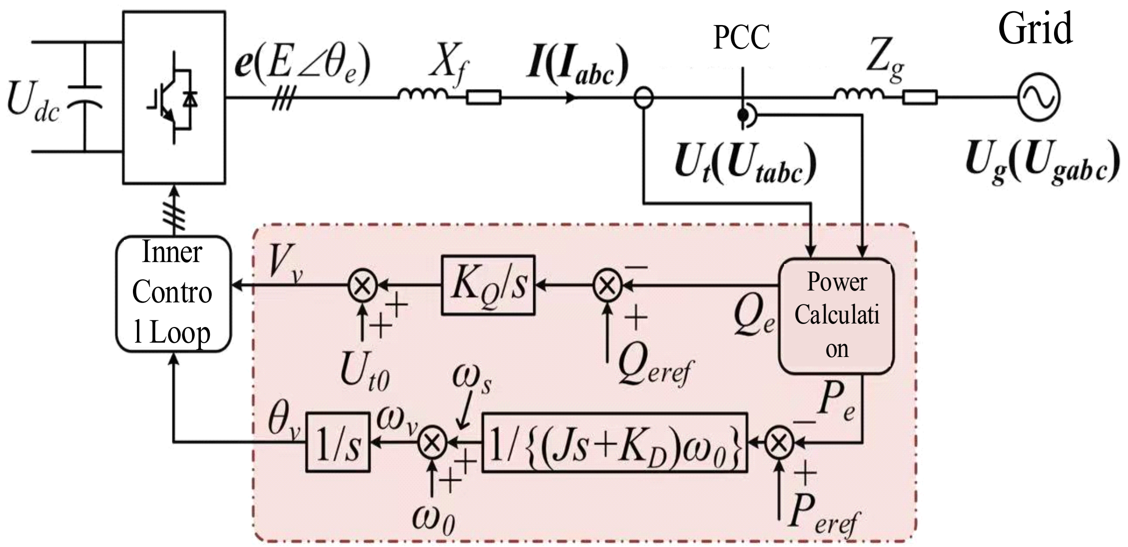

Grid-feeding Converter Features:

- GFM equipment can be used as an independent power source to supply power to the load
- Controlled voltage source

- **Grid-Following Convert (GFL)**

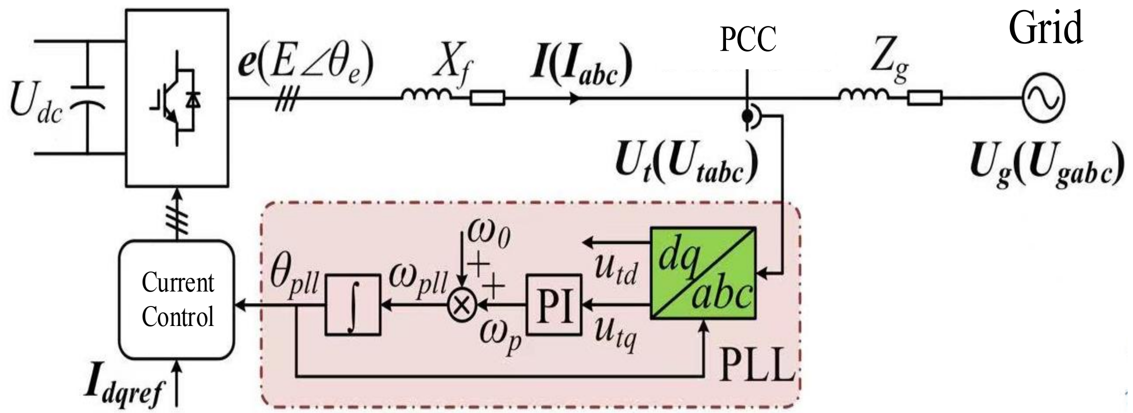

Grid-following Converter Features:

- Relying on the phase-locked loop PLL to observe the PCC voltage of the common coupling point to complete the grid connection;
- Controlled current source.

1.2 Grid-connected Converter

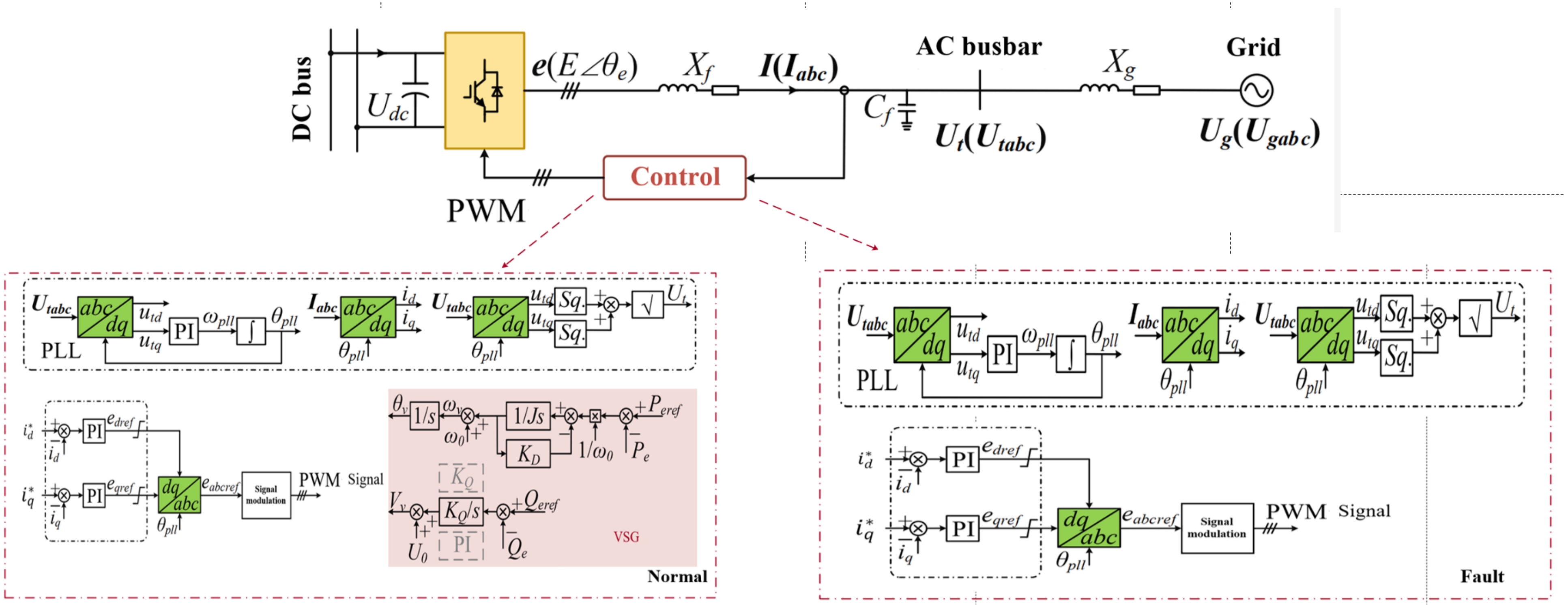

When the grid-connected inverter is **operating in the normal condition**, its control strategy can be **grid-following control or grid-forming control.**

When the grid-connected inverter is **operating in the fault condition**, its control strategy turns to be **grid-following control mode** to limit the fault current.

2 Modelling

2 Modelling

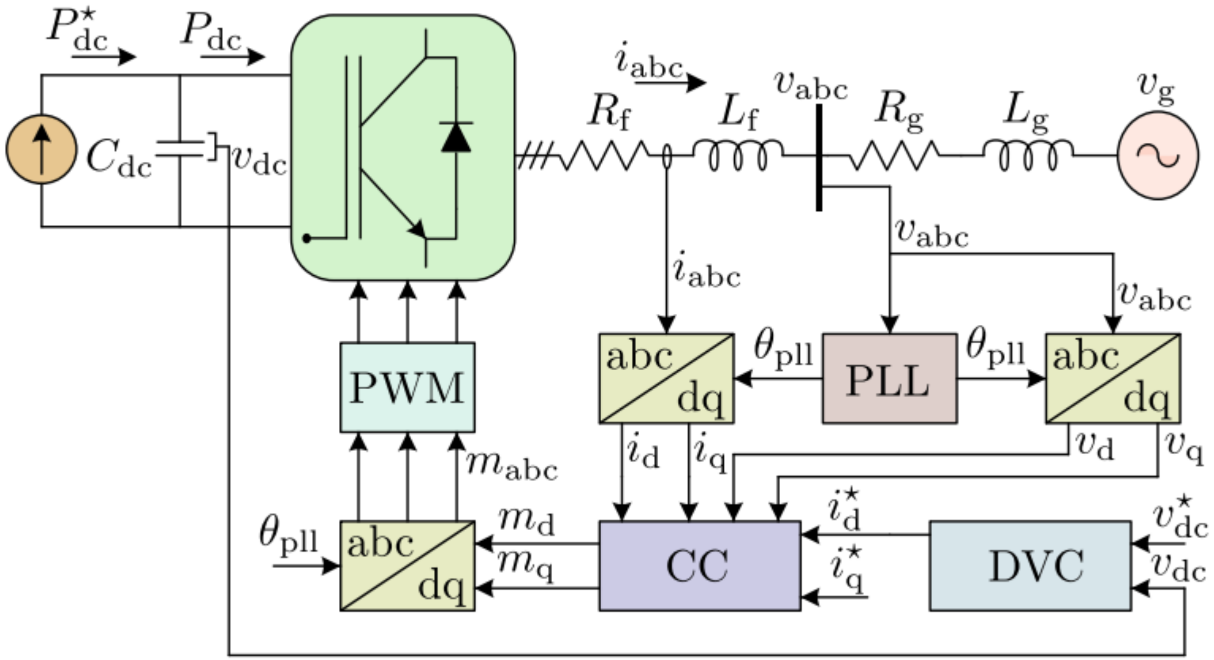

CC – current controller
DVC – dc-bus voltage controller
PLL – phase-locked loop

The full model of the grid-feeding converter can be seperated into four parts including **electric circuit, PLL , current control dynamics** and **DC-Bus voltage control dynamics.**

2.1 Modelling: *Full Model*

- Electric circuit

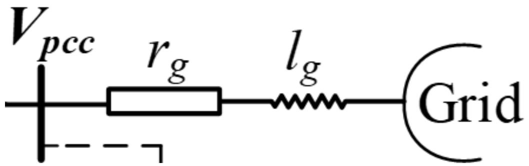

$$\begin{bmatrix} v_d \\ v_q \end{bmatrix} = \begin{bmatrix} cos\delta & sin\delta \\ -sin\delta & cos\delta \end{bmatrix}\begin{bmatrix} v_g \\ 0 \end{bmatrix} + R_g\begin{bmatrix} i_d \\ i_q \end{bmatrix} + \omega_{pll}L_g\begin{bmatrix} -i_q \\ i_d \end{bmatrix}$$

- PLL dynamic

$$\frac{d\delta}{dt} = \Delta\omega_{pll} = \omega_{pll} - \omega_n$$

$$\frac{d\Delta\omega_{pll}}{dt} = k_p^{pll}\frac{dv_q}{dt} + k_i^{pll}v_q$$

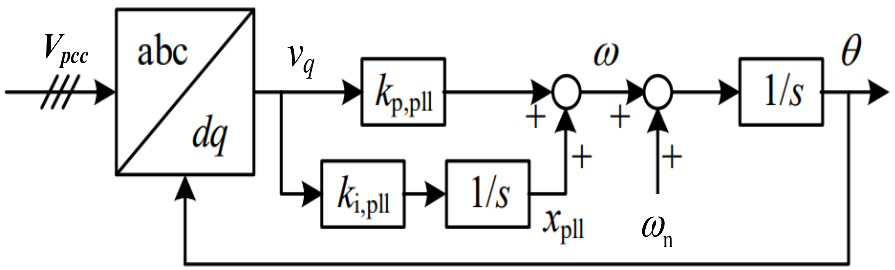

- Current control dynamic

$$\begin{cases} e_{dref} = k_{ip}(i_{dref} - i_d) + \int k_{ii}(i_{refd} - i_d)dt \\ e_{qref} = k_{ip}(i_{qref} - i_q) + \int k_{ii}(i_{refq} - i_q)dt \end{cases}$$

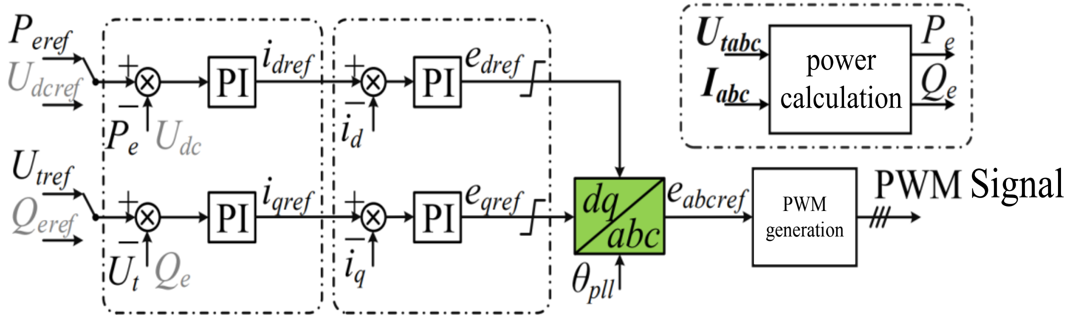

- DC-Bus voltage dynamic

$$\frac{1}{2}C_{dc}\cdot\frac{d\left(v_{dc}^2\right)}{dt} = v_{dc}I_c - v_{dc}i_{dc}$$

$$\begin{cases} \dfrac{d\gamma_{dc}}{dt} = v_{dc}^2 - v_{dc}^{\star 2} \\ i_d^{\star} = k_p^{dc}\dfrac{d\gamma_{dc}}{dt} + k_i^{dc}\gamma_{dc} \end{cases}$$

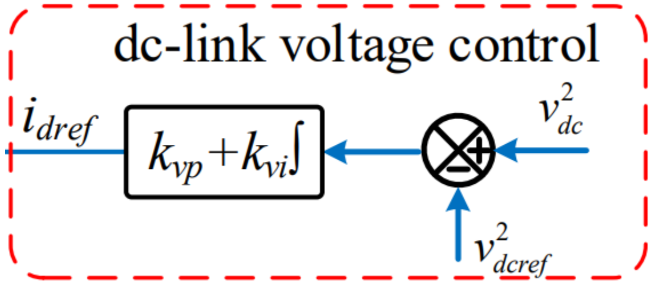

2.1 Modelling: *Full Model(Time Scale)*

The grid-connected convert system contains **multiple control loops** in the **multiple time scales**.

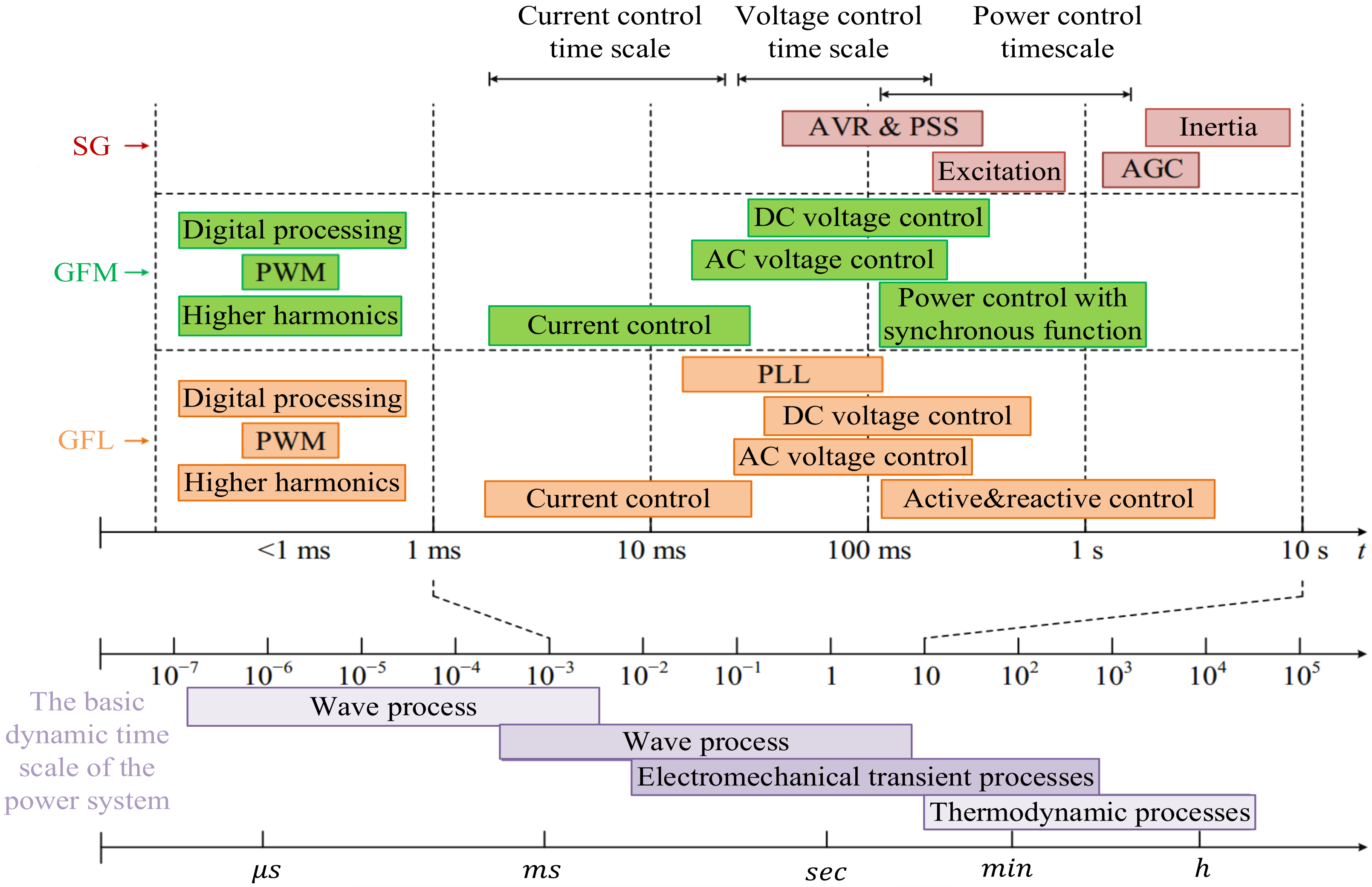

2.2 Modelling: *PLL Dynamics Effect (2nd QSLS Model)*

- Synchronization transients at PCC:

$$V_c = V_g - I_c Z_g$$

$$v_q = V_g \sin(-\delta_{pll}) + r_g i_q + \omega_{pll} l_g i_d$$

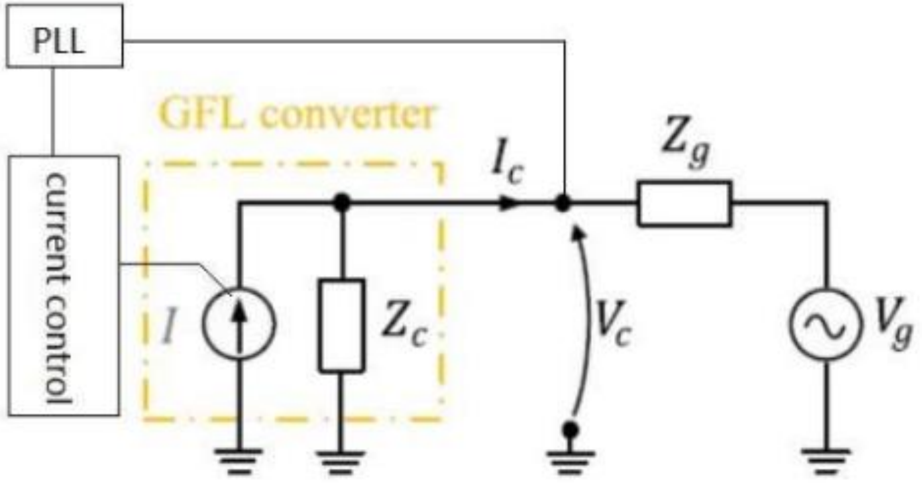

<u>The grid impedance makes the PCC voltage coupling with the converter output</u>

2.2 Modelling: *PLL Dynamics Effect (2nd QSLS Model)*

- Time Scale : ***PLL dynamic***

The dynamics of the current controller is much **faster than** the PLL mechanism

➢ **Neglecting the current controller transients** and converter works on the **constant current mode**

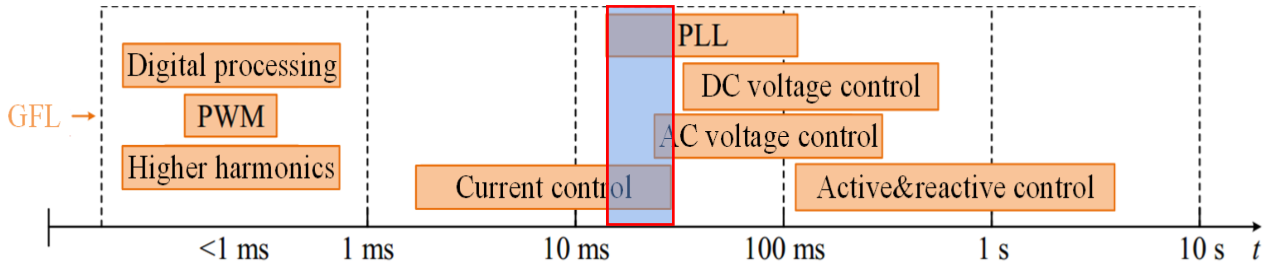

$$\frac{d\delta_{pll}}{dt} = \Delta\omega_{pll}$$

$$\Delta\omega_{pll} = K_{ppll} v_q + \int K_{ipll} v_q$$

$$v_q = \underbrace{V_g \sin(-\delta_{pll})}_{\text{Grid synchronization}} + \underbrace{r_g i_q^* + \omega_{pll} l_g i_d^*}_{\text{Self-synchronization}}$$

QLSL model

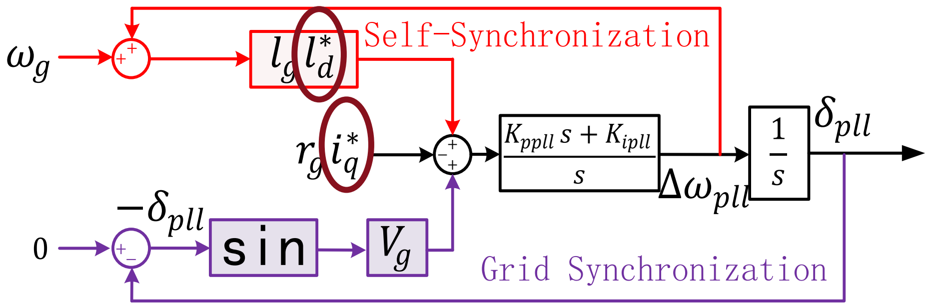

Quasi-Static Large-Signal (QSLS) model of the PLL

2.3 Modelling: *Current Control Dynamic Effect (4^nd QLSL Model)*

- The grid-following converter is based on the voltage sourced converter (VSC), of which PWM directly drives the terminal voltage output.
- At the instant of fault, due to a delayed action in the current controller, the VSC terminal voltage remains unchanged, and resulting in an significant fault current in transients.

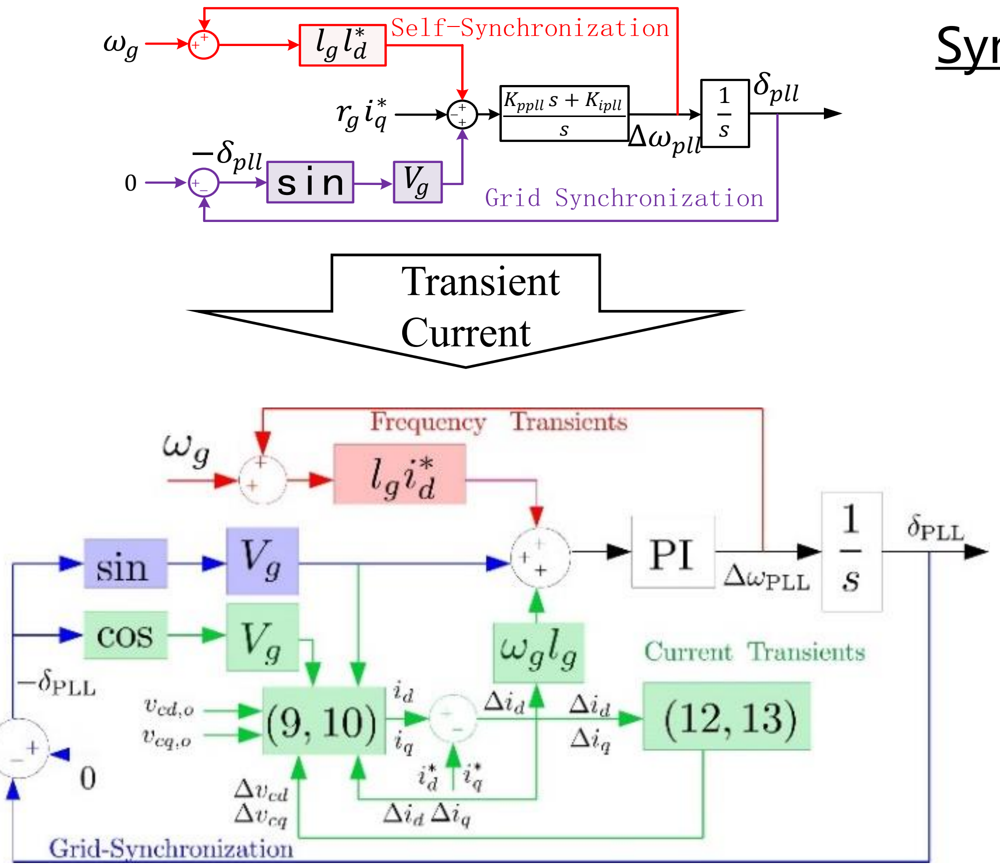

Synchronization transients at PCC:

$$v_q = V_g \sin(-\delta_{pll}) + (\omega_g + \Delta\omega_{pll}) l_g (i^*_d + \Delta i_d)$$

Current transients

$$i_d = \frac{v_{cd} - v_d}{\omega_{pll} l_f}$$

$$i_q = -\frac{v_{cq} - v_q}{\omega_{pll} l_f}$$

Current Controller

$$\Delta v_{cd} = K_{pc}\Delta i_d + \int K_{ic}\Delta i_d - \omega_{pll} l_f \Delta i_q$$

$$\Delta v_{cq} = K_{pc}\Delta i_q + \int K_{ic}\Delta i_q - \omega_{pll} l_f \Delta i_d$$

Converter Voltage

$$v_{cd,0} + \Delta v_{cd} = V_g \cos(-\delta_{pll}) + \omega_{pll}(l_f + l_g)(i_q^* + \Delta i_q)$$

$$v_{cq,0} + \Delta v_{cq} = V_g \sin(-\delta_{pll}) - \omega_{pll}(l_f + l_g)(i_d^* + \Delta i_d)$$

2.3 Modelling: *Current Control Dynamic Effect* (*4nd QLSL Model*)

A real-time Electromagnetic Transients (EMT) simulation solved in Matlab/Simulink is used to validate the 4th-order model in comparison with the conventional QSLS methods.

Parameter	Value
Nominal voltage $V_{g,0}$	10kv
Rated Capacity	1MVA
Nominal frequency ω_g	50HZ
PLL PI $K_{p,pll}$ / $K_{i,pll}$	0.022/0.392
Current limit in amplitude	81.65A
l_g	0.1H
Maximizing the active power during the voltage(i_d^*, i_q^*)	81.65A ,0A

- Case 1: $l_f = 0.12\ H$, $K_{pc} = 1200$, $K_{pi} = 2433$; for which the current controller time constant is 0.1 ms.
- Case 2: $l_f = 0.12\ H$, $K_{pc} = 240$, $K_{pi} = 486.6$; for which the current controller time constant is 0.5 ms.
- Case 3: $l_f = 0.05\ H$, $K_{pc} = 500$, $K_{pi} = 2433$; for which the current controller time constant is 0.1 ms.
- Case 4: $l_f = 0.05\ H$, $K_{pc} = 100$, $K_{pi} = 486.6$; for which the current controller time constant is 0.5 ms.

2.3 Modelling: *Current Control Dynamic Effect* (*4th QLSL Model*)

Minimum fault voltage (pu) for which the converter remains stable as computed by the different methods for the different cases. *The higher the value of voltage, the lower the synchronization stability

Case	1	2	3	4
(l_f, t_s)	Large filter small controller time constant	Large filter large controller time constant	Small filter small controller time constant	Small filter small controller time constant
QSLS	0.341	0.341	0.341	0.341
Proposed	0.362	0.439	0.382	0.543
EMT	0.363	0.449	0.386	0.569

The minimum allowable grid voltage sag, when the converter is critically stable.

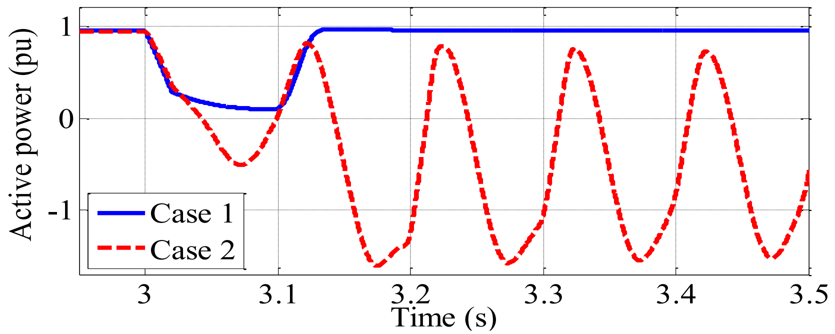

Comparison between QSLS\4th-order

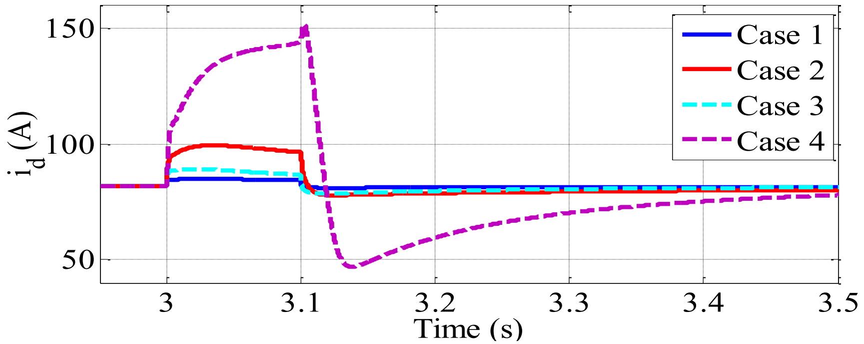

d-axis current transient result when V_g steps down to 0.569 pu and recovered at 3.1 s

① The increase of the current controller time constant decreases the synchronization stability.
② The reduction in the filter inductance worsens the synchronization.
③ The 2nd QSLS method cannot capture the transient repones in above scenarios.

2.4 Modelling: *Current Control Dynamic Effect (Feed-forward QLSL Model)*

***Feed-forward control objectives*:**

- ✓ Feeding the PCC voltage into the converter control
- ✓ Decouple the converter control from the AC system
- ✓ Speed up the current control transients

Advantage:

- ➢ This could help decouple the current control dynamics from the PLL dynamics
- ➢ This could help alleviate the negative impact from the current transients.
- ➢ This potentially can improve the synchronization stability.

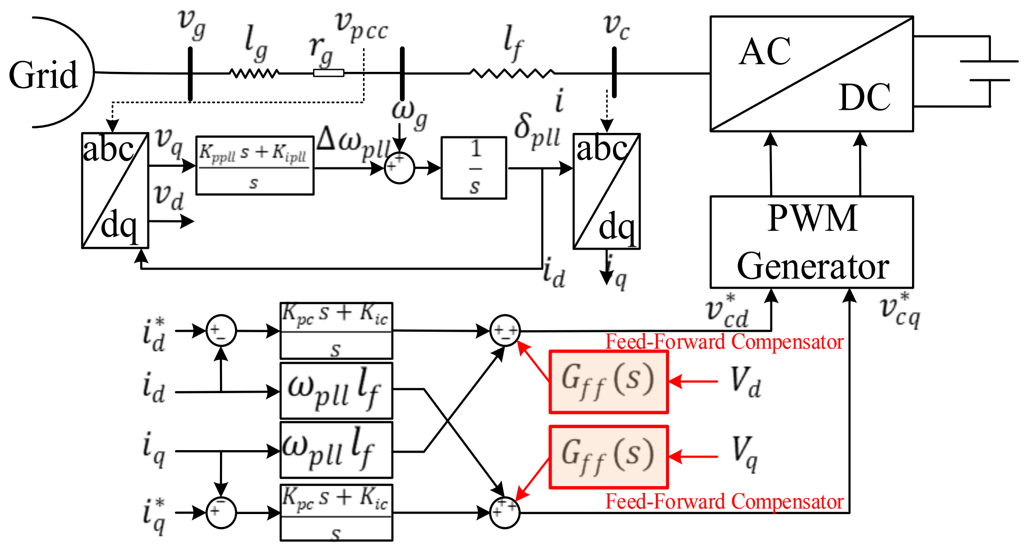

2.4 Modelling: *Current Control Dynamic Effect (Feed-forward QLSL Model)*

We modified QSLS model into a 4th-order model by including the current control dynamics and the current flow from the converter terminal.

$$\Delta v_{cd} = K_{pc}\Delta i_d + \int K_{ic}\Delta i_d - \omega_{pll} l_f \Delta i_q + G_{ff}(s)\Delta v_d$$

$$\Delta v_{cq} = K_{pc}\Delta i_q + \int K_{ic}\Delta i_q - \omega_{pll} l_f \Delta i_d + G_{ff}(s)\Delta v_q$$

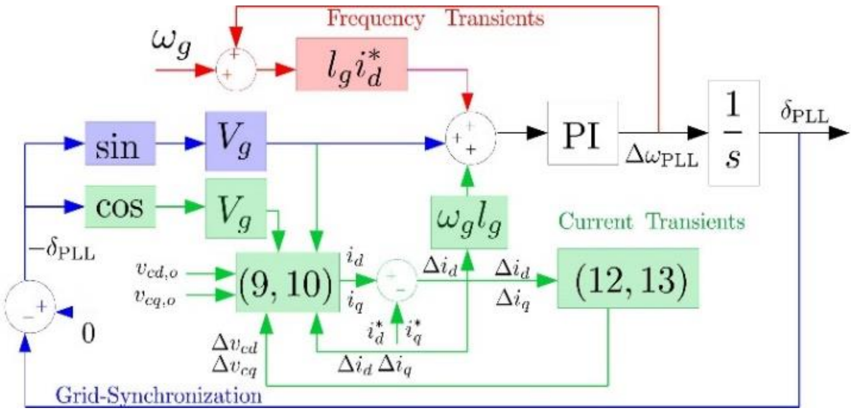

feed-forward compensator

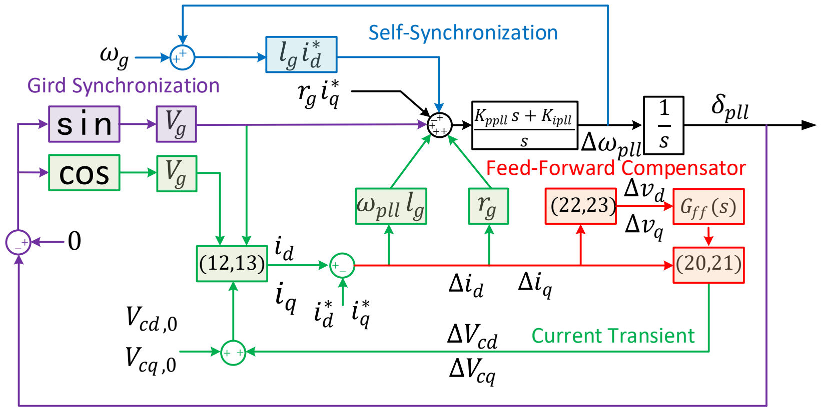

Current transients

$$i_d = \frac{v_{cd} - v_d}{\omega_{pll} l_f}$$

$$i_q = -\frac{v_{cq} - v_q}{\omega_{pll} l_f}$$

Current Controller

$$\Delta v_{cd} = K_{pc}\Delta i_d + \int K_{ic}\Delta i_d - \omega_{pll} l_f \Delta i_q + G_{ff}(s)\Delta v_d$$

$$\Delta v_{cq} = K_{pc}\Delta i_q + \int K_{ic}\Delta i_q - \omega_{pll} l_f \Delta i_d + G_{ff}(s)\Delta v_q$$

Converter Voltage

$$v_{cd,0} + \Delta v_{cd} = V_g \cos(-\delta_{pll}) + \omega_{pll}(l_f + l_g)(i_q^* + \Delta i_q)$$

$$v_{cq,0} + \Delta v_{cq} = V_g \sin(-\delta_{pll}) - \omega_{pll}(l_f + l_g)(i_d^* + \Delta i_d)$$

2.4 Modelling: *Current Control Dynamic Effect (Feed-forward QLSL Model)*

- Without the feed-forward compensator, the changed terminal voltage is merely compensated by the integral part of the current control at the settling time t_s :

$$\int_0^{t_s} K_{ic}\Delta i = \Delta v_{c,t_s} = v_{g,t_s} - v_{g,0}$$

- However, with the feed-forward compensator, the changed terminal voltage is fully compensated by the feed-forward voltage:

$$\Delta v_{t_s} = v_{g,t_s} - v_{g,0}$$

- And then the integral part stabilizes at 0:

$$\int_0^{t_s} K_{ic}\Delta i = 0$$

$$|v_{g,t_s} - v_{g,0}| > 0$$

The accumulation of the integral in the converter without feed-forward compensator is greater than that with feed-forward compensator.

The effectivity of the feed-forward compensator depends on the control time constant.

$$G_{ff}(s) = \frac{\tilde{v}}{v} = \frac{1}{T_{ff}s + 1}$$

- In the worst case,

$$T_{ff} = \infty$$

- In the best case:

$$T_{ff} = 0$$

Note: A too fast feed-forward compensator injects the high harmonic component at the PCC and lead to resonance with the PWM. For the synchronization stability, the faster feed-forward compensator, the higher stability.

2.4 Modelling: *Current Control Dynamic Effect (Feed-forward QLSL Model)*

Case1: Effect of the Feed-Forward Compensator on the Synchronization Stability

- A strong current control, of which time constant is 0.1 ms;
- A weak current control, of which time constant is 0.5 ms.

	Case 1	Case 2
$G_{ff}(0)=0$	0.35	0.45
$G_{ff}(0)=1$	0.34	0.35
QSLS	0.34	0.34

The minimum allowable grid voltage sag, when the converter is critically stable.

① The feed-forward control can nearly eliminate the negative effect of the current transients.

② **<u>The converter with feed-forward control can be modelled in QSLS model effectively.</u>**

Case2: Feed-Forward Compensator Time Constant

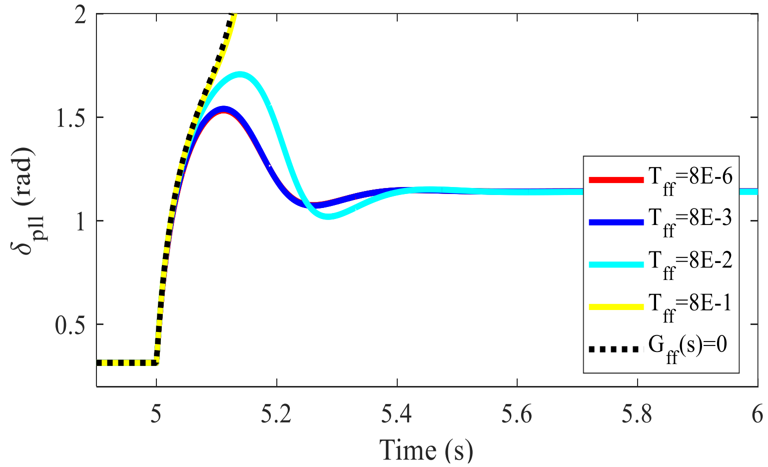

① The increase in the time constant of the feed-forward compensator worsens the synchronization stability.

② When the time constant is large enough, its transients will approach to the converter without the feed-forward compensator.

2.5 Modelling: *DC-Bus Voltage Control Effect*

- DC-Bus voltage dynamic

$$
\begin{cases}
\dfrac{\mathrm{d}v_{\mathrm{dc}}^2}{\mathrm{d}t} = \dfrac{1}{\tau_{\mathrm{dc}}}\left(P^\star - P^{\mathrm{e}}\right) \\
\tau_{\mathrm{dc}} = 2P_{\mathrm{dc}}^\star / \left(C_{\mathrm{dc}} v_{\mathrm{dc}}^{\star 2}\right) \\
P^{\mathrm{e}} = \underbrace{v_{\mathrm{g}}\left(i_{\mathrm{d}}^\star \cos\delta - I_{\mathrm{q}} \sin\delta\right) + R_{\mathrm{g}}\left(i_{\mathrm{d}}^{\star 2} + I_{\mathrm{q}}^2\right)}_{=f_P(\delta, i_{\mathrm{d}}^\star, I_{\mathrm{q}})}
\end{cases}
$$

$$
\begin{cases}
\dfrac{\mathrm{d}\gamma_{\mathrm{dc}}}{\mathrm{d}t} = v_{\mathrm{dc}}^2 - v_{\mathrm{dc}}^{\star 2} \\
i_{\mathrm{d}}^\star = k_{\mathrm{p}}^{\mathrm{dc}} \dfrac{\mathrm{d}\gamma_{\mathrm{dc}}}{\mathrm{d}t} + k_{\mathrm{i}}^{\mathrm{dc}} \gamma_{\mathrm{dc}}
\end{cases}
$$

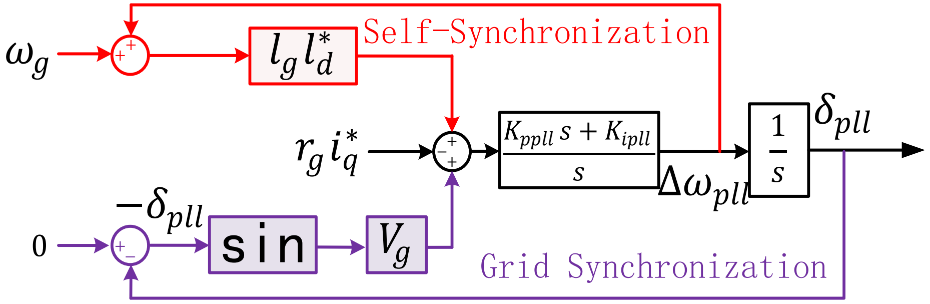

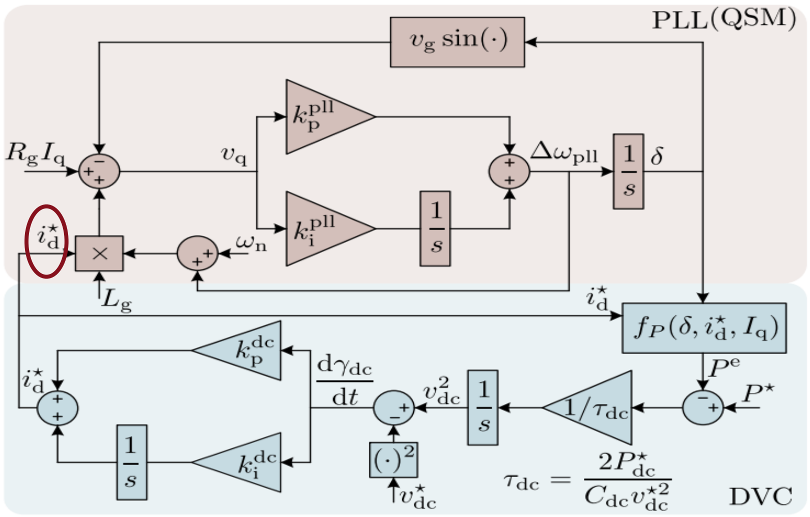

QSM− quasi-static model

2.6 Summary

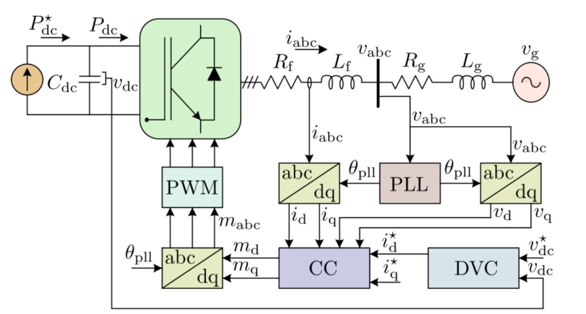

CC – current controller
DVC – dc-bus voltage controller
PLL – phase-locked loop

Full model

DC-Bus voltage control

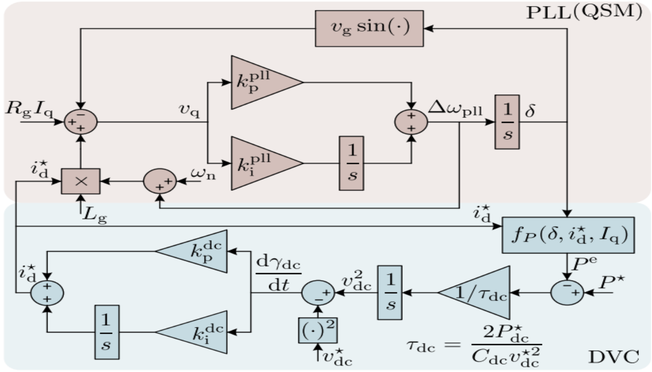

QSM – quasi-static model

CC+DVC

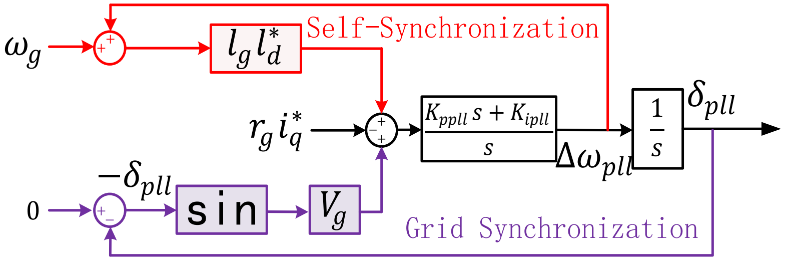

2th-order QSLS model

Transient Current

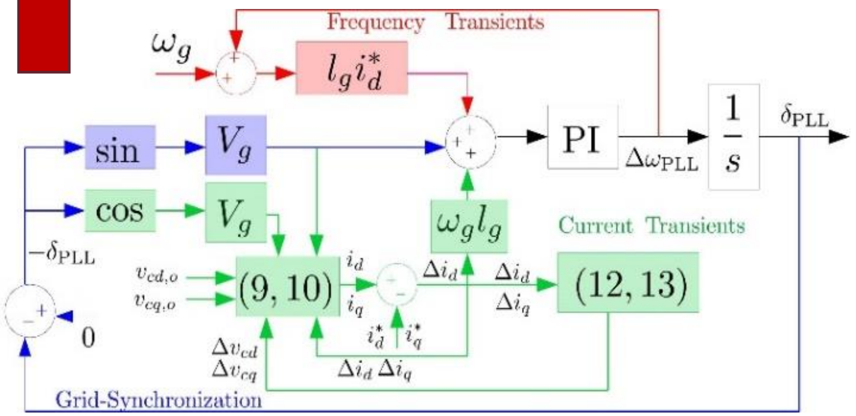

4th-order QSLS

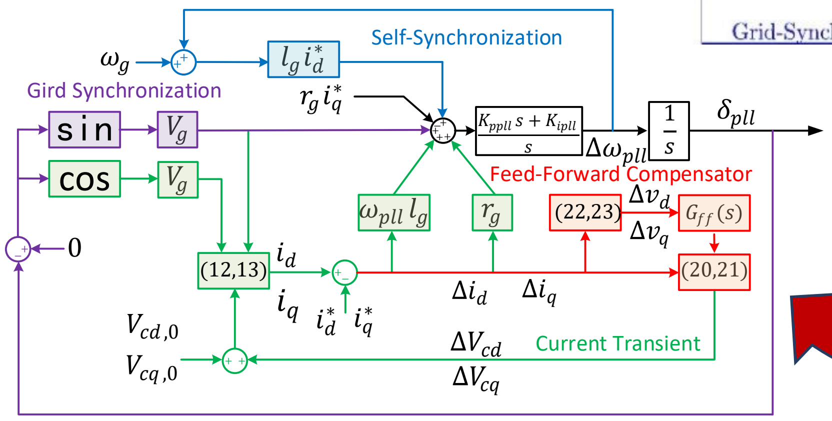

Feed-forward 4th-order QSLS

Feed-Forward Control

Use case of the QSLS model:

- GFL with feed-forward compensator
- A large filter
- A short current controller time constant

2 Analysis

3.1 Stability Analysis *Method: Equal Area Criterion*

- **GFL dynamic**

$$(1-K_{\mathrm{p\_pll}}L_{\mathrm{g}}i_{\mathrm{d}}^{*})\ddot{\delta}=$$

$$K_{\mathrm{i\_pll}}(\omega_{\mathrm{g}}L_{\mathrm{g}}i_{\mathrm{d}}^{*}+(L_{\mathrm{g}}i_{\mathrm{d}}^{*}-\frac{K_{\mathrm{p\_pll}}U_{\mathrm{g}}\cos\delta}{K_{\mathrm{i\_pll}}})\dot{\delta}-U_{\mathrm{g}}\sin\delta)$$

$$T_{J_{eq}}\frac{\mathrm{d}\omega_{pll}}{\mathrm{d}t}=u_q-D_{eq}\left(\omega_{pll}-\omega_g\right)$$

$$T_{J_{eq}}=\frac{\omega_b}{k_i}\left(1-\frac{k_pL_{eq}i_d^*}{\omega_b}\right)\approx\frac{\omega_b}{k_i},\ D_{eq}=\frac{k_pU_{eq}\omega_b}{k_i}\cos\delta$$

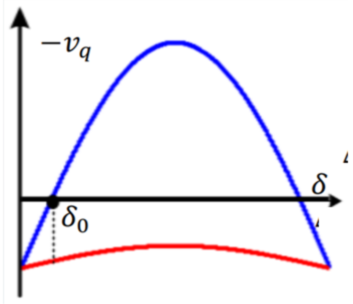

No equilibrium point:

GFL lose synchronization

$$\boxed{T_{J_{eq}}\frac{\mathrm{d}\omega_{pll}}{\mathrm{d}t}=u_q}$$

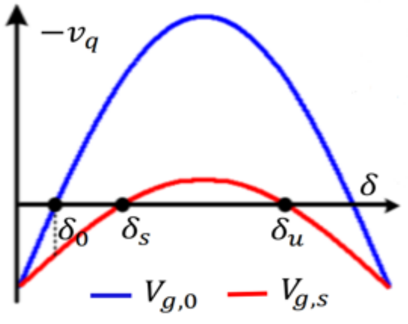

with equilibrium point:

- If **acceleration area >decceleration area** : GFL lose synchonization stability
- If **acceleration area = decceleration area :** GFL critial stability
- If **acceleration area < decceleration area :** GFL keep synchronization stability

- The equal area criterion **neglect the effect of damping.**
- This method is inaccurate, especially when the GFL have the **negative damping**

3.1 Stability Analysis *Method: Phase Protrait*

Ordinary Differential Equation

$$\begin{cases} \dfrac{d\delta_{pll}}{dt} = \Delta\omega_{pll} \\ \dfrac{d\Delta\omega_{pll}}{dt} = \dfrac{-k_{p,pll}\Delta\omega_{pll}v_g\cos\delta_{pll}}{1-k_{p,pll}l_g i_d} + \\ \qquad + \dfrac{k_{i,pll}(r_g i_q + (\omega_g + \Delta\omega_{pll})l_g i_d - v_g\sin\delta_{pll})}{1-k_{p,pll}l_g i_d} \end{cases}$$

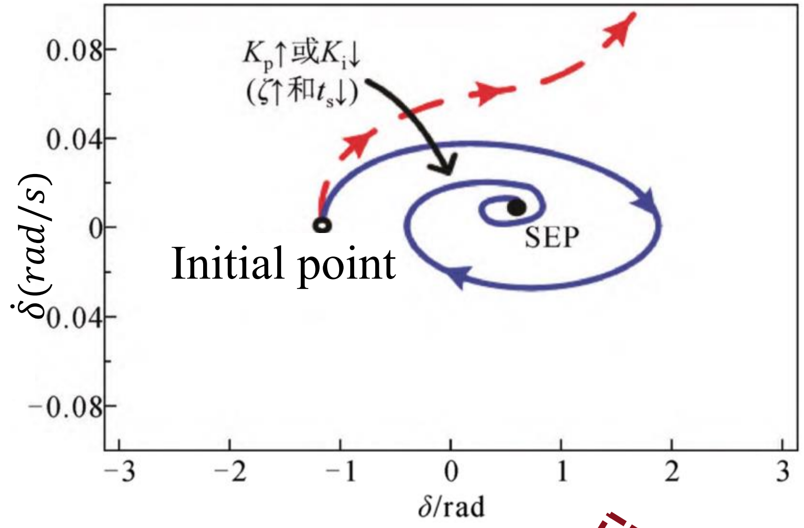

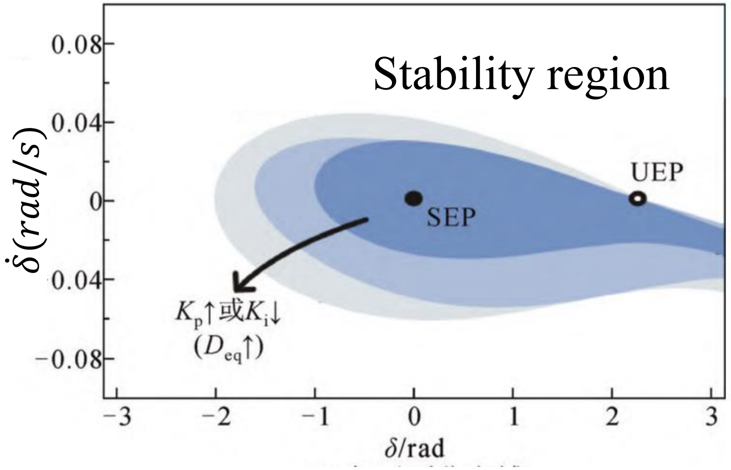

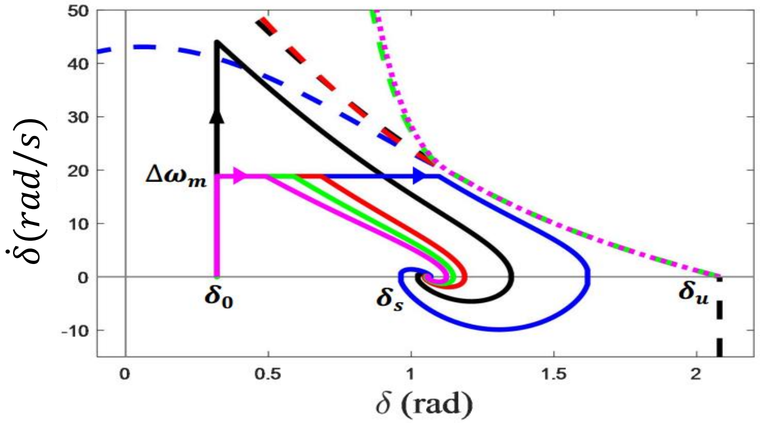

3.1 Stability Analysis *Method: Lyapunov Direct Method*

The energy function of PLL: $$V(\delta,\omega)=\frac{H_{pll}}{2}\omega^2-(T_m\delta+U_g cos\delta)$$

The difference between the acceleration area and the deceleration area after the fault:

$$S_{\text{I}}-S_{\text{II}}=\int_{\delta_0}^{\delta_2}T_m-T_e(\delta)d\delta$$
$$=(T_m\delta+U_g cos\delta)\Big|_{\delta_0}^{\delta_2}=V(\delta,0)-V_{cr}$$

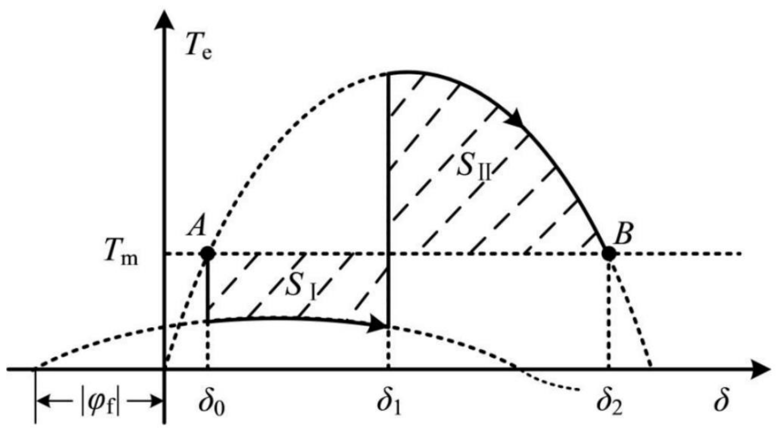

Critical energy: $V_{cr}=V(\delta_2,0)$

Test the dissipation of the energy function

$$\dot{V}(\delta,\omega)=H_{pll}\cdot\omega\dot{\omega}-(T_m-T_e)\dot{\delta}=-D_{pll}\cdot\omega^2$$

- The stable domain estimated by the energy function exceeds the true stable domain boundary in some regions.
- This approach is usually computationally complex and difficult to obtain analytical solutions for general dynamic systems.

3.2 Stability Analysis: *GFL Inertial/Damping Effect*

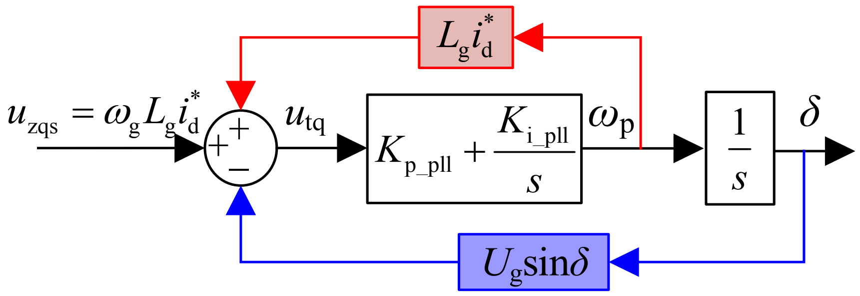

QSLS model

$$(1 - K_{p\_pll} L_g i_d^*)\ddot{\delta} =$$

$$K_{i\_pll}\left(\omega_g L_g i_d^* + \left(L_g i_d^* - \frac{K_{p\_pll} U_g \cos\delta}{K_{i\_pll}}\right)\dot{\delta} - U_g \sin\delta\right)$$

T_j and D are the equivalent inertial and damping coefficient of GFL, respectively.

$$T_j = \frac{1 - K_{p\_pll} L_g i_d^*}{K_{i\_pll}},\ D = \frac{K_{p\_pll} U_g \cos\delta}{K_{i\_pll}} - L_g i_d^*.$$

The damping of the GFL :

- Inconstant and varies with the grid states and converter outputs.
- May turn to be negative.

A poorly damped PLL

- may move the operating point beyond the unstable equilibrium point (UEP) during the transients resulting in the synchronization instability.

3.2 Stability Analysis: *GFL Inertial/Damping Effect*

A.Static analysis

For a stable operating point, the damping must be positive.

a)Impact of PLL parameters

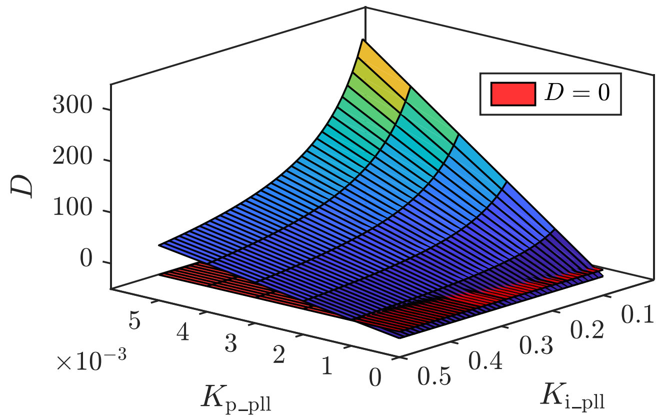

The relationship between the damping and the PLL parameters when SCR=2.

b)Impact of SCR

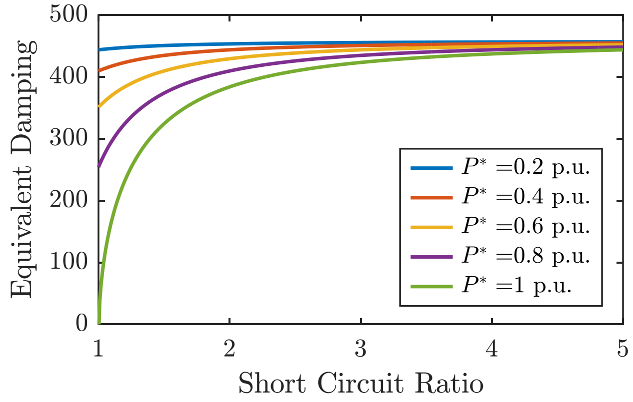

Effect of SCR on the equivalent damping *D* with different reference power P^*.

- A negative damping will appear when the ratio of $K_{\mathrm{p\_pll}}$ and $K_{\mathrm{i\_pll}}$ is small.

- The damping of GFL decreases with the SCR reduction.

3.2 Stability Analysis: *GFL Inertial/Damping Effect*

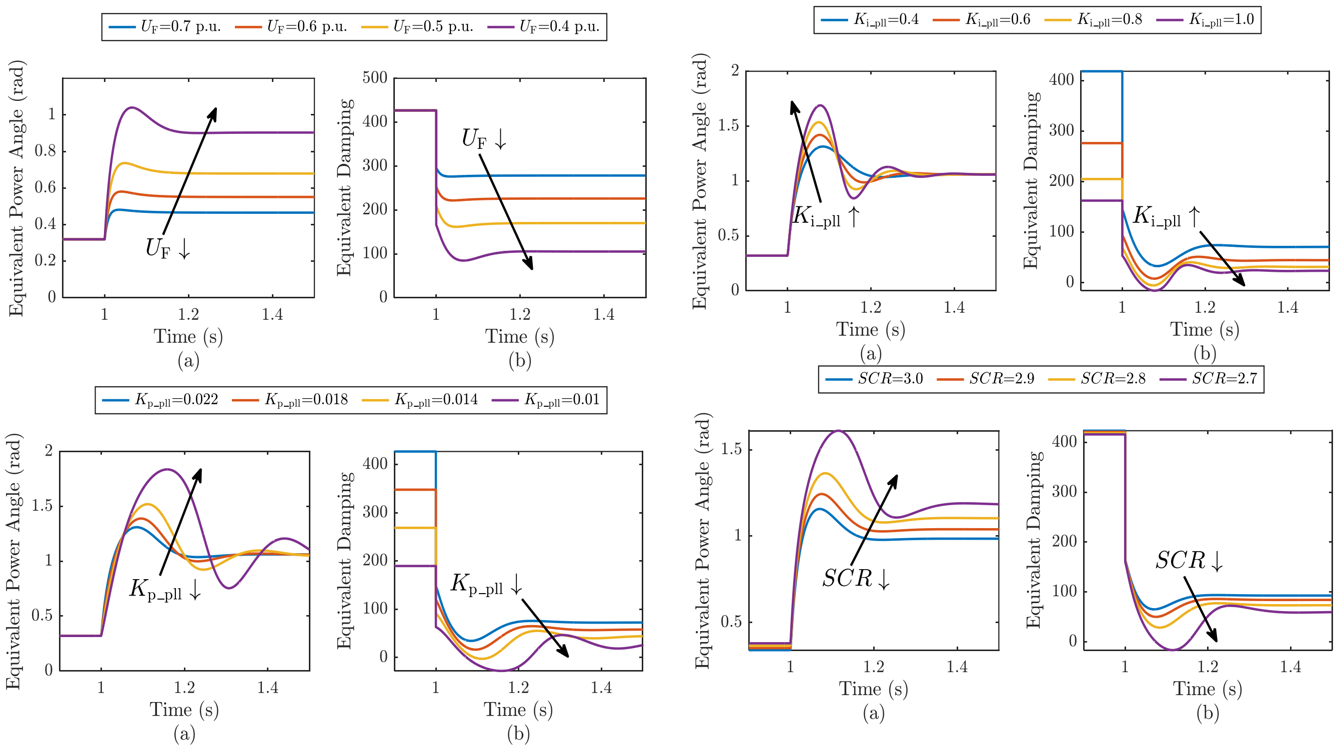

Effect of fault voltage U_F and PLL parameter on the EPA δ and the equivalent damping D.

B. Dynamic analysis

a) Impact of fault voltage

- The lower fault voltage, the worse damping /synchronization stability, the higher overshoot.

b) Impact of PLL parameters

- the decrease in K_{p_pll} or the increase in K_{i_pll} lows the damping / synchronization stability.

c) Impact of SCR

- The lower SCR, the worse damping /synchronization stability, the higher overshoot.

The damping of GFL is inconstant and may be negative with small ratio of PI parameters of PLL or in a weak grid following a sever fault. The negative damping of GFL is one of root cause of the synchronization instability.

3.3 Stability Analysis: *DC-Bus Voltage Control Effect*

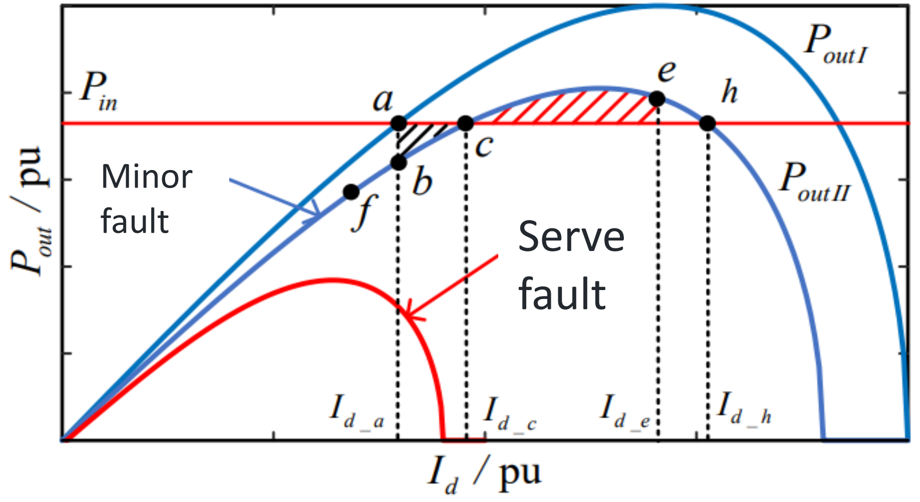

$$v_q = V_g \sin(-\delta_{pll}) + r_g i_q^* + \omega_{pll} l_g i_d^*$$

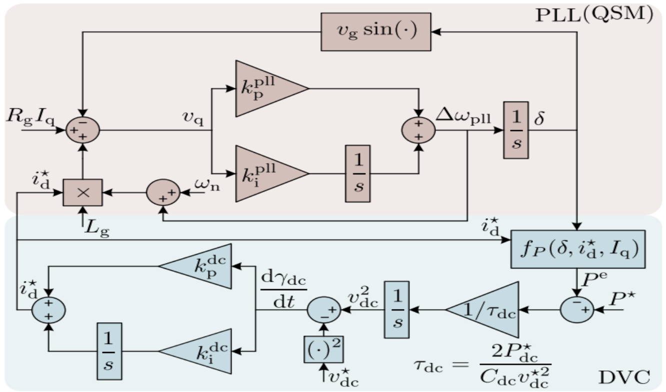

QSM− quasi-static model

$$\underbrace{\left[\frac{\left(1-k_p^{pll} L_g i_d^\star\right)}{k_i^{pll}}\right]}_{=M(i_d^\star)} \frac{d^2\delta}{dt^2} + \underbrace{\left[\frac{k_p^{pll}}{k_i^{pll}} v_g \cos\delta - L_g i_d^\star - \frac{k_p^{pll} k_p^{dc} L_g}{\tau_{dc} k_i^{pll}} (P^\star - P^e) - \frac{k_p^{pll} k_i^{dc} L_g}{k_i^{pll}} \left(v_{dc}^2 - v_{dc}^{\star 2}\right)\right]}_{=D(\delta, i_d^\star, v_{dc})} \frac{d\delta}{dt} + v_g \sin\delta$$

$$= \underbrace{\left(X_g i_d^\star + R_g I_q\right) + \frac{k_p^{pll} k_p^{dc} X_g}{\tau_{dc} k_i^{pll}} (P^\star - P^e) + \frac{k_p^{pll} k_i^{dc} X_g}{k_i^{pll}} \left(v_{dc}^2 - v_{dc}^{\star 2}\right)}_{=\text{Acting Force}(F_a)}$$

DC-Bus voltage control **decreases the synchronization stability.**

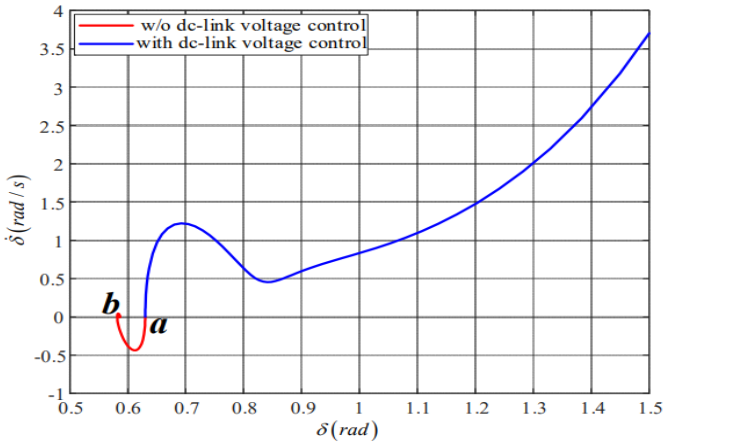

Phase portraits of the VSC with and without the dc-link voltage control when E drops from 1 p.u. to 0.9 p.u. and SCR = 2.

3.4 Stability Analysis: *X/R Ratio Effect*

Synchronization transients at PCC:

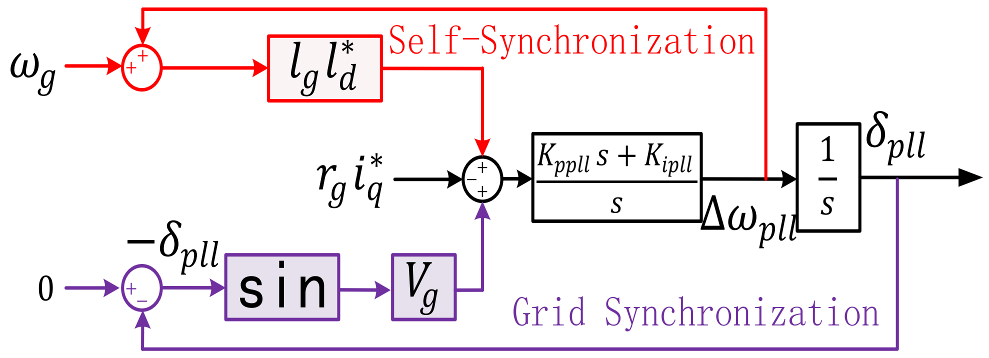

$$v_q = V_g \sin(-\delta_{pll}) + r_g i_q^* + \omega_{pll} l_g i_d^*$$

define: $\gamma = \omega_{pll} l_g / r_g$

- If $(i_{max} - i_d^*)/\ i_q^* < \gamma < -i_d^*/i_q^*$, the phase angle δ_{pll} is positive. The capacitive current through the grid resistance $r_g i_q$ could partially cancel the positive effect of the $\omega_{pll} l_g i_d$ term on $V_g \sin(-\delta_{pll})$.
- If $-i_d^*/i_q^* < \gamma < -(i_{max} + i_d^*)/\ i_q^*$, the phase angle δ_{pll} is negative. A further increase in $r_g i_q$ will enlarge the phase negatively thus degrade the converter stability.
- If $\gamma > -(i_{max} + i_d^*)/\ i_q^*$ or $\gamma < (i_{max} - i_d^*)/\ i_q^*$, no equilibrium point exists. The converter is unstable.

3.4 Stability Analysis: *X/R Ratio Effect*

$\gamma < -i_d^* / i_q^*$

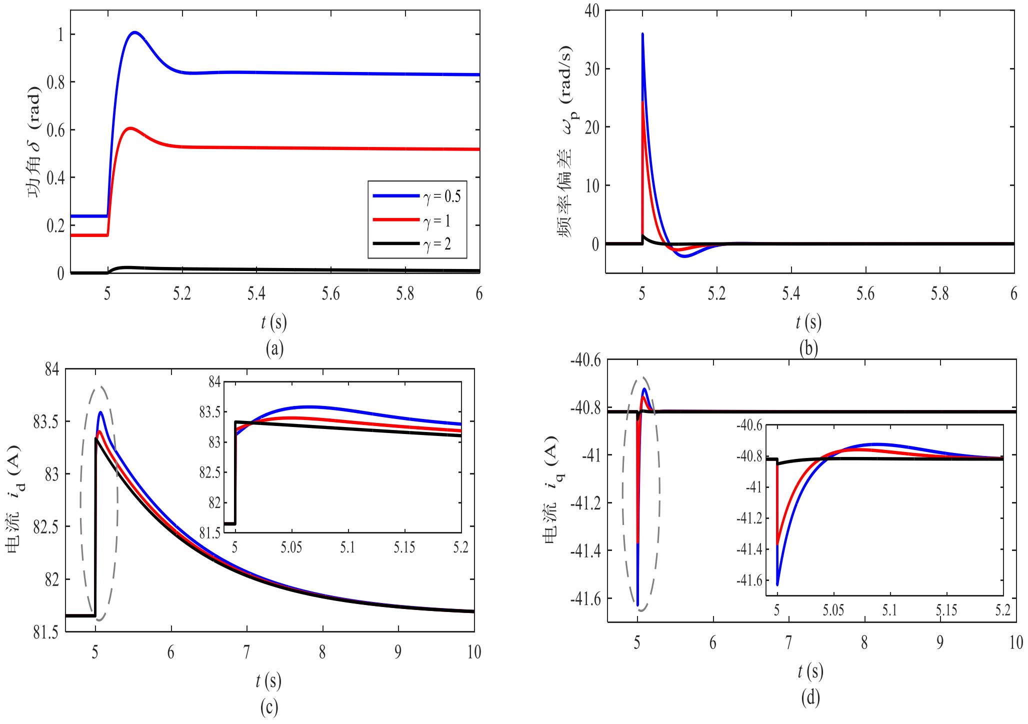

$\gamma > -i_d^* / i_q^*$

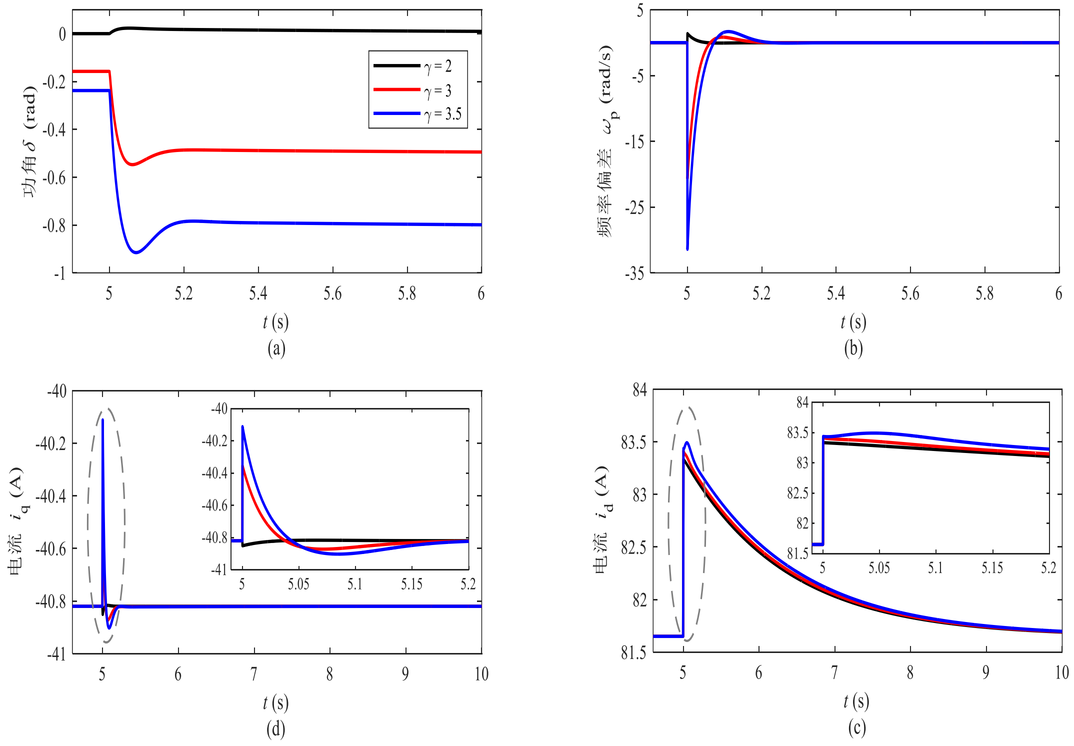

- The increase in impedance ratio γ enhances the synchronization stability.
- The decrease in impedance ratio γ enhances the synchronization stability.

3.4 Stability Analysis: *Grid Effect*

1) ***voltage sag***: the grid voltage amplitude V_g step reduces

2) ***short-circuit fault***: the grid impedance $\boldsymbol{Z_g}$ changes with respect to the short-circuit impedance, which could be equivalent to $V_g e^{j\theta_g} + Z_g I e^{j(\delta+\angle Z_g)}$ that the equivalent **grid voltage changes with respect to both the amplitude and phase.**

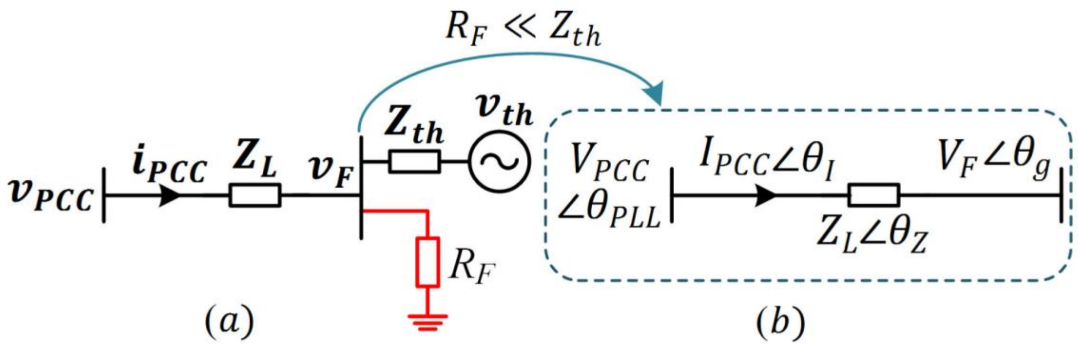

$$v_q = (V_{g,0} + \Delta V_g)\sin(\Delta\omega_g t + \Delta\theta_g - \delta) + r_g i_q + \omega_{pll} l_g i_d$$

3.4 Analysis: *Grid Effect*

- **Phase-angle jump**

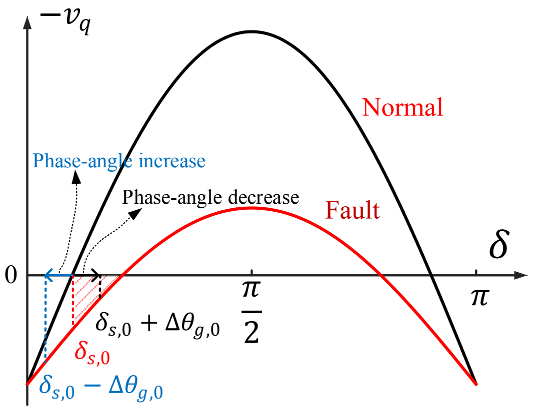

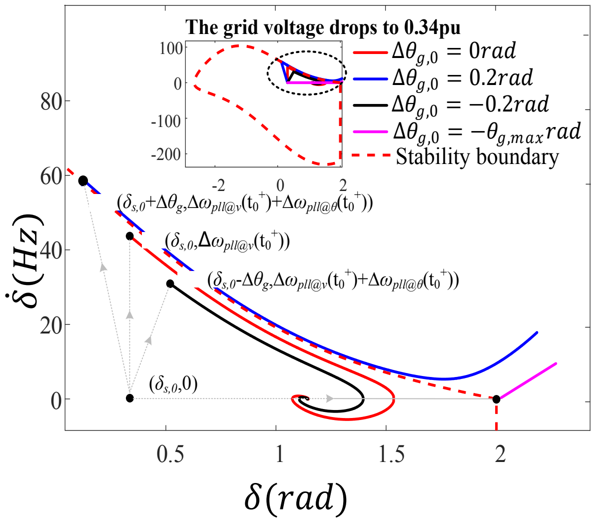

The larger the negative phase jump $\Delta\theta_g$, the better the GFL synchronous response

- **Frequency variation**

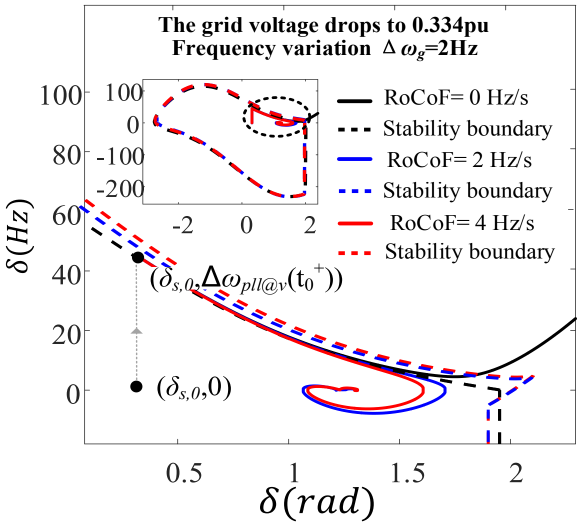

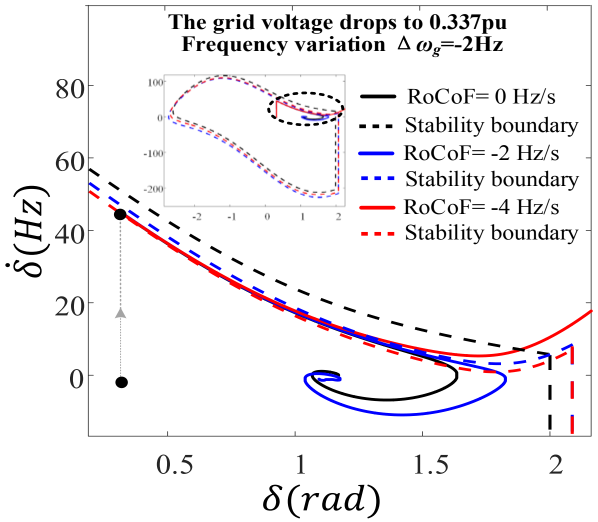

The negatively increase in RoCoF shrinks the stability boundary and may lead to the loss of the synchronization.

The phase jump only has an impact on the initial perturbance while the grid frequency influences the transient behavior of the GFL.

3.4 Analysis: *Grid Effect*

Case 1: Frequency variation

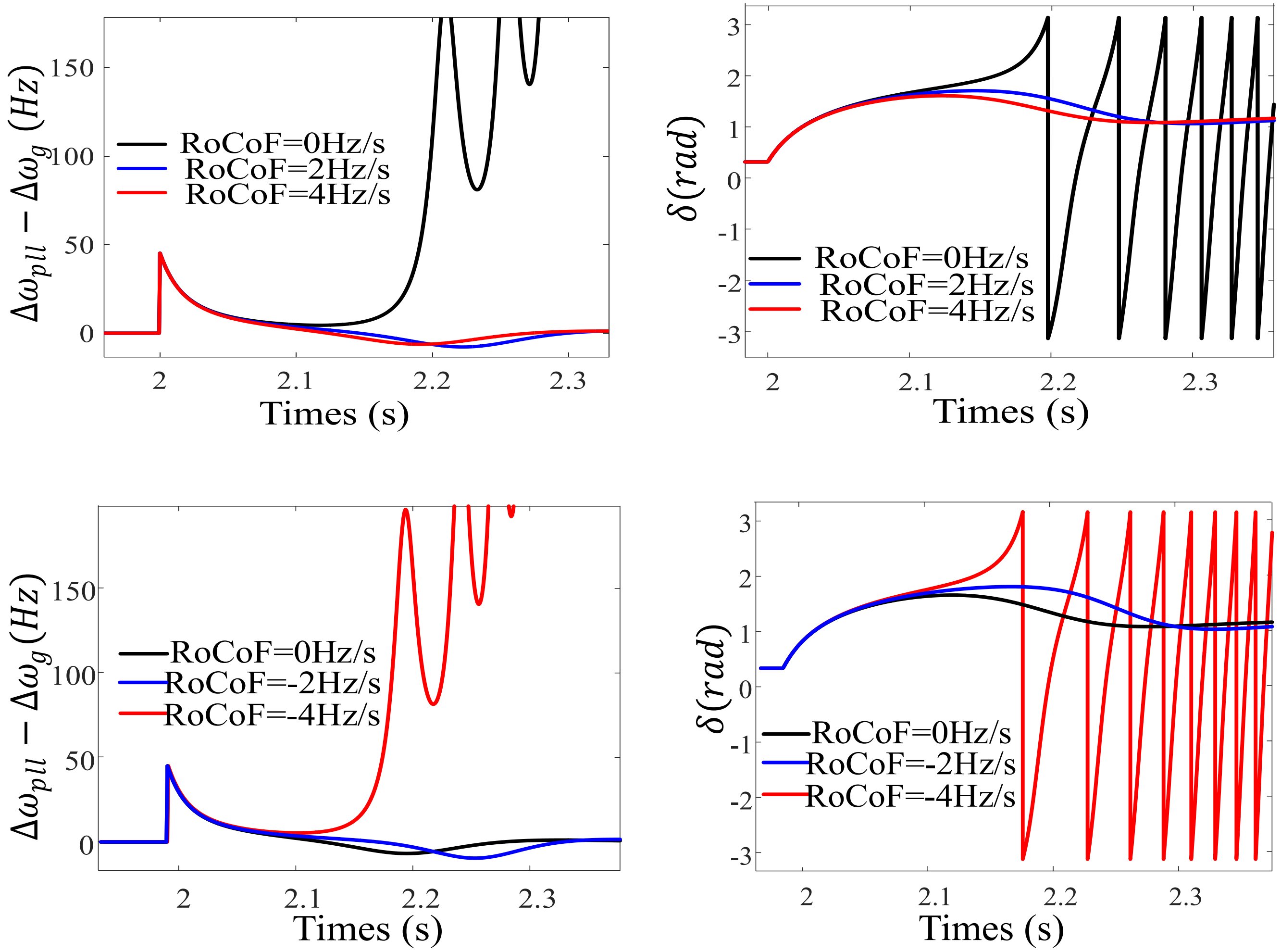

The grid frequency increase helps enhance the synchronization stability, and, even more interestingly, the higher the RoCoF, the better the transient response.

3.4 Analysis: *Grid Effect*

Case 2: Effect of phase-angle jumps

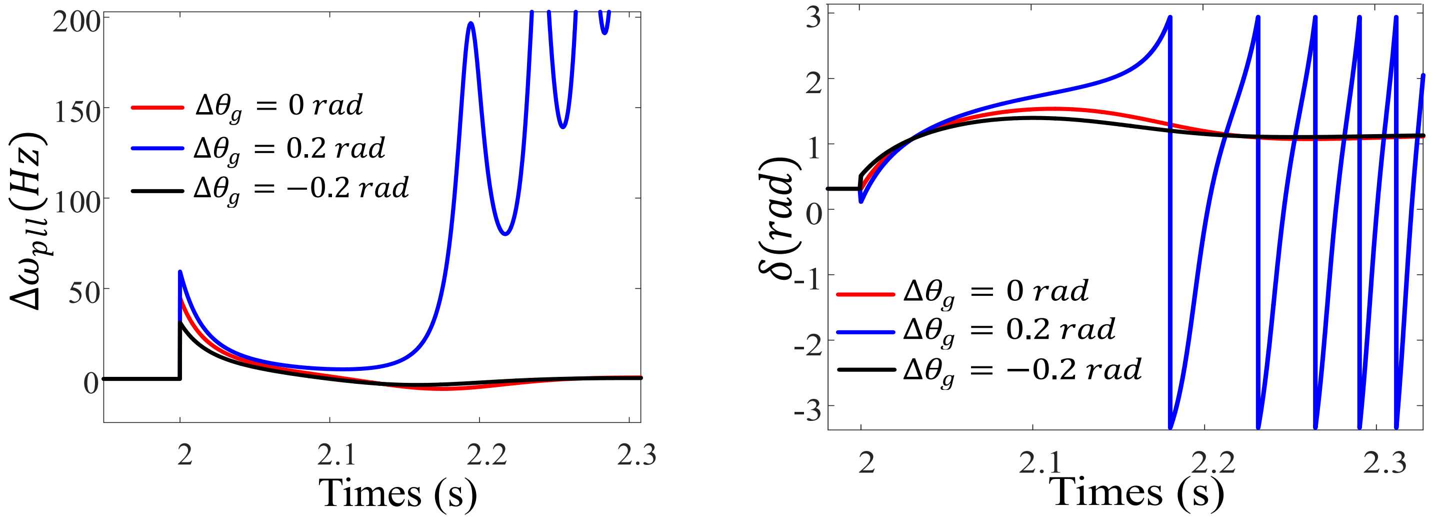

Positive phase jump can enlarge the acceleration area and over amplify the PLL frequency change. In extreme cases, this effect **can result in the loss of synchronization of the GFL.**

4 Limiter Effect

4.1 Limiter Effect: *Frequency Limiter*

Frequency Limiter (**FL**) is widely used in reality to avoid a significant frequency mismatch between the GFL and the grid

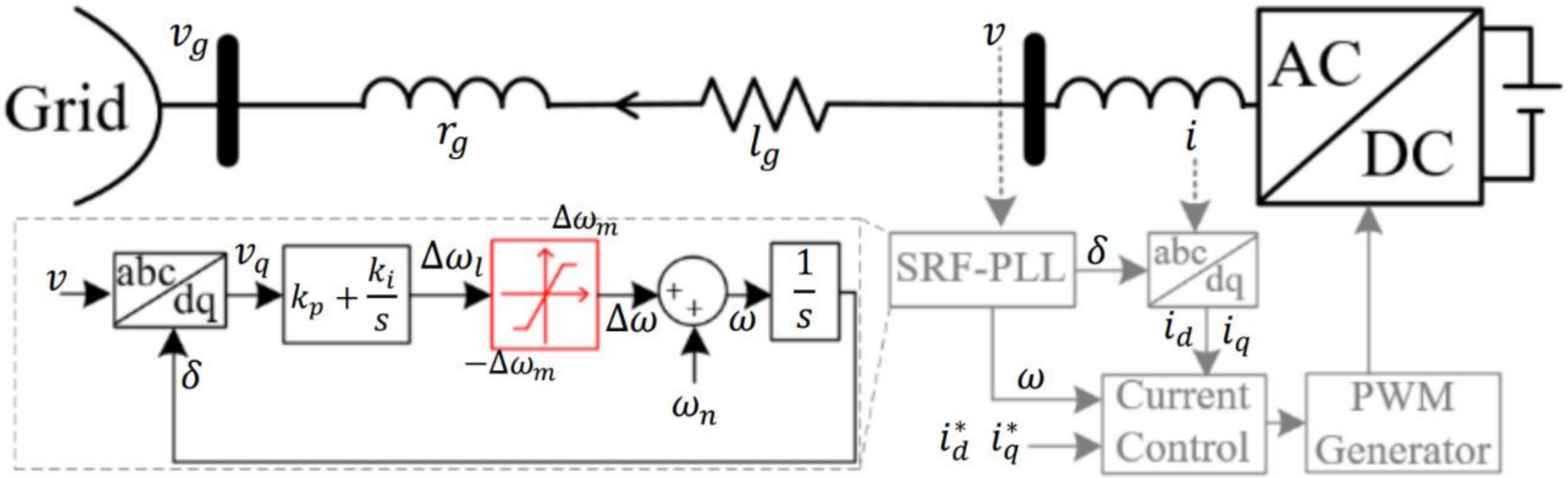

4.1 Limiter Effect: *Frequency Limiter (Equilibrium Points Existing)*

When the equilibrium points exist, the frequency limiter slow the frequency recover to zero, and increase the decceleration area area.

$$\int_{t_0}^{t_1}(\Delta\omega_l(t)-\Delta\omega_m)dt$$
$$=\int_{t_1}^{t_2}\left(\Delta\omega_m-\Delta\omega(t)\right)dt+\int_{t_2}^{t_3}\left(\Delta\omega_l(t)-\Delta\omega(t)\right)dt$$

The smaller $\Delta\omega_m$, the larger t_3.

When $(\Delta\omega(t_4)=\Delta\omega_l(t_5)=0)$, $\delta(t_4)<\delta(t_5)$

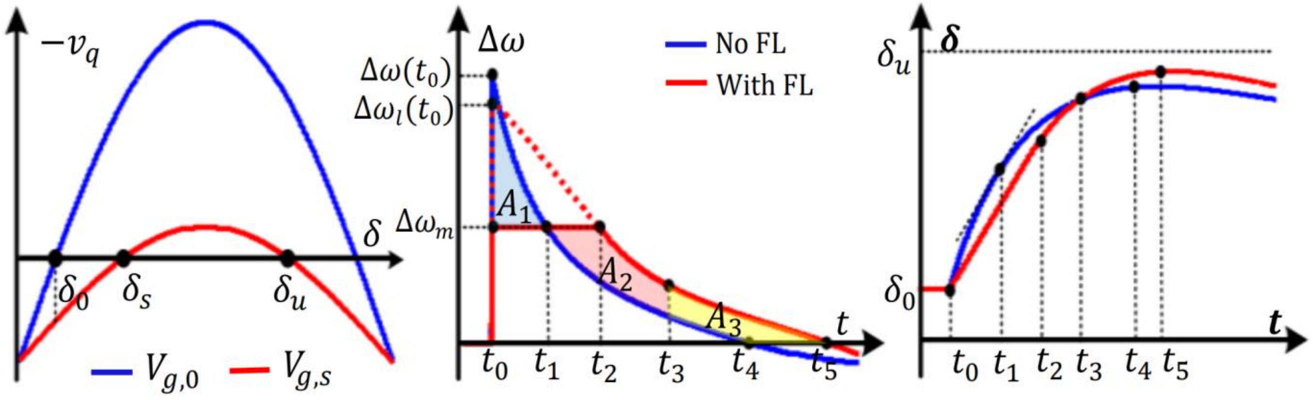

FL **worsens the synchronization stability** $\Delta\omega_m<\Delta\omega(t_0)$.

The smaller $\Delta\omega_m$, the larger A_1 resulting in a longer t_3 and a worse synchronization stability.

4.1 Limiter Effect: *Frequency Limiter (No Equilibrium Points)*

When no equilibrium points, the frequency limiter slows the frequency increase

- The FL slows down the phase increase from the instant of the fault.

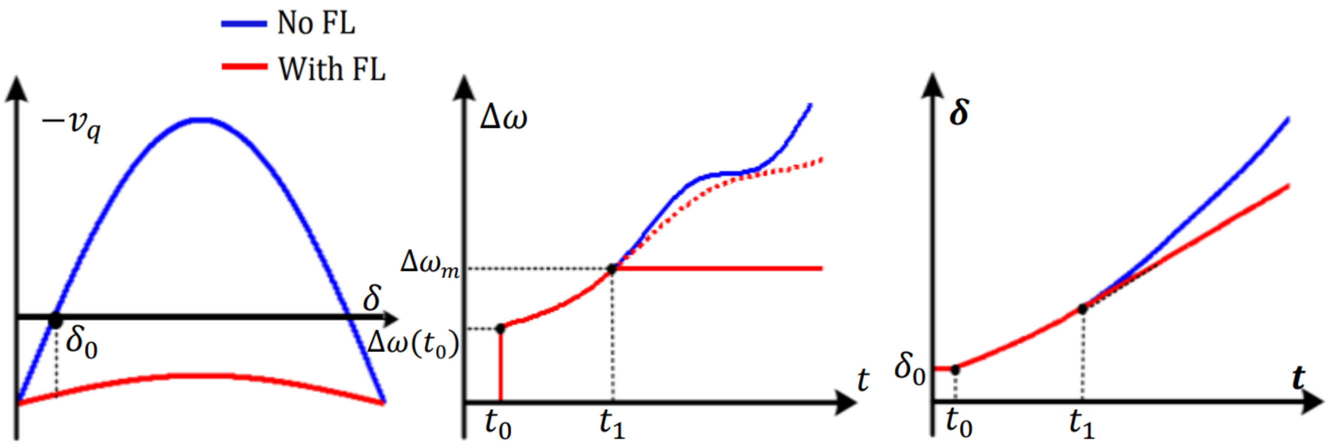

$\boldsymbol{Case 1}$: $\Delta\boldsymbol{\omega}_{\boldsymbol{m}} < \boldsymbol{\omega}(\boldsymbol{t_0})$ **and** $\Delta\dot{\boldsymbol{\omega}}(\boldsymbol{t_0}) > \mathbf{0}$

$$\Delta\boldsymbol{\omega}(\boldsymbol{t_1}) = \Delta\boldsymbol{\omega}_{\boldsymbol{m}}$$

FL can improve the synchronization stability and the lower $\Delta\omega_m$ the higher the stability.

4.1 Limiter Effect: *Frequency Limiter (No Equilibrium Points)*

When no equilibrium points , the frequency limiter restricts the frequency change

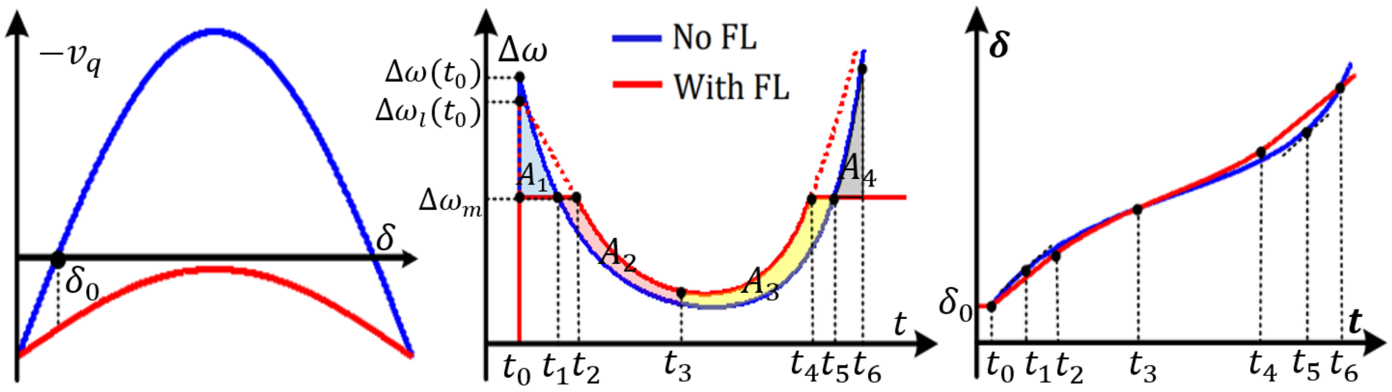

Fig. 5. Phase movements at the situation of $\Delta\omega_m < \omega(t_0)$ and $\Delta\dot{\omega}(t_0) < 0$.

$Case2$: $\Delta\omega_m < \omega(t_0)$ and $\Delta\dot{\omega}(t_0) < 0$

- In the period $t_0 \sim t_3$, the phase of the converter with FL is smaller than without FL
- In the period $t_3 \sim t_6$, the phase of the converter with FL is larger than without FL **(Fault cleared)**

$$\int_{t_3}^{t_4} (\Delta\omega(t) - \Delta\omega_l(t))dt + \int_{t_4}^{t_5} (\Delta\omega_m - \Delta\omega(t))dt = \int_{t_5}^{t_6} (\Delta\omega(t) - \Delta\omega_m)dt$$

4.1 Limiter Effect: *Frequency Limiter* (*Case Study*)

With Equilibrium Point

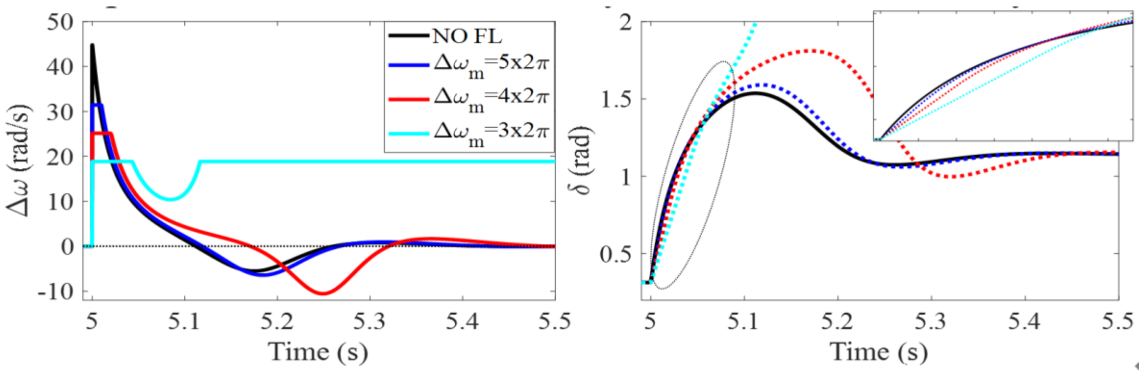

- The FL restricts the error
- Prolongs the settling time
- Worsening the stability

Without Equilibrium Point

$\boldsymbol{Case1}$: $\Delta\omega_m < \omega(t_0)$ **and** $\Delta\dot{\omega}(t_0) > 0$

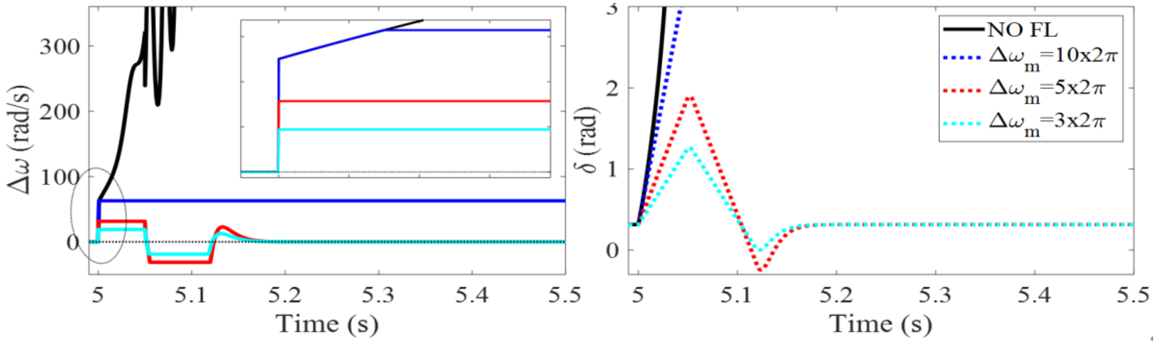

$\boldsymbol{Case2}$: $\Delta\omega_m < \omega(t_0)$ **and** $\Delta\dot{\omega}(t_0) < 0$

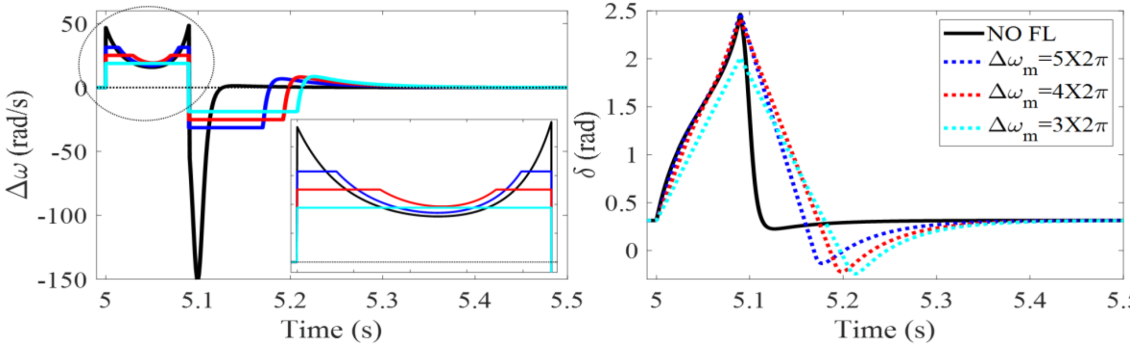

- Suppresses the change rate of the phase.
- Allow more time to clear the fault.

4.2 Limiter Effect: *Frequency anti-windup*

Different PI control limiters have the different transient response of the SRF-PLL

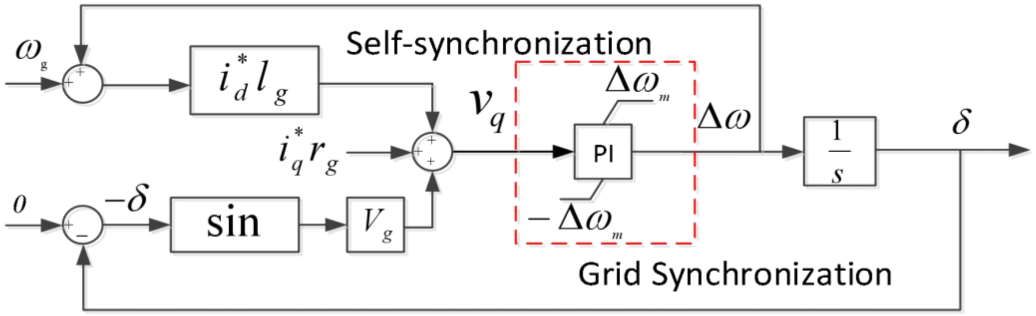

Grid-Following Converter quasi-steady-state model

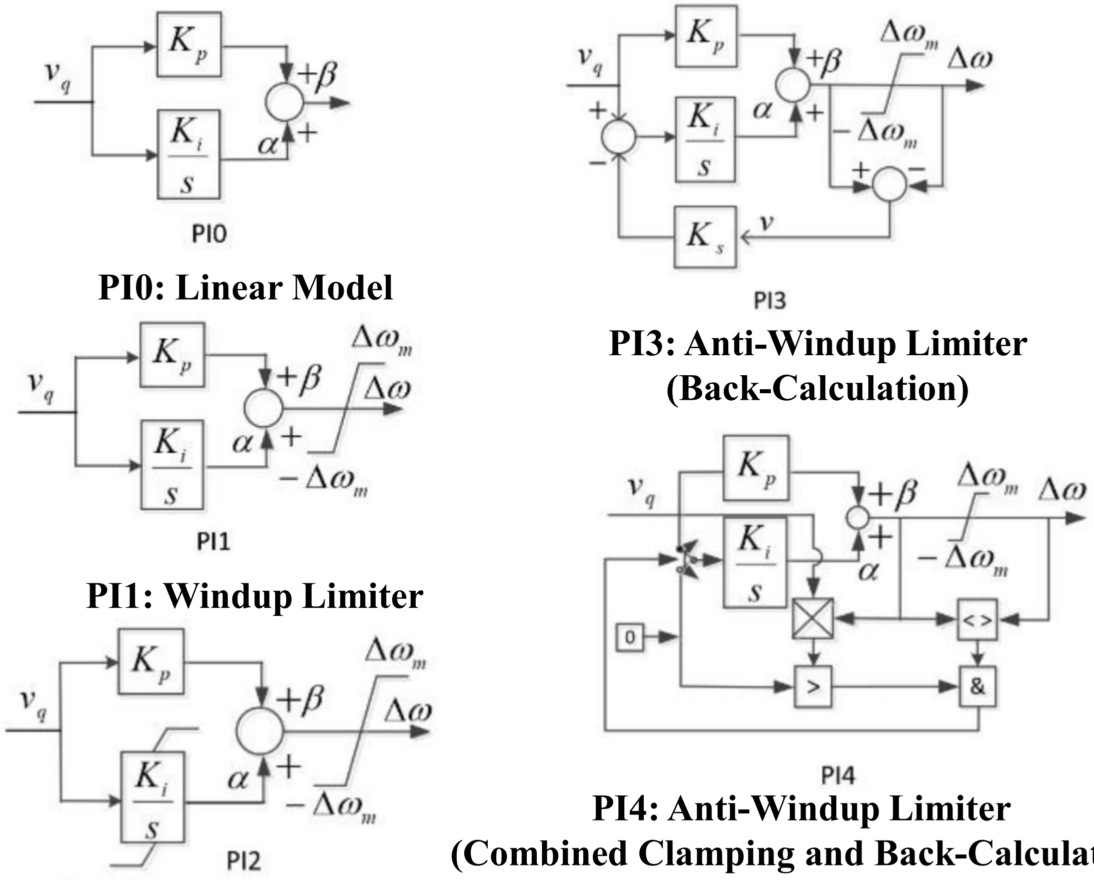

PI0: Linear Model

PI1: Windup Limiter

PI2: Anti-Windup Limiter (Clamping)

PI3: Anti-Windup Limiter (Back-Calculation)

PI4: Anti-Windup Limiter (Combined Clamping and Back-Calculation)

4.2 Limiter Effect: *Frequency anti-windup(Equilibrium Points Existing)*

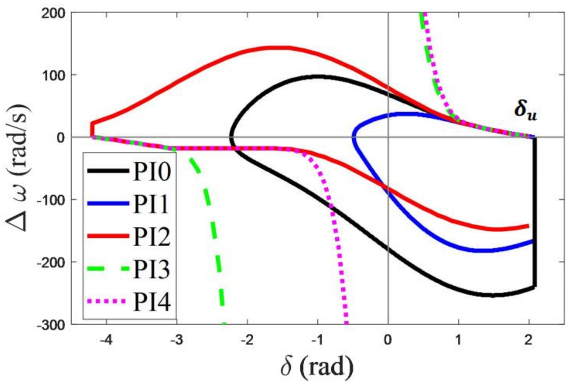

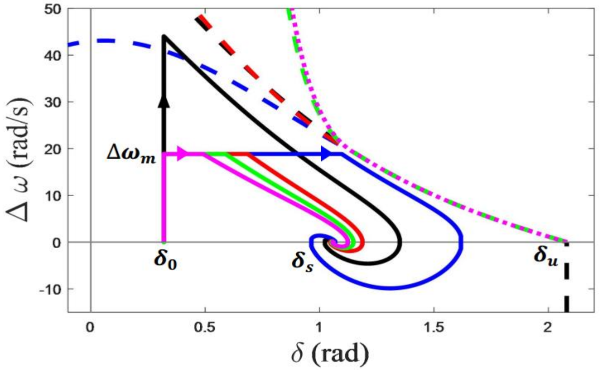

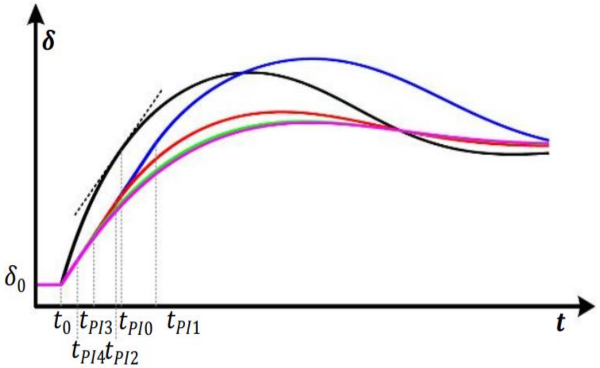

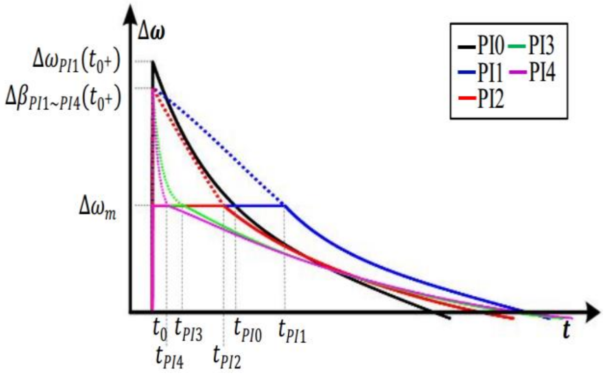

The area of stability region:

PI4>PI3>PI2>PI0>PI1

Critical time:

$$t_{PI\{\blacksquare\}}\ at\ \beta_{PI\{\blacksquare\}}(t_{PI\{\blacksquare\}}) = \Delta\omega_m$$

The shorter $t_{PI\{\blacksquare\}}$, the better the stability margin

PI4>PI3>PI2>PI0>PI1

4.2 Limiter Effect: *Frequency anti-windup(No Equilibrium Points)*

- **No Equilibrium Point**

The area of stability region:

PI3>PI4>PI0>PI2>PI1

The frequency ξ_{PI} {■}is at the time t_c which is the fault is cleared

The smallerξ_{PI} {■}, the better the stability margin

PI4>PI3>PI2>PI1>PI0

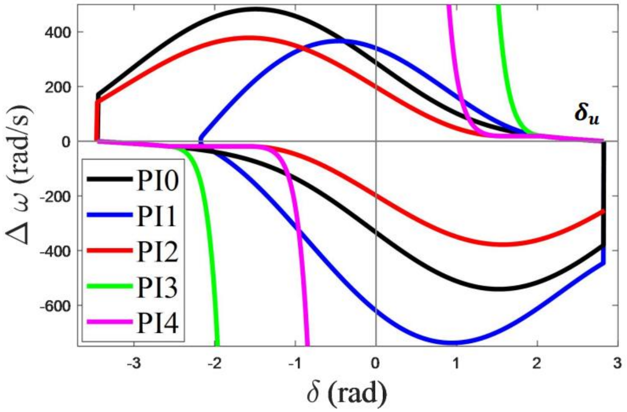

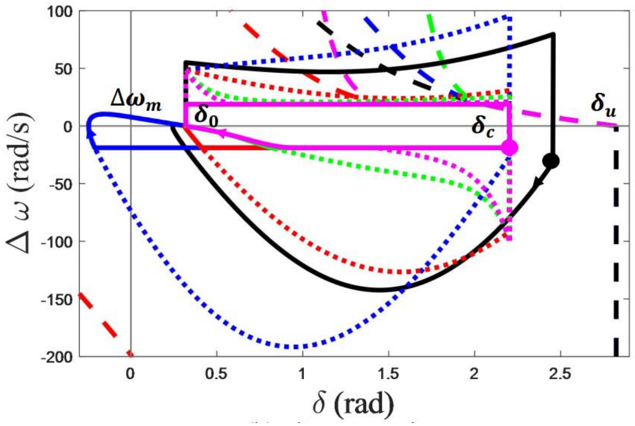

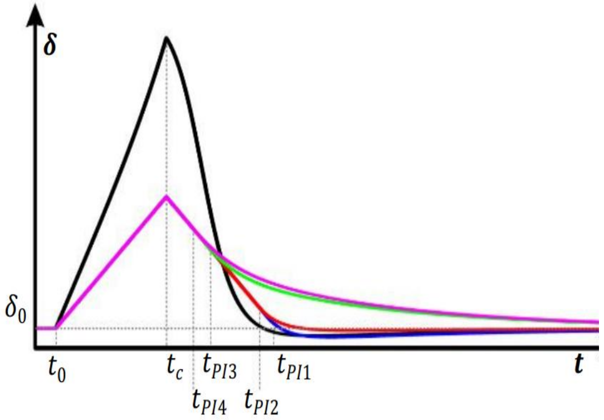

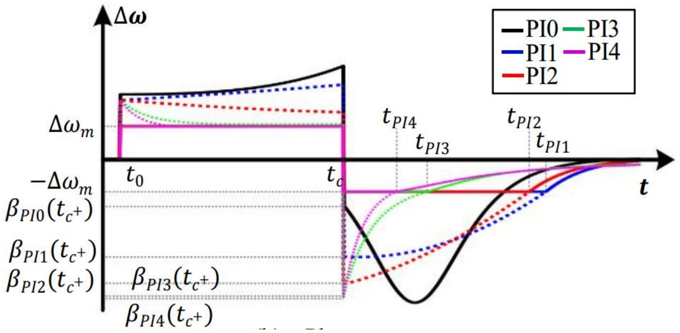

5 Conclusion

5 Conclusion

1. The grid impedance introduces a positive feedback on the synchronism. In a weak grid (low SCR, low X/R ratio), the grid-following converter may lose the synchronization.
2. Power electronic device consists of a serial of controller and switches in multiple timescales. The dynamics in the small-timescale and limiters can affect the synchronous transients and overturn the stability assessment results.
3. The synchronization characteristics are nonlinear and high-order, of which stability assessment is very difficult. The present methods are based on the 2^{nd}-order QSLS

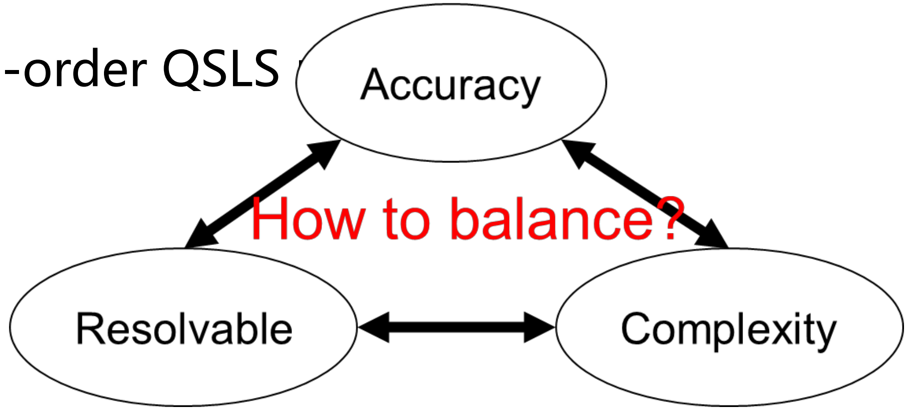

6 List of References

6 List of Reference

[1]**J. Chen**, M. Liu, T. O'Donnell and F. Milano, "Impact of Current Transients on the Synchronization Stability Assessment of Grid-Feeding Converters," in IEEE Transactions on Power Systems, vol. 35, no. 5, pp. 4131-4134, Sept. 2020.

[2]**J. Chen**, C. Ge and H. Ye, "Impact of the Feed-Forward Compensation on the Synchronization Stability," The 10th Renewable Power Generation Conference (RPG 2021), 2021, pp. 218-224.

[3]**J. Chen**, F. Milano and T. O'Donnell, "Assessment of Grid-Feeding Converter Voltage Stability," in IEEE Transactions on Power Systems, vol. 34, no. 5, pp. 3980-3982, Sept. 2019 .

[4]**J. Chen**, M. Liu, H. Geng, T. O'Donnell and F. Milano, "Impact of PLL Frequency Limiter on Synchronization Stability of Grid Feeding Converter," in IEEE Transactions on Power Systems, vol. 37, no. 3, pp. 2487-2490, May 2022.

[5] **J. Chen,** G. Li, M. Liu, H. Ye, “Influence Mechanism of R/X Ratio on Synchronization Stability of Grid-following Converter, ” in Proceedings of the CSEE, vol.43, no. 6, March 2023

[6] Q. Shen, G. Li, H. Ye, Y. Xie and **J. Chen**, "Modelling and Analysis of Damping Characteristics of Grid Following Converter," 2022 IEEE Power & Energy Society General Meeting (PESGM), Denver, CO, USA, 2022, pp. 1-5.

[7] **J. Chen**, C. Ge, D. Qiang, H. Geng, T. O'Donnell and F. Milano, "Impact of frequency anti-windup limiter on synchronization stability of grid feeding converter," in CSEE Journal of Power and Energy Systems.

[8] **J. Chen**, M. Liu, T. O'Donnell and F. Milano, "On the Synchronization Stability of Converters connected to Weak Resistive Grids," 2021 IEEE Power & Energy Society General Meeting (PESGM), Washington, DC, USA, 2021, pp. 1-5.

[9] **J. Chen**, W. Si, M. Liu and F. Milano, "On the Impact of the Grid on the Synchronization Stability of Grid-Following Converters," in IEEE Transactions on Power Systems.

Thanks for your attention!

Junru Chen
junru.chen@xju.edu.cn

Federico Milano

Federico Milano received from the University of Genoa, Italy, the Ph.D. in Electrical Engineering in 2003. In 2013, he joined the UCD School of Electrical and Electronic Engineering, where he is currently a full professor. He has authored more than 300 publications, and 8 books. He is an IEEE Fellow, an IET Fellow, a member of the IEEE PES Distinguished Lecturer Program, the chair of the IEEE Power System Stability Controls Subcommittee, Chair of the Technical Programme Committee of the PSCC 2024, Senior Editor of the IEEE Transactions on Power Systems, a member of the Cigré Irish National Committee, and Editor in Chief of the IET Transmission, Generation & Distribution.

Complex Modelling of Converter-Interfaced Generation

Federico Milano

University College Dublin

25th June 2023

Table of Contents

Challenges

- The electric power system is currently undergoing a period of unprecedented changes
- This transition involves the major challenge of substituting synchronous machines with power electronics-interfaced generation (CIG)
- The regulation and interaction with the rest of the system of CIG is yet to be fully understood!

Time scales

Typical time scales related to inertia and frequency control

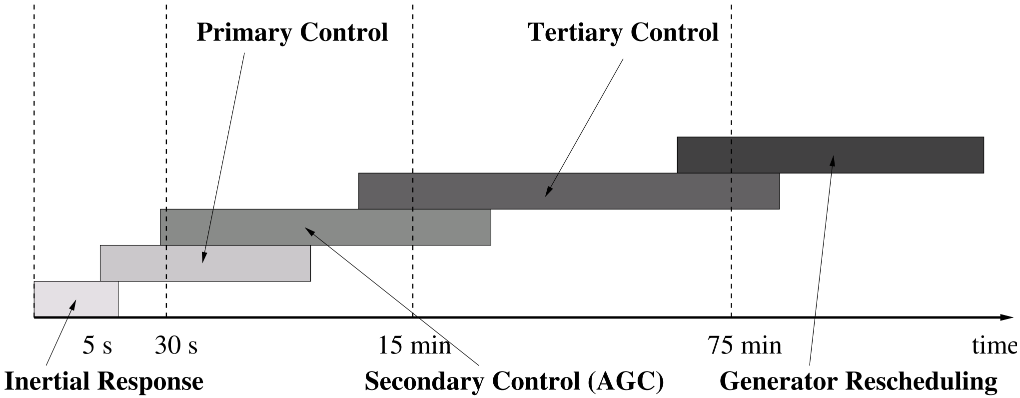

Time Scales

CIG controllers can be fast (is this good?)

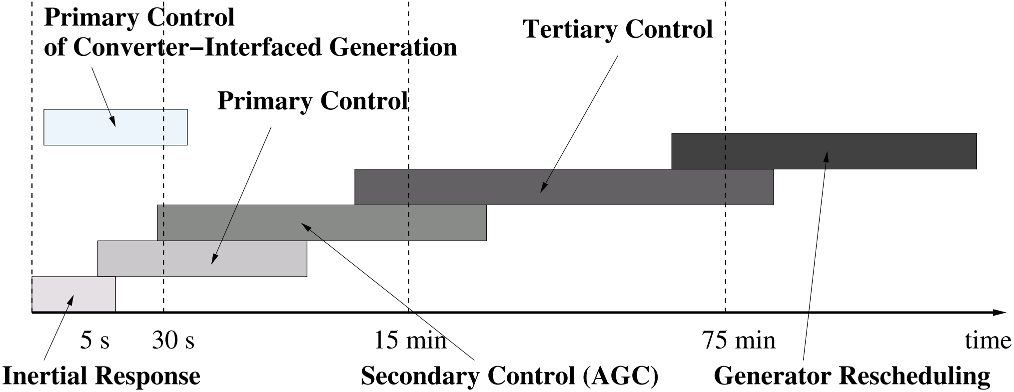

Electro-Mechanical Dynamics – I

Neglecting network topology, a conventional system where generation is attained with synchronous generation can be represented as

$$M\omega' = p_{\rm syn} - p_{\rm load} - p_{\rm losses} ,$$

where

- M is the total inertia of the synchronous machines
- ω is the average frequency of the system
- ω' is called Rate of Change of Frequency (RoCoF)
- $p_{\rm syn}$ is the power of synchronous machines
- $p_{\rm load} + p_{\rm losses}$ are load demand and losses respectively.

Electro-mechanical Dynamics – II

A system where generation is attained with synchronous as well as non-synchronous generation can be represented as

$$\tilde{M}\omega' = p_{\rm syn} + p_{\rm cig} - p_{\rm load} - p_{\rm losses} \, ,$$

where

- $\tilde{M}$ is the total inertia of the synchronous machines, with $\tilde{M} < M$ or, in certain periods and certain systems, $\tilde{M} \ll M$
- $p_{\rm cig}$ is the powers provided by CIG

Volatility of the inertia

$\tilde{M}$ is a function of time!

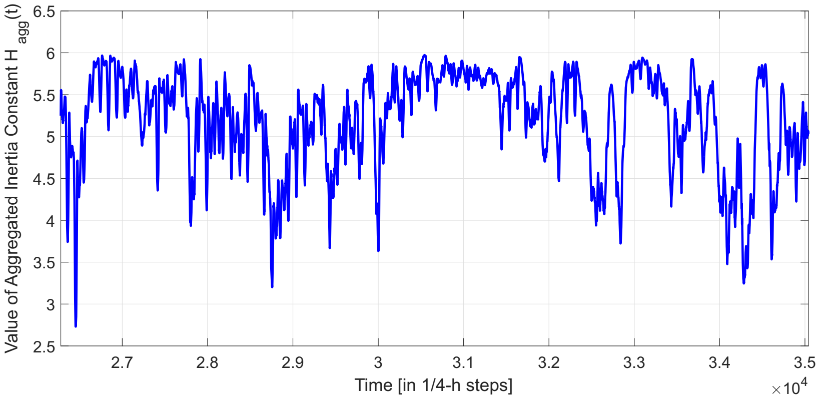

Acknowledgment: Thanks to A. Ulbig and G. Andersson for data and script to generate figure

Extreme Case

In a hypothetical system where there are no synchronous machines at all, $\tilde{M} \approx 0$ and the frequency is completely decoupled from the power balance of the system:

$$0 = p_{\mathrm{cig}} - p_{\mathrm{load}} - p_{\mathrm{losses}}$$

This operating condition has never really happened in large networks (only in microgrids and small islanded systems)

Open Question

If the inertia is null, is still the frequency meaningful?

Analogy between Synchronous Machine and CIG

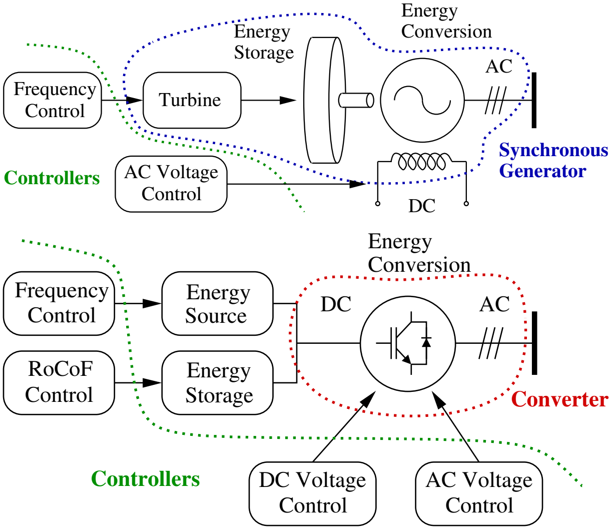

Drawbacks of CIG

- Reduce the inertia
- The local frequency must be measured (and properly defined) first!
- Often introduce volatility and uncertainty (e.g., wind and solar power plants)
- Often do not provide primary and/or secondary frequency control

Remark

Since it is based on a converter, CIG controllers can be very fast

Advantages of CIG

- Can provide primary and secondary control (if the resources are properly handled and/or storage is included)
- Quantities other than the frequency can be utilized (voltage?)

Remark

Since it is based on a converter, CIG controllers can be very fast

Inconsistency of the Conventional Model - I

Let's consider a two-machine system:

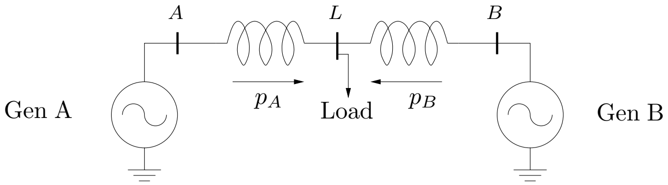

Conventional model:

$$
\begin{aligned}
\delta'_A &= \omega_A - \omega_o \\
M_A \omega'_A &= p_{m,A} - p_{e,A} \\
p_{e,A} &= \frac{e_{q1,A} v_L}{x_{d1,A} + x_{AL}} \sin(\delta_A - \delta_L)
\end{aligned}
$$

$$
\begin{aligned}
\delta'_B &= \omega_B - \omega_o \\
M_B \omega'_B &= p_{m,B} - p_{e,B} \\
p_{e,B} &= \frac{e_{q1,B} v_L}{x_{d1,A} + x_{BL}} \sin(\delta_B - \delta_L)
\end{aligned}
$$

Turkey Blackout on 31st of March 2015 – I

- The blackout in Turkey led to the outage of 32 GW.

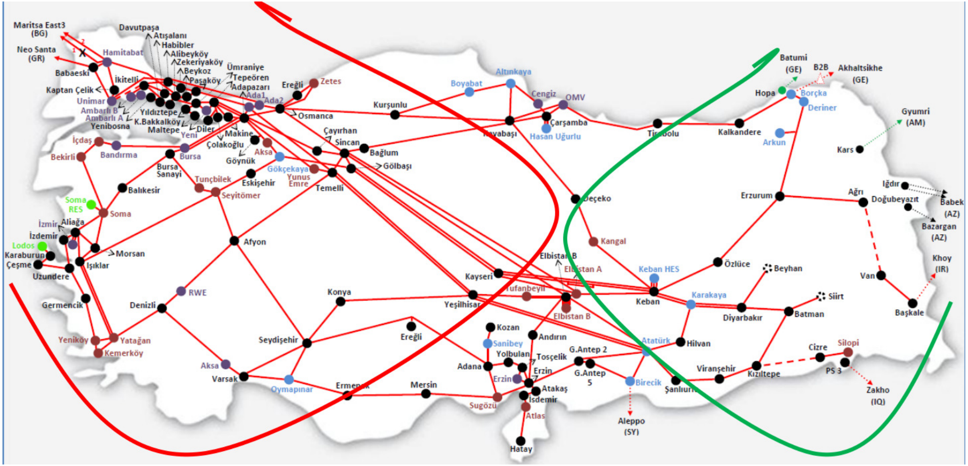

Turkey Blackout on 31st of March 2015 – II

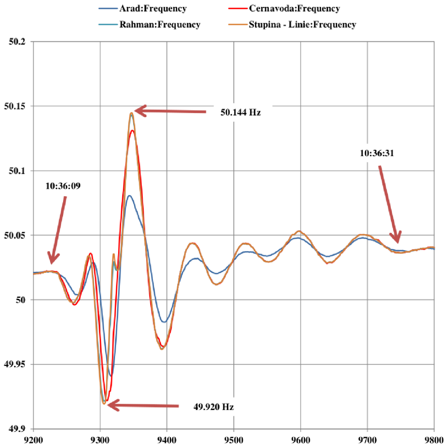

- As a consequence of the line outages and the blackout in Turkey, the Romanian system experimented severe frequency oscillations.
- Bigger oscillations were measured at locations geographically closer to Turkey.

Inconsistency of the Conventional Model - II

We know that the frequency at different points of the grids are different during an electromechanical transient.

However, the conventional transient stability model assumes that the frequency can only change in the rotor of the synchronous machines, not in the grid.

In turn, the conventional model assumes that the frequency is equal to the synchronous reference ω_o everywhere in the circuit.

Modeling Issues – I

- The conventional power system model for transient stability analysis is based on the assumption of quasi-steady-state phasors for voltages and currents.
- The crucial hypothesis on which such a model is defined is that the frequency required to define all phasors and system parameters is constant and equal to its nominal value.
- This model is appropriate as long as only the rotor speed variations of synchronous machines is needed to regulate the system frequency through standard primary and secondary frequency regulators.

Modeling Issues – II

- An increasing number of devices other than synchronous machines are expected to provide frequency regulation.
- These include, among others:
  - distributed energy resources, e.g., wind and solar generation
  - flexible loads providing load demand response
  - HVDC transmission systems
  - energy storage devices
- These devices do not impose the frequency at their connection point with the grid.
- There is thus the need to define with accuracy the local frequency at every bus of the network.

Application to CIG and Non-Synchronous Devices – I

Once the frequency has been estimated, one can use it to regulate the frequency through CIGs and other non-synchronous devices, such as flexible thermostatic loads.

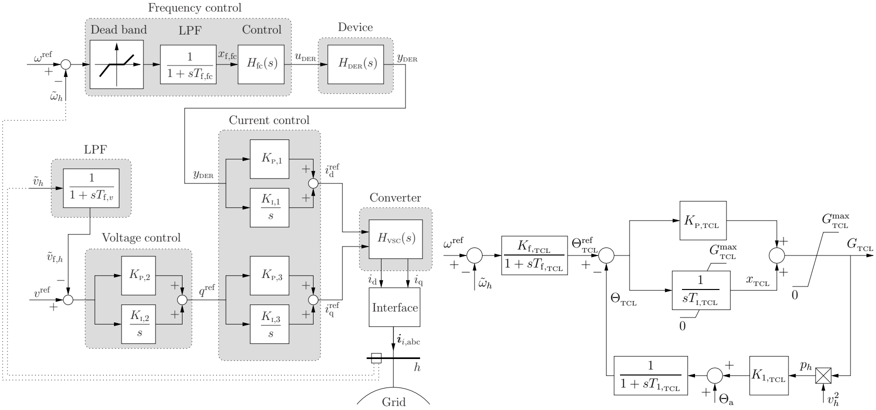

Application to CIG and Non-Synchronous Devices – II

In this example, wind energy conversion system (WECS) are equipped with frequency control.

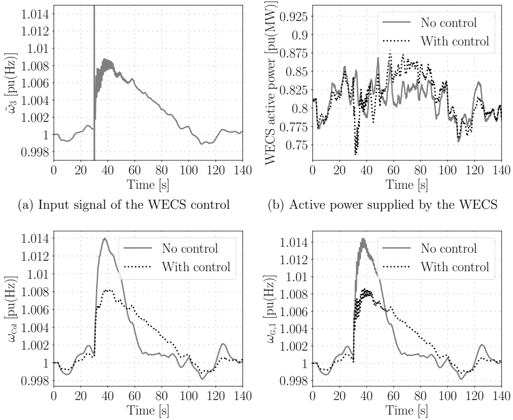

(a) Input signal of the WECS control (b) Active power supplied by the WECS

(c) Frequency of the CoI (d) Rotor speed of machine at bus 1

Chattering due to the Frequency Control of WECS

Real-world recording of the frequency in the Irish grid.

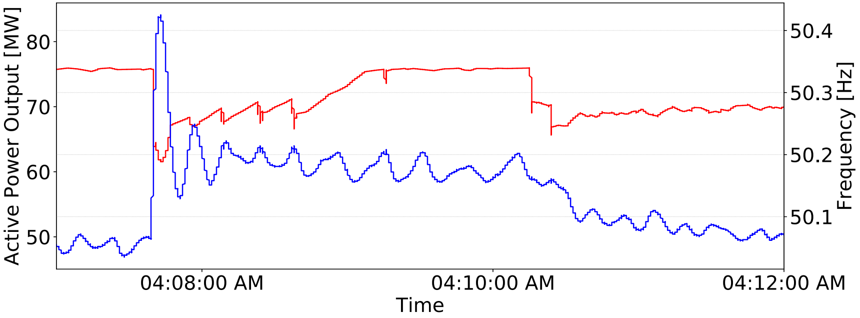

The issue causing the chattering is the deadband included in the frequency controller of a large WECS.

All-Island Irish Transmission System with 100% Non-Synchronous Generation

In this example, we consider a scenario of the Irish system with 100% non-synchronous generation.

The load is 2.36 GW, and the contingency is the outage of the HVDC line to the UK outage (400 MW) at $t = 1$ s.

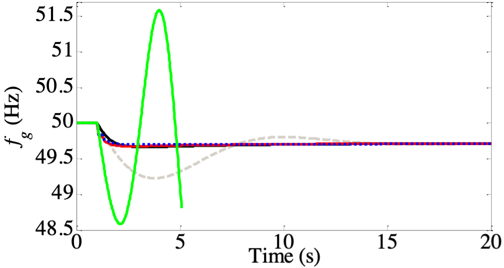

(a) Grid frequency zoom-out

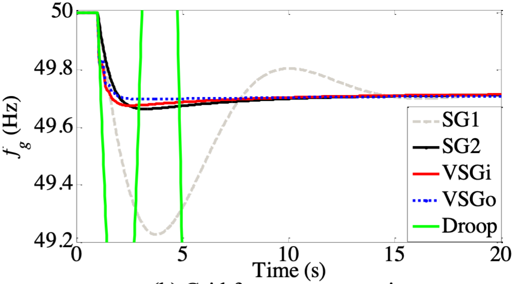

(b) Grid frequency zoom-in

Table of Contents

Frequency and Power Variations

This section defines the link between complex power and *complex frequency* in ac power systems.

Let us consider the power injection at network buses:

$$\bar{\boldsymbol{s}}(t) = \boldsymbol{p}(t) + \jmath \boldsymbol{q}(t) = \bar{\boldsymbol{v}}(t) \circ \bar{\boldsymbol{\imath}}^*(t) \, ,$$

where voltages and currents are Park's vectors (or analytic signals), i.e., are valid in transient conditions:

$$\bar{\boldsymbol{v}}(t) = \boldsymbol{v}_{\mathrm{d}}(t) + \jmath \boldsymbol{v}_{\mathrm{q}}(t) \, .$$

Assumption

Let us assume that transmission line dynamics are fast, hence:

$$\bar{\imath}(t) \approx \bar{\mathbf{Y}}\, \bar{\boldsymbol{v}}(t)\,,$$

where $\bar{\mathbf{Y}}$ is the conventional admittance matrix of the grid.

Hence the power injections into the grid nodes can be rewritten as:

$$\bar{\boldsymbol{s}}(t) = \bar{\boldsymbol{v}}(t) \circ [\bar{\mathbf{Y}}\, \bar{\boldsymbol{v}}(t)]^{*}\,.$$

Complex Frequency

Let us rewrite the Park vector of the voltage in polar coordinates:

$$\bar{v} = v\, e^{\jmath\theta} = e^{(u+\jmath\theta)}$$

where $u = \ln(v)$.

Then, the *complex frequency* is defined as follows:

$$\bar{\eta} = \frac{d}{dt}(u + \jmath\theta) = u' + \jmath\theta' = \rho + \jmath\omega\,,$$

It is possible to show that the complex frequency is a special case of *geometric frequency*.

Link of the Complex Frequency with the Current

From the previous definition, the following identity holds:

$$\bar{\boldsymbol{v}}' = \frac{d}{dt}\bar{\boldsymbol{v}} = \bar{\boldsymbol{v}} \circ \bar{\boldsymbol{\eta}} \, .$$

Then, from $\bar{\boldsymbol{\imath}} \approx \bar{\mathbf{Y}}\,\bar{\boldsymbol{v}}$, one obtains:

$$\bar{\boldsymbol{\imath}}' = \bar{\mathbf{Y}}\,\bar{\boldsymbol{v}}' = \bar{\mathbf{Y}}\,(\bar{\boldsymbol{v}} \circ \bar{\boldsymbol{\eta}}) = \bar{\mathbf{Y}}\,\mathrm{diag}(\bar{\boldsymbol{v}})\,\bar{\boldsymbol{\eta}} = \bar{\mathbf{I}}\,\bar{\boldsymbol{\eta}} \, .$$

Link of the Complex Frequency with the Complex Power

Then taking the conjugate and multiplying by the voltage

$$\bar{\boldsymbol{v}} \circ \bar{\boldsymbol{\imath}}'^{*} = \bar{\mathbf{S}}\, \bar{\boldsymbol{\eta}}^{*} \, .$$

Where $\bar{\mathbf{S}}$ is a matrix whose elements are the complex power flow in the branches of the grid.

Rate of Change of Power (RoCoP) [grid side]

And finally, we note that:

$$
\begin{aligned}
\bar{\boldsymbol{s}}' &= \frac{d}{dt}(\bar{\boldsymbol{v}} \circ \bar{\boldsymbol{\imath}}^*) \\
&= \bar{\boldsymbol{v}}' \circ \bar{\boldsymbol{\imath}}^* + \bar{\boldsymbol{v}} \circ \bar{\boldsymbol{\imath}}'^* \\
&= \bar{\boldsymbol{v}} \circ \bar{\boldsymbol{\eta}} \circ \bar{\boldsymbol{\imath}}^* + \bar{\boldsymbol{v}} \circ \bar{\boldsymbol{\imath}}'^* \\
&= \bar{\boldsymbol{s}} \circ \bar{\boldsymbol{\eta}} + \bar{\boldsymbol{v}} \circ \bar{\boldsymbol{\imath}}'^*
\end{aligned}
$$

So we obtain the expression:

$$
\boxed{\bar{\boldsymbol{s}}' - \bar{\boldsymbol{s}} \circ \bar{\boldsymbol{\eta}} = \bar{\mathrm{S}}\, \bar{\boldsymbol{\eta}}^*}
$$

We need now an expression for $\bar{\boldsymbol{s}}'$ from the device side . . .

Alternative Expression of the RoCoP

Note that, in general, the complex frequency of the voltage is not equal to the complex frequency of the current, hence:

$$\bar{v}' = \bar{\eta}_v \bar{v}$$

$$\bar{\imath}' = \bar{\eta}_\imath \bar{\imath}$$

Then, one obtains:

$$p' = (\rho_v + \rho_\imath)p - (\omega_v - \omega_\imath)q$$

and

$$q' = (\omega_v - \omega_\imath)p - (\rho_v + \rho_\imath)q$$

System Model

Let consider the conventional DAE model for transient stability analysis:

$$
\begin{aligned}
\boldsymbol{z}' &= \boldsymbol{f}(\boldsymbol{z}, \boldsymbol{y}) \\
\boldsymbol{0} &= \boldsymbol{g}(\boldsymbol{z}, \boldsymbol{y})
\end{aligned}
$$

Under usual assumptions, we can write:

$$
\begin{aligned}
\boldsymbol{y}' = \frac{\partial \boldsymbol{\phi}}{\partial \boldsymbol{z}} \boldsymbol{z}' &= \left(\frac{\partial \boldsymbol{g}}{\partial \boldsymbol{y}} \right)^{-1} \frac{\partial \boldsymbol{g}}{\partial \boldsymbol{z}} \boldsymbol{z}' \\
&= \left(\frac{\partial \boldsymbol{g}}{\partial \boldsymbol{y}} \right)^{-1} \frac{\partial \boldsymbol{g}}{\partial \boldsymbol{z}} \boldsymbol{f}(\boldsymbol{z}, \boldsymbol{\phi}(\boldsymbol{z})) \, .
\end{aligned}
$$

Rate of Change of Power (RoCoP) [device side]

In the conventional DAE model of power systems, voltages and powers are algebraic variables.

Let assume we can write the expression of the power injections of each device connected to the grid as:

$$\bar{\boldsymbol{s}}' = \bar{\boldsymbol{s}}'(\bar{\boldsymbol{v}}, \boldsymbol{z}, \boldsymbol{y})$$

Then, the time derivatives of $\bar{\boldsymbol{s}}'$ can be written as:

$$\bar{\boldsymbol{s}}' = \frac{\partial \bar{\boldsymbol{s}}}{\partial \bar{\boldsymbol{v}}}\, \bar{\boldsymbol{v}}' + \left[\frac{\partial \bar{\boldsymbol{s}}}{\partial \boldsymbol{z}} + \frac{\partial \bar{\boldsymbol{s}}}{\partial \boldsymbol{y}} \left(\frac{\partial \boldsymbol{g}}{\partial \boldsymbol{y}} \right)^{-1} \frac{\partial \boldsymbol{g}}{\partial \boldsymbol{z}} \right] \boldsymbol{z}'$$

where we already know that $\bar{\boldsymbol{v}}' = (\rho + \jmath\omega) \circ \bar{\boldsymbol{v}} = \bar{\boldsymbol{\eta}} \circ \bar{\boldsymbol{v}}$, hence:

$$\boxed{\bar{\boldsymbol{s}}' = \frac{\partial \bar{\boldsymbol{s}}}{\partial \bar{\boldsymbol{v}}}\, \bar{\boldsymbol{\eta}} \circ \bar{\boldsymbol{v}} + \left[\frac{\partial \bar{\boldsymbol{s}}}{\partial \boldsymbol{z}} + \frac{\partial \bar{\boldsymbol{s}}}{\partial \boldsymbol{y}} \left(\frac{\partial \boldsymbol{g}}{\partial \boldsymbol{y}} \right)^{-1} \frac{\partial \boldsymbol{g}}{\partial \boldsymbol{z}} \right] \boldsymbol{z}'}$$

Component of the RoCoP

From the definition of complex frequency we can define the following components of the RoCoP:

$$\bar{\boldsymbol{s}}'_1 = \jmath \bar{\boldsymbol{s}} \circ \boldsymbol{\omega} - \jmath \bar{\mathrm{S}}\, \boldsymbol{\omega} \,,$$
$$\bar{\boldsymbol{s}}'_2 = \bar{\boldsymbol{s}} \circ \boldsymbol{\varrho} + \bar{\mathrm{S}}\, \boldsymbol{\varrho} \,.$$

where

$$\bar{\boldsymbol{s}}' = \bar{\boldsymbol{s}}'_1 + \bar{\boldsymbol{s}}'_2 \,.$$

Special Cases: Constant Power Injection

The constraint is $\bar{s} = \mathrm{const.}$

Then, we obtain:

$$\bar{s}' = 0 \quad \Rightarrow \quad \bar{s}_1' = -\bar{s}_2'$$

This is a quite interesting result as it indicates that, during a transient, a constant power device (even a constant power load) affects the frequency at a bus if the voltage magnitude changes, and *vice versa*!

Special Cases: Constant Admittance

The constraint is $\bar{\imath} = \bar{Y}_o \bar{v}$

Then (after some tedious algebra), we obtain:

$$\bar{s}_1' = 0 \quad \text{and} \quad \bar{s}' = \bar{s}_2'$$

This is another interesting result as it indicates that a constant admittance cannot impact the frequency. It only impacts the voltage magnitude.

Special Cases: Constant Current and Power Factor

The constraint is $|\bar{\imath}| = \text{const.}$ and $\phi = \text{const.}$

Then (after some tedious algebra), we obtain:

$$\bar{s}'_2 = 0 \quad \text{and} \quad \bar{s}' = \bar{s}'_1$$

Yet another interesting result. This tells us that a constant current device cannot impact the voltage. It only impacts the frequency.

Approximated Expressions

Then, one can define some approximated expressions:

$$\boldsymbol{p}_1' \approx \mathbf{B}_1 \boldsymbol{\omega} \,,$$
$$\boldsymbol{q}_1' \approx \mathbf{G}_1 \boldsymbol{\omega} \,,$$

and

$$\boldsymbol{p}_2' \approx \mathbf{G}_2 \boldsymbol{\varrho} \,,$$
$$\boldsymbol{q}_2' \approx \mathbf{B}_2 \boldsymbol{\varrho} \,,$$

where $\mathbf{B}_1$, $\mathbf{G}_1$, $\mathbf{B}_2$ and $\mathbf{G}_2$ are approximated susceptance and conductance matrices obtained from $\bar{\mathbf{Y}}$.

Example: ρ and ω

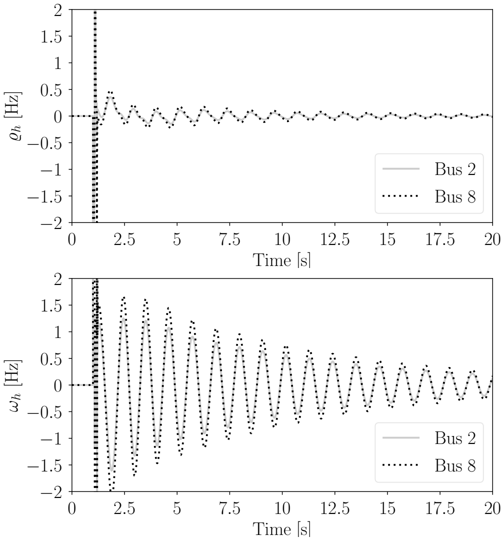

Example: Synchronous Machine and DER

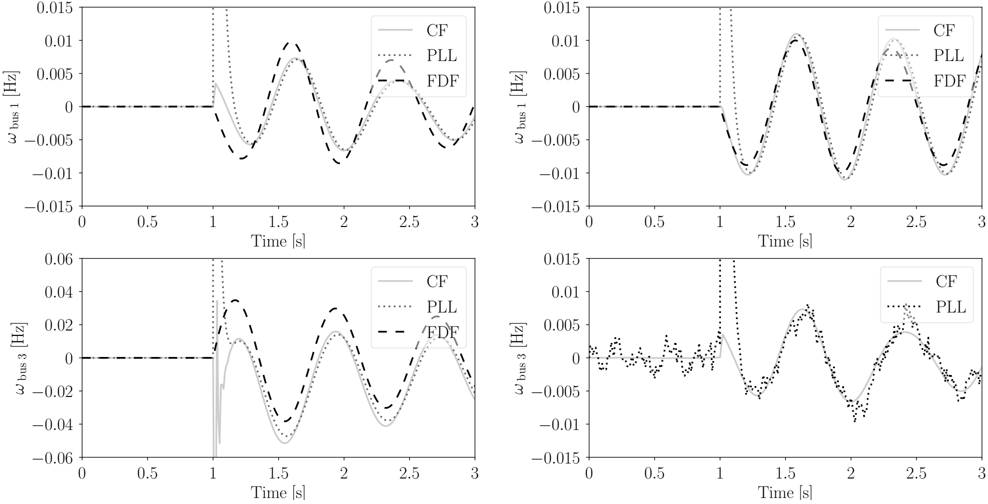

Complex Frequency as a Modelling Tool

A byproduct of the complex frequency approach is that it can be utilised as a modelling tool.

Remark

As a differential operator, the formulation based on the complex frequency does not provide "new" equations.

However, it provides "new" insights on the behaviour of the components.

What is the "internal" frequency of a converter?

We know well that the internal frequency of a synchronous machine is the rotor angular speed.

The rotor speed is the frequency of the internal emf of the machine

Can we define a similar "internal" frequency for converters and, more in general, for devices that do not have a rotor?

What is the link between internal frequency and power injection of a converter?

This is a relevant question because, if we know this link, then:

- We can understand better what to expect from existing controllers
- It is easier to design new and effective controllers

Generalization of the Complex Frequency

So far we have considered exclusively the complex frequency of the bus voltage.

In effect, one can define the complex frequency of any time dependent complex quantity, e.g., voltage and current:

$$\bar{v}'_h = \bar{\eta}_v \, \bar{v}_h \, , \qquad \bar{\imath}'_h = \bar{\eta}_\imath \, \bar{\imath}_h \, .$$

Note that the complex frequency of the voltage and the current at a given bus are not equal, in general.

The only case where $\bar{\eta}_v = \bar{\eta}_\imath$ is when the device connected at bus h is a constant admittance.

Components of the Complex Frequency

The complex frequency includes:

Translation

A real part, which represents a **translation** and depends only on the magnitude of the Park vector; and

Rotation

An imaginary part, which represents a **rotation** and depends only on the phase angle of the Park vector.

Rate of Change of Complex Power

Let us consider the VSC complex power injection into the grid:

$$\bar{s} = \bar{v}\bar{\imath}^*$$

The rate of change of complex power is:

$$\bar{s}' = (\bar{\eta}_v + \bar{\eta}_\imath^*)\bar{s}$$

Ideal Controllers – I

Ideal constant current control:

$$
\begin{aligned}
\bar{\imath}' &= 0 \\
\bar{\eta}_{\imath} &= 0 \\
\bar{s}' &= \bar{\eta}_{v}\bar{s}
\end{aligned}
$$

Constant current source and constant power factor:

$$
\begin{aligned}
\rho_{\imath} &= 0 \\
\omega_{v} &= \omega_{\imath} \\
\bar{s}' &= \rho_{v}\bar{s}
\end{aligned}
$$

Ideal Controllers – II

Constant active and reactive power:

$$\bar{s}' = 0$$

$$\bar{\eta}_v = -\bar{\eta}_\imath^*$$

Constant admittance:

$$\rho_v = \rho_\imath$$

$$\omega_v = \omega_\imath$$

$$\bar{s}' = 2\rho_v \bar{s}$$

Ideal Controllers – III

Constant active power and constant voltage:

$$
\begin{aligned}
\rho_v &= 0 \\
p' &= 0 \\
\frac{q}{p} &= \frac{\rho_\imath}{\omega_v - \omega_\imath}
\end{aligned}
$$

Terminal bus vs. “internal” bus

The goal is to use the complex frequency to find the equations that describe what happens in the box.

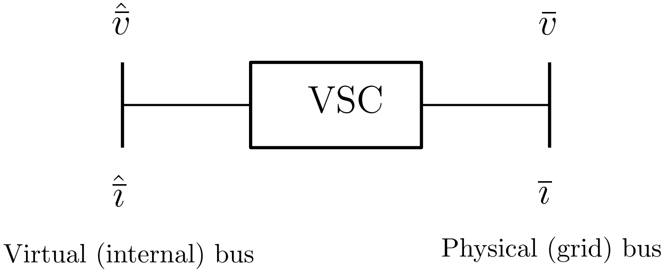

Rate of Change of Complex Power as an Invariant

Let us consider the VSC complex power injection into the grid:

$$\bar{s} = \bar{v}\bar{\imath}^* = \hat{\bar{v}}\hat{\bar{\imath}}^*$$

The complex power is an invariant, that is, it is the same independently from the reference frame:

$$\bar{s}' = (\bar{\eta}_v + \bar{\eta}_\imath^*)\bar{s} = (\hat{\bar{\eta}}_v + \hat{\bar{\eta}}_\imath^*)\bar{s}$$

Effect of PLL

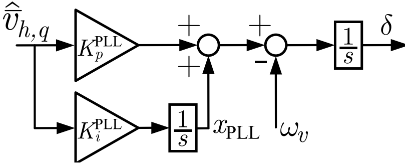

$$
\begin{aligned}
\bar{v}_h &= \exp(\jmath\,\delta)\,\hat{\bar{v}}_h \\
\bar{\imath}_h &= \exp(\jmath\,\delta)\,\hat{\bar{\imath}}_h \\
&\Downarrow \\
\hat{\bar{\eta}}_v &= \bar{\eta}_v - \jmath\delta' \\
\hat{\bar{\eta}}_\imath &= \bar{\eta}_\imath - \jmath\delta'
\end{aligned}
$$

The very first device that we can consider within the DER is the PLL which introduces a (transient) shift between the grid and the internal reference frame of the voltage and current of the DER:

PLL

The PLL introduces a **transient rotation**.

Inner Current Control

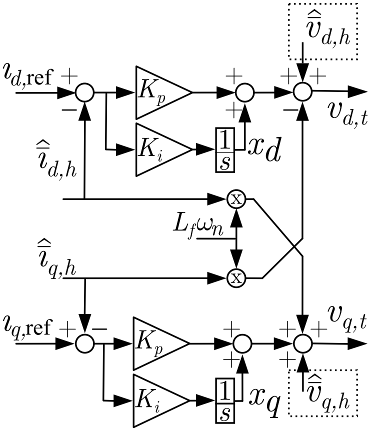

The effect of the current control is only on the real part of the complex frequency:

$$\bar{s}_h' = (\bar{\eta}^*_{\imath_{\mathrm{ref}}} + \kappa_{\mathrm{PI}})\,\hat{\bar{v}}_h\,\bar{\imath}^*_{\mathrm{ref}} + (\hat{\bar{\eta}}_v - \kappa_{\mathrm{PI}})\,\bar{s}_h$$

where $\kappa_{\mathrm{PI}} = K_i/K_p$ and:

$$(\bar{\eta}_\imath')^* + \kappa_{\mathrm{PI}} = \bar{\eta}_\imath^* + (\kappa_{\mathrm{PI}} + \jmath\delta')\,,$$
$$\bar{\eta}_v' - \kappa_{\mathrm{PI}} = \bar{\eta}_v - (\kappa_{\mathrm{PI}} + \jmath\delta')$$

Current Control

The Current Control introduces a **translation**.

Voltage Feed Forward (VFF)

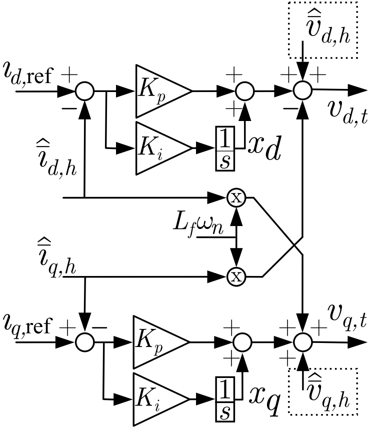

The effect of the VFF (dotted boxes in the figure) is inversely proportional to the proportional gain of the current controller:

$$
\begin{aligned}
\bar{s}'_h = {} & (\bar{\eta}^*_{\imath_\text{ref}} + \kappa_\text{PI})\, \bar{v}'_h\, \bar{\imath}^*_\text{ref} \\
& + (\bar{\eta}'_v - \kappa_\text{PI})\, \bar{s}_h \\
& - \frac{1}{K_p} (\bar{\eta}'_v)^* v_h^2
\end{aligned}
$$

VFF

The VFF introduces both a **rotation** and a **translation**.

GFL Control

Current control with constant current reference:

$$\bar{s}'_h = \kappa_{\mathrm{PI}}\, \bar{v}'_h\, \bar{\imath}^*_{\mathrm{ref}} + (\bar{\eta}'_v - \kappa_{\mathrm{PI}})\, \bar{s}_h$$

Current control with constant power reference:

$$\bar{s}'_h = (\bar{\eta}'_v - \kappa_{\mathrm{PI}})\,(\bar{s}_h - \bar{s}_{\mathrm{ref}})$$

Current control with virtual admittance loop:

$$\bar{s}'_h = -v_h^2\, \bar{Y}^*_v 2\rho_v + \bar{Y}^*_v \bar{\eta}'_v \bar{v}'_h \bar{v}_{\mathrm{ref}}$$

GFM Control

Voltage control:

$$\bar{s}'_h = (K^v_p \bar{\eta}^*_{v_{\rm ref}} + K^v_i)\bar{v}'_h \bar{v}^*_{\rm ref} - (K^v_p(\bar{\eta}'_v)^* + K^v_i)v^2_h + (\bar{\eta}'_v - \kappa_{\rm PI})\,\bar{s}_h$$

Synchronization:

$$\delta' = \omega_{\rm VSM} - \omega_v \,,$$

$$\omega'_{\rm VSM} = \frac{1}{J_v}\Big(\frac{p_{\rm ref}}{\omega_n} - \frac{p_h}{\omega_{\rm VSM}} + D_p(\omega_n - \omega_{\rm VSM})\Big)$$

Outer voltage loop:

$$\bar{v}_{\rm ref} = \jmath v_{q,{\rm ref}} = \jmath \psi_v \omega_{\rm VSM} \,,$$

$$\Rightarrow \quad \bar{\eta}_{v_{\rm ref}} \bar{v}_{\rm ref} = \jmath(\dot{\psi}_v \omega_{\rm VSM} + \psi_v \dot{\omega}_{\rm VSM})$$

$$\bar{\eta}_{v_{\rm ref}} = \rho_{v_{\rm ref}}$$

Case Study - I

Case Study 1

The following examples show how to utilise the complex frequency as a "metric" of the effectiveness of the control.

We use a modified version of the WSCC 9-bus system:

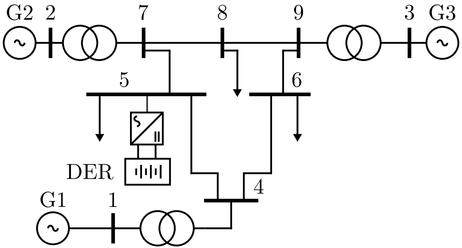

Effect of the Bandwidth of the PLL

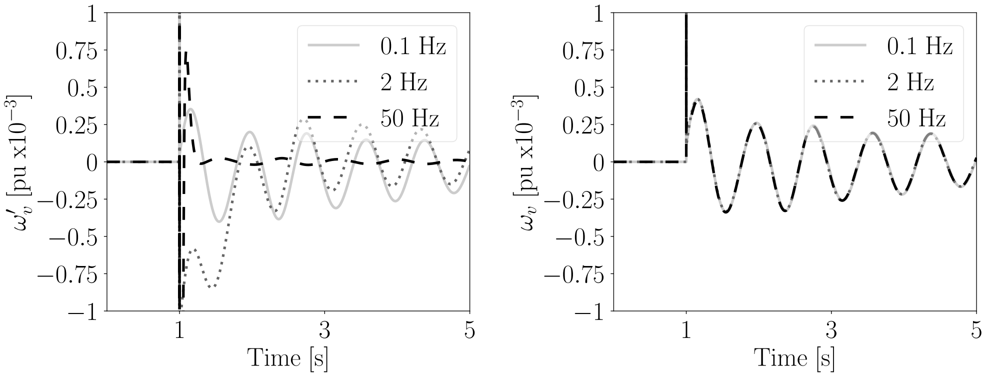

Effect of Current Control Gains

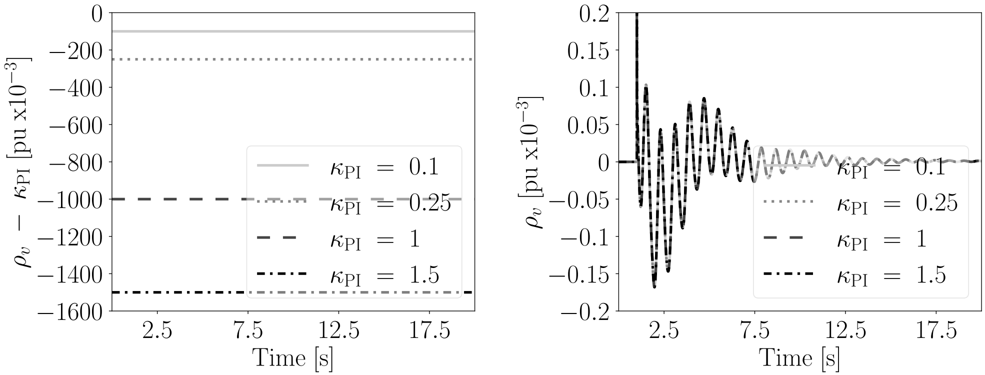

Effect of VFF

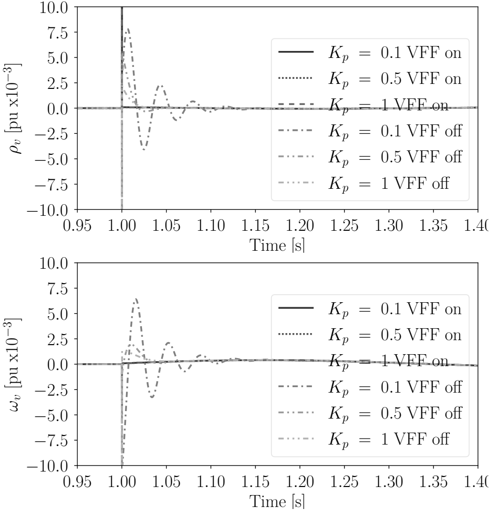

GFL Current Control - Outer Loops

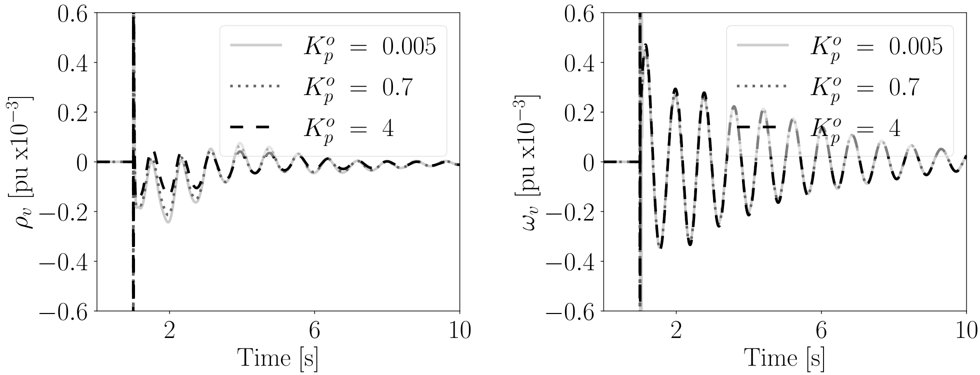

GFL Current Control - Active Power Droop

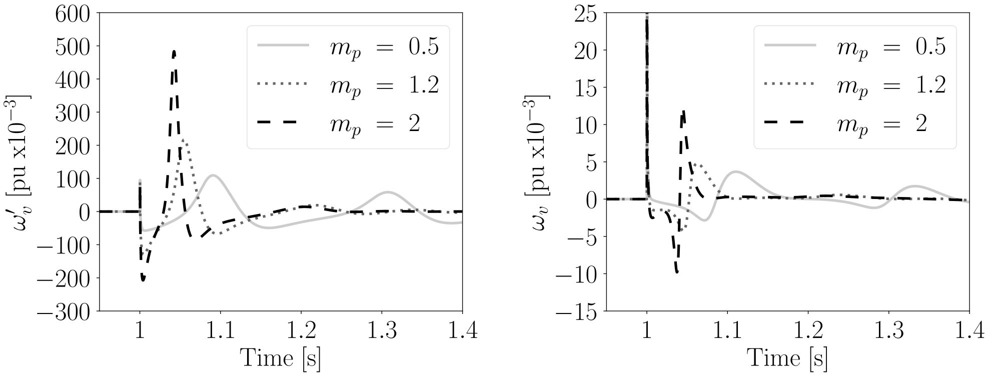

GFM Virtual Shaft

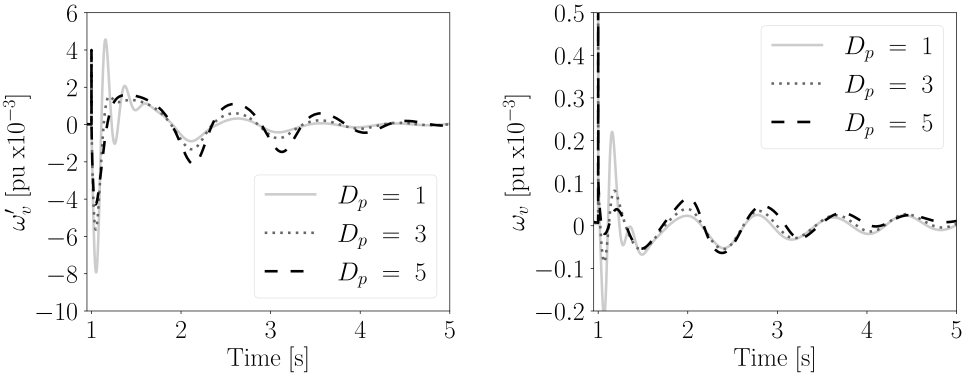

Case Study - II

Case Study 2

The following examples show how to utilise the complex frequency as a tool to design more effective controllers.

We use again a modified version of the WSCC 9-bus system:

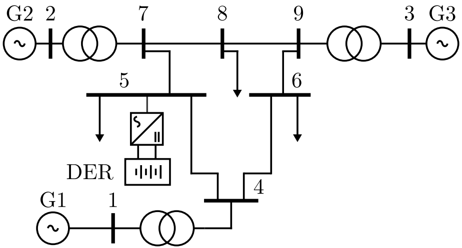

Complex Modelling of Converter-Interfaced Generation

Federico Milano

Low-Inertia Systems

Complex Frequency

Concluding Remarks

Design of the PLL

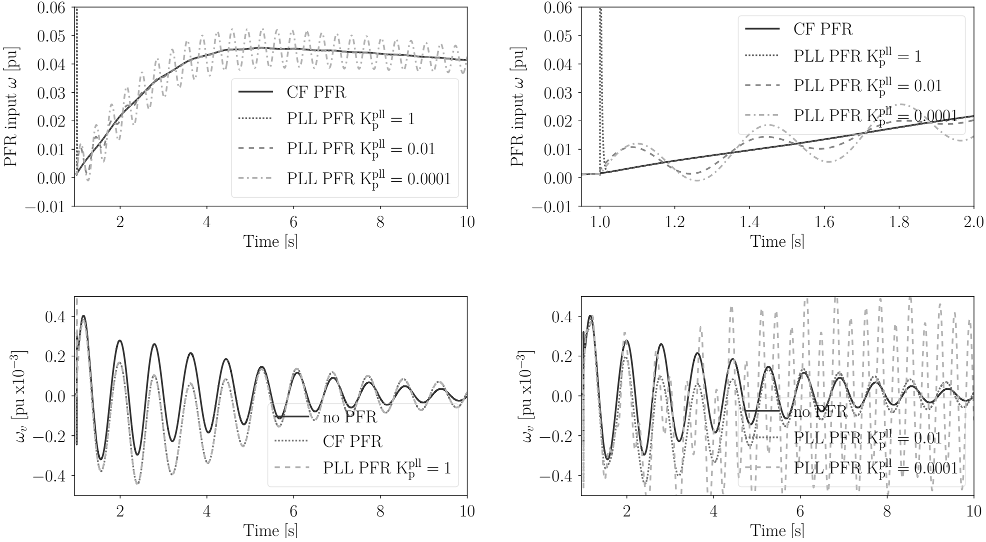

Design of the droop of GFL

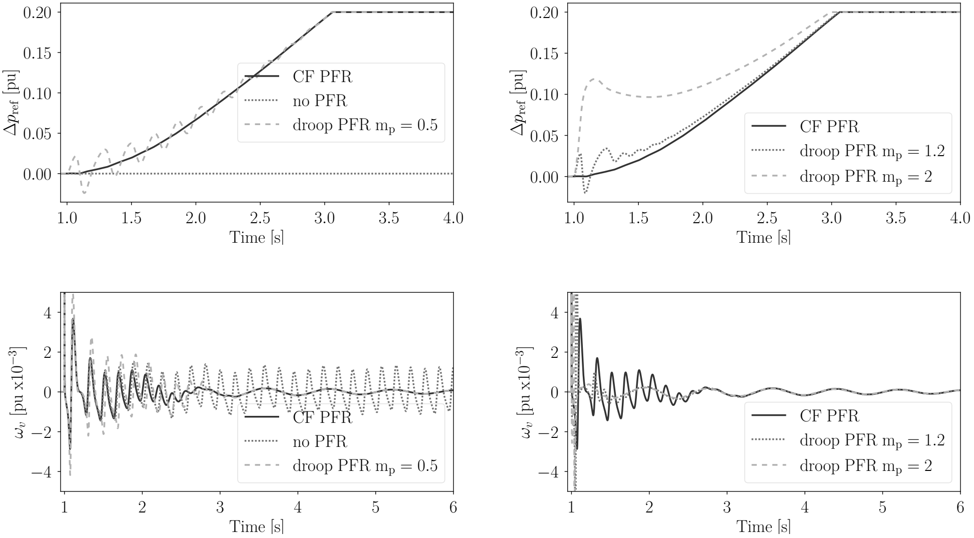

Interaction among SM, VSM and GFL

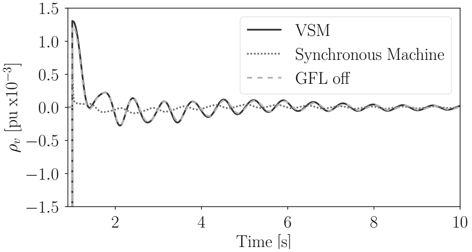

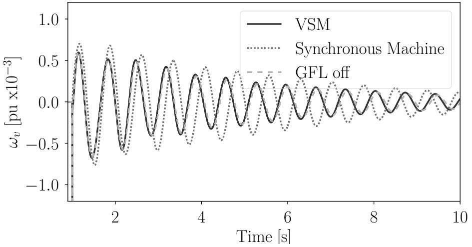

Remarks – I

CF approach decouples the contribution on the local frequency of each sub-controller and identifies critical control parameters.

The current controller is shown to represent a constant translation of the real part of the CF while the synchronization control, regardless of its type, affects the imaginary part.

Remarks – II

For GFL configurations, the PLL parameters are shown to have the largest impact on the local frequency.

For GFM, active power droop parameter as well as VSM damping parameter are shown to affect the frequency response after a contingency.

For the GFM case, the internal frequency of the controller achieves a better transient response than the exact frequency.

Remarks – III

It seems to be relevant to extend the use of the calculated internal frequencies of the converters for control applications.

There seem to be a potential of using non-conventional controllers based on CF or controllers based on non-conventional input signals (based on the real part of CF).

The effect on CF of multiple converters, their dynamic interaction and the impact of this interaction on converter frequency control will also be studied.

Example: Control of DERs – I

Control 1 (conventional)

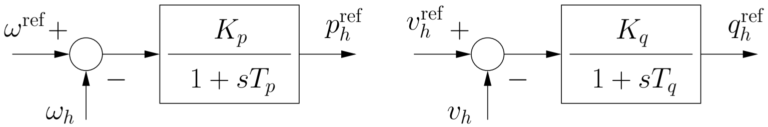

Control 2 (based on complex frequency findings)

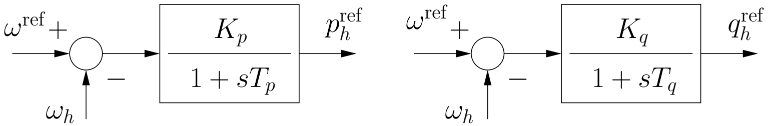

Example: Control of DERs – II

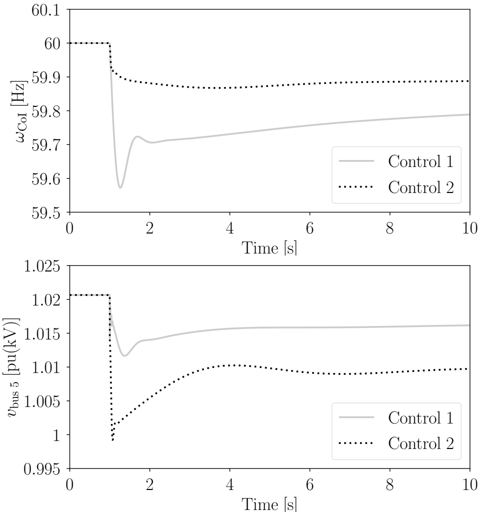

Example: Frequency-Voltage Control – I

The derivation of the complex frequency shows that both voltage and frequency are link to both active and reactive power.

This observation cannot be easily exploited with conventional synchronous machines as their frequency control is *too slow* to couple dynamically with the voltage control.

However, one can utilize this idea of a mixed voltage-frequency control for DERs.

Example: Frequency-Voltage Control – II

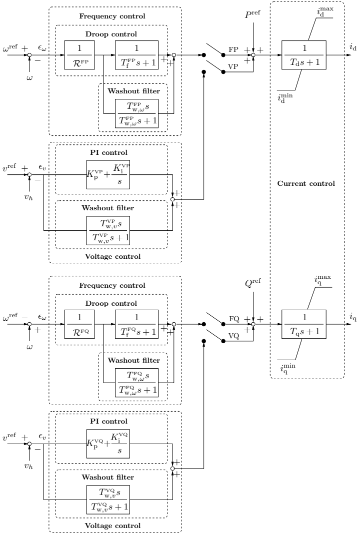

Example: Frequency-Voltage Control – III

The available control modes for the active power are:

- FP: The active power is employed to regulate the frequency.
- VP: The active power is employed to regulate the voltage.
- FVP: The active power reference is modified to control both the frequency and the voltage.

The available modes for the control of the reactive power are:

- VQ: The reactive power is utilized to regulate the voltage.
- FQ: The reactive power is utilized to regulate the frequency.
- FVQ: Both VQ and FQ are switched on in a combined control of the reactive power.

Example: Frequency-Voltage Control – IV

Since the control combines "everything with everything", we need some metric to be able to compare results.

We define the magnitude of the complex frequency as:

$$\eta_h = \sqrt{(\omega_h^2 + \rho_h^2)}$$

and then the cumulative metric (the smaller the better!):

$$\mu_h = \int_{t_0}^{t} \eta_h \, dt$$

The property of this metric is that the two components of the complex frequency have the same units and, thus, are directly comparable.

Example: Frequency-Voltage Control – V

Modified New England 39-bus system

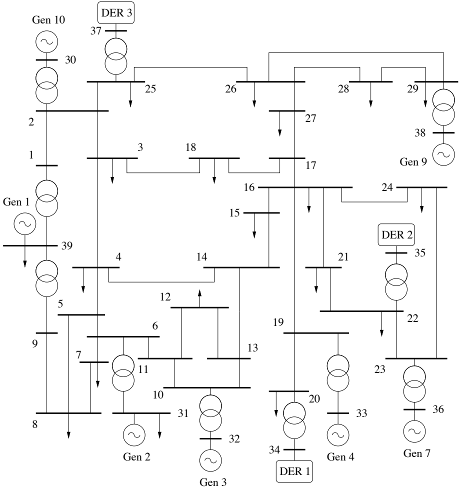

Example: Frequency-Voltage Control – VI

Outage of the load connected at bus 3. Impact on frequency.

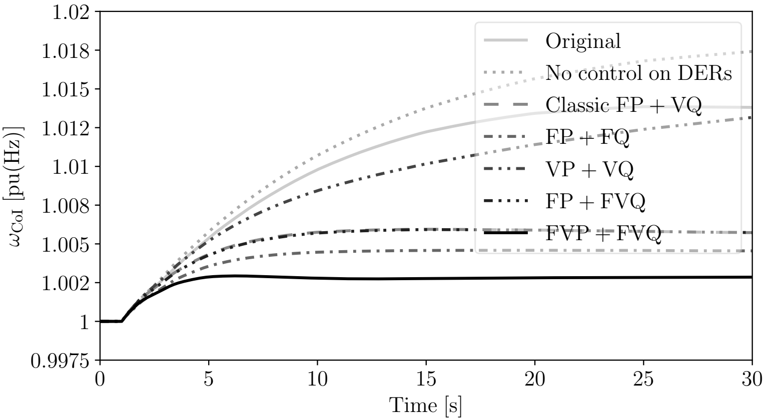

Example: Frequency-Voltage Control – VII

Outage of the load connected at bus 3. Impact on voltage.

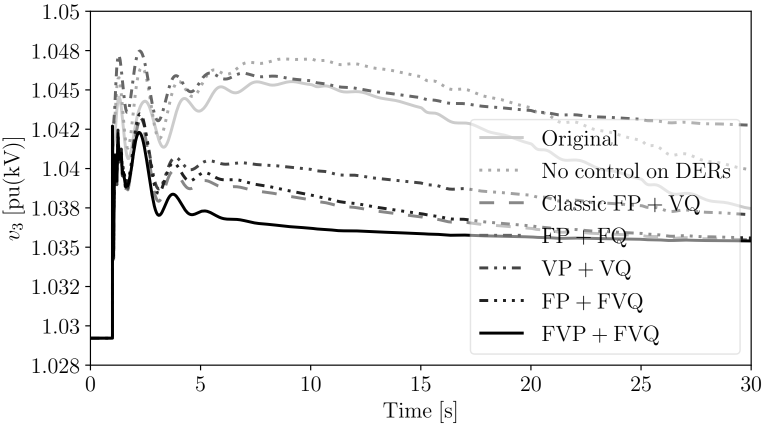

Example: Frequency-Voltage Control – VIII

Outage of the load connected at bus 20. Various control combinations.

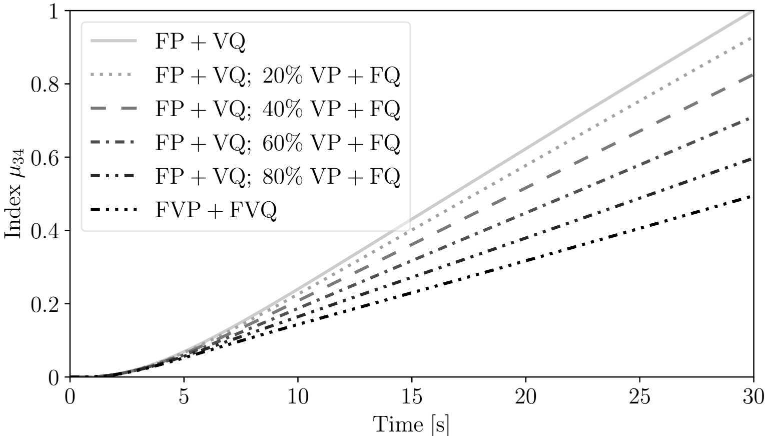

Example: Frequency-Voltage Control – IX

Outage of the generator 10. Effect of line resistance.

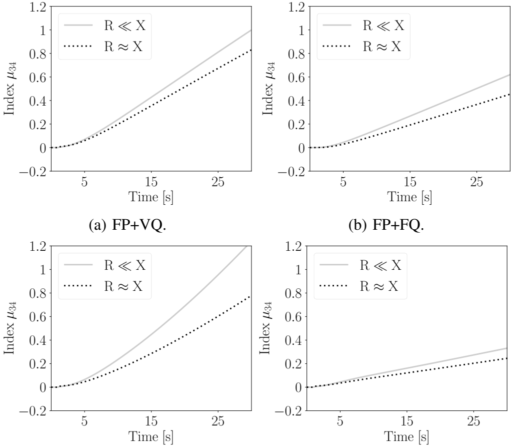

(a) FP+VQ. (b) FP+FQ.

(c) VP+VQ. (d) FVP+FVQ.

Outage of the generator 10. Effect of DER penetration.

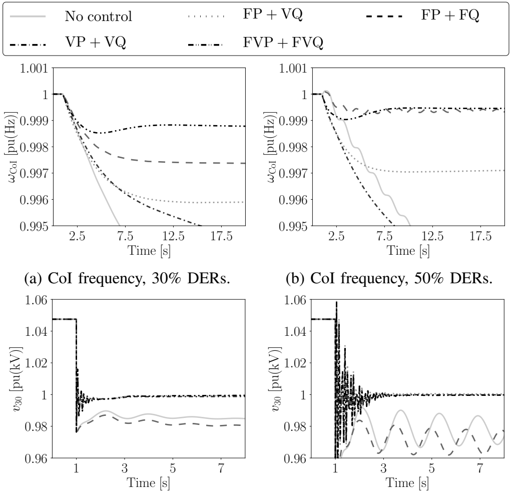

(a) CoI frequency, 30% DERs.

(b) CoI frequency, 50% DERs.

Frequency Control with Voltage Feedback - I

Let us consider again the differentiation of the active power injection at a bus:

$$dp_h = dp_{1,h} + dp_{2,h}$$

The term $dp_{1,h}$ is the component of the active power that can effectively modify or impact the frequency in the grid.

The idea is thus to design a control that imposes the following constraint:

$$dp_{2,h} = 0$$

Frequency Control with Voltage Feedback - II

The expression of $dp_{2,h}$ is:

$$dp_{2,h} = \sum_{k \in \mathbb{B}} \tilde{B}^{hk}(t)\, d[v_h(t)\, v_k(t)]$$

or, equivalently,

$$dp_{2,h} = \sum_{k \in \mathbb{B}} \tilde{B}^{hk}(t) \left(v_k \, dv_h + v_h \, dv_k \right)$$

So our control must satisfy the constraint:

$$\sum_{k \in \mathbb{B}} \left(v_k(t)\, dv_h + v_h(t)\, dv_k \right) = 0$$

Frequency Control with Voltage Feedback - III

The last equation is equivalent to:

$$v_h(t) \sum_{k \in \mathbb{B}} v_k(t) = c_o$$

where c_o is a constant, which, following from the system initialization, takes the value:

$$c_o = v_{h,o}(t) \sum_{k \in \mathbb{B}} v_{k,o}(t)$$

Finally, the new reference voltage of the modified remote voltage controller (MRVC) becomes:

$$v^{\mathrm{ref}}(t) = \frac{c_o}{\sum_{k \in \mathbb{B}} v_k(t)}$$

Frequency Control with Voltage Feedback - IV

We compare the following scenarios for the DER control:

1. CPC (Constant Power Control), i.e. without the frequency and voltage control loops;
2. FC, i.e. with the frequency loop connected and the voltage control disconnected;
3. FC+VC, i.e. with both frequency and voltage control connected and the voltage control constant reference;
4. FC+MRVC, i.e. with both frequency and voltage control connected and with the modified voltage control reference.

Frequency Control with Voltage Feedback - V

Let us consider a modified version of the WSCC 9-bus system.

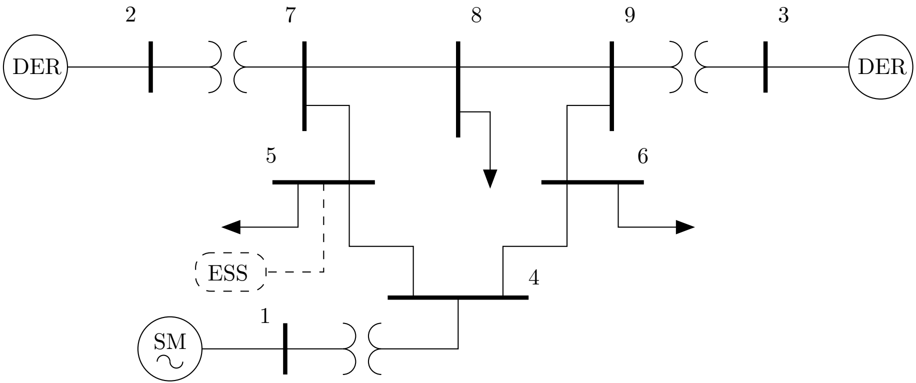

Frequency Control with Voltage Feedback - VIII

Let consider now the effect of the ESS following a fault.

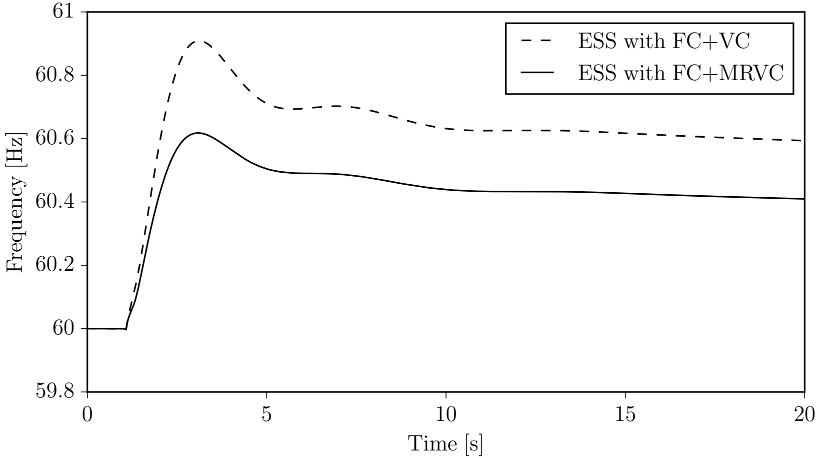

Frequency Control with Voltage Feedback - IX

With the MRVC, the ESS requires less energy to do a better control.

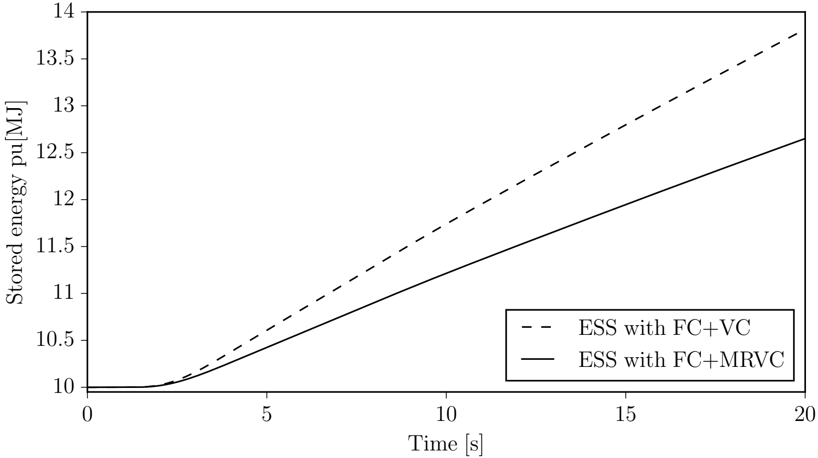

Table of Contents

Conclusions – I

Paradigm shift

Power systems are undergoing one of the most dramatic paradigm shift since the beginning of ac transmission systems: the move from synchronous to non-synchronous devices.

Adequacy of conventional models

Conventional transient stability models might be inadequate, especially with respect to the modeling of converter-interface resources.

Adequacy of conventional controllers

Conventional controllers might be inadequate, especially with respect to the estimation and regulation of the "frequency."

Conclusions – II

Need of New Approaches

Differential geometry provides a consistent (and visual) interpretation of the instantaneous frequency of the voltage

Many Frequencies

Based on a geometric interpretation, one can see that there are "many" different frequencies. The correct understanding of the physical meaning of each frequency is crucial.

Conclusions – III

Rate of Change of Power

The rate of change of power (RoCoP) appears as a relevant quantities to determine the properties of the dynamic behavior of the system.

Novel Controllers

Understanding properly the role of the RoCoP and its relationship with frequency variations can help design better controllers.

Frequency Divider

The "frequency divider," which is a special case of the RoCoP equations, is an effective simple tool that have several applications in modeling and state estimation.

Open Questions

What is the role of “frequency” in a system without synchronous machines?

In a zero-inertia system, can the controllers that balance the power be decentralized or have to be centralized?

Which signal (measured quantity) should these controllers use?

References – I

- Á. Ortega, F. Milano, *Comparison of Bus Frequency Estimators for Power System Transient Stability Analysis*, IEEE PowerCon, Wollongong, Australia, September-October 2016.
- F. Milano, Á. Ortega, *Frequency Divider*, IEEE Transactions on Power Systems, Vol. 32, No. 2, pp. 1493-1501, March 2017.
- Á. Ortega, F. Milano, *Impact of Frequency Estimation for VSC-based Devices with Primary Frequency Control*, IEEE PES ISGT Europe 2017, Turin, Italy, 26-29 September 2017.
- F. Milano, *Rotor Speed-free Estimation of the Frequency of the Center of Inertia*, IEEE Transactions on Power Systems, Vol. 33, No. 1, pp. 1153-1155, January 2018.

References – II

- J. Zhao, L. Mili, F. Milano, *Robust Frequency Divider for Power System Online Monitoring and Control*, IEEE Transactions on Power Systems, Vol. 33, No. 4, pp. 4414-4423, July 2018.
- Á. Ortega, A. Musa, A. Monti, F. Milano, *Hardware-in-the-Loop Validation of the Frequency Divider Formula*, IEEE PES General Meeting, Portland, OR, August 2018.
- Á. Ortega, F. Milano, *Frequency Control of Distributed Energy Resources in Distribution Networks*, 10th Symposium on Control of Power and Energy Systems (IFAC CPES2018), Tokyo, Japan, September 2018.

References – III

- Á. Ortega, F. Milano, *Frequency Participation Factors, IEEE Transactions on Power Systems*, Vol. 33, No. 5, pp. 5563-5571, September 2018.
- F. Milano, Á. Ortega, A. J. Conejo, *Model-Agnostic Linear Estimation of Generator Rotor Speeds based on Phasor Measurement Units*, IEEE Transactions on Power Systems, Vol. 33, No. 6, pp. 7258-7268, November 2018.
- M. Liu, Á. Ortega, F. Milano, *PMU-based Estimation of the Frequency of the Center of Inertia and Generator Rotor Speeds*, IEEE PES General Meeting, Atlanta, GA, August 2019.

References – IV

- F. Milano, Á. Ortega, *Frequency-dependent Model for Transient Stability Analysis*, IEEE Transactions on Power Systems, Vol. 34, No. 1, pp. 806-809, January 2019.
- Á. Ortega, F. Milano, *Estimation of Voltage Dependent Load Models through Power and Frequency Measurements*, IEEE Transactions on Power Systems, Vol. 35, No. 4, pp. 3308-3311, July 2020.
- J. Chen, M. Liu, F. Milano, T. O'Donnell, *100% Converter-Interfaced Generation using Virtual Synchronous Generator Control: A Case Study based on the Irish System*, EPSR, vol. 187, October 2020.
- F. Milano and Á. Ortega, *A Method for Evaluating Frequency Regulation in an Electrical Grid Part I: Theory*, in IEEE Transactions on Power Systems, Vol. 36, No. 1, pp. 183-193, January 2021.

References – V

- Á. Ortega and F. Milano, *A Method for Evaluating Frequency Regulation in an Electrical Grid Part II: Applications to Non-Synchronous Devices*, in IEEE Transactions on Power Systems, Vol. 36, No. 1, pp. 194-203, January 2021.
- M. Liu, J. Chen, F. Milano, *On-line Inertia Estimation for Synchronous and Non-Synchronous Devices*, IEEE Transactions on Power Systems, vol. 36, no. 3, pp. 2693-2701, May 2021.
- G. Tzounas, F. Milano, *Improving the Frequency Response of DERs through Voltage Feedback*, IEEE PES General Meeting, Washington, DC, on-line event, 25-29 July 2021.

References – VI

- F. Milano, *Complex Frequency*, IEEE Transactions on Power Systems, vol. 37, no. 2, pp. 1230-1240, March 2022.
- F. Milano, *A Geometrical Interpretation of Frequency*, IEEE Transactions on Power Systems, vol. 37, no. 1, pp. 816-819, January 2022.
- F. Milano, G. Tzounas, I. Dassios, T. Kërçi, *Applications of the Frenet Frame to Electric Circuits*, IEEE Transactions on Circuits and Systems I: Regular Papers, vol. 69, no. 4, pp. 1668-1680, April 2022.

References – VII

- F. Sanniti, G. Tzounas, R. Benato, F. Milano, *Curvature-Based Control for Low-Inertia Systems*, IEEE Transactions on Power Systems, vol. 37, no. 5, pp. 4149-4152, Sept. 2022.
- W. Zhong, G. Tzounas, F. Milano, *Improving the Power System Dynamic Response through a Combined Voltage-Frequency Control of Distributed Energy Resources*, IEEE Transactions on Power Systems, vol. 37, no. 6, pp. 4375-4384, Nov. 2022.
- W. Zhong, G. Tzounas, M. Liu, F. Milano, *On-line Inertia Estimation of Virtual Power Plants*, EPSR, Volume 212, November 2022, 108336. Presented at PSCC 2022.

References – VIII

- F. Milano, *The Frenet Frame as a Generalization of the Park Transform*, vol. 70, no. 2, pp. 966-976, Feb. 2023.
- D. Moutevelis, J. Roldán-Pérez, M. Prodanovic and F. Milano, *Taxonomy of Power Converter Control Schemes based on the Complex Frequency Concept*, in IEEE Transactions on Power Systems, preprint available. arXiv: 2209.11107
- D. Moutevelis, J. Roldán-Pérez, M. Prodanovic, F. Milano, *Design of Virtual Impedance Control Loop using the Complex Frequency Approach*, PowerTech, Belgrade, Serbia, 25-29 June 2023.

Book on Frequency Variations

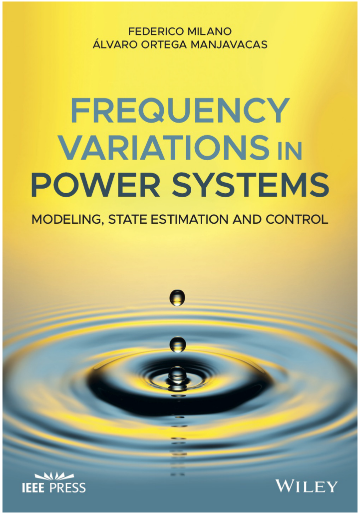

THANK YOU FOR YOUR ATTENTION!

PowerTech
Belgrade 2023

LEADING INNOVATIONS FOR RESILIENT
& CARBON-NEUTRAL POWER SYSTEMS

25-29 JUNE, 2023, BELGRADE, SERBIA